

COMPARATIVE LIFE CYCLE ASSESSMENT OF URANIUM RECOVERY  
FROM BRINE

A THESIS SUBMITTED TO  
THE GRADUATE SCHOOL OF NATURAL AND APPLIED SCIENCES  
OF  
MIDDLE EAST TECHNICAL UNIVERSITY

BY

MELIKE BENAN ALTAY

IN PARTIAL FULFILLMENT OF THE REQUIREMENTS  
FOR  
THE DEGREE OF MASTER OF SCIENCE  
IN  
ENVIRONMENTAL ENGINEERING

APRIL 2022



Approval of the thesis:

**COMPARATIVE LIFE CYCLE ASSESSMENT OF URANIUM RECOVERY  
FROM BRINE**

submitted by **MELIKE BENAN ALTAY** in partial fulfillment of the requirements  
for the degree of **Master of Science in Environmental Engineering Department,**  
**Middle East Technical University** by,

Prof. Dr. Halil Kalıpçılar  
Dean, Graduate School of **Natural and Applied Sciences**

\_\_\_\_\_

Prof. Dr. Bülent İçgen  
Head of Department, **Environmental Engineering**

\_\_\_\_\_

Assist. Prof. Dr. Zöhre Kurt  
Supervisor, **Environmental Engineering, METU**

\_\_\_\_\_

**Examining Committee Members:**

Prof. Dr. Filiz Bengü Dilek  
Environmental Engineering, METU

\_\_\_\_\_

Assist. Prof. Dr. Zöhre Kurt  
Environmental Engineering, METU

\_\_\_\_\_

Prof. Dr. Ayşegül Aksoy  
Environmental Engineering, METU

\_\_\_\_\_

Prof. Dr. Derek Baker  
Mechanical Engineering, METU

\_\_\_\_\_

Assist. Prof. Dr. Burçin Atılgan Türkmen  
Chemical Engineering, Bilecik Şeyh Edebali University

\_\_\_\_\_

Date: 15.04.2022

**I hereby declare that all information in this document has been obtained and presented in accordance with academic rules and ethical conduct. I also declare that, as required by these rules and conduct, I have fully cited and referenced all material and results that are not original to this work.**

Name, Surname: Melike Benan Altay

Signature :

## **ABSTRACT**

### **COMPARATIVE LIFE CYCLE ASSESSMENT OF URANIUM RECOVERY FROM BRINE**

Altay, Melike Benan

M.S., Department of Environmental Engineering

Supervisor: Assist. Prof. Dr. Zöhre Kurt

April 2022, 193 pages

With the increase in world population and the associated increase in raw material, clean water, and energy demands, seeking for innovative and sustainable methods to decrease the human-made environmental footprint becomes a task of utmost importance. Uranium-based atomic energy the generation has an enormous potential to efficiently supply energy demand at the cost of high environmental impact on water bodies. Therefore, estimating the environmental impacts of the uranium recovery systems from desalination waste is a necessity. This study assessed the environmental impact of the uranium recovery methods from brine with amidoximated adsorbents and compared them with the conventional uranium mining methods. This study also aims to analyze the environmental load of desalination plants integrated with uranium recovery methods from brine. The results showed that recovery of uranium from brine in the long run is more effective than the conventional procedures. The other results claim that the combination of uranium recovery from brine systems with desalination plants causes to impact reduction in marine ecotoxicity. The sensitivity analysis results reveal that hydroxylamine and hazardous waste disposal are the most influential parameters during uranium recovery with adsorbent methods. The results of sensitivity analyses about desalination plants reveal that electricity production and chemical

consumption are the most sensitive parameters. Comparative analysis between energy sources used in adsorbent recovery processes and desalination methods indicated that solar energy has the lowest environmental impacts among all kinds of energy scenarios. This study concluded that an alternative sustainable industrial process to obtain uranium is actually applicable and it can be integrated with the desalination plants.

**Keywords:** uranium recovery, life cycle assessment, solar energy, amidoximated adsorbent, desalination

## ÖZ

### **TUZLU SUDAN URANYUM GERİ KAZANIMININ KARŞILAŞTIRMALI YAŞAM DÖNGÜSÜ ANALİZİ**

Altay, Melike Benan

Yüksek Lisans, Çevre Mühendisliği Bölümü

Tez Yöneticisi: Dr. Öğr. Üyesi. Zöhre Kurt

Nisan 2022 , 193 sayfa

Dünya nüfusundaki artış ve buna bağlı olarak hammadde, temiz su ve enerji taleplerindeki artış ile insan kaynaklı çevresel ayak izini azaltmak için yenilikçi ve sürdürülebilir yöntemler aramak son derece önemli bir görev haline gelmiştir. Uranyum bazlı atom enerjisi üretimi su kaynakları üzerinde yüksek çevresel etkiler pahasına enerji talebini verimli bir şekilde karşılamak için muazzam bir potansiyele sahiptir. Bu nedenle tuzdan arındırma tesislerinin atığından uranyum geri kazanım sistemlerinin çevresel etkilerinin analiz edilmesi bir zorunluluktur. Bu çalışma amidoksimlenmiş adsorbanlarla tuzlu sudan uranyum geri kazanım yöntemlerinin çevresel etkilerini değerlendirir ve bunları geleneksel uranyum madenciliği yöntemleri ile kıyaslar. Bu çalışma aynı zamanda tuzlu sudan uranyum geri kazanım yöntemleri ile entegre edilmiş tuzdan arındırma tesislerinin çevresel yükünü analiz etmeyi amaçlar. Sonuçlar uzun vadede uranyumun tuzlu sudan geri kazanımının geleneksel uranyum prosedürlerinden daha etkili olduğunu göstermiştir. Diğer sonuçlar tuzlu su sistemlerinden uranyum geri kazanımının tuzdan arındırma tesisleriyle entegre edilmesinin deniz ekotoksitesinde azalmaya neden olduğunu iddia etmektedir. Duyarlılık ana-

lizinin sonuçları hidroksilamin ve tehlikeli atık bertarafının adsorbanlarla uranyum geri kazanımında en etkili parametreler olduğunu ortaya çıkarmıştır. Tuzdan arındırma tesisleriyle ilgili duyarlılık analizlerinin sonuçları elektrik üretimi ve kimyasal tüketimin en hassas parametreler olduğunu ortaya koymaktadır. Adsorbanla uranyum geri kazanımı yöntemlerinde ve tuzdan arındırma metodlarında kullanılan enerji kaynakları arasında yapılan karşılaştırmalı analizler güneş enerjisinin diğer bütün enerji senaryoları arasında en düşük çevresel etkiye sahip olduğunu göstermiştir. Bu çalışma uranyum elde etmek için alternatif sürdürülebilir endüstriyel yöntemin aslında uygulanabilir ve bunun tuzdan arındırma tesislerine entegre edilebileceği sonuçlarına varmıştır.

Anahtar Kelimeler: uranyum geri kazanımı, yaşam döngüsü analizi, solar enerji, amidoksimlenmiş adsorbant, tuzdan arındırma

To Cleaner Nuclear Science World

## ACKNOWLEDGMENTS

First of all, I would like to express my sincere gratitude and thanks to Assist. Prof. Dr. Zöhre Kurt for her great encouragement, support, and supervision during the studies introduced in this thesis.

I also would like to thank the members of the thesis committee, Prof. Dr. Filiz Bengü Dilek, Prof. Dr. Ayşegül Aksoy, Prof. Dr. Derek Baker, and Asst. Prof. Burçin Atılğan Türkmen for their considerable contributions to this thesis.

I am also grateful to Science Academy's Young Scientist Awards Program (BAGEP), Turkey, L'Oréal Women in Science, Turkey, Sistema Nacional de Investigación (SNI), Panama, the Secretaría Nacional de Ciencia, Tecnología e Innovación (SENACYT), PSA-CIEMAT, Panama project IOMA17-010 and SolarTwins project funded by the European Union's Horizon 2020 research and innovation program under grant agreement No 856619 for their financial and scientific support.

Furthermore, I would like to express my special thanks to the Sustainable Treatment Technology Research group, Bahar Evren, Mert Erkanlı, Ceyda Kalıpcıoğlu, İlayda Sipahi and Gözde Taylan, for their valuable cooperation and comments during my analyses.

I'd like to also thank my dear friends Tuğçe Simge Arslan, Melis Dülger, Musa Binay, Ayşe Sena Akdeniz, Cansu Polat, Sema Başarır, Özge Yücel Bilen, Tercan Çataklı and Zeynep Özcan for being supportive and understanding during my journey. Thanks to you, I was able to complete my master journey with good memories.

I also would like to thank my roommates Merve Gülveren, Emrehan Berkay Çelebi, and Sarp Çelebi for their endless support at all times. I would like to express my special gratitude to Sarp Çelebi for sharing his wisdom and valuable experience during my journey and for being my mentor, who gave strength to endure in difficult times. I owe my special gratitude to Güldane Kalkan for her kindness and great patience in

my master's degree.

I would like to specially thank my dearest mother and my father, who taught me to work in a disciplined way, for being thoughtful and supportive all the time. Behind everything I have accomplished, the biggest factor was their belief in me and their support in every decision I made.

Lastly, my biggest thanks go to my dear fiancée, Hasan Geren. His contribution to my life is enormous. Hasan is my best friend, closest advisor, and life partner. He supported me every step of the way with patience, humor, and great wisdom.

## TABLE OF CONTENTS

ABSTRACT . . . . .	v
ÖZ . . . . .	vii
ACKNOWLEDGMENTS . . . . .	x
TABLE OF CONTENTS . . . . .	xii
LIST OF TABLES . . . . .	xvi
LIST OF FIGURES . . . . .	xix
LIST OF ABBREVIATIONS . . . . .	xxiii
CHAPTERS	
1 INTRODUCTION . . . . .	1
1.1 General Background . . . . .	1
1.2 Problem Statement . . . . .	3
1.3 Significance of the Study . . . . .	4
1.4 Objective of the Thesis . . . . .	4
1.5 Structure of the Thesis . . . . .	4
2 LITERATURE REVIEW . . . . .	7
2.1 Life Cycle Assessment . . . . .	7
2.1.1 Goal and Scope Definition . . . . .	9
2.1.2 Inventory Analysis . . . . .	9
2.1.3 Impact Assessment . . . . .	10
2.1.4 Interpretation . . . . .	14
2.1.5 Software and Database . . . . .	15
2.2 Conventional Uranium Extraction Methods . . . . .	17
2.2.1 Open-Pit Mining . . . . .	17
2.2.2 Underground Mining . . . . .	18
2.2.3 Uranium Milling and Extraction . . . . .	19
2.2.4 In-situ Leaching . . . . .	21

2.3	Other Uranium Extraction Methods from Water Media . . . . .	23
2.4	Desalination Technologies . . . . .	26
2.4.1	Thermal Desalination Technologies . . . . .	27
2.4.1.1	Multi-stage Flash Distillation . . . . .	27
2.4.1.2	Multi-effect Distillation . . . . .	28
2.4.1.3	Vapor Compression . . . . .	28
2.4.1.4	Co-generation Systems . . . . .	29
2.4.2	Membrane Desalination Technologies . . . . .	31
2.4.2.1	Reverse Osmosis . . . . .	31
2.4.2.2	Electrodialysis . . . . .	32
2.4.2.3	Membrane Distillation . . . . .	32
2.4.3	Alternative Desalination Technologies . . . . .	33
2.4.4	Renewable Energy Driven Desalination Technologies . . . . .	33
3	LIFE CYCLE ASSESSMENT OF URANIUM RECOVERY FROM BRINE	35
3.1	INTRODUCTION . . . . .	35
3.2	METHODOLOGY . . . . .	36
3.2.1	Goal and Scope Definition . . . . .	36
3.2.2	Inventory Analysis . . . . .	39
3.2.2.1	Calculation of Required Substances Amount and Energy	39
3.2.2.1.1	AF1 Adsorbent Calculations . . . . .	42
3.2.2.1.1.1	Mass Calculations . . . . .	42
3.2.2.1.1.2	Adaptation of Experimental Values to Realistic Values . . . . .	49
3.2.2.1.1.3	Energy Calculations . . . . .	51
3.2.2.1.1.4	Adsorbed Uranium Calculations for AF1 Adsorbent . . . . .	59
3.2.2.1.2	PAN-AO Adsorbent Calculations . . . . .	60
3.2.2.1.2.1	Mass Calculations . . . . .	61
3.2.2.1.2.2	Adaptation of Experimental Values to Realistic Values . . . . .	62
3.2.2.1.2.3	Energy Calculations . . . . .	62
3.2.2.1.2.4	Adsorbed Uranium Calculations for PAN-AO Adsorbent . . . . .	65
3.2.2.2	Elution Process Selection and Estimation . . . . .	65
3.2.2.2.1	Elution Process Selection . . . . .	65

3.2.2.2.2	Required Eluant Amount Estimation . . . . .	66
3.2.2.2.3	Purification by Vanadium Elution from Concentrated Solution . . . . .	68
3.2.2.3	Disposal Calculations . . . . .	71
3.2.2.3.1	AF1 Adsorbent Disposal Amount . . . . .	74
3.2.2.3.2	PAN-AO Adsorbent Disposal Amount . . . . .	75
3.2.2.4	Recycling of Adsorbents . . . . .	76
3.2.3	Life Cycle Impact Assessment . . . . .	78
3.3	RESULTS AND DISCUSSION . . . . .	78
3.3.1	Characterization Results . . . . .	78
3.3.1.1	AF1 Adsorbent . . . . .	78
3.3.1.2	PAN-AO Adsorbent . . . . .	81
3.3.1.3	Different Energy Scenarios . . . . .	81
3.3.2	Comparative Results of Adsorbent and Conventional Uranium Recovery Methods . . . . .	87
3.3.3	Sensitivity Analysis . . . . .	95
3.3.4	Recycling of Adsorbent Scenarios . . . . .	102
3.3.5	Comparison of Results with Literature . . . . .	104
3.3.6	Environmental Sustainability Concept of This Study . . . . .	107
3.4	CONCLUSION . . . . .	108
4	LIFE CYCLE ASSESSMENT OF DESALINATION PLANT COMBINED WITH URFB SYSTEM . . . . .	109
4.1	INTRODUCTION . . . . .	109
4.2	METHODOLOGY . . . . .	117
4.2.1	Goal and Scope Definition . . . . .	117
4.2.2	Inventory Analysis . . . . .	118
4.2.3	Life Cycle Impact Assessment . . . . .	121
4.3	RESULTS and DISCUSSION . . . . .	122
4.3.1	Characterization and Normalization Results of Solar-Driven MED Plant . . . . .	122
4.3.2	Sensitivity Analysis . . . . .	126
4.3.3	Comparative Characterization and Normalization Results of Solar-Driven MED Plant Combined with URFB System . . . . .	131
4.3.3.1	Comparison of Results with Conventional Reverse Osmosis Integrated with URFB Systems . . . . .	135
4.4	CONCLUSION . . . . .	142

5 CONCLUSION AND RECOMMENDATION . . . . .	143
REFERENCES . . . . .	147
APPENDICES . . . . .	170
A APPENDIX . . . . .	171
A.1 DETAILS OF INVENTORIES . . . . .	171
B APPENDIX . . . . .	183
B.1 COMPARATIVE CHARACTERIZATION AND NORMALIZATION RESULTS WITH DIFFERENT IMPACT CATEGORIES . . . . .	183

## LIST OF TABLES

### TABLES

Table 2.1	Uranium Recovery from Water Media Methods Comparison . . . .	25
Table 2.2	Thermal Desalination Technologies Comparison . . . . .	30
Table 3.1	Conventional Uranium Mining LCA Studies . . . . .	37
Table 3.2	Assumptions Made During the Input Calculation . . . . .	41
Table 3.3	Given Parameters and Variables in the Literature . . . . .	42
Table 3.4	AF1 Adsorbent Elemental Analysis Results During Production (Das, Tsouris, et al., 2016) . . . . .	47
Table 3.5	The Amount of Chemicals Required for AF1 Adsorbent Production for All Normalization Cases . . . . .	49
Table 3.6	Specific Heat Values of Chemicals Used in Adsorbent Preparation .	52
Table 3.7	Energy Requirement and Operational Temperature Values for AF1 Adsorbent Production Processes . . . . .	59
Table 3.8	Given Parameters and Variables in the Literature for PAN Adsorbent	60
Table 3.9	The Amount of Chemicals Required for PAN-AO Adsorbent Pro- duction for All Normalization Cases . . . . .	62
Table 3.10	Energy Requirement and Operational Temperature Values for PAN- AO Adsorbent Production Processes . . . . .	65
Table 3.11	Pros and Cons of Uranium Elution Methods and Their Experimental Conditions . . . . .	67
Table 3.12	Vanadium Elution Methods Comparison . . . . .	69
Table 3.13	Chemical Used in Uranium and Vanadium Separation from Alkaline Media (Z. Zhu et al., 2013) . . . . .	70
Table 3.14	Summary of Chemical Amounts Required for Carbonate Elution and Vanadium and Uranium Separation for AF1 and PAN Adsorbents and both Normalization Cases . . . . .	71

Table 3.15 Disposal Methods of Waste Produced from Uranium Recovery from Brine Processes . . . . .	74
Table 3.16 Disposal Methodology for AF1 Adsorbent Case . . . . .	75
Table 3.17 Disposal Methodology for PAN Adsorbent Case . . . . .	76
Table 3.18 Input and Output Data for Uranium Recovery from Brine via AF1 and PAN-AO Adsorbents for Different Cycles (Ecoinvent) . . . . .	77
Table 3.19 All Energy Sources Results Comparison of AF1 Case with Conventional Mining Results . . . . .	82
Table 3.20 All Energy Sources Results Comparison of PAN Case with Conventional Mining Results . . . . .	83
Table 3.21 Name of the Most Affected Impact Categories based on the Energy Scenarios . . . . .	84
Table 3.22 Characterization Results of Uranium Recovery from Brine via Amidoximated Adsorbents and Conventional Uranium Extraction and Mining Methods (Ecoinvent) . . . . .	90
Table 3.23 Main Pollutants and Processes Released in All Uranium Extraction Methods in All Impact Categories . . . . .	91
Table 3.24 Sensitivity Results (%) of Uranium Recovery via AF1 adsorbent (Only Positive Perturbation Ratio) . . . . .	95
Table 3.25 Sensitivity Results (%) of Uranium Recovery via AF1 adsorbent (Only Negative Perturbation Ratio) . . . . .	96
Table 3.26 Sensitivity Results (%) of Uranium Recovery via PAN-AO adsorbent (Only Positive Perturbation Ratio) . . . . .	96
Table 3.27 Sensitivity Results (%) of Uranium Recovery via PAN-AO adsorbent (Only Negative Perturbation Ratio) . . . . .	96
Table 4.1 Desalination LCA Studies Performed in the last 10 years . . . . .	112
Table 4.1 Desalination LCA Studies Performed in the last 10 years continue.. .	113
Table 4.1 Desalination LCA Studies Performed in the last 10 years continue.. .	114
Table 4.2 The Main Contributors Affecting the LCA Results in Desalination Technologies based on the Previously Presented LCA Studies . . . . .	115
Table 4.3 Important Design Parameters of Solar-Driven MED LCA to Produce 1 m <sup>3</sup> Distillate . . . . .	120

Table 4.4 Electricity Sources of the Selected Countries in 2016 (Ecoinvent 3.6)	128
Table 4.5 The Characterization Results of Solar-Driven MED System Integrated with URFB via AF1 and PAN-AO Adsorbent (ReCiPe 2016 Midpoint)	134
Table A.1 Details of Inventory for Uranium Recovery via AF1 and PAN-AO Adsorbent Methods	172
Table A.1 Details of Inventory for Uranium Recovery via AF1 and PAN-AO Adsorbent Methods	173
Table A.2 Conversion Factors (%) for Amidoximated Adsorbent Production	174
Table A.3 The Inventory of Solar Driven MED Plant	175
Table A.4 CSP Technologies Comparison	178
Table A.4 CSP Technologies Comparison	179
Table A.4 CSP Technologies Comparison	180
Table B.1 The Characterization Results of Solar-Driven MED System Integrated with URFB via AF1 and PAN-AO Adsorbent with ILCD 2011 Midpoint+ Method	191
Table B.2 Main Pollutants and Relevant Processes Causing to Spread These Pollutants During 1 kg of U Production from RO Plant Combined With URFB System	192

## LIST OF FIGURES

### FIGURES

Figure 2.1	LCA Framework (Muralikrishna & Manickam, 2017) . . . . .	8
Figure 2.2	General Unit Process Flow Diagram (Muthu, 2014) . . . . .	10
Figure 2.3	Cotton Fibre Production Detailed Unit Process Flow Diagram (Muthu, 2014) . . . . .	11
Figure 2.4	Schema of the ILCD characterisation at Midpoint and Endpoint Level for Different Impact Categories and Areas of Protection (Guinee et al., 2011) . . . . .	14
Figure 2.5	The link between Interpretation Phase and Other Phases of LCA (Hauschild et al., 2018) . . . . .	15
Figure 2.6	Annual Number of LCA Publications Performed With Distinct LCA Software (Silva et al., 2019) . . . . .	16
Figure 2.7	Schematic view of (a) open-pit mining (Espinoza et al., 2013) (b) underground mining (Hamrin, 1980) . . . . .	19
Figure 2.8	The Flow Chart of Uranium Processing (Council et al., 2012) . .	21
Figure 2.9	Schematic view of In-situ Leaching (Hore-Lacy, 2016) . . . . .	22
Figure 2.10	Classification Major Desalination Technologies (Shatat & Rif- fat, 2014) . . . . .	26
Figure 2.11	MSF Process Flow Chart (Shatat & Riffat, 2014) . . . . .	27
Figure 2.12	MED Process Flow Chart (Shatat & Riffat, 2014) . . . . .	28
Figure 2.13	Vapor Compression Evaporation Flow Chart (Shatat & Riffat, 2014) . . . . .	29
Figure 2.14	Renewable Energy Driven Desalination Technologies Distribu- tion (Jijakli et al., 2012) . . . . .	34

Figure 3.1	System Boundaries for This Study Including Uranium Recovery from Desalination Plants Brine via (a) AF1 Adsorbent and (b) PAN-AO Adsorbent . . . . .	40
Figure 3.2	System Boundaries for Conventional Uranium Mining Methods .	41
Figure 3.3	Breakthrough Curve for Optimum Cycle of AF1 Adsorbent . . .	60
Figure 3.4	Breakthrough Curve for Optimum Cycle for PAN-AO Adsorbent	66
Figure 3.5	Process Steps and Chemicals and Energy Requirements of AF1 Adsorbent Production for Normalization 1 (a) & Normalization 2 (b) . .	72
Figure 3.6	Process Steps and Chemicals and Energy Requirements of PAN-AO Adsorbent Production for Normalization 1 (a) and Normalization 2 (b) . . . . .	73
Figure 3.7	Characterization Results of Uranium Recovery from brine via AF1 Adsorbent Method . . . . .	79
Figure 3.8	Characterization Results of Uranium Recovery from brine via PAN-AO Adsorbent Method . . . . .	80
Figure 3.9	Characterization Results of Uranium Recovery from brine via AF1 Adsorbent for Different Energy Sources . . . . .	85
Figure 3.10	Characterization Results of Uranium Recovery from brine via PAN-AO Adsorbent for Different Energy Sources . . . . .	86
Figure 3.11	Normalization Results from Comparison for Uranium Recovery via Amidoximated Adsorbents and Conventional Uranium Extraction and Mining Methods . . . . .	92
Figure 3.12	Comparative Single Score Results for All Uranium Mining Methods . . . . .	93
Figure 3.13	Comparative Single Score Results for Only Uranium Recovery with Adsorbent Methods . . . . .	94
Figure 3.14	Sensitivity Analysis Results of Uranium Extraction in (a) CC, (b) HTC, (c) FET, and (d) MFRRD Impact Categories for AF1 and PAN-AO Adsorbent Methods (* means negative perturbation ratio, and all results are given in absolute value.) . . . . .	97
Figure 3.15	Comparative Characterization Results of All Uranium Recovery Methods Under the Worst and Best Case Scenarios of Adsorbent Methods based on Hydroxylamine Consumption . . . . .	101

Figure 3.16	Comparative Characterization Results of AF1 and PAN-AO Adsorbents for Different Cycles or Reuse Numbers and Conventional Uranium Mining Methods . . . . .	103
Figure 3.17	Comparative Characterization Results of Adsorbent Calculated in Our Study and Compiled Conventional Mining Methods given in (Farjana et al., 2018) . . . . .	106
Figure 4.1	Overview of Systems Investigated in This Study . . . . .	118
Figure 4.2	The System Boundary of Solar-Driven MED Plant Investigated in This Study . . . . .	119
Figure 4.3	The System Schema of PTC+MED Plant (Adapted from the Study (Taylan, 2019)) . . . . .	121
Figure 4.4	Characterization Result of Solar Driven MED Plant . . . . .	124
Figure 4.5	Normalization Result of Solar Driven MED Plant . . . . .	125
Figure 4.6	Sensitivity Analysis Results in (a) GW, (b) FE, (c) ME, and (d) HTC Impact Categories for Solar-Driven MED Plant (* refer to negative perturbation ratio and all results are presented in absolute value.) . . . . .	129
Figure 4.7	Electricity Mix Impact on Results in GW, FE, ME, and HTC Impact Categories for Solar-Driven MED Plant . . . . .	130
Figure 4.8	Comparative Characterization Results of Solar-Driven MED Plant and Solar-Driven MED Plant Integrated with URFB Systems via AF1 and PAN-AO Adsorbents (ReCiPe 2016 Midpoint) . . . . .	133
Figure 4.9	Comparative Characterization Results of Base Case Solar-Driven MED Plant and Conventional RO Plant Combined with URFB Systems (ReCiPe 2016) . . . . .	137
Figure 4.10	Comparative Normalization Results of Base Case Solar-Driven MED and RO Plants Combined with URFB Systems (ReCiPe 2016) . . . . .	138
Figure 4.11	Characterization Results Comparison of Totally Solar Case Solar-Driven MED Plant Combined with URFB Systems and Conventional Reverse Osmosis Method Combined with URFB Systems (ReCiPe 2016)	139
Figure 4.12	Normalization Results Comparison of Totally Solar Case Solar-Driven MED Plant Combined with URFB Systems and Conventional Reverse Osmosis Method Combined with URFB Systems (ReCiPe 2016)	141

Figure A.1	MED Plant Chart Designed by PSA-CIEMAT . . . . .	181
Figure B.1	Characterization Results of Uranium Recovery from brine via (a) AF1 Adsorbent with EF 3.0 Method . . . . .	184
Figure B.2	Characterization Results of Uranium Recovery from brine via PAN-AO Adsorbent with EF 3.0 Method . . . . .	185
Figure B.3	Comparative Characterization Results of Uranium Recovery from Brine via Amidoximated Adsorbents and Conventional Uranium Ex- traction and Mining Methods with EF 3.0 Method . . . . .	186
Figure B.4	Comparative Normalization Results of Uranium Recovery from Brine via Amidoximated Adsorbents and Conventional Uranium Ex- traction and Mining Methods with EF 3.0 Method . . . . .	187
Figure B.5	Comparative Characterization Results of URFB Systems with Distinct Combined Energy Sources with ILCD 2011 Midpoint+ Method (AF1 Adsorbent) . . . . .	188
Figure B.6	Comparative Characterization Results of URFB Systems with Distinct Combined Energy Sources with ILCD 2011 Midpoint+ Method (PAN-AO Adsorbent) . . . . .	189
Figure B.7	Comparative Characterization Results of MED Plant Driven by PTC and Flat Plate Collectors with ReCiPe 2016 Midpoint Method . . .	190
Figure B.8	Comparative Characterization Results of Totally Solar Case and Conventional RO Plants Case Combined With URFB Systems with ReCiPe 2016 Midpoint+ . . . . .	193

## LIST OF ABBREVIATIONS

ACD	Acidification
AF1	Specific Kind of Adsorbent prepared by Oak Ridge National Laboratory
AN	Acrylonitrile
CC	Climate Change
CSP	Concentrated Solar Power
DMSO	Dimethyl Sulfoxide
FET	Freshwater Ecotoxicity
FEU	Freshwater Eutrophication
FPMF	Fine Particulate Matter Formation
FRS	Fossil Resource Scarcity
GHG	Greenhouse Gas
GW	Global Warming
HTC	Human Toxicity, Cancer Effects
HTNC	Human Toxicity, Non-cancer Effects
HW	Hazardous Waste
ITA	Itaconic Acid
IRE	Ionizing Radiation E (Interim)
IRHH	Ionizing Radiation Human Health
LCA	Life Cycle Assessment
LCIA	Life Cycle Impact Assessment
LU	Land Use
MED	Multi Effect Distillation
MEU	Marine Eutrophication
MFRRD	Mineral, Fossil & Renewable Resource Depletion
MRS	Mineral Resource Scarcity
MSF	Multistage Flash Distillation
OD	Ozone Depletion

OFHH	Ozone Formation Human Health
OFTE	Ozone Formation Terrestrial Ecosystems
PAN-AO	Polyacrylonitrile Amidoximated Adsorbent
PTC	Parabolic Trough Collector
PCO	Photochemical Ozone Formation
PM	Particulate Matter
PV	Photovoltaic
RO	Reverse Osmosis
SDG	Sustainable Development Goal
SHIP	Solar Heat for Industrial Processes
SOD	Stratospheric Ozone Depletion
TA	Terrestrial Acidification
TEU	Terrestrial Eutrophication
URFB	Uranium Recovery from Brine
WC	Water Consumption
WRD	Water Resource Depletion

# CHAPTER 1

## INTRODUCTION

### 1.1 General Background

Population growth culminates in rising energy and clean water demand problems throughout the world. According to the United Nations prediction, the world population will increase nearly 20% by 2050 (Leridon, 2020). It is also predicted that by 2050 the world energy consumption will have risen by nearly 50% (Zhongming et al., 2019). Therefore, the role of nuclear energy will gain huge importance in the energy sector between the years 2015 and 2030 (Tsouris, 2017). Although there is a debate about nuclear energy posing a danger to the health of society, it is the safest energy production technology based on the statistics of annual mortality rates occurring in non-OECD, OECD, and another 15 European countries per one gigawatt (Brook et al., 2014). Moreover, nuclear energy is a reliable and environmentally friendly energy generation method because it can provide continuous electricity supply on a large scale and it leads to the minimum carbon dioxide emissions among all energy sources. Furthermore, nuclear energy is an economically viable energy production method since it has low sensitivity to fuel costs and electricity generation cost is also low, so nuclear energy is a strong competitor in the energy sector (Karakosta et al., 2013). The other prognosis which was made by The United Nations World Water Development Report 2018 specifies that nearly 60% of the total population will suffer from clean water scarcity by 2050 (Water, 2018). Therefore, developing systems that can supply energy and water demands becomes compulsory for the sake of humanity.

Uranium is a metal mainly found in terrestrial ores but its reserve is 1000 times higher in seawater (Bardi, 2010). While uranium can be extracted from deposits in the land by open-pit, in-situ leaching, and underground (Farjana et al., 2018), ocean mining

has gained prominence with a concept introduced in literature nearly 50 years ago (Tang et al., 2020). The main issue with uranium extraction is its low concentration in the ocean (3.3 ppb), hence developing a new method for uranium separation from seawater has become crucially important (Tang et al., 2020). One solution to the low concentration of uranium in the ocean is to combine its recovery with already present technologies to concentrate it. Desalination is a method that is used to obtain drinking water from the seawater, producing brine as a waste. Major desalination processes can be separated into two classes named thermal and membrane desalination (Shatat & Riffat, 2014). There is a fact that thermal desalination technologies have advantages in terms of operation simplicity, higher permeate quality, and ability to deal with more saline water (Fritzmann et al., 2007a), so there has been an increasing trend towards global thermal desalination installed capacity in time (Curto et al., 2021). Although water is treated by using different principles in both categories, produced brine composition can be similar to each other (Fard et al., 2015) (Ahmad et al., 2019) (Wiechert et al., 2018).

Uranium concentration in the brine of reverse osmosis desalination plants can be nearly two times higher than the seawater uranium content with fewer impurities depending on the desalination processes (Wiechert et al., 2018) (Wongsawaeng et al., 2021). The most common metals being recovered from brine are lithium, magnesium, and vanadium with different extraction steps (X. Zhao et al., 2020) (Ruan et al., 2021). That is, every element has its extraction methods, so they should be investigated comprehensively and separately for their industrial applicability. However, in this study uranium has been chosen as the desired element among other ions found in seawater because it can meet all demands presented above. Moreover, brine as waste from desalination plants is highly saline and has a high temperature, so it has substantial adverse impacts on the environment and especially on marine life. Although various brine management methods are available in the market (Giwa et al., 2017), it is generally discharged directly into the water bodies without applying any treatment (Morillo et al., 2014). One way to reuse brine is via metal recovery. Thanks to the metal recovery from desalination plants reject, brine commonly classified as waste can be converted into the main source for another system and this brings up the concept of sustainability in this study. Adsorption, coagulation and co-precipitation,

membrane filtration, and solvent extraction are the alternative methods of uranium recovery from brine (URFB) or seawater (J. Kim et al., 2013) (Yun, 1982). However, adsorption is the most appropriate method among other alternatives depending on mainly higher efficiency (J. Kim et al., 2013) (Tang et al., 2020). Up to date, various adsorbents materials were analyzed for uranium extraction, but the most promising adsorbent types are reported as amidoximated polymers (Kuo et al., 2016) (Pan et al., 2015) (Tamada, 2010).

## **1.2 Problem Statement**

In the literature, most reports have focused on the performance of amidoximated adsorbents under different conditions for the URFB system in the laboratory conditions (Ladshaw et al., 2017) (Na et al., 2012) (Pan et al., 2020) (Wongsawaeng et al., 2021). Obtaining uranium from brine was considered before (Wiechert et al., 2018) (Wongsawaeng et al., 2021), however, the studies were only conducted in the laboratory and no industrial level evaluation was performed. (Chouyyok et al., 2016) claims that this recovery method can be more environmentally benign as compared to the other conventional uranium stripping methods. Likewise, (B. Parker et al., 2018) specifies that oceanic uranium extraction processes lead to fewer environmental problems than terrestrial methods. However, there is no industrial evaluation such as life cycle assessment (LCA) studies of this system or any numerical results that confirm these ideas and provide a comparative analysis for the commercial viability of this technology.

The environmental impact of most manufacturing systems is considered after system industrialization, but preliminary LCA studies must be examined before the URFB process. LCA helps to evaluate the environmental impacts of manufacturing technologies on diverse categories like climate change, ozone depletion, and human toxicity with distinct approaches such as the cradle-to-grave or cradle-to-cradle (Krishna et al., 2017) (Zuckerandl & Pauling, 1965). Because the URFB system offers an alternative way to produce uranium for a society whose energy needs will increase in the future, a detailed investigation of this area must be conducted with a life cycle perspective to avoid potential environmental problems. Moreover, brine management is not included in most desalination plants' life cycle assessment studies (Mannan et al.,

2019) (Zhou et al., 2011) (Alhaj et al., 2022) so that their real environmental impact cannot be detected clearly. In the studies covering the brine disposal step, the real value of brine in the metal recovery field has not been evaluated with LCA analysis (Abdul Ghani et al., 2020).

### **1.3 Significance of the Study**

This study has the potential to prove the real or quantitative environmental impact of uranium extraction from seawater via amidoximated adsorbent. From this aspect, it is the first study conducted in this field. Then, the results can be compared with the conventional uranium extraction and mining methods and decided whether it is an alternative and environmentally friendly uranium production method or not. On the other hand, this study can help the optimization process of this system by evaluating the results. To illustrate, before the system industrializes, the chemicals that have a high environmental load can be decided and replaced with the other ones which have a comparatively lower environmental impact, so a problem can be prevented before it occurs. Also, this study will help to understand the environmental impact of desalination plants integrated with uranium recovery technologies to detect the potential of this method in the desalination field.

### **1.4 Objective of the Thesis**

This study aims to evaluate the life cycle assessment (LCA) of uranium production from brine, compare it with readily available techniques and evaluate the sustainable techniques to indicate whether this is an alternative method to obtain uranium as a possibility. Also, evaluating the environmental impact of desalination plants combined with uranium extraction technologies via amidoximated adsorbents is the other objective of this thesis.

### **1.5 Structure of the Thesis**

This thesis consists of five chapters. In the Chapter 1, brief information about the background of the study is provided and the problem statement, significance, and objective of the thesis are clarified. Chapter 2 includes information about the LCA

structure. It also reviews the conventional and alternative uranium extraction methods from different media and uranium milling stages, as well as the desalination technologies. Chapter 3 elaborates on the LCA study about the environmental impact of URFB via adsorbent technologies and these results are compared with the conventional extraction techniques. This chapter discusses the results of different scenarios related to the main energy of the system and adsorbent recycling. Chapter 4 focuses on the comparative environmental analysis of desalination plants and URFB integrated desalination plants. Finally, a summary of all results and major findings of this thesis along with future suggestions are presented in Chapter 5.



## **CHAPTER 2**

### **LITERATURE REVIEW**

In this chapter, the section 2.1 will provide an information about LCA. The part 2.2 will explain the uranium extraction methods detail. In the section 2.2.1, the background information about the conventional uranium mining from ore deposits will be discussed and the alternative methods for uranium recovery from aqueous media will be clarified in the section 2.2.2. The part 2.3 will provide an information about desalination technologies. After thermal desalination methods will be explained detail in the section 2.3.1, membrane technologies in desalination field will be discussed in the section 2.3.2. Finally, alternative and renewable-energy-driven desalination technologies will be clarified in the sections 2.3.3 and 2.3.4, respectively.

#### **2.1 Life Cycle Assessment**

LCA is a method for assessing the potential environmental impact of a product or service over its life cycle. Although the history of this method dates back to the 1960s, consistency was not achieved in the applied methods for nearly 30 years, so the international organization for standardization (ISO) 14040 series of standards concerning the methodology of LCA was developed to harmonize the evolving methods in 1997. This set of standards on LCA covers four standards named ISO 14040 (the principles and framework), ISO 14041 (the goal and scope definition), ISO 14042 (the life cycle impact assessment), and ISO 14043 (the life cycle interpretation). Details of these standards will be discussed in the following parts, but the relationship between these phases is shown in Figure 2.1.

Various impact assessment methods that aim to quantify all necessary environmental loads and prevent burden-shifting were developed during the 1990s. The CML92

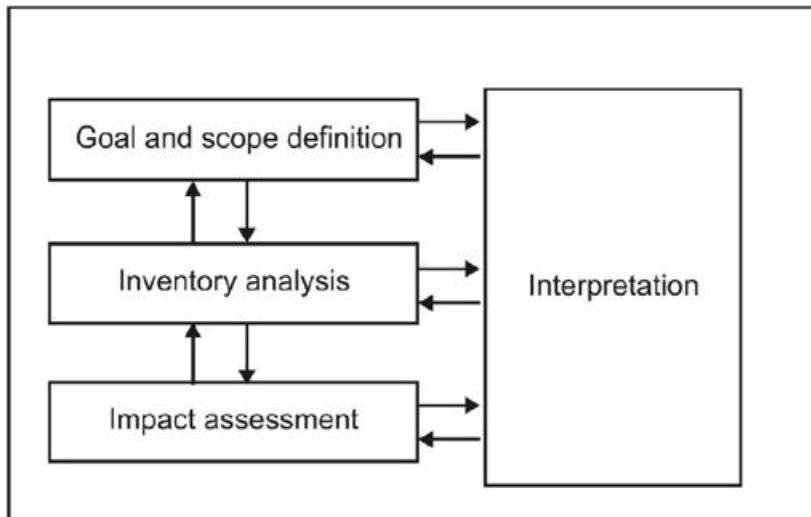


Figure 2.1: LCA Framework (Muralikrishna & Manickam, 2017)

which includes extensive series of midpoint impact categories was the first impact assessment methodology. Then, other methodologies such as Eco-indicator 99 which is a more science-based approach were released. The database used in life cycle inventory (LCI) was developed during these years, but there were differences in data quality and standards, so the first Ecoinvent database was improved to achieve consistency between them in 2003. Then, different approaches called attributional and consequential were applied in LCI and the main difference between them is related to the perception of the LCA and product life cycle and its potential implementation (Guinee et al., 2011). In the former perspective, the fundamental aim is to estimate the share of the global environmental burdens of the processes and material flows used in the product life cycle. Assessing the environmental impact of the production and use of a product on the global environmental burdens as a result of the possible decision is the main logic behind the latter approach (Ekvall, 2019). That is, while attributional LCA is convenient for the studies about accounting of the consumption-based emissions, consequential LCA is preferred in the applications related to informing policy-makers or clients on total emission change under different policy decisions or purchasing (Brander et al., 2008).

The application area of LCA is very comprehensive. It can be used in decision-making in the area of product design, strategic planning, efficient operation, and con-

sumption of resources by monitoring the most environmentally friendly process or products and product development. Moreover, LCA can be applied in the marketing field with the aspect of business communication by declaring the environmental products or practices. For example, eco-labeling can be one example of this communication application in the marketing area (Hauschild et al., 2018).

### **2.1.1 Goal and Scope Definition**

The first step of an LCA or goal and scope definition must be clearly defined in all applications. In the goal definition, the background of the decision and objectives of the study should be outlined. Moreover, the system, target audience, time, and resources should be identified in this step. In the scope definition, the functional unit of the system which is a quantified characterization of the system product's performance should be defined. Furthermore, the basic process flow map that is represented as an example in Figure 2.2 and the system boundary should be selected for the particular study. Variants of LCA can be formed depending on the system boundaries. To illustrate, cradle-to-grave is a kind of LCA that covers all phases from use to disposal of a product system. In the cradle-to-gate analysis, the resource extraction phase is the only included step, and use and disposal phases are neglected in these LCA studies (Guinee et al., 2011).

### **2.1.2 Inventory Analysis**

In the life cycle inventory analysis step, all inputs and outputs of a product over its life cycle are compiled and quantified. This is the most time-consuming step for most LCA studies. Firstly, a detailed process flow diagram example that is shown in Figure 2.3 is formed by showing each subsystem to depict their contributions clearly. Then, the quantitative and qualitative data are included for all unit processes within the system boundaries. The type of data can be changed depending on its collection method. For example, the data collected at the production site is called primary data, but if the data is obtained or estimated from the literature or published references, the term secondary data is used.

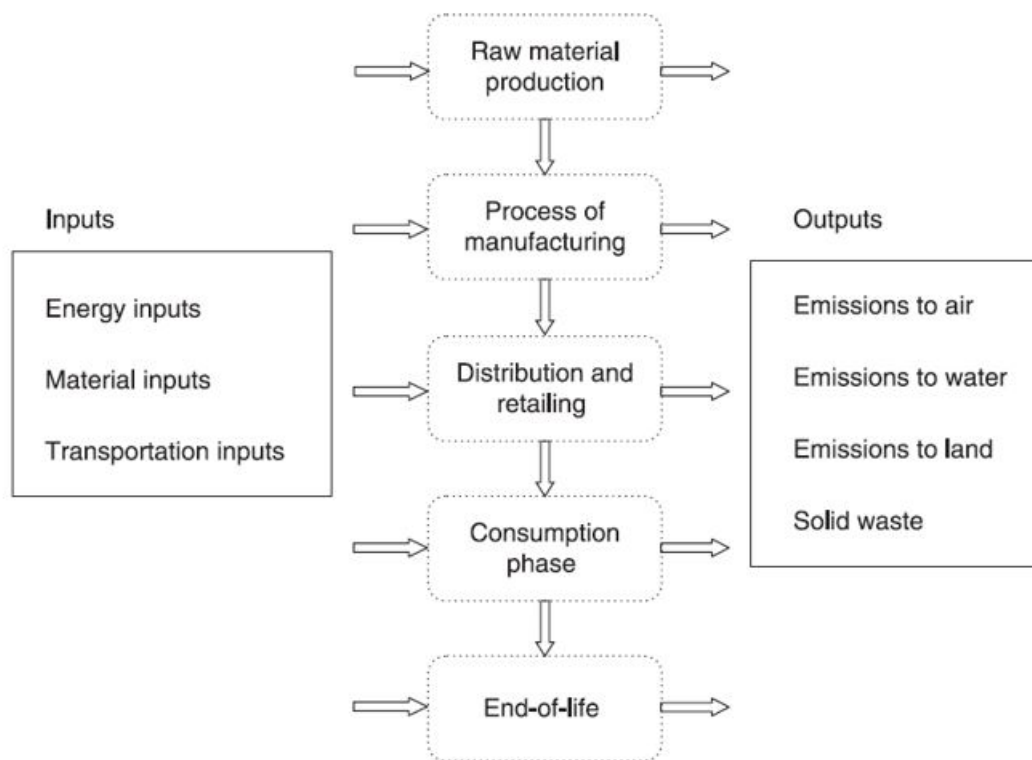


Figure 2.2: General Unit Process Flow Diagram (Muthu, 2014)

Moreover, various data quality indicators such as time-related coverage, completeness, and representatives are found to assess the quality of data. After all data is collected, it is normalized based on the functional unit of the system and all environmental loads are distributed within a given unit process all over its different products depending on the scope of the study. As a final step of inventory analysis, inventory results covering significant items such as air emissions and energy consumption are reported (Guinee et al., 2011).

### 2.1.3 Impact Assessment

The main goal of the third phase of LCA is to evaluate the potential environmental and human health impacts of the unit processes or systems defined in the LCI and convert them into specific impact categories. The unit processes that contribute the highest environmental impact and the most critical potential impacts can be identified with this step. Also, the relative environmental impacts of each system can be

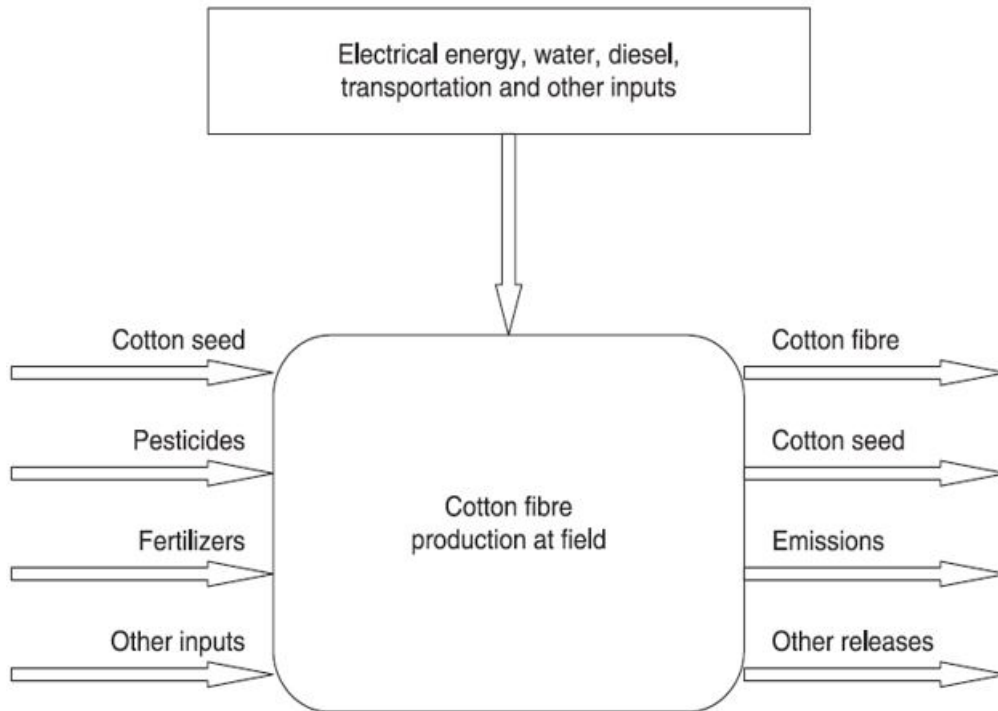


Figure 2.3: Cotton Fibre Production Detailed Unit Process Flow Diagram (Muthu, 2014)

compared. The life cycle impact assessment (LCIA) covers three mandatory steps explained below (Guinee et al., 2011).

**\*Selection of Impact Categories, Category Indicators, and Characterisation Model:**

The main target of this step is to find the most useful items for a specified goal and scope of the study. Therefore, selected categories differ from study to study. Global warming, ozone depletion, and acidification are examples of these impact categories (Mu et al., 2020).

**\*Classification:** LCI results are assigned to particular impact categories based on their potential effects in this step (Mu et al., 2020). To illustrate, carbon dioxide is emitted from fossil fuels based on LCI results. In this step, this pollutant is assigned to related impact categories such as climate change.

**\*Characterization:** LCI results are converted and combined into representative impact indicators by using characterization factors. That is, the potential category indi-

cators are estimated in the characterization step, so a direct comparison of LCI results within all impact categories can be applied (Mu et al., 2020). To characterize impact indicators following equation is applied ((SAIC) & Curran, 2006):

$$ImpactIndicators = InventoryData * CharacterizationFactor \quad (2.1)$$

These characterization factors are provided by models. For example, the global warming potential factor for chloroform is defined as 9 by Intergovernmental Panel on Climate Change (IPCC) Model ((SAIC) & Curran, 2006).

Apart from these three compulsory phases of LCIA, it has also optional components listed below.

**\*Normalisation:** This tool is used to compare impact indicator data among impact categories by dividing indicator results by a selected normal or reference value. To select a normal value, various methods can be applied ((SAIC) & Curran, 2006):

- \* The baseline
- \* The highest result among all alternatives
- \* Global, regional, or local geographical zone
- \* Resident of a geographical zone

The important point in the normalization phase is that the comparison of normalized data within different impact categories is not possible. That is, this data can only be compared within the same impact category. To illustrate, the impacts of global warming cannot be compared directly with the effects of ozone depletion because of the application of different characterization factor calculations for these two impact categories ((SAIC) & Curran, 2006).

**\*Grouping:** Impact category indicators are sorted by considering properties such as location and emission type (eg. air and water) or ranked by considering their priorities in this optional component of LCIA (Guinee et al., 2011).

**\*Weighthing:** Relative values or weights are assigned to the distinct impact cate-

gories considering their importance in the weighting phase of LCIA. Moreover, it is focused on the most important potential impact. Since the most important impact category depends on the goal and scope of the study or stakeholders' perspective and in some cases their value judgment may differ with time or location, there is no scientific basis for the weighting step. Therefore, it is crucial to clarify the weighting methodology clearly (Guinee et al., 2011).

The last step in LCIA is to evaluate and document the LCIA results to provide a better understanding of the results with a reliable way (Guinee et al., 2011).

Various LCIA methods have been released in the literature since 1984. For example, TRACI, ILCD, ReCiPe, CML, and IMPACT 2002+ are the most well-known LCIA methods. All LCIA methods vary in different aspects such as selected impact categories, time horizon, characterization factors, and evaluation methods, but the difference between midpoint and endpoint approaches is one of the most important distinctions between them. In the midpoint method, a group of substances that can contribute to the same environmental impact is gathered and classified to assess the potential impacts of the system in more detail. To illustrate, the substances that may have a carcinogenic impact on humans can be classified as toxic carcinogens in the same category and their contributions to this impact category are estimated via characterisation. Moreover, the earlier or short-term environmental impact in any cause-effect chain can be analyzed in this method. On the other hand, midpoint indicators are expanded or linked by extra modeling elements that represent areas of protection related to human health, ecosystem, and natural resources in the endpoint approach, so the long-term environmental impacts of the cause-effect chain can be evaluated (Guinee et al., 2011). The link between midpoint and endpoint methods is represented in Figure 2.4. During the selection of the LCIA methodology, the system requirements, internal and external factors, and limitations of the study should be considered. Any recommendations about which LCIA methodology should be used are provided in the ISO 14040 series of standards. However, the particular recommendations for midpoint and endpoint impact categories were given by the European Commission (Guinee et al., 2011).

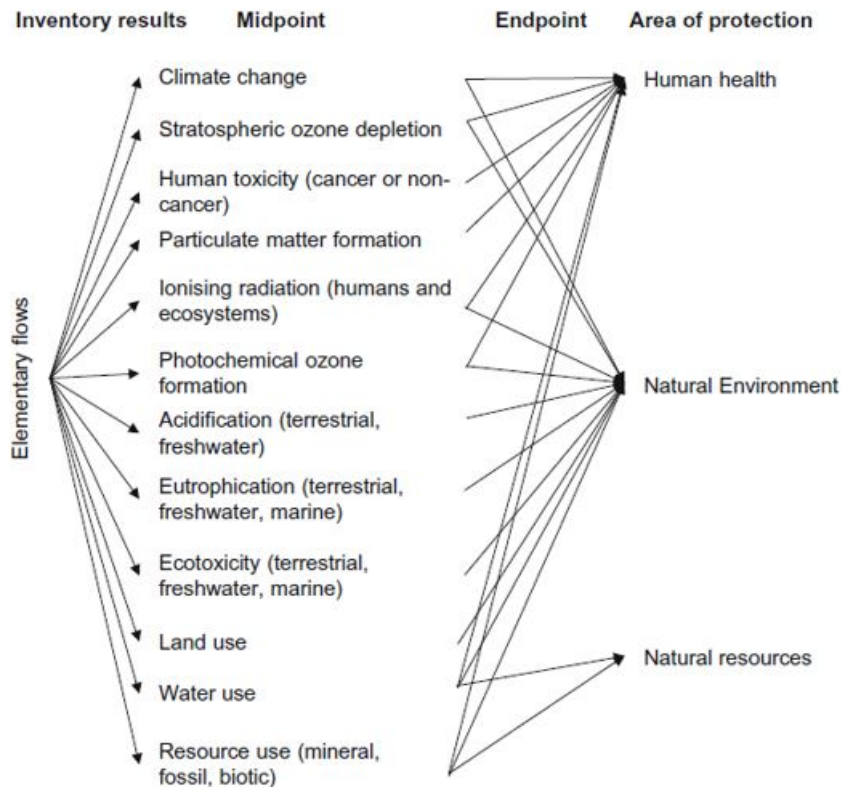


Figure 2.4: Schema of the ILCD characterisation at Midpoint and Endpoint Level for Different Impact Categories and Areas of Protection (Guinee et al., 2011)

### 2.1.4 Interpretation

Life cycle interpretation which is the last phase of LCA is a method used for the description of significant arguments and assessing the data completeness, sensitivity, and consistency at the end of the study. Also, after formulating conclusions and recommendations, all results are reported in the most objective way (Hauschild et al., 2018). All interpretation phases along with the other stages of LCA are presented in Figure 2.5.

In the first step of interpretation, the data that has the greatest influence on impact results are identified because this result is used in the second phase of interpretation to evaluate the completeness, sensitivity, and consistency of the LCA study. Before identifying the component or part that contributes to the results most, preceding steps should be reanalyzed extensively. Then, the second step of interpretation is initiated to

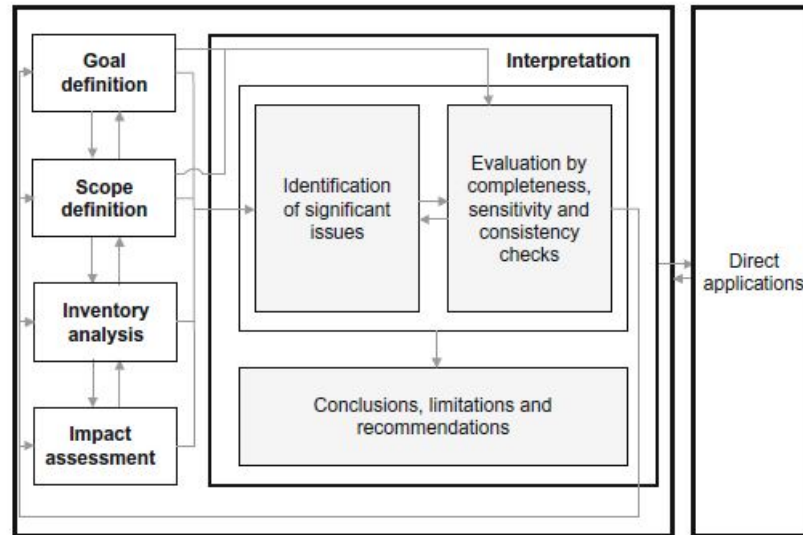


Figure 2.5: The link between Interpretation Phase and Other Phases of LCA (Hauschild et al., 2018)

establish the reliance of the study outcomes. In the completeness check which is one of the tasks performed during the second phase, it is ensured that all data required for the study is completed by developing a checklist. Then, a sensitivity check is applied to learn whether the uncertainty of significant arguments or issues described clearly in the previous step influences the policy maker’s capability of comparative deduction. Moreover, the parameters are changed deliberately in this analysis and the robustness of the results corresponding to these variations are determined. After it is investigated whether the applied methods, assumptions, and data are consistent with the goal and scope of the study, the second step of interpretation is completed. Finally, the results of LCIA are interpreted to select the option that has the overall least effect on the environment and human health and/or the other areas of concern identified in the goal and scope of the study and they are reported in an organized manner ((SAIC) & Curran, 2006).

### 2.1.5 Software and Database

Since the number of inventory data, impact assessment methods, and modeling studies covering complicated product systems has been increasing, the need for software that can handle this complexity has arisen. Thanks to the software, the product sys-

tems or inventory can be modeled easily and LCIA results for all the impact categories can be estimated by performing the impact assessment. Furthermore, uncertainty and sensitivity analyses can be run with this software within a short time by using the uncertainty information given in the LCI databases. SimaPro, GaBi, OpenLCA, and Umberto are the most prevalent software used in LCA studies. They differ from each other with regard to some aspects such as the method of system expansion. SimaPro is one of the professional tools which enables us to collect, analyze and observe the product or service sustainability performance (Hauschild et al., 2018). Although GaBi was the first commercial LCA software, according to the Web of Science database, the annual number of LCA publications performed with SimaPro software was the highest one as compared to the GaBi, OpenLCA, and Umberto between the years 2001 and 2018 (Silva et al., 2019). The result of this study is presented in Figure 2.6.

After the logic and structure of LCA are discussed in detail, information about conventional uranium mining methods will be given in the following part since the environmental impact results of this study will be compared with conventional uranium mining methods results.

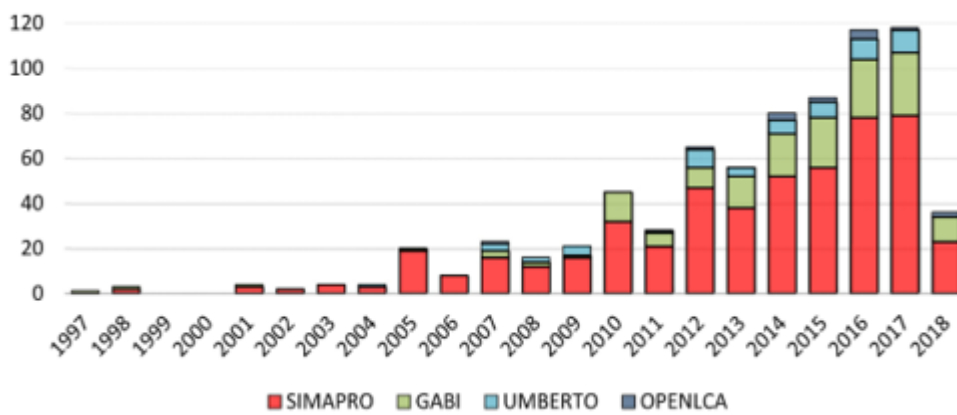


Figure 2.6: Annual Number of LCA Publications Performed With Distinct LCA Software (Silva et al., 2019)

## **2.2 Conventional Uranium Extraction Methods**

Uranium is a radioactive chemical element that has an atomic number of 92. Moreover, the radioactive isotopes of uranium that occurs naturally are  $^{234}\text{U}$ ,  $^{235}\text{U}$  and  $^{238}\text{U}$ . It is also a typical element found in the crust of Earth. Australia, Canada, the Russian Federation, and Kazakhstan are the main uranium producers in the world. However, its concentrations of it are low in most parts of the world. To illustrate, while it is 3 ppm on average in the upper part of the crust, its concentration of it in the overall crust is equal to 1.7 ppm. However, in the ore bodies, their concentrations are higher and they are classified based on concentration values. For example, while very low-grade uranium ore that is found in Namibia includes 0.01% or 100 ppm of uranium, very high-grade ore that is located in Canada involves 20% of uranium (Hore-Lacy, 2016).

In most nuclear reactors, 500 GJ which is nearly 20000 times higher than the case of 1 kg black coal consumption energy can be produced by using only 1 kg uranium (Hore-Lacy, 2016) and the annual uranium requirement for a nuclear reactor with a capacity of 50 GWe is 10000 tonnes (Macfarlane & Miller, 2007). This exclusive energy density of uranium was exploited in the 1930s. Although it was initially used for military purposes, the effort to produce energy with nuclear reactions has also been the main purpose of this technology. The pioneer of today's nuclear reactors was operated in Idaho in 1951 and the topic of controlled, safe, economic and durable nuclear plants has been studied since then (Hore-Lacy, 2016). Although the safety, economic and environmental management in nuclear power plants is crucial, the extraction of raw materials used in these plants is also important to ensure the sustainability of nuclear energy technology (Hore-Lacy, 2016). Open-pit, underground and in-situ leaching are the three common uranium mining methods applied all over the world, and details of them will be discussed in the following parts.

### **2.2.1 Open-Pit Mining**

It is one of the mining techniques used to extract the ore found at or near the surface of ground (Piro & Lipkina, 2020). The position of ore in this technique is especially crucial since ore can be reached by removing the overburden or waste rocks and if

it is in a very deep part of the soil, it may not make sense to use this method. In this method, ramps are constructed at a particular width and slope that is sufficient for access to mining equipment. During the design of walls, geotechnical properties of the soil, rock or sediment has to be considered. Moreover, groundwater inflow and the possibility of flood have to be checked and necessary precautions have to be taken in considering these circumstances. It can be generalized that steeper pits are more economically viable. However, there is a possibility of wall failure that has to be taken into consideration. Also, the open-pit mining field can be kilometers wide and hundreds of meters deep depending on the grade and the amount of deposit. To determine the suitable mining method used in open-pit mining, rock characteristics have to be well defined. To illustrate, if the rocks are friable, they can be removed via scraper technology. However, drilling and blasting which are the most common methods in open-pit mining are applied for the rocks that have higher strength (Hore-Lacy, 2016).

### **2.2.2 Underground Mining**

In this method, the ores found below the underground surface are extracted. The attempt of underground mining that produces a significant amount of byproduct has started with mechanized mining. There are main indispensable constituents in this mining field. Firstly, shafts that are generally a few meters in width or diameter are called vertical openings. Their depth can reach a thousand meters depending on the situation and concrete is generally used to line shafts. Secondly, horizontal openings are called adits that are similar to horizontal and vertical dimensions to shafts. Also, they can be used for the transportation of miners and ore materials via railway or wheeled vehicles. If there is a potential to collapse in the mining field, concrete, steel, or timber lining may be necessary together with the shafts. Thirdly, declines that have a spiral form are named inclined ramps and they provide vehicular access to the ore material. The maximum slope value is typically 15% for this component and the width of it has to be wide enough for a vehicle that has the largest dimensions. Also, 2-way vehicle traffic can be made possible at distinct intervals via passing spaces and lining can be applied depending on the stability of rock (Gertsch & Bullock, 1998). In the design of this mining, the location of the ore, physical resistance of rocks, ground surface topography, and road access conditions have to be considered. Also,

ventilation is a crucial factor that has to be taken into account, especially in uranium underground mines since the radioactive decay products of uranium such as radon can be found in dust. The four mining methods are applied to extract ore from underground mining fields depending on the ore characteristics and geometry. While the narrow vein mining method is used for small underground mines, the stoping technique is applicable for the larger uranium mining field that includes a larger ore mass. Moreover, the room and pillar method is applied for the orebody that is found relatively extensive and horizontal position. The last method called raise bore is suitable for Canada where high-grade uranium ore is located (Hore-Lacy, 2016). The visual representation of open-pit and underground mining is shown in Figure 2.7.

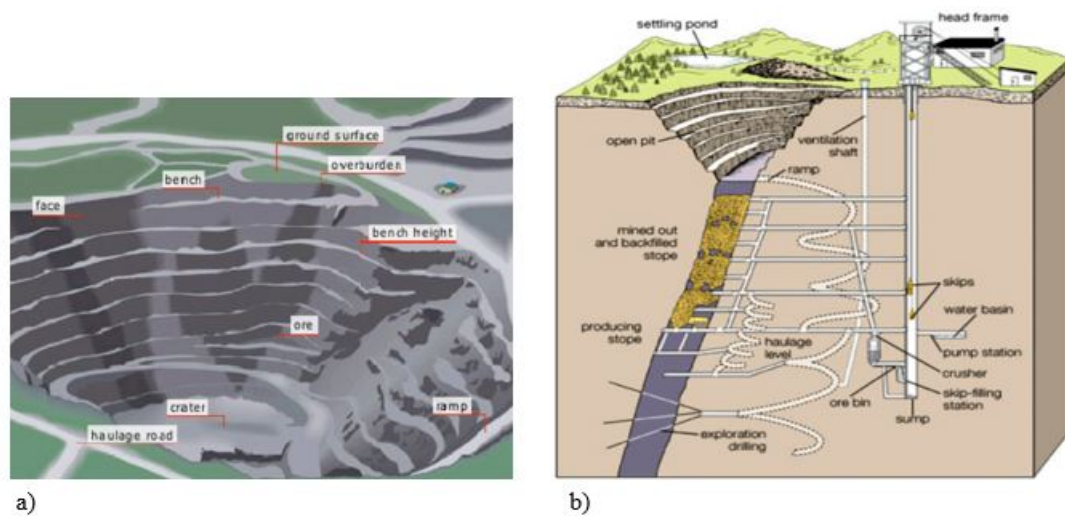


Figure 2.7: Schematic view of (a) open-pit mining (Espinoza et al., 2013) (b) underground mining (Hamrin, 1980)

### 2.2.3 Uranium Milling and Extraction

After the ore is excavated, milling is applied to generate concentrated uranium ore. It includes chemical and physical processes and six essential steps discussed below are generally applied to extract uranium from ore and concentrate it (L. K. Kim, 2018).

**\*Ore Preparation:** After coarse uranium ore is analyzed to evaluate the moisture and uranium content, it is blended to supply constant input to the mill. Then, ore with a suitable size for the following step is produced by a set of crushing and grinding steps with water addition (L. K. Kim, 2018).

**\*Uranium Extraction:** Lixivants and oxidants are used to extract uranium from ore by a set of air or mechanical mixing in a container, so concentrated leach slurry can be produced. Acid leaching with sulfuric acid is the most common method because sulfuric acid is economically favorable on an industrial scale. However, alkaline leaching is more favorable for carbonate ores. Moreover, sodium chlorate and hydrogen peroxide are commonly utilized as an oxidant (Hore-Lacy, 2016).

**\*Solid Liquid Separation:** Counter current decantation, filtration, and slime-sand separation machinery are used to separate the solution including uranium from ore residues, so a purified leach solution is obtained. In general, the following solvent extraction is needed to clarify the solution. Moreover, solid settling can be promoted by using flocculants (L. K. Kim, 2018).

**\*Purification:** Solvent extraction and ion exchange processes are used to remove impurities from the uranium-containing solution. These methods can be applied on a large scale. In solvent extraction, a set of mixer-settlers are utilized to increase the reaction surface between leach solutions and organic solvent together with modifiers or diluents, so amine salts formation is reduced and organic separation from aqueous media is enhanced. Then, the stripping of uranium from the organic phase to the aqueous one is applied. The Amex process that covers amine isodecanol kerosene usage in the extraction step followed by stripping via ammonium sulfate is the most prevalent method to produce uranium sulfate. In the other method which is ion exchange, resins are used to adsorb uranyl anions from purified solutions. The adsorption, elution, and regeneration of resin are the most common steps of this method. The competing ions with uranyl anions are separated from the resin in the regeneration step (L. K. Kim, 2018).

**\*Precipitation:** Uranium is precipitated from solution using different chemicals depending on the type of solution. The cost, environmental impact, feed solution purity, and the ultimate goal issues should be considered to choosing precipitating chemicals. To illustrate, if the stripping solution is acidic, ammonia is the most common chemical to generate ammonium diuranate. On the other hand, sodium hydroxide is utilized to produce sodium diuranate from alkaline stripping solution (*Uranium Extraction Technology*, 1993).

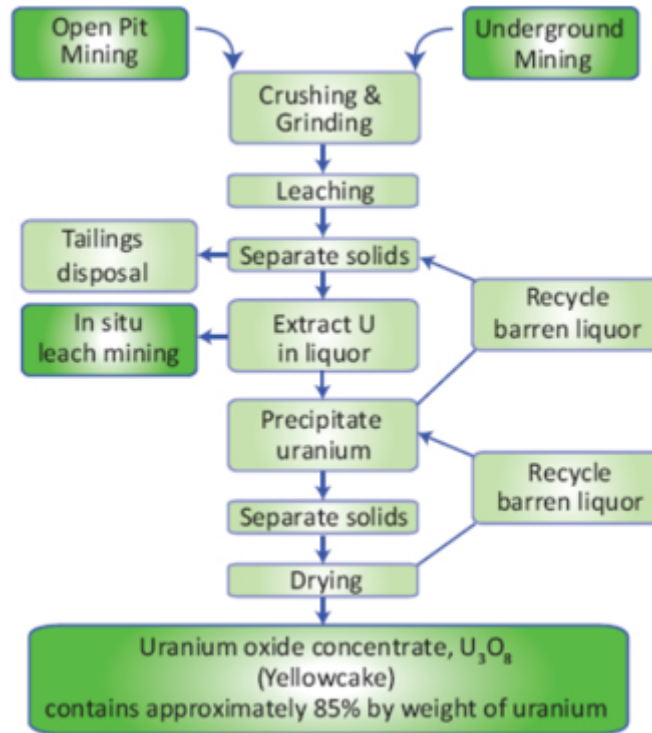


Figure 2.8: The Flow Chart of Uranium Processing (Council et al., 2012)

**\*Drying and Calcination:** After washing is applied to uranium concentrate, the wet product is dried to remove moisture and volatile chemicals via a set of equipment such as thickeners, spray driers, and centrifuges. Then, calcination is achieved by heating dried uranium concentrate at up to 700-800 °C depending on the type of final uranium product (*Uranium Extraction Technology*, 1993).

The flow diagram of uranium processing is shown in Figure 2.8.

#### 2.2.4 In-situ Leaching

In this technique, host rock leaves in place while uranium is recovered by injecting a solution called lixiviant into the ore field. This solution helps to dissolve uranium found in the host rock. Then, the uranium enriched solution is drawn by a pump and sent to the processing plant where uranium recovery is achieved via a series of methods called ion exchange, chemical treatment, and drying. This process is repeated until the desired amount of uranium is extracted. The detailed visual representation of in-situ leaching is shown in Figure 2.9. Hydrodynamic control with sufficient

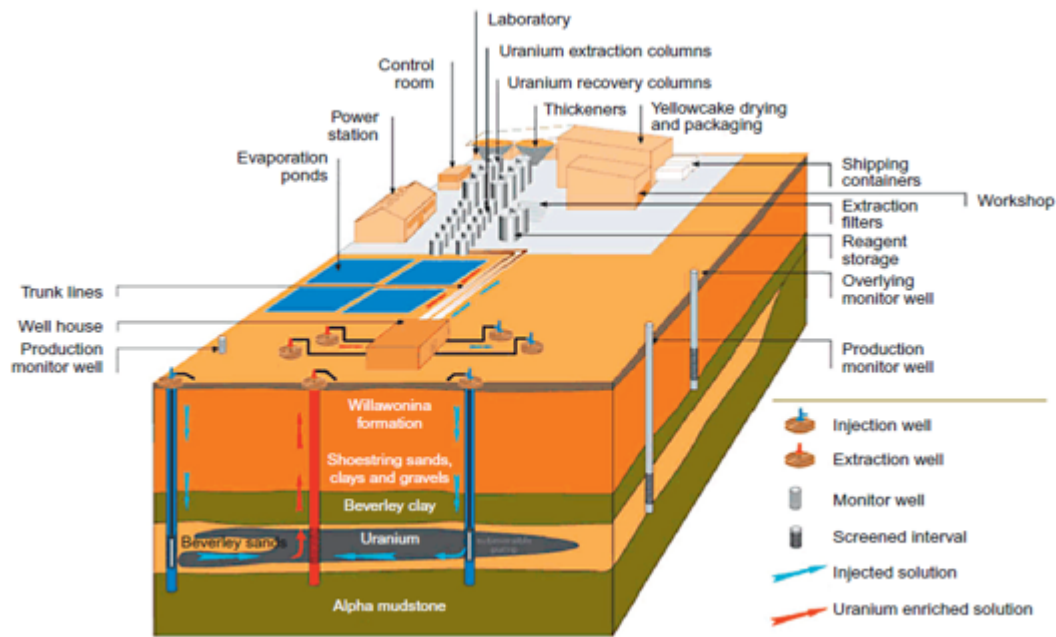


Figure 2.9: Schematic view of In-situ Leaching (Hore-Lacy, 2016)

groundwater and transmissivity, proper contact of uranium mineral with the lixiviant, and solubility of lixiviant are crucial concepts in the in-situ leaching method. Also, an alkaline or an acidic leaching solution or lixiviant can be used for a particular location depending on the geotechnical parameters and regulatory standards of that region (Hore-Lacy, 2016). Because of the high dissolution of uranium in sulfuric acid solution, sulfuric acid which is one of the most common acidic leaching solutions is used to leach uranium as a sulfate. Moreover, after uranium dioxide ( $UO_2$ ) is reacted with oxygen to produce uranium trioxide ( $UO_3$ ), uranium is dissolved as carbonate in an alkaline mixture such as sodium carbonate (Council et al., 2012). It is claimed that in-situ leaching has a less environmental impact as compared to the open-pit mining methods because of some features such as less water requirement and surface disturbance, minimal heavy equipment usage, and radioactive waste production. Furthermore, 46% of produced global uranium is produced by the in-situ leaching method, and Australia, China, Kazakh, Russia, and United States are the pioneer of this technology in the world (Hore-Lacy, 2016).

After conventional uranium mining methods are explained, the details of alternative uranium extraction methods from aqueous media will be discussed in the next part.

### 2.3 Other Uranium Extraction Methods from Water Media

To contribute and guarantee today's and future demand for uranium, other uranium extraction methods have been investigated. Alternative to conventional uranium mining methods, uranium found in mainly tricarbonyl uranium complex ( $(\text{UO}_2(\text{CO}_3)_3)^{4-}$ ) in aqueous media can be recovered from this media via different methods such as coagulation and co-precipitation, membrane filtration, adsorption (J. Kim et al., 2013) and solvent extraction (Campbell et al., 1979). The principles of these well-known methods are summarized below.

**\*Coagulation and Co-precipitation:** The dissolved material or uranium is converted to an insoluble form in this method. Also, the solubility of the target and removed products are crucial (Dulama et al., 2013). As a precipitation chemicals or agents aluminium hydroxide ( $\text{Al}(\text{OH})_3$ ), iron (III) hydroxide ( $\text{Fe}(\text{OH})_3$ ) and calcium phosphate ( $\text{Ca}_3(\text{PO}_4)_2$ ) can be utilized (Sodaye et al., 2009).

**\*Membrane Filtration:** Fine particulates or dissolved materials can be separated from the solution via a membrane acting as a microporous barrier. Membrane processes can be classified into four different groups named reverse osmosis, nanofiltration, ultrafiltration, and microfiltration depending on their pore sizes. Nanofiltration is one of the most common membrane filtration methods utilized in uranium recovery (Favre-Reguillon et al., 2003).

**\*Solvent Extraction:** A target molecule or uranium is dissolved by using a liquid compound called solvent. Then, the solvent is separated from the target molecule and the solute became more concentrated. The selection of extractant or solvent material has a critical position in solvent extraction techniques. This chemical has to be non-volatile, non-toxic, non-flammable, and adaptable to an industrial scale. Nitrogen-based, phosphorus-based, and sulfur-based extractants are the most common extractants types in the uranium recovery field (J. R. Kumar et al., 2011).

**\*Adsorption:** Thanks to the different physico-chemical interactions between the target compound and adsorbent material, uranium or the target compound can be recovered from the solution via adsorption. Coordination is one of the most substantial mechanisms for the adsorption of chemicals selectively. The efficiency of this process

strongly depends on the construction of adsorbents including affinity ligands such as amidoxime and phosphoryl groups. Moreover, the solid carrier is also a crucial part of the adsorbent and this material has to be durable and adjustable (Wang & Zhuang, 2019). Up to date, various adsorbents materials like synthetic polymers (Huang et al., 2018), inorganic materials (Manos & Kanatzidis, 2012), biopolymers (Oshita et al., 2008), and porous carbon-based materials (Romanchuk et al., 2013) were tested for uranium extraction. The most promising adsorbent type was reported to be amidoximated polymers because of their high uranium selectivity and mechanical strength (Kuo et al., 2016) (Pan et al., 2015) (Tamada, 2010).

The comparison of all these uranium recovery methods from aqueous media based on operational, economic, capacity-related, and environmental issues are represented in Table 2.1. In brief, coagulation and coprecipitation method utilizes toxic substance (J. Kim et al., 2013) and high amounts of hydroxide (Campbell et al., 1979) (Sodaye et al., 2009) to be implemented. Membrane filtration has low environmental impact (Favre-Réguillon et al., 2005), but carries economic and operational problems like biofouling (Favre-Réguillon et al., 2005) (J. Kim et al., 2013). In comparison with other extraction methods, the highest uranium yield is obtained from the solvent extraction method. However, it has also the complicated operational procedure (Sodaye et al., 2009), high environmental risk (Kanno, 1984) and is a high-priced method (Best, Driscoll, et al., 1980). Therefore, solvent extraction is not a preferred method for uranium extraction from aqueous media. Among these options' adsorption is the most efficient, convenient, and low-priced method (J. Kim et al., 2013) (Tang et al., 2020). Therefore, adsorption has been chosen as an extraction method of uranium from water media in this study.

Table 2.1: Uranium Recovery from Water Media Methods Comparison

Name of Method	Operation Simplicity	Cost	Uptake Capacity	Environmental Risk
Coagulation and Co-precipitation	*Not simple because additional sedimentation and filtration processes can be required (J. Kim et al., 2013). *Long precipitation time is needed, so it is not practical for large seawater volume (Sodaye et al., 2009).	Economically not feasible because a lot of hydroxides are required for the large-scale applications (Campbell et al., 1979).	1100-2600 ton U/year with iron(III) hydroxide (Savenko, 1997).	High, since toxic substances can be produced (J. Kim et al., 2013).
Membrane Filtration	Not simple because of the fouling tendency (J. Kim et al., 2013)	*Do not economically viable process for uranium recovery (Favre-Régouillon et al., 2005) *High operational cost (J. Kim et al., 2013)	0.85 mg U/ g polyethylene membrane, it has lower capacity than the adsorption (J. Kim et al., 2013).	Low environmental impact (Favre-Régouillon et al., 2005)
Solvent Extraction	*Solvent loss is occurred by entrainment (Singh & Gupta, 2000). *Complicated procedure (Sodaye et al., 2009)	Because of solubility, it is prohibitively expensive (Best, Driscoll, et al., 1980).	Attractive specific uranium yield. It is higher than the other methods (Campbell et al., 1979).	High (Kanno, 1984)
Adsorption	Easy (J. Kim et al., 2013).	*\$610/kg of U (J. Kim et al., 2014) *It has potential to be economical for large scale (Singh & Gupta, 2000)	*1.54 mg U / g with polyamidoxime material (J. Kim et al., 2014) *1200 ton U/year (J. Kim et al., 2014)	Low environmental risk and environmentally sustainable (C. Wai et al., 2014)

In the following part, the details of desalination technologies will be focused since the environmental impact of desalination plants integrated with uranium recovery from brine systems will also be analyzed in this study.

## 2.4 Desalination Technologies

Water scarcity and lack of access to clean water caused by mainly population growth, climate change, industrial and agricultural activities are among the biggest global challenges of today’s world. Because of these reasons, the stress on the world’s water sources and sanitation problems have been growing over time. The amount of water that can be used directly is less than 3% of the world’s water reserves as freshwater and the remaining part or mostly ocean water has high salinity that makes it unsuitable for direct consumption. Therefore, the need to convert high saline water to fresh water has emerged. Desalination systems have been developed to meet this need by extracting salts and other minerals from inlet or saline water (Ahmed et al., 2021). The desalination technologies can be separated into two main categories named thermal and membrane (Micale et al., 2009) and major technologies in these categories are presented in Figure 2.10. Details of them will be discussed in the following parts.

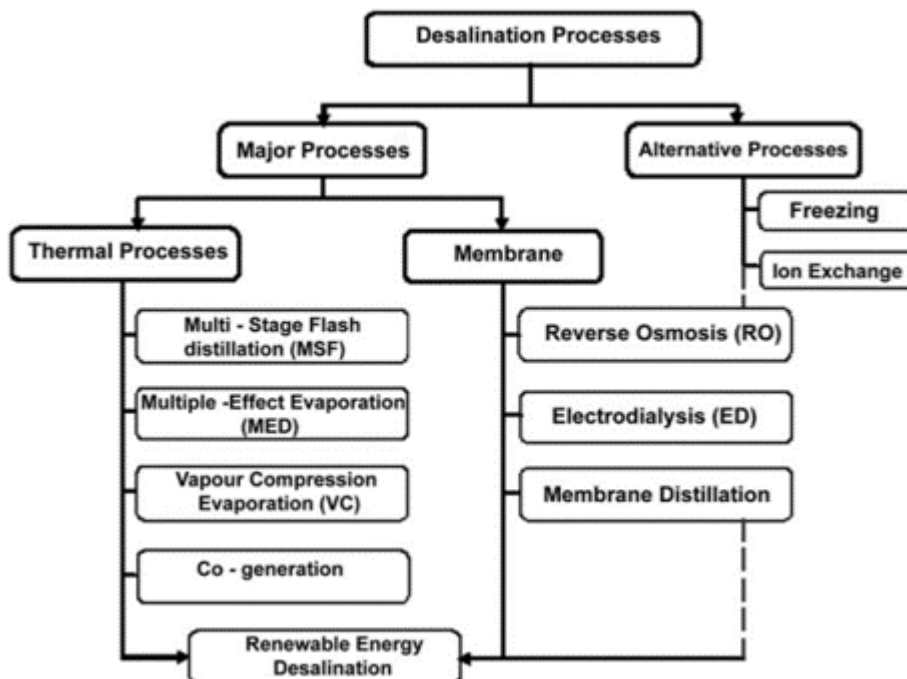


Figure 2.10: Classification Major Desalination Technologies (Shatat & Riffat, 2014)

## 2.4.1 Thermal Desalination Technologies

This form of desalination technology was developed in the 1950s which is earlier than the membrane desalination technologies. It covers the evaporation of salty water by using thermal energy sources and condensation of the resulting steam to produce freshwater. This type of technology is generally applied to large-scale facilities to achieve high economic feasibility. There are three main thermal desalination processes called multi-stage flash distillation (MSF), multi-stage distillation (MED), and vapor compression (VC). While MSF forms 18% of global desalination capacity, 7% of it results from MED. Moreover, they have distinct working principles that will be discussed in the next parts (Elsaid et al., 2020).

### 2.4.1.1 Multi-stage Flash Distillation

In this method, saline water is heated to near boiling point in a brine heater and the heated saline water passes through a series of effects or stages. Since the pressure inside these stages decreases gradually, water can boil rapidly and vapor is generated. Then, the conversion of this vapor steam to freshwater is achieved by condensation on the tubes of the heat exchanger. Also, when incoming saline water flows through the heater, it is used to cool these tubes, but incoming water is also warmed up at the same time.

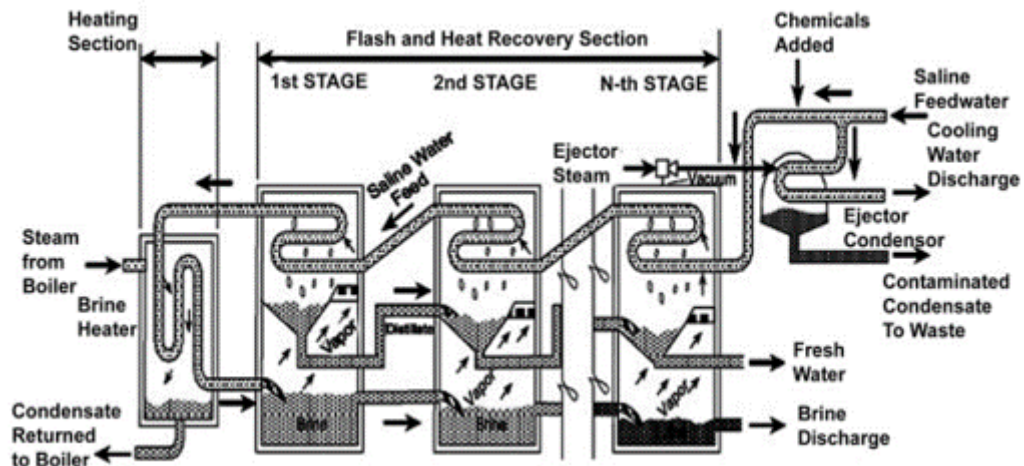


Figure 2.11: MSF Process Flow Chart (Shatat & Riffat, 2014)

Therefore, the thermal efficiency of the heater increases by reducing the thermal en-

ergy requirement to increase the temperature of feed water (Shatat & Riffat, 2014). The process schema is shown in Figure 2.11.

### 2.4.1.2 Multi-effect Distillation

This method is the oldest distillation method in large-scale used in the seawater desalination process. High unit capacity, high distillate quality, and high heat efficiency are the most important features of MED distillation. Its working principle of it is also based on evaporation and condensation by decreasing the ambient pressure in a variety of effects like in MSF distillation. The major difference between MSF and MED is related to the technique of heat transfer and evaporation. In MED saline seawater enters the first effect and its temperature is increased to the boiling point via preheating in tubes. Then, it is sprayed onto the evaporator tube's surface that is heated by steam, so rapid evaporation is promoted. Also, the used steam is condensed on the opposite side of the evaporator tubes and is directed to a boiler to regeneration (Shatat & Riffat, 2014). The flow chart of this process is represented in Figure 2.12.

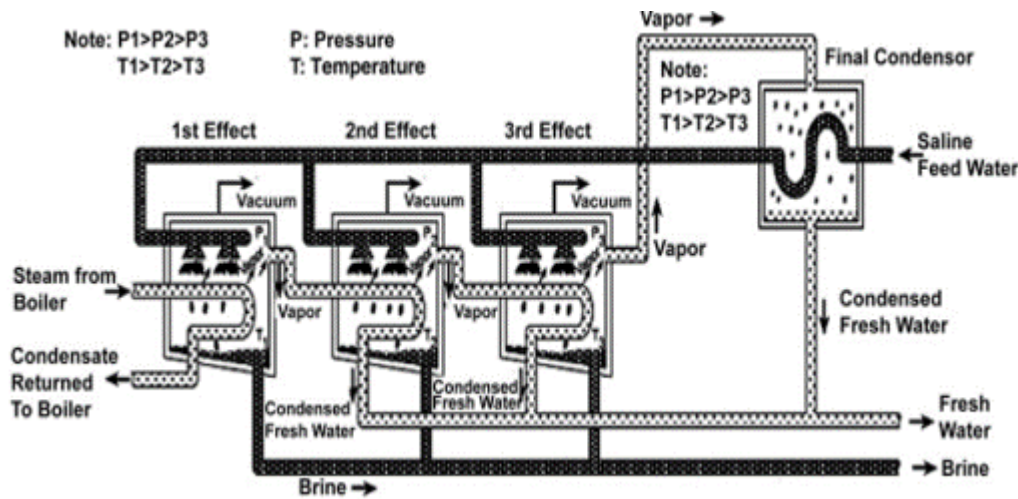


Figure 2.12: MED Process Flow Chart (Shatat & Riffat, 2014)

### 2.4.1.3 Vapor Compression

This method is based on the principle of decreasing the boiling temperature by lowering the pressure. Mechanical vapor compression via mechanical compressor and thermal vapor compression via steam jet are the two types of vapor compression methods. They are applied to condense the water vapor to generate a heat that is

sufficient to evaporate incoming saline water (Shatat & Riffat, 2014). The flow chart of this process is represented in Figure 2.13.

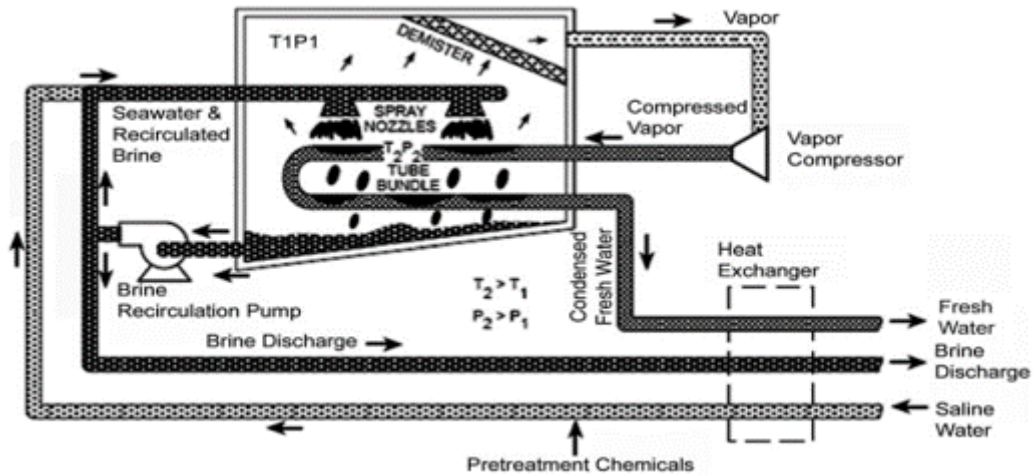


Figure 2.13: Vapor Compression Evaporation Flow Chart (Shatat & Riffat, 2014)

All these three thermal desalination methods have their own characteristics and they can be preferred depending on the different items. For example, if the main issue is related to the water quality, then MSF distillation is the best option, but in the operation phase of this method, scaling can be a problem because of the high temperature requirement. This and other types of differences between thermal desalination methods are discussed in Table 2.2.

#### 2.4.1.4 Co-generation Systems

In this process, the energy sources can be used in water production with desalination and electricity production. After electricity is generated with high pressure steam in the turbine, the steam that has a lower temperature and energy level because of the expansion in the turbine can be used in desalination plants. Moreover, the used steam is sent back to the boiler where reheat is applied. Less energy requirement is the main advantage of co-generation systems as compared to the separate operation of desalination and electricity generation plants (Shatat & Riffat, 2014).

Table 2.2: Thermal Desalination Technologies Comparison

Name of Method	MSF	MED	VC	Reference
Energy Consumption (kWh/m <sup>3</sup> )	Electrical: 2.5-5.0 Thermal: 15.83-23.5	Electrical: 1.0-2.5 Thermal: 12.2-19.1	Electrical: 7-12 (for MVC) and 1.6-1.8 (for TVC) Thermal: 0 (for MVC) and 14.5 (for TVC)	(Mehta, n.d.)
Product of Water Quality	2-10 ppm dissolved solids	5-50 ppm total dissolved solids	8-11 ppm total dissolved solid	(Shatat & Riffat, 2014) (Mehta, n.d.) (Bahar et al., 2004)
Maximum Top Brine Temperature	Approximately 120 °C	Approximately 70 °C	Approximately 70 °C	(Deng et al., 2010)
Reliability	Very High	Very High	-	(Mehta, n.d.)
Production Unit Capacity (m <sup>3</sup> /d)	<76000	<36000	<3000 (for MVC) <26000 (for TVC)	(Shatat & Riffat, 2014) (Mehta, n.d.)
Capital Expenditures (\$/m <sup>3</sup> * day)	1425	1150	1000	(Castro et al., 2020)
Operating Expenses (\$/m <sup>3</sup> )	0.232	0.232	0.232	(Castro et al., 2020)
Water Production Cost (\$/m <sup>3</sup> )	0.56-1.75	0.52-1.5	2.0-2.6 (for MVC) 0.87-0.95 (for TVC)	(Al-Qaraghuli & Kazmerski, 2012)
Advantages	*Relatively simple construction and operation *No moving parts, other than conventional pumps and a small number of connection tubes *More stage means improvement of efficiency and water production	*Less sensitive to scaling because of less temperature requirement *Being the oldest large-scale distillation method used for seawater desalination	*Simplicity and reliability lead to making it attractive for small scale desalination units *Low operating temperature (below 70°C) causes to simple and efficient process in terms of power requirement *Because of low operating temperature, the low potential of scale formation and tube corrosion	(Shatat & Riffat, 2014)
Disadvantages	*Higher temperature requirement (over 115 °C) for operation. This improves efficiency but may lead to scaling problems *More stage means higher capital cost and operational complexity	*Risk of contamination of the condensate water because of the saline-soaked wicks placed above the condensing surfaces	*Requirement of greater maintenance of compressors and heat exchangers than other systems *Requirement of spare parts	(Shatat & Riffat, 2014) (Tanaka et al., 2000) (Lubis & Holtzaple, 2012)

## **2.4.2 Membrane Desalination Technologies**

Membrane desalination technologies were developed in the 1970s. Since energy cost has increased and remarkable developments have progressed in membrane science, membrane desalination has been favored more than thermal technologies. Low energy requirement, the flexibility of capacity, and adaptability to a broad range of inlet salinity are the other advantages of membrane desalination processes. In membrane desalination technology, the semi-permeable membrane that allows the passage of only water is used. The method used in membrane desalination technology differs from each other depending on the driving force. For example, while in reverse osmosis this force is pressure, an electrical field is the driving force in electrodialysis (Elsaid et al., 2020). Details of these methods will be argued in the following parts.

### **2.4.2.1 Reverse Osmosis**

Reverse osmosis is a method of applying pressure to solvent from a field that has a high solute concentration to a field that has low solute concentration through a membrane. Therefore, water passes through the membrane, and the dissolved salts remain on the other side of the membrane (Kucera, 2015). A conventional reverse osmosis plant covers five main parts named seawater supply, pre-treatment, high pressure pumping, membrane separation, and post-treatment processes (Elsaid et al., 2020). The advantages and disadvantages of this method are given below:

Advantages: Because of the lower ambient temperature during operation, corrosion problems are seen less as compared to the MSF and MED technologies (Miller et al., 2015). Developments in the field of energy recovery equipment and membrane by improving the durability and lowering the price have helped to decrease the operational cost in this process (Shatat & Riffat, 2014).

Disadvantages: To produce water from seawater, a high amount of water can be required depending on the recovery ratio. Moreover, membrane scaling is a prevalent problem in reverse osmosis systems depending on the salt precipitation. Also, membranes tend to be plugged because of the biological and colloidal activities, so operational problems can be observed in these plants (Shatat & Riffat, 2014).

### **2.4.2.2 Electrodialysis**

Electrodialysis that is an electrochemical separation method used in water desalination area was released commercially in nearly 10 years before the reverse osmosis process. In this method, positively or negatively charged ions dissolved in water move towards electrodes that has opposite charge because of the electrical potential difference that is created between selective ion exchange membranes (Liu & Cheng, 2020). Energy consumption of this method strongly depends on the salinity of feed water like in the case of reverse osmosis (Patel et al., 2021). The advantages and drawbacks of this method are listed below.

Advantages: It has a high recovery ratio by achieving less brine and more distillate production. Also, the chemical requirement used in pre-treatment is low and the capital cost is lower than reverse osmosis systems (Patel et al., 2021). Moreover, treatment of inlet water that has a higher concentration of suspended solids than reverse osmosis can be achieved (Shatat & Riffat, 2014).

Disadvantages: Electrodialysis is not suitable for brackish water with dissolved solids of lower than 0.4 g/L and it is not an economic method for water that has a concentration of dissolved solids higher than 30 g/L (Shatat & Riffat, 2014). Also, the energy efficiency is lower as compared to reverse osmosis and electrodialysis cannot cope with the removal of uncharged large and small materials (Patel et al., 2021).

### **2.4.2.3 Membrane Distillation**

Membrane distillation is a method based on the transport of pure water vapor through a hydrophobic membrane. While impure liquid water that has a high temperature and its corresponding vapor pressure based on the heating process is found on one side of a membrane, lower temperature and pressure than those of inlet saline liquid water are available on the other side of this membrane. Because of the vapor pressure difference between these two sides of the membrane, pure water vapor flows from saline liquid water to the vapor side of the membrane. Then, the flowing pure vapor is condensed and pure liquid water is produced (Drioli et al., 2015). The advantages and disadvantages of membrane distillation are discussed below.

Advantages: It requires a low operation temperature and its operation is simple. As

compared to the other pressure-driven conventional membrane technologies, lower operating pressure is needed (Shatat & Riffat, 2014).

Disadvantages: It requires more area than the other membrane-based desalination processes. The energy requirement of the membrane distillation process is nearly the same as that of MSF and MED technologies. Moreover, because of the necessity of the inlet water that has to be free of organic pollutants, it has limited usage (Shatat & Riffat, 2014).

### **2.4.3 Alternative Desalination Technologies**

Freezing and solvent extraction are the other alternatives to desalination processes (Shatat & Riffat, 2014). The freezing method is based on the principle of the generation of ice crystals that are formed from pure water. It covers three main components named ice formation, cleaning, and melting of ice (Lu & Xu, 2010). Since it requires low theoretical energy and corrosion and scaling problems are seen less, it is preferred in some countries. However, since moving and processing ice and water are mechanically complicated, the freezing process includes operational difficulties.

In the ion exchange method, one type of anion or cation that is fixed in the solid can be exchanged with another type of anion or cation found in the solution. In the processes that require high purity, the ion exchange method can be favorable, but because of the cost issues, it is not suitable for seawater or brackish water desalination. However, both freezing and ion exchange processes do not achieve high productive performance as compared to the MSF, RO, and ED processes, so they are not preferred so much in desalination area (Shatat & Riffat, 2014).

### **2.4.4 Renewable Energy Driven Desalination Technologies**

Integration of renewable energy into desalination technologies results in renewable energy-driven desalination plants. Coupling these two technologies can lead to nearly 80% - 90% reduction in environmental impacts as compared to the fossil fuel scenario (Najjar et al., 2021). Various renewable energy sources named solar, wind, biomass, geothermal, and ocean can be applied to these plants for the purpose of sustainable water production, but as can be seen in Figure 2.14, solar energy is a commonly

used energy source in this field with a 51% ratio depending on the various factors such as climate, geography, capacity, the topography of study area and cost of project (Jijakli et al., 2012). The reason why solar energy combination is preferred more in desalination field can be explained that desalination plants are generally built in dry and isolated areas across the world (Tarpani et al., 2019) and conversion of solar energy into electrical and thermal energy is achieved easily (Alhaj et al., 2022).

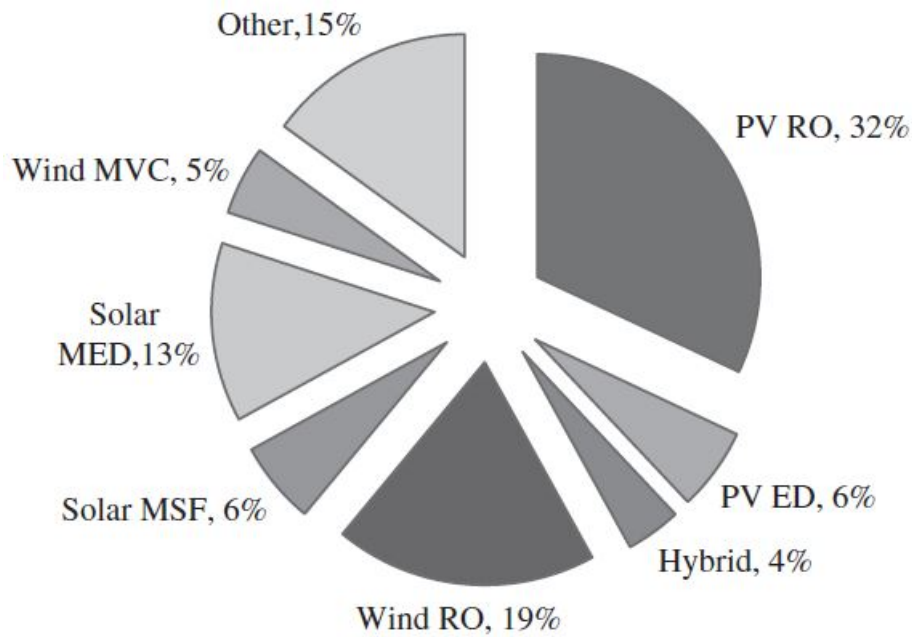


Figure 2.14: Renewable Energy Driven Desalination Technologies Distribution (Jijakli et al., 2012)

## CHAPTER 3

### LIFE CYCLE ASSESSMENT OF URANIUM RECOVERY FROM BRINE

#### 3.1 INTRODUCTION

Most European countries have a target to net-zero to decrease the GHG emissions by 2050 in accordance with combating climate change by inhibiting the increase in average global temperature to below 2°C above the level observed in the pre-industrial era (Sachs et al., 2016) (Paulillo et al., 2021). Since the largest contributor of GHG emissions is the energy production sector, switching the energy sources from fossil fuel to low carbon alternative energy sources like solar, nuclear, and wind has the potential to decrease emissions substantially and quickly (Paulillo et al., 2021). It is proved that nuclear power has a critical position in GHG mitigation where it can save nearly 10% of CO<sub>2</sub> emissions from global energy use. Moreover, it is also predicted by European Union that it is not possible to make any considerable impact on mitigating CO<sub>2</sub> emissions without depending on nuclear energy for Europe (Menyah & Wolde-Rufael, 2010). Therefore, the production of uranium which is a main raw material of nuclear power plants is also important (Norgate et al., 2014). Uranium can be produced from both water and earth with the conventional technologies and alternative ones that have been discussed in detail in Chapter 2.

Although nuclear energy offers an alternative way to reduce GHG emissions, it has also a negative impact on the environment depending on a set of processes from uranium mining and milling to final waste disposal (McCombie & Jefferson, 2016). Up to now, various LCA studies about conventional uranium mining methods have been conducted to detect these impacts. According to the study conducted by Sovacool (2008), uranium mining and milling have an important position in the life assessment of nuclear power plants in terms of global carbon dioxide emission, so a detailed

analysis should be conducted for these steps. The examples of these studies and their main properties are discussed in Table 3.1.

According to the information provided in Table 3.1, while most studies have been conducted for particular regions by using the site-specific input and output values, global scenarios have been considered in the other ones. Moreover, while the main focus was only on the GHGs emission from uranium mining and milling activities or nuclear fuel cycle in the previous studies, the impacts in other categories have also been taken into consideration especially in studies conducted in recent years. Although different impact assessments methods or methodologies have been followed in these studies, it was concluded that uranium mining and milling processes have severe environmental impacts in different impact categories depending on the ore grade and energy source. Therefore, the need for alternative uranium production methods has been created, but a preliminary LCA study is mandatory to detect the possible environmental impacts caused by these technologies.

## **3.2 METHODOLOGY**

LCA is used as a tool of quantitative sustainability assessment to find solutions to current challenges and to comply with the environmental sustainability for any product, process, or system considering all environmental impacts resulting from its entire life stages. The methodology of LCA follows the International Organization for Standards 14040 and 14044 as its principles, framework, requirements, and guidelines (Hauschild, 2018).

### **3.2.1 Goal and Scope Definition**

LCA of URFB produced as waste from desalination is performed by using the most studied and well-known materials: amidoximated adsorbents AF1 and PAN-AO. Evaluation of the environmental load of URFB from cradle to gate and comparing it with the conventional methods including in-situ leaching, underground and open-pit mining for extracting uranium from land is completed (Farjana et al., 2018). Gate represents the uranium processing factory gate, where before it is transported to nuclear power plants in this study. Therefore, all the data about inputs and waste emissions required up to this point have been included in the system boundaries of this study.

Table 3.1: Conventional Uranium Mining LCA Studies

No	Authors	Location	Goal of the Study	Functional Unit	System Boundary	Method and Software	Data Quality	Key Findings
1	(Lee & Koh, 2002)	Korea	Evaluating the environmental impacts of different nuclear fuel cycles and making a decision about nuclear energy policy	1 GWh electricity generation from nuclear power plants	Starting with uranium mining and milling and ending up disposal phase after the usage phase	Selection of environmental impact categories and finding necessary components such as classification factors from reports, Manual Calculation	Real Plant Data and Assumptions	Deciding the most harmful stage to the environment as uranium mining and milling in various impact categories such as climate change, acidification, and radiological impact potential
2	(Simons & Bauer, 2012)	Switzerland and France	Evaluating the specific human health and environmental loads arising from electricity production with the European pressurized reactor and detecting the influence of various fuel cycle strategies on the results	1 kWh electricity generation with the European pressurized reactor	Starting with uranium mining and milling with all conventional uranium extraction methods and ending up disposal phase after the usage phase including construction and decommissioning	ReCiPe, SimaPro	Ecoinvent v2.0 Database and Assumptions	The importance of uranium composition on the LCA results and indicating the main reason for highest environmental load in all indicators except for metals depletion as uranium milling step
3	(Norgate et al., 2014)	Global	Determining the global average GHGs caused by nuclear power generation and analyzing the uranium ore grade effect on the footprint result	1 MWh electricity production via pressurized water nuclear reactor with a capacity of 1 Gwe	Starting with uranium ore mining and milling with all conventional uranium extraction methods and ending up disposal phase after operation including decommissioning step	the ISO 14044 guidelines to compute GHG emissions, process-chain approach together with the economic input-output method depending on the scarcity or availability of data, SimaPro	Publicly available reports, company websites and LCA studies, Ecoinvent and SimaPro Databases and Assumptions	Estimating the GHG footprint as 33.9 kg CO <sub>2</sub> -e per 1 MWh electricity production from the ore grade of 0.15% and resulting in a high GHG footprint depending on the higher input and energy requirement with decreasing of the uranium ore grade degree
4	(Haque & Norgate, 2014)	Australia	Analyzing the GHG footprint caused by the in-situ leaching (ISL) mining method and comparing it with the other conventional mining methods	1 kg uranium production with ISL method (the other metals named gold and copper were also considered.)	Uranium extraction from ore-body with ISL and uranium milling	Australian Impact Method, SimaPro	Publicly available literature sources, contacts in the industry, and SimaPro database including Ecoinvent and assumptions	Resulting in a total GHG footprint from ISL as 38 kg CO <sub>2</sub> -e per 1 kg U <sub>3</sub> O <sub>8</sub> yellowcake production from the ore grade of 0.24% and detecting the main GHG emission contributors as sulphuric acid consumption and electricity requirement for pumping activities of leaching solutions
5	(D. J. Parker et al., 2016)	Canada	detecting the GHG emissions caused by the uranium mining and milling steps of the nuclear fuel cycle	1 kg of (U <sub>3</sub> O <sub>8</sub> ) production	Uranium mining with open-pit and underground methods and milling including construction, operation, and decommissioning phases	the ISO 14044 standards and process-chain analysis, SimaPro	Ecoinvent v3.0 Database, publicly available sources such as company websites and regulatory reports, and real plants data and assumptions	Resulting in a total GHG footprint of 81 kg CO <sub>2</sub> -e per 1 kg (U <sub>3</sub> O <sub>8</sub> ) yellowcake production from the ore grade of 0.74% and claiming the largest GHGs emission contributors as electricity consumption and direct emissions from non-renewable energy sources
6	(Farjana et al., 2018)	Australia	Detecting the environmental impact caused by all conventional uranium mining methods and compare them to detect the most suitable method	1 kg of uranium production as yellowcake	Uranium mining and milling with all conventional uranium extraction methods	ILCD and CED, SimaPro	Ecoinvent and AusLCI Databases	Indicating the method that causes the greatest radioactivity as underground mining and detecting the method that leads to more severe environmental impacts except for ionizing radiation than other mining methods depending on the energy and chemical consumption as in-situ leaching
7	(Farjana et al., 2019)	Global	Analyzing the environmental load caused by different metal production methods including uranium extraction with ISL comparatively and conducting sensitivity analysis by replacing the energy source from fossil fuel to solar	1 kg of uranium production (the other metals named aluminum, copper, etc. were considered also.)	Ore or uranium mining	IMPACT 2002+, SimaPro	Publicly available literature sources and Ecoinvent Database	Revealing that uranium mining combined with solar energy leads to reduce the environmental impacts substantially as compared to the mining methods using fossil energy as a primary energy source
8	(Pauffilo et al., 2021)	United Kingdom	Evaluating the environmental loads of two methods applied in used nuclear fuels management named once-through cycle and twice-through cycle	Management of used nuclear fuels including 1 ton uranium before being transformed partially in the advanced gas-cooled reactor	Starting with uranium mining carried out in different countries (Australia, Canada, and Kazakhstan) since there are no uranium mining sites in UK and uranium milling and ending up reprocessing or direct disposal steps	ILCD, Gabi	Publicly available literature sources and Ecoinvent Database	Comparing all conventional uranium mining methods applied in different regions in different impact categories and deciding the most harmful mining method as ISL in most impact categories, but observing also the lowest environmental impact in ISL in the ionizing radiation impact category. Also, concluding that uranium mining methods affect only radiological impacts in a once-through cycle approach

Climate change (CC), ozone depletion (OD), human toxicity (HTC & HTNC), particulate matter (PM), ionizing radiation (IRE & IRHH), photochemical ozone formation (PCO), acidification (ACD), freshwater and marine eutrophication (FEU & MEU), freshwater ecotoxicity (FET), land use (LU), and water-resource depletion (WRD), mineral, fossil and renewable resource depletion (MFRRD) were the parameters evaluated with life cycle assessment. Also, the consequential system model has been applied in this study and allocation is avoided. The functional unit providing systems to be compared has been taken as “1 kg of uranium production as yellowcake with a purity of 90%” for cradle to gate evaluation of life cycle (Rebitzer et al., 2004). SimaPro 9.0 Software has been used as an LCA tool for quantitative analysis of environmental load in this study. For the conventional uranium extraction alternatives, system boundaries include the raw material extraction and processing into yellowcake. The system boundaries include adsorbent preparation, uranium elution, and purification processes Figure 3.1. While AF1 adsorbent is prepared by radiation induced graft polymerization method that consists of four processes called electron beam irradiation, graft copolymerization, amidoximation, and conditioning, for PAN-AO adsorbent amidoximation is the only required step. The electron beam irradiation step is applied to produce radicals on the trunk of polymer (Oyola & Dai, 2016). Then, comonomers are bonded covalently to side chains onto the prime polymer chain, so graft copolymerization is achieved (Sherazi, 2016). After the conversion of the ligand from cyano to amidoxime group that is very selective for uranium adsorption (Pan et al., 2016) is completed with amidoximation process, amidoximated adsorbent preparation is completed with conditioning step whose purpose is improving the uranium loading capacity depending on the increase in the hydrophilicity of fiber (Das, Tsouris, et al., 2016) (Oyola & Dai, 2016).

After adsorbent materials are produced, they are exposed to the brine solution and uranium is adsorbed onto them. Then, desorption process is achieved by using alkaline eluant (Oyola & Dai, 2016) (Tsouris et al., 2015) (X. Zhao et al., 2020). After the alkaline elution process, the solution includes some impurities because of the competing ions such as vanadium (J. Kim et al., 2014). To achieve purification, a separation step that is explained in detail in the article conducted by (Z. Zhu et al., 2013) must be conducted. Also, some elements like infrastructures, required areas from nature,

and transportation have been excluded from both adsorbent system boundaries.

The data about conventional uranium mining methods were obtained from the literature (Farjana et al., 2018)(Haque & Norgate, 2014)(D. J. Parker et al., 2016), but those systems' boundaries and assumptions differ from this study. Therefore, the datasets provided in Ecoinvent v3.6 database for uranium ore extraction and yellow-cake production have been combined and compiled to obtain accurate results to compare conventional and adsorbent uranium recovery methods. Also, infrastructures and transportation data have been excluded for all conventional alternatives as applied in adsorbent methods. The system boundary for conventional uranium mining is represented in Figure 3.2.

In the following parts, details about the calculation of input & outputs values for this study will be explained.

### **3.2.2 Inventory Analysis**

Required data related to the raw materials, resources, and energy inputs and output waste emissions for the processes found in the system boundary have been collected both quantitatively and qualitatively. The life cycle of amidoximated adsorbent and purification processes by extracting vanadium has been introduced to SimaPro 9.2.0.1. (PhD version) manually and the dataset is considered from ecoinvent v3.6 database. Detailed information about required energy, chemicals, and waste has been obtained with the help of the experimental studies given in the goal and scope definition section of this study, and calculation steps will be shown in the next parts.

#### **3.2.2.1 Calculation of Required Substances Amount and Energy**

Before embarking upon detailed calculations, some assumptions listed in Table 3.2 have been made to ease the calculation. During this process, literature values have been used. Moreover, for this study it was considered that: all electricity is supplied with solar energy; incineration is the disposal method.

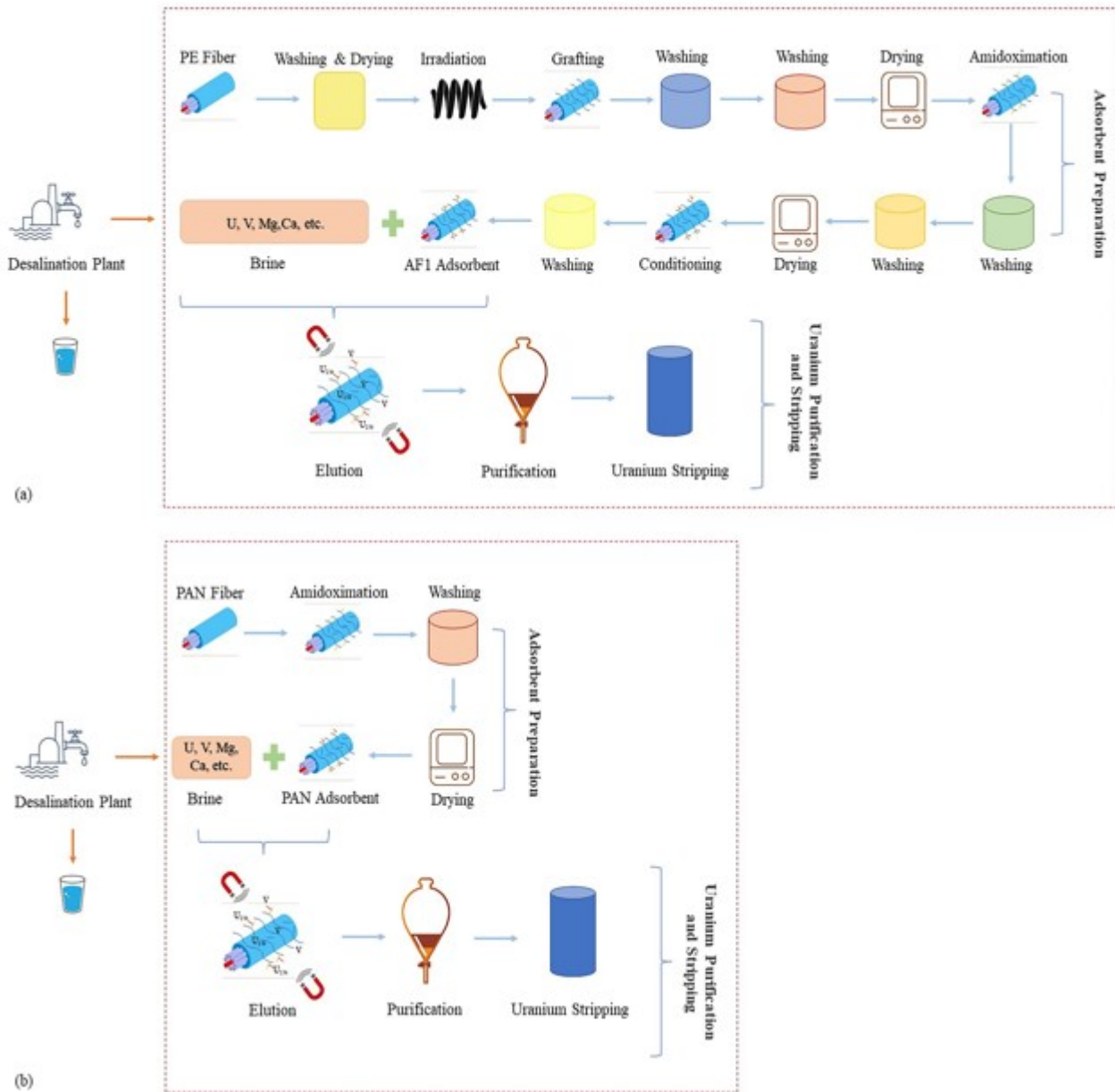


Figure 3.1: System Boundaries for This Study Including Uranium Recovery from Desalination Plants Brine via (a) AF1 Adsorbent and (b) PAN-AO Adsorbent

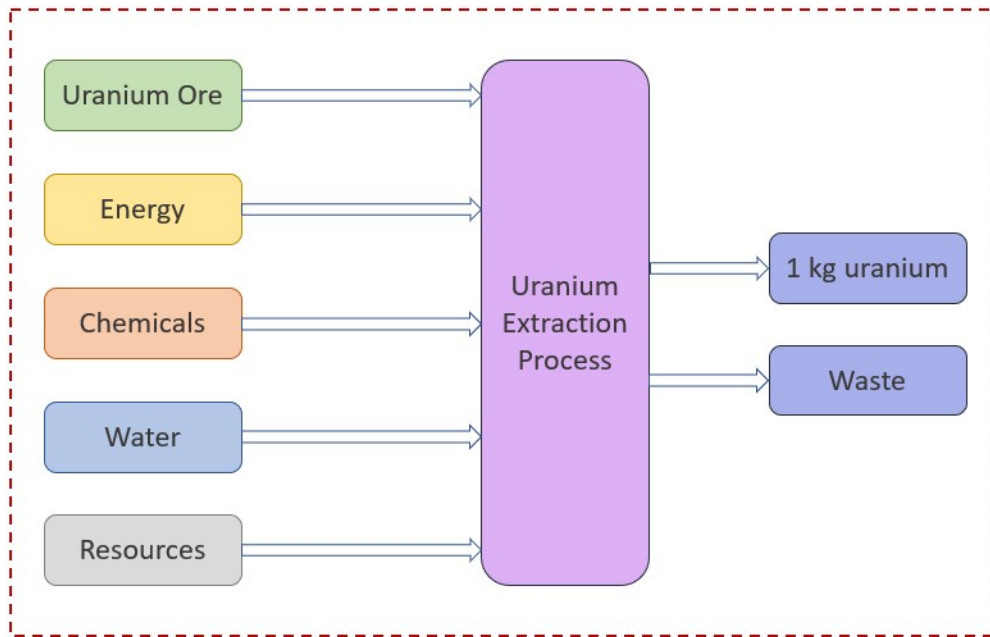


Figure 3.2: System Boundaries for Conventional Uranium Mining Methods

Table 3.2: Assumptions Made During the Input Calculation

Assumptions	References
Initial fiber volume was assumed as 10 mL by considering the volume of a flask and the other added chemicals during AF1 adsorbent calculations.	(Oyola & Dai, 2016)
After every reuse, 3% of adsorbent capacity is lost.	(Flicker Byers & Schneider, 2016) (Wongsawaeng et al., 2021)
The adsorbent is used 40 and 50 times for AF1 and PAN-AO adsorbents.	(Flicker Byers & Schneider, 2016)
By using 1 kg AF1 adsorbent, 4.72 g U and 15.33 g V are obtained.	(Oyola & Dai, 2016)
By using a 1 kg PAN-AO adsorbent, 6.02 g U and 6.38 g V are obtained.	(Pan et al., 2020)
Because of the lack of information in the Ecoinvent v3.6 database and chemical structure similarity between succinic acid and itaconic acid, itaconic acid was entered into the system as succinic acid. A similar situation is valid for potassium carbonate.	(Hogle et al., 2002)
Required heating energy for the fiber was neglected because it has a very small mass as compared to the other chemicals.	(Oyola & Dai, 2016)

### 3.2.2.1.1 AF1 Adsorbent Calculations

Some parameters and variables which have been used during calculations are listed in Table 3.3

Table 3.3: Given Parameters and Variables in the Literature

Name of Parameter	Value	References
Density and porosity of fiber before grafting	0.941 g/cm <sup>3</sup>	(Grasselli et al., 2003) (Kuo et al., 2016)
The volume of the flask during grafting	250 mL	
Used Acrylonitrile (AN) amount during grafting	2.471 mol	
Used Dimethyl sulfoxide (DMSO) amount during grafting	0.799 mol	
Used Itaconic acid (ITA) amount during grafting	0.327 mol	
Degree of Grafting	376 %	(Oyola & Dai, 2016)
The mass of fiber before amidoximation	150 mg	
The characteristics and volume of hydroxylamine in Methanol/Water solution for amidoximation	15 ml of 10% hydroxylamine hydrochloride in 50/50 (w/w) water/methanol solution	
Degree of Amidoximation	4.77 mmol/g	
The mass of fiber before KOH conditioning	30 mg	
The characteristic and volume of KOH during conditioning	15 mL of 2.5% KOH	

#### 3.2.2.1.1.1 Mass Calculations

##### Before Irradiation

The mass of polyethylene fiber before irradiation has been calculated by using the density and flask volume information of this fiber. In the article presented by Oyola and Dai (2016), flask volume was specified as 250 mL, and the total volume of AN, DMSO, and ITA solution was nearly 240 mL as mentioned in the article, so it has been assumed that the volume of fiber is approximately 10 mL. Then, the mass of fiber has been calculated as;

$$\rho_{fiber} = \text{mass of fiber} / \text{volume of fiber} \quad (3.1)$$

$$\text{mass of fiber} = 0.941 \text{ g/cm}^3 * 10 \text{ mL} = 9.41 \text{ g}$$

Also, to remove readily dissolvable polylactic acid, fiber is submerged into tetrahy-

drofuran solution (Oyola & Dai, 2016). It is assumed as the required volume is nearly equal to fiber volume, so by using density information of tetrahydrofuran ( $\rho = 0.889 \text{ g/cm}^3$  at  $20^\circ\text{C}$ ), the required tetrahydrofuran amount has been estimated as;

$$\text{Mass of tetrahydrofuran} = 10 \text{ mL} * 0.889 \text{ g/cm}^3 = 8.89 \text{ g}$$

In the same study, used chemicals during grafting were given as volume and molar basis, but in the life cycle assessment studies, mass is the most common functional unit type. Hence, all parameters have been calculated or converted on a mass basis in our study. For AN, DMSO, and ITA used in the grafting step, this conversion has been made by using the molecular weight of these substances. As a result, these mass values have been calculated as given below.

$$\text{MW of AN} = 53.06 \text{ g/mole}$$

$$\text{MW of DMSO} = 78.14 \text{ g/mole}$$

$$\text{MW of ITA} = 130.1 \text{ g/mole}$$

$$\text{Required mass of AN} = (2.471 \text{ mol}) * (53.06 \text{ g / mole}) = 131.11 \text{ g}$$

$$\text{Required mass of DMSO} = (0.799 \text{ mol}) * (78.14 \text{ g / mole}) = 62.43 \text{ g}$$

$$\text{Required mass of ITA} = (0.327 \text{ mol}) * (130.1 \text{ g / mole}) = 42.54 \text{ g}$$

All these chemical mol values are presented in Table 3.3.

### **After Grafting**

Mass of polyethylene fiber after grafting has been calculated by using the degree of grafting which is one of the experimental variables and given in the study conducted by Oyola and Dai (2016), and the related formula is given below.

$$\%DOG = ((wtAG - wtBG)/wtBG) * 100 \quad (3.2)$$

where,

wtAG: the weight of fiber after grafting

wtBG: the weight of fiber before irradiation

$$\%DOG = 376 = ((wtAG - 9.41 \text{ g}) * 100) / 9.41 \text{ g}$$

$$\Rightarrow wtAG = 44.79 \text{ g}$$

It is assumed as the density of fiber does not change after grafting. Then, by using the density and mass information, the volume of the fiber after grafting has been estimated as 47.6 mL. In the article, there is no information about the volume of chemicals that were used in washing, so assumptions have been made by considering the volume of the fiber after processes. To illustrate, after grafting nearly 48 mL fiber has been found as explained above, and it has been deduced that 48 mL dimethylformamide is enough for submerging and washing the produced polymer. The same assumption has been made for the methanol washing after washing with dimethylformamide. That is, it is assumed that a 48 mL methanol solution is enough for washing the fiber. Then, by using density information of dimethylformamide and methanol which are 0.944 g/cm<sup>3</sup> and 0.792 g/cm<sup>3</sup> at 25 °C respectively (Joshi et al., 1990) (Albaiti et al., 2016), the amount of them has been calculated below.

$$\text{Required dimethylformamide mass for washing} = 0.944 \text{ g/cm}^3 * 48 \text{ mL} = 45.31 \text{ g}$$

$$\text{Required methanol mass for washing} = 0.792 \text{ g/cm}^3 * 48 \text{ mL} = 38.02 \text{ g}$$

The other important assumption in this part is that during the washing and drying steps, there is no mass change of fiber.

### **Before Amidoximation**

To be able to calculate the mass of hydroxylamine in the amidoximation solution, the density of hydroxylamine, methanol, and water must be known. These values are 1.227 g/cm<sup>3</sup>, 0.792 g/cm<sup>3</sup>, and 1 g/cm<sup>3</sup> at 20 °C respectively (Guard, 1999) (Albaiti et al., 2016). Also, other information presented in the Oyola and Dai (2016) paper is that the mass of hydroxylamine forms 10% of the total solution and while methanol and water mass are equal, the total volume of the solution is 15 mL. By using this

information and mass conversion, firstly the volume of chemicals has been estimated as below.

$$\rho_{NH_2OH} * V_{NH_2OH} + \rho_{H_2O} * V_{H_2O} + \rho_{MeOH} * V_{MeOH} = 15mL * \rho_{solution} \quad (3.3)$$

$$0.1x \qquad \qquad \qquad 0.45x \qquad \qquad \qquad 0.45x$$

$$\Rightarrow 4.5 * (1.227 \text{ g/cm}^3 * V_{NH_2OH}) = 1 \text{ g/cm}^3 * V_{H_2O} \rightarrow V_{NH_2OH} = V_{H_2O}/5.5215$$

$$\Rightarrow 0.792 \text{ g/cm}^3 * V_{MeOH} = 1 \text{ g/cm}^3 * V_{H_2O} \rightarrow V_{MeOH} = V_{H_2O}/0.792$$

$$\Rightarrow V_{H_2O} / 5.5215 + V_{H_2O} + V_{H_2O} / 0.792 = 15 \text{ mL}$$

$$\rightarrow V_{H_2O} = 6.14 \text{ cm}^3$$

$$\rightarrow V_{MeOH} = 7.75 \text{ cm}^3$$

$$\rightarrow V_{NH_2OH} = 1.11 \text{ cm}^3$$

Then, by using the density of these substances their masses have been calculated.

$$\text{Mass of Hydroxylamine} = 1.11 \text{ cm}^3 * 1.227 \text{ g/cm}^3 = 1.36 \text{ g}$$

$$\text{Mass of Methanol} = 7.75 \text{ cm}^3 * 0.792 \text{ g/cm}^3 = 6.2 \text{ g}$$

$$\text{Mass of Water} = 6.14 \text{ cm}^3 * 1 \text{ g/cm}^3 = 6.2 \text{ g}$$

However, these values are valid for nearly 150 mg fiber as specified in the same article, so it should be normalized for nearly 45 g fiber calculated previous part to obtain more meaningful and comparable results. After normalization, new values can be listed as 406 g, 1833 g, and 1833 g respectively.

### **After Amidoximation**

The mass of fiber after amidoximation can be calculated by using the degree of amidoximation or the density of amidoxime group values which are one of the experimental variables and other information. The related equation is given below.

$$AOGD = (W_t - W_0) * 1000 / (W_t * M_t) \quad (3.4)$$

where,

AOGD: the degree of amidoximation or the density of amidoxime groups (4.77 mmol/g)

$W_t$ : the weight of fiber after amidoximation

$W_0$ : the weight of fiber before amidoximation

$M_t$ : molecular weight of hydroxylamine (33 g/mole)

Then, by using this equation, the mass of fiber can be estimated as:

$$4.77 \text{ mmol/g} = ((W_t - 150\text{mg}) * 1000) / (W_t * 33 \text{ g/mole})$$

$$\Rightarrow W_t = 178.02 \text{ mg}$$

Normally by weighing the fiber after and before amidoximation, the degree of amidoximation is calculated, but in the article final mass was not specified. Therefore, the procedure given above has been followed. Then, the normalization step has been applied again, and the final mass has been calculated as 53.16 g. In the following washing steps, again any information about the amount of the used chemicals was not given on the paper. Therefore, density has been assumed as the same as the initial density which is 0.941 g/cm<sup>3</sup>, and by using mass and density information, approximate volume values have been calculated as 56.49 mL for 53.16 g amidoximated fiber. By using this information, the required deionized water and methanol volume have been assumed as 57 mL. Then, using this volume and density information of them, the required mass values have been calculated as 57 g and 45.14 g for deionized water and methanol, respectively. Also, this assumption has been applied to another scenario.

### **Before Conditioning**

Since a 2.5% KOH solution is very dilute ( $\rho = 1.028 \text{ g/cm}^3$  at 20 °C), it can be said that in 1 mL of solution 25 mg KOH is found (Lee and Lin, 2007). Also, in the article, it is specified that for 30 mg adsorbent 15 mL of KOH solution is used (Oyola & Dai, 2016). The mass of the adsorbent has been calculated as 53.16 g in the previous part, so it can be concluded that a 26.6 L KOH solution is required for that amount of adsorbent. Then, the mass water of this solution can be estimated as below.

Mass of KOH = (25 mg KOH / 1 mL solution) \* 26579.7 mL solution = 0.67 kg

Mass of solution = (1.028 g/cm<sup>3</sup>) \* 26579.7 mL = 27.32 kg

Mass of water = (27.32 – 0.67) kg = 26.66 kg

Then, potassium and hydroxide mass can be calculated separately by using molar mass information of them which are 39.0983 g and 17.008 g and these calculations are shown below.

$$\text{Mass of Potassium} = (\text{Total Mass of KOH} / ((\text{MW of K}^+ / \text{MW of OH}^-) + 1)) * (\text{MW of K}^+ / \text{MW of OH}^-) \quad (3.5)$$

$$= (664.49 \text{ g} / ((39.0983 / 17.008) + 1)) * (39.0983 / 17.008)$$

$$\Rightarrow 463.06 \text{ g}$$

$$\text{Mass of Hydroxide} = \text{Total Mass of Solution} - \text{Mass of K}^+ \quad (3.6)$$

$$= (664.49 - 463.06) \text{ g}$$

$$\Rightarrow 201.43 \text{ g}$$

### After Conditioning

During the calculation of adsorbent mass after conditioning, elemental analysis results have been used, and these are shown in Table 3.4.

Table 3.4: AF1 Adsorbent Elemental Analysis Results During Production (Das, Tsouris, et al., 2016)

Sample ID	Elements (wt %)				Total
	C	H	N	O	
Amidoximated AF1	48.95	8.13	20.15	22.53	100
AF1- %2.5 KOH @80 °C for 3 h	45.43	7.6	16.88	24.27	94*

\*: The rest ( 6%) is K.

After amidoximation, nearly 53.2 g AF1 adsorbent can be produced, but in the experiment, 30 mg fiber was used for KOH conditioning. As can be seen in Table 3.4, 48.95% of this adsorbent which is equal to 14.69 mg composed of carbon (C). After conditioning with KOH, hydrogen mass changes because of deprotonation. Furthermore, some of the amidoxime groups can convert into other functional groups such as carboxylate during conditioning (Das, Tsouris, et al., 2016). Therefore, the mass of N and O differ also at this step. On the other hand, the mass of C does not change during this process, so by using this mass, the total mass of the final adsorbent can be estimated below.

Mass of C before conditioning = Mass of C after Conditioning = Total mass of adsorbent \* 45.43%

14.69 mg = Total mass of adsorbent \* 45.43% (This percentage value is given in Table 3.4)

⇒ The total mass of adsorbent after conditioning = 32.34 mg

Then, this calculated fiber mass value has been normalized as 57.3 g by using the value presented above.

In this study, 3 types of normalization have been applied and the logic behind all of them is a linear scale-up procedure. In the first one, article values have been arranged with the initial fiber amount which is 9.41 g. These steps are explained in detail in the upper parts. Secondly, 1 kg polyethylene fiber usage has been considered as a base case, and the ratio between the first case and this case has been estimated as 106.27 by dividing the second case fiber amount (1000 g) by the first one (9.41). That is, all required mass amounts have been multiplied by 106.27 for this case to make a relationship between the two scenarios. However, for just washing chemical amounts, re-assumption has been done to prevent overestimation. Finally, for 1kg uranium production, the related ratio which is 157.55 has been found by using produced uranium amount and adsorbent mass in the first case. That is, this time required chemical mass values are 157.55 times higher than the first normalization values. All these normalized values are given in Table 3.5. Moreover, detailed uranium amount calculation values which help to form Table 3.5 are explained in the following part.

Table 3.5: The Amount of Chemicals Required for AF1 Adsorbent Production for All Normalization Cases

Name of Chemical	Required Amount for Normalized Article Values	Normalized Amount for 1 kg Polyethylene	Normalized Amount for 1 kg U Production
Polyethylene Fiber	9.41 g	1 kg	1.48 kg
Tetrahydrofuran	8.89 g	1 kg	1.40 kg
Acrylonitrile	131.11 g	13.93 kg	20.66 kg
Dimethyl Sulfoxide	62.43 g	6.63 kg	9.84 kg
Itaconic Acid	42.54 g	4.52 kg	6.70 kg
Dimethylformamide	45.31 g	4.23 kg	6.27 kg
Methanol (for Washing 2 and 4)	83.16 g (38.02 g + 45.14 g)	7.76 kg (3.55 kg + 4.21 kg)	11.5 kg (5.26 kg + 6.24 kg)
Hydroxylamine	406.7 g	43.22 kg	64.01 kg
Methanol/Water	Methanol: 1832.9 g	Methanol: 194.8 kg	Methanol: 288.8 kg
	Water: 1832.9 g	Water: 194.8 kg	Water: 288.8 kg
Deionized Water (Washing 3 and 5)	87 g (57 g + 30 g)	11.05 kg	17.48 kg
		(5.32 kg + 5.73 kg)	(7.88 kg + 9.60 kg)
Potassium Hydroxide/Water	KOH: 664.5 g	KOH: 70.62 kg	KOH: 104.69 kg
	Water: 26659.5 g	Water: 2833.1 kg	Water: 4200.32 kg

### 3.2.2.1.1.2 Adaptation of Experimental Values to Realistic Values

Until this part, required chemical amounts have been calculated by adapting lab protocol values from listed articles with a 1:1 scaling ratio on a weight basis or linear scale-up procedure. However, using these chemical amounts directly may cause wrong results or a higher environmental load more than actually in life cycle assessment studies since people work with small amounts of chemicals in the lab, so redundant chemicals sometimes can be added to ensure the reaction happens. However, this would not be logical in real life because financial and environmental concerns should be considered during any production process. Therefore, adapting the required amount of chemicals with an engineering approach is a necessity. In the adaptation process, the chemical amounts have been calculated again by considering the conversion factor, reusability, and recyclability of chemicals. Catalysts such as DMSO, washing water, and chemicals have not been included as an input of this

study, since they are not found within adsorbent structure, and they can be reused. To illustrate, tetrahydrofuran, methanol, water, dimethyl formamide, dimethyl sulfoxide, and the other organic chemicals used in solvent extraction can be reused and recycled up to 90% ratio (Flicker Byers & Schneider, 2016), so their required amount for 1 kg uranium production is comparatively lower than the other input, so they can be neglected.

#### Real AN and ITA Values

During real values calculation, the mass of fiber before and after grafting has been used. The difference between these two values shows the amount of AN and ITA involved in the fiber formation. This value is divided by the amount of these chemicals used in the experiment and is multiplied by 100. The conversion factor can be found on a percentage basis with these steps that are shown below for the 1 kg uranium production scenario.

$$\text{Conversion Factor (\%)} = ((7.057 - 1.483) \text{ kg} / (20.657 + 6.703) \text{ kg}) * 100 = 20.37\%$$

This means that only 20.37 percent of chemicals added into the solution which are 4.21 kg AN and 1.37 kg ITA are seen in the fiber structure. For the other scenario, which is 1 kg Polyethylene, the same steps have been followed, and the required chemical amounts have been estimated as 2.84 kg AN and 0.92 kg ITA.

#### Real Amidoximation Chemicals Values

By using the same method, the hydroxylamine amount has been estimated by subtracting the mass of fiber measured before amidoximation from the fiber mass measured after amidoximation. Then, this value again has been divided by the initial amount of added chemicals. The related step is summarized below.

$$\text{Conversion Factor (\%)} = ((8.376 - 7.057) \text{ kg} / (192.232) \text{ kg}) * 100 = 0.69\%$$

That is, only 0.69 percent of additional hydroxylamine which is 1.32 kg contributes to fiber structure. The same steps have been followed for the other scenario and the required hydroxylamine amount has been calculated as 0.9 kg.

### Real Conditioning Chemicals Values

A similar procedure is valid for conditioning chemical or KOH solution. In this step, the conversion factor is calculated on the initial and final mass of potassium found in the fiber structure. Initial mass calculation of K ions found in fiber was shown in the "Before Conditioning" part. To calculate the final mass of K ions presented in fiber, the fiber mass calculated in the "After Conditioning" part is multiplied by the relevant percentage ratio (6%) given in Table 3.4. The conversion factor for K ions can be estimated below by using the values for the 1 kg uranium scenario.

$$\text{Conversion Factor (\%)} = (\text{The Amount of K}^+ \text{ Found in Fiber} / \text{Initial Addition of K}^+) * 100 \quad (3.7)$$

$$= (0.542 \text{ kg} / 72.968 \text{ kg}) * 100 = 0.74\%$$

That is, only 0.74 percent of additional potassium which is 0.54 kg contributes to fiber structure. By using this amount, the required potassium hydroxide amount has been calculated as 0.78 kg by using the molecular mass ratio of  $\text{K}^+$  and KOH. After calculating KOH mass, the required water amount found in the KOH solution has been calculated by using the mass ratio between these two chemicals shown in the "Before Conditioning" part. The water amount was found as 21.02 kg and 31.17 kg for the first and second normalization scenarios. Summarizing all values used in SimaPro 9.2.0.1. excluding all washing chemicals and catalysts are given in Table 3.18.

#### **3.2.2.1.1.3 Energy Calculations**

##### Heat Energy

Heating energy is required for almost all steps which are drying, grafting, amidoximation and conditioning during the amidoximated adsorbent preparation. Also, specific heat values of chemicals are required to calculate the required heating energy, and these values are listed in Table 3.6.

Table 3.6: Specific Heat Values of Chemicals Used in Adsorbent Preparation

Name of Chemical	Specific Heat Value	Reference
Irradiated Polyethylene Fiber	2.3 J/g*°C	(H. Kumar et al., 2011) (Wunderlich & Jones, 1969)
Tetrahydrofuran	1.72 J/g*°K	(Lebedev et al., 1978)
AN	2.09 J/g*°K	(Guerrero-Pérez & Banares, 2015)
DMSO	1.91 J/g*°K	(Grolier et al., 1993)
ITA	1.30 J/g*°K**	(Vanderzee & Westrum Jr, 1970)
Hydroxylamine	1.42 J/g*°K	(Michopoulos & Rode, 1991)
Methanol	2.48 J/g*°K	(Filatov & Afanas' ev, 1992)
Water	4.18 J/g*°K	(Kluitenberg, 2002)
Potassium Hydroxide	1.16 J/g*°K	(Kubaschewski et al., 1993)

\*\*Because of the very similar molecular structure with succinic acid, and lack of information, succinic acid specific heat value has been assumed as the same as ITA.

During the grafting, amidoximation, and conditioning steps, heating energy must be supplied to the chemicals and fiber to increase the temperature from room temperature which is assumed as 25 °C to a higher one such as 80 °C. This amount of energy can be estimated by using the formula below.

$$Q = m * c * \Delta T \text{ (Lienhard \& John, 2005)} \quad (3.8)$$

where,

Q = heat energy (J)

m = mass of chemical absorbing the heat (g)

c = specific heat capacity (J/g\*°C)

ΔT = change in temperature (°C)

All the heating calculations are done for both normalized situations.

Heat Energy for Fiber Preparation via Tetrahydrofuran

Heat energy is required for the tetrahydrofuran submerging step that is applied to remove readily dissolvable polylactic acid from the fiber. The required temperature

for this process is specified as 60 °C and related energy calculations are shown below.

$$*Q1 \text{ for Polyethylene Fiber} = 1000 \text{ g} * 2.3 \text{ J/g}^{\circ}\text{C} * (60-25) \text{ }^{\circ}\text{C}$$

$$Q1 = 80500 \text{ J} (1\text{J} = 2.77*10^{-7} \text{ kWh}) \Rightarrow Q = 0.02 \text{ kWh (for normalization 1)}$$

$$Q2 \text{ for Polyethylene Fiber} = (1482.6 \text{ g} * 2.3 \text{ J/g}^{\circ}\text{C} * (60-25) \text{ }^{\circ}\text{C}) * 2.77*10^{-7} \text{ kWh/J}$$

$$Q2 = 0.033 \text{ kWh (for normalization 2)}$$

$$*Q1 \text{ for Tetrahydrofuran} = 1000 \text{ g} * 1.72 \text{ J/g}^{\circ}\text{C} * (60-25) \text{ }^{\circ}\text{C}$$

$$Q1 = 60200 \text{ J} \Rightarrow Q = 0.02 \text{ kWh (for normalization 1)}$$

$$Q2 \text{ for Tetrahydrofuran} = 1401.1 \text{ g} * 1.72 \text{ J/g}^{\circ}\text{C} * (60-25) \text{ }^{\circ}\text{C}$$

$$Q1 = 84347 \text{ J} \Rightarrow Q = 0.023 \text{ kWh (for normalization 1)}$$

$$\text{Total Heat Energy for Normalization 1} = (0.02 + 0.02) \text{ kWh} = 0.04 \text{ kWh}$$

$$\text{Total Heat Energy for Normalization 2} = (0.033 + 0.023) \text{ kWh} = 0.06 \text{ kWh}$$

### Heat Energy for Grafting

In the grafting step, energy is applied for increasing the temperature of chemicals which are AN, DMSO, ITA, and Polyethylene fiber from 25 °C to 60 °C. These energy calculations are given below.

$$*Q1 \text{ for Polyethylene Fiber} = 1000 \text{ g} * 2.3 \text{ J/g}^{\circ}\text{C} * (60-25) \text{ }^{\circ}\text{C}$$

$$\Rightarrow Q1 = 80500 \text{ J} (1\text{J} = 2.77*10^{-7} \text{ kWh}) \Rightarrow Q = 0.02 \text{ kWh (for normalization 1)}$$

$$Q2 \text{ for Polyethylene Fiber} = (1482.6 \text{ g} * 2.3 \text{ J/g}^{\circ}\text{C} * (60-25) \text{ }^{\circ}\text{C}) * 2.77*10^{-7} \text{ kWh/J}$$

$$\Rightarrow Q2 = 0.03 \text{ kWh (for normalization 2)}$$

$$*Q1 \text{ for Acrylonitrile} = (13933.18 \text{ g} * 2.09 \text{ J/g}^{\circ}\text{C} * (60-25) \text{ }^{\circ}\text{C}) * 2.77*10^{-7} \text{ kWh/J}$$

$$\Rightarrow Q1 = 0.28 \text{ kWh (for normalization 1)}$$

$$Q2 \text{ for Acrylonitrile} = (20657.17 \text{ g} * 2.09 \text{ J/g}^{\circ}\text{C} * (60-25) \text{ }^{\circ}\text{C}) * 2.77*10^{-7} \text{ kWh/J}$$

$$\Rightarrow Q2 = 0.42 \text{ kWh (for normalization 2)}$$

$$\text{*Q1 for Dimethyl Sulfoxide} = (6633.993 \text{ g} * 1.91 \text{ J/g}^{\circ}\text{C} * (60-25) \text{ }^{\circ}\text{C}) * 2.77*10^{-7} \text{ kWh/J}$$

$$\Rightarrow \text{Q1} = 0.12 \text{ kWh (for normalization 1)}$$

$$\text{Q2 for Dimethyl Sulfoxide} = (9835.48 \text{ g} * 1.91 \text{ J/g}^{\circ}\text{C} * (60-25) \text{ }^{\circ}\text{C}) * 2.77*10^{-7} \text{ kWh/J}$$

$$\Rightarrow \text{Q2} = 0.18 \text{ kWh (for normalization 2)}$$

$$\text{*Q1 for ITA} = (4520.97 \text{ g} * 1.30 \text{ J/g}^{\circ}\text{C} * (60-25) \text{ }^{\circ}\text{C}) * 2.77*10^{-7} \text{ kWh/J}$$

$$\Rightarrow \text{Q1} = 0.08 \text{ kWh (for normalization 1)}$$

$$\text{Q2 for ITA} = (6702.74 \text{ g} * 1.30 \text{ J/g}^{\circ}\text{C} * (60-25) \text{ }^{\circ}\text{C}) * 2.77*10^{-7} \text{ kWh/J}$$

$$\Rightarrow \text{Q2} = 0.12 \text{ kWh (for normalization 2)}$$

$$\text{Total Heat Energy for Normalization 1} = (0.02+0.28+0.12+0.08) \text{ kWh} = 0.51 \text{ kWh}$$

$$\text{Total Heat Energy for Normalization 2} = (0.03+0.42+0.18+0.12) \text{ kWh} = 0.76 \text{ kWh}$$

#### Heat Energy for Amidoximation

Because of the smaller fiber mass than hydroxylamine chloride in methanol-water solution mass noticeably, the required energy for heating the fiber is also very low as compared to this solution. Therefore, energy for heating the fiber can be neglected for this step, and the main heating energy calculations are presented below.

$$\text{*Q1 for Hydroxylammonium} = (43219.9 \text{ g} * 1.42 \text{ J/g}^{\circ}\text{C} * (80-25) \text{ }^{\circ}\text{C}) * 2.77*10^{-7} \text{ kWh/J} \Rightarrow \text{Q1} = 0.94 \text{ kWh (for normalization 1)}$$

$$\text{Q2 for Hydroxylammonium} = (64077.2 \text{ g} * 1.42 \text{ J/g}^{\circ}\text{C} * (80-25) \text{ }^{\circ}\text{C}) * 2.77*10^{-7} \text{ kWh/J} \Rightarrow \text{Q2} = 1.39 \text{ kWh (for normalization 2)}$$

$$\text{*Q1 for methanol} = (194779.2 \text{ g} * 2.48 \text{ J/g}^{\circ}\text{C} * (80-25) \text{ }^{\circ}\text{C}) * 2.77*10^{-7} \text{ kWh/J}$$

$$\Rightarrow \text{Q1} = 7.36 \text{ kWh (for normalization 1)}$$

$$\text{Q2 for methanol} = (288777.3 \text{ g} * 2.48 \text{ J/g}^{\circ}\text{C} * (80-25) \text{ }^{\circ}\text{C}) * 2.77*10^{-7} \text{ kWh/J}$$

$$\Rightarrow Q_2 = 10.91 \text{ kWh (for normalization 2)}$$

$$*Q_1 \text{ for water} = (194779.2 \text{ g} * 4.18 \text{ J/g}^{\circ}\text{C} * (80-25) \text{ }^{\circ}\text{C}) * 2.77 * 10^{-7} \text{ kWh/J}$$

$$\Rightarrow Q_1 = 12.40 \text{ kWh (for normalization 1)}$$

$$Q_2 \text{ for water} = (288777.3 \text{ g} * 4.18 \text{ J/g}^{\circ}\text{C} * (80-25) \text{ }^{\circ}\text{C}) * 2.77 * 10^{-7} \text{ kWh/J}$$

$$\Rightarrow Q_2 = 18.39 \text{ kWh (for normalization 2)}$$

$$\text{Total Heat Energy for Normalization 1} = (0.94+7.36+12.4) \text{ kWh} = 20.7 \text{ kWh}$$

$$\text{Total Heat Energy for Normalization 2} = (1.39+10.91+18.39) \text{ kWh} = 30.69 \text{ kWh}$$

### Heat Energy for KOH Conditioning

Related heat energy calculation for the conditioning is given below.

$$*Q_1 \text{ for Potassium Hydroxide} = (70615.6 \text{ g} * 1.16 \text{ J/g}^{\circ}\text{C} * (70-25) \text{ }^{\circ}\text{C}) * 2.77 * 10^{-7} \text{ kWh/J} \\ \Rightarrow Q_1 = 1.02 \text{ kWh (for normalization 1)}$$

$$Q_2 \text{ for Potassium Hydroxide} = (104693.86 \text{ g} * 1.16 \text{ J/g}^{\circ}\text{C} * (70-25) \text{ }^{\circ}\text{C}) * 2.77 * 10^{-7} \text{ kWh/J} \\ \Rightarrow Q_2 = 1.51 \text{ kWh (for normalization 2)}$$

$$*Q_1 \text{ for water} = (2833097.95 \text{ g} * 4.18 \text{ J/g}^{\circ}\text{C} * (70-25) \text{ }^{\circ}\text{C}) * 2.77 * 10^{-7} \text{ kWh/J}$$

$$\Rightarrow Q_1 = 147.61 \text{ kWh (for normalization 1)}$$

$$Q_2 \text{ for water} = (4200316.57 * 4.18 \text{ J/g}^{\circ}\text{C} * (70-25) \text{ }^{\circ}\text{C}) * 2.77 * 10^{-7} \text{ kWh/J}$$

$$\Rightarrow Q_2 = 218.85 \text{ kWh (for normalization 2)}$$

$$\text{Total Heat Energy for Normalization 1} = (1.02+147.61) \text{ kWh} = 148.6 \text{ kWh}$$

$$\text{Total Heat Energy for Normalization 2} = (1.51+218.85) \text{ kWh} = 220.4 \text{ kWh}$$

### Heat Energy for Drying After Submerging via Tetrahydrofuran

Fiber can hold the washing chemical in proportion with its porosity value which is 0.71 in this study. This means that fiber can hold chemicals with a volume of 71% of the total fiber volume. Initial volumes of fiber are 1062.7 mL and 1575.5 mL. It means that 754.5 mL and 1118.6 mL of tetrahydrofuran can be kept inside the fiber pore. By

using density information, required masses have been estimated as 671.5 g and 995.6 g. Therefore, these amounts of liquid can be vaporized via drying. However, the temperature must be increased first. The drying temperature is specified as 50 °C in the article, so the required heat calculations are shown below.

$$Q1 = (671.5 \text{ g} * 1.72 \text{ J/g} \cdot \text{K} * (50-25) \text{ }^\circ\text{C}) * 2.77 * 10^{-7} \text{ kWh/J}$$

$$\Rightarrow Q = 0.008 \text{ kWh (for normalization 1)}$$

$$Q2 = (995.6 \text{ g} * 1.72 \text{ J/g} \cdot \text{K} * (50-25) \text{ }^\circ\text{C}) * 2.77 * 10^{-7} \text{ kWh/J}$$

$$\Rightarrow Q = 0.012 \text{ kWh (for normalization 1)}$$

This energy is used to increase the temperature of the solution. However, more energy is required to evaporate tetrahydrofuran inside the pore. Therefore, by using latent heat of tetrahydrofuran which is 459.02 kJ/kg (Stephenson, 2012), the required energy is calculated.

$$Q1 \text{ for Evaporation} = (459.02 \text{ kJ/kg} * 0.672 \text{ kg} * 1000 \text{ J/kJ}) * 2.77 * 10^{-7} \text{ kWh/J}$$

$$\Rightarrow Q = 0.09 \text{ kWh (for normalization 1)}$$

$$Q2 \text{ for Evaporation} = (459.02 \text{ kJ/kg} * 0.996 \text{ kg} * 1000 \text{ J/kJ}) * 2.77 * 10^{-7} \text{ kWh/J}$$

$$\Rightarrow Q = 0.13 \text{ kWh (for normalization 2)}$$

$$\text{Total Heat Energy for Normalization 1} = (0.008+0.09) \text{ kWh} = 0.1 \text{ kWh}$$

$$\text{Total Heat Energy for Normalization 2} = (0.012+0.13) \text{ kWh} = 0.14 \text{ kWh}$$

### Heat Energy for Drying 1

The same theory is valid for this step. By using porosity information, the volume of chemicals that are held in the fiber pores can be calculated. After grafting, fiber volume is 4479.16 mL and 6640.75 mL in the normalized condition 1 and 2, respectively, and 71% of them are equal to 3180.2 mL and 4714.93 mL. That is, these calculated amounts of methanol stay inside the fiber, and the main objective in drying is removing this methanol, but the mass of methanol must be estimated by using density information first, and these are listed as 2518.72 g and 3734.23 g respectively. Then,

the required heat applied for methanol is calculated by using the same formula, and these steps are given below.

$$Q1 = (2518.72 \text{ g} * 2.48 \text{ J/g} \cdot \text{K} * (60-25) \text{ }^\circ\text{C}) * 2.77 * 10^{-7} \text{ kWh/J}$$

$$\Rightarrow Q = 0.06 \text{ kWh (for normalization 1)}$$

$$Q2 = (3734.23 \text{ g} * 2.48 \text{ J/g} \cdot \text{K} * (60-25) \text{ }^\circ\text{C}) * 2.77 * 10^{-7} \text{ kWh/J}$$

$$\Rightarrow Q = 0.09 \text{ kWh (for normalization 2)}$$

The energy calculated above is not enough to evaporate methanol, it is just used to increase the temperature of methanol solution from 20°C to 60°C. Therefore, the latent heat of evaporation of methanol value should be known to estimate the required heat for evaporation, and this value is given as 1087 kJ/kg (Anand et al., 2011). Additional heat value is estimated below.

$$Q1 \text{ for Evaporation} = (1087 \text{ kJ/kg} * 2.519 \text{ kg} * 1000 \text{ J/kJ}) * 2.77 * 10^{-7} \text{ kWh/J}$$

$$\Rightarrow Q = 0.76 \text{ kWh (for normalization 1)}$$

$$Q2 \text{ for Evaporation} = (1087 \text{ kJ/kg} * 3.734 \text{ kg} * 1000 \text{ J/kJ}) * 2.77 * 10^{-7} \text{ kWh/J}$$

$$\Rightarrow Q = 1.12 \text{ kWh (for normalization 2)}$$

$$\text{Total Heat Energy for Normalization 1} = (0.06+0.76) \text{ kWh} = 0.82 \text{ kWh}$$

$$\text{Total Heat Energy for Normalization 2} = (0.09+1.12) \text{ kWh} = 1.21 \text{ kWh}$$

### Heat Energy for Drying 2

To calculate the volume of the polyethylene fiber after the second methanol washing, it has been assumed that the initial density of fiber is constant which is 0.941 g/cm<sup>3</sup>. Then, by using the mass and density information, fiber volume has been estimated as 5315.94 mL and 7881.35 mL for normalization 1 and 2, respectively. Also, the porosity of fiber has been assumed again to be the same as the initial condition (0.71). Then, by using the fiber volume and porosity information, the volume of methanol which is held inside the fiber has been estimated as 3774.32 mL and 5595.76 mL for normalization 1 and 2. Moreover, the mass of methanol was calculated as 2989.26 g

and 4431.84 g. Finally, the required heat to increase methanol temperature from 20 °C to 50 °C can be estimated as below.

$$Q1 = (2989.26 \text{ g} * 2.48 \text{ J/g} * \text{K} * (50-25) \text{ } ^\circ\text{C}) * 2.77 * 10^{-7} \text{ kWh/J}$$

$$\Rightarrow Q = 0.05 \text{ kWh (for normalization 1)}$$

$$Q2 = (4431.84 \text{ g} * 2.48 \text{ J/g} * \text{K} * (50-25) \text{ } ^\circ\text{C}) * 2.77 * 10^{-7} \text{ kWh/J}$$

$$\Rightarrow Q = 0.08 \text{ kWh (for normalization 2)}$$

Then, the required energy for evaporation is calculated below.

$$Q1 \text{ for Evaporation} = (1087 \text{ kJ/kg} * 2.989 \text{ kg} * 1000 \text{ J/kJ}) * 2.77 * 10^{-7} \text{ kWh/J}$$

$$\Rightarrow Q = 0.9 \text{ kWh}$$

$$Q2 \text{ for Evaporation} = (1087 \text{ kJ/kg} * 4.431 \text{ kg} * 1000 \text{ J/kJ}) * 2.77 * 10^{-7} \text{ kWh/J}$$

$$\Rightarrow Q = 1.334 \text{ kWh}$$

$$\text{Total Heat Energy for Normalization 1} = (0.05+0.9) \text{ kWh} = 0.95 \text{ kWh}$$

$$\text{Total Heat Energy for Normalization 2} = (0.08+1.334) \text{ kWh} = 1.41 \text{ kWh}$$

Then, all the information which is related to the energy calculation is given in Table 3.7.

### Irradiation Energy

Irradiation energy is used to prepare polyethylene fiber for grafting. In the Oyola and Dai study, the RDI Dynamitron electron beam machine was used, and irradiation conditions are listed in the supporting information of this article (2016). By using approximate total dose information which is 200 kGy and machine efficiency which is specified as 0.3 (Zimek, 2018), required energy has been calculated and shown below.

$$\text{Total Irradiation Energy for Normalization 1} = (200 \text{ kGy} / 0.3) * 1 \text{ kg} = 666.7 \text{ kJ}$$

$$\Rightarrow 666.7 \text{ kJ} / (3600 \text{ kJ/kWh}) = 0.19 \text{ kWh}$$

Total Irradiation Energy for Normalization 2 = (200 kGy / 0.3) \* 1.48 kg = 986.7 kJ

⇒ 986.7 kJ / (3600 kJ/kWh) = 0.3 kWh

As a result of this calculation, the overall energy for AF1 adsorbent production is listed in Table 3.7.

Table 3.7: Energy Requirement and Operational Temperature Values for AF1 Adsorbent Production Processes

Process Name	Temperature	Energy Values for 1 kg Polyethylene	Energy Values for 1 kg Uranium
Submerging	60 °C	0.04 kWh	0.06 kWh
Grafting	60 °C	0.51 kWh	0.76 kWh
Amidoximation	70 °C	20.70 kWh	30.69 kWh
KOH Conditioning	70 °C	148.64 kWh	220.37 kWh
Drying After Submerging	50 °C	0.10 kWh	0.14 kWh
Drying After Washing 1	50-60 °C	0.82 kWh	1.21 kWh
Drying After Washing 2	50-60 °C	0.95 kWh	1.41 kWh
Irradiation		0.2 kWh	0.3 kWh
<b>Total Energy (kWh)</b>		<b>171.9 kWh</b>	<b>254.9 kWh</b>

#### 3.2.2.1.1.4 Adsorbed Uranium Calculations for AF1 Adsorbent

In the paper provided by Oyola and Dai (2016), after 11 weeks, 4.72 g U was obtained by using a 1 kg adsorbent. However, this was the just first use of adsorbent. After the desorption process, the adsorbent can be reused. Also, it is specified that no more than 50 uses of the same adsorbent are economically feasible (Flicker Byers & Schneider, 2016). Therefore, to be able to reach the optimum cycle number, the breakthrough curve is drawn by considering a 3% loss after every use, and the optimum cycle or reuse number has been accepted as 40 cycles. The related curve is given in Figure 3.3

Then, 110.81 g uranium can be obtained by using 1 kg adsorbent after the 40th usage based on the results presented in Figure 3.3. Moreover, even if the biofouling effect seems to be omitted, it has been considered from the beginning of this calculation and has affected the other part of the uranium capacity calculation since the initial value of adsorbent capacity is low depending on this effect.

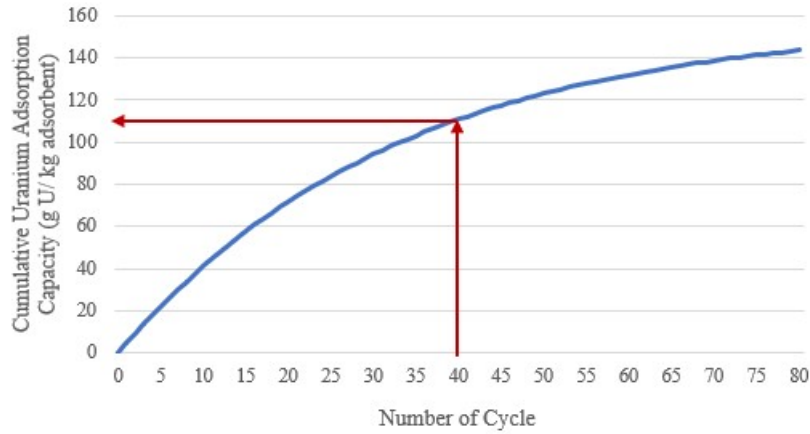


Figure 3.3: Breakthrough Curve for Optimum Cycle of AF1 Adsorbent

### 3.2.2.1.2 PAN-AO Adsorbent Calculations

In the uranium extraction from the brine field, other adsorbent types such as polyacrylonitrile-based can be used. This method requires a fewer amount of chemicals, and competition between uranium and vanadium is less compared to the first adsorbent type (Pan et al., 2020). Some parameters and variables which have been used during input and output calculations are listed in Table 3.8.

Table 3.8: Given Parameters and Variables in the Literature for PAN Adsorbent

Name of Chemical	Required Amount	Reference
The density of PAN Fiber	1.18 g/cm <sup>3</sup>	(Ko et al., 1988)
The porosity of PAN Fiber	0.76	(Moradi et al., 2019)
Polyacrylonitrile fiber (PAN)	0.4 g	
Amidoximation Degree	1.9 mmol/g	
Conversion Ratio	10.8%	
Hydroxylamine	1.05 g	(H. Zhao et al., 2015)
Methanol/Water	60 mL water (= 60 g) 40 mL methanol (= 31.6 g)	
Sodium Hydroxide	0.6 g	
PAN Fiber Specific Heat Value (J/g*°C)	0.75	(Athanasopoulos et al., 2012)
Sodium Hydroxide Specific Heat Value (J/g*°C)	1.49	(Chase, 1996)
Latent Heat of Water (kJ/kg)	2358	(Ayoub et al., 2014)

### 3.2.2.1.2.1 Mass Calculations

By using density information of water and methanol, the required mass of these substances can be calculated as below.

$$\rho_{water} = 1 \text{ g/cm}^3 \text{ at } 25 \text{ }^\circ\text{C}$$

$$\Rightarrow \text{mass of water} = 1 \text{ g/cm}^3 * 60 \text{ mL} = 60 \text{ g}$$

$$\rho_{methanol} = 0.79 \text{ g/cm}^3 \text{ at } 25 \text{ }^\circ\text{C} \text{ (Albaiti et al., 2016)}$$

$$\Rightarrow \text{mass of methanol} = 0.79 \text{ g/cm}^3 * 40 \text{ mL} = 31.68 \text{ g}$$

Then, the final mass of the adsorbent can be calculated by putting the presented amidoximation degree (AOGD) value as 1.9 mmol/g in the article conducted by Zhao et al. (2015) into the equation (3.2). This step is shown below.

$$1.9 \text{ mmol/g} = ((Wt - 0.4 \text{ g}) * 1000) / (Wt * 33 \text{ g/mole})$$

$$\Rightarrow Wt = 0.43 \text{ g}$$

That is, 0.4 g PAN is used to produce 0.43 g PAN-AO fiber.

Also, the required hydroxylamine amount has been already given in Table 3.8. After all these reaction steps, PAN-AO fiber should be washed with deionized water to remove the remaining salts (H. Zhao et al., 2015). In this article, there is no information about the volume or amount of this water. After the density of fiber has been assumed as the same as the initial value which is 1.18 g/cm<sup>3</sup>, the volume of fiber has been calculated as 0.5 mL and the required distilled water volume has been assumed as 2.5 mL by considering the calculated volume of fiber. Again, all these chemicals have been arranged for two normalization conditions which are 1 kg PAN-AO adsorbent usage and 1 kg U production. The related ratio which was explained in the "AF1 Adsorbent Calculations" part is 2500 for the first normalization scenario, and this value is equal to 14933.9 for the second one. That is, the input values calculated and/or presented in literature should be multiplied by these ratios to create an inventory for both normalization cases. During this calculation, 6.02 g U / kg adsorbent of uranium adsorption capacity has been used (Pan et al., 2020), and a detailed calculation of

adsorbed uranium will be discussed in the following part. Finally, overall inputs consumed for PAN-AO adsorbent production are listed in Table 3.9 for all normalization cases.

Table 3.9: The Amount of Chemicals Required for PAN-AO Adsorbent Production for All Normalization Cases

Name of Chemical	Required Amount for Normalized Article Values	Normalized Amount for 1 kg PAN-AO	Normalized Amount for 1 kg U Production
PAN Fiber	0.4 g	1 kg	5.97 kg
Hydroxylamine	1.05 g	2.63 kg	15.68 kg
Methanol	31.68 g	79.20 kg	473.11 kg
Deionised Water	60 g	150 kg	896.03 kg
Sodium Hydroxide	0.60 g	1.50 kg	8.96 kg
Distilled Water	2.50 g	1.26 kg	7.52 kg

### 3.2.2.1.2.2 Adaptation of Experimental Values to Realistic Values

The same procedure for adaptation of calculated experimental values with linear scale-up has been applied for PAN-AO adsorbent.

#### Real Hydroxylamine Value

In this part, the conversion factor is given as 10.8 % in the article (H. Zhao et al., 2015). Therefore, the real hydroxylamine amount was estimated by multiplying this number by the previous mass of hydroxylamine which is 2.625 kg and 15.681 kg for normalized situations. Therefore, the real mass of hydroxylamine was calculated as 0.284 kg and 1.694 kg for them. These are the masses that were used in the system modeling via SimaPro 9.2.0.1.(PhD version).

### 3.2.2.1.2.3 Energy Calculations

In PAN-AO adsorbent preparation, energy is required for amidoximation and drying steps to increase temperature, and the calculation steps of the required energy for these processes are the same as the AF1 adsorbent energy calculation part.

### Heat for Amidoximation

The heating energy calculations are shown below. During this process, the temperature is increased from 25°C to 70°C (H. Zhao et al., 2015).

$$*Q1 \text{ for PAN fiber} = (1000 \text{ g} * 0.75 \text{ J/g}^{\circ}\text{C} * (70-25) \text{ }^{\circ}\text{C}) * 2.77 * 10^{-7} \text{ kWh/J}$$

$$\Rightarrow Q1 = 0.01 \text{ kWh (for normalization 1)}$$

$$Q2 \text{ for PAN fiber} = (5974 \text{ g} * 0.75 \text{ J/g}^{\circ}\text{C} * (70-25) \text{ }^{\circ}\text{C}) * 2.77 * 10^{-7} \text{ kWh/J}$$

$$\Rightarrow Q2 = 0.06 \text{ kWh (for normalization 2)}$$

$$*Q1 \text{ for Hydroxylammonium} = (2625 \text{ g} * 1.42 \text{ J/g}^{\circ}\text{C} * (70-25) \text{ }^{\circ}\text{C}) * 2.77 * 10^{-7} \text{ kWh/J} \Rightarrow Q1 = 0.05 \text{ kWh (for normalization 1)}$$

$$Q2 \text{ for Hydroxylammonium} = (15681 \text{ g} * 1.42 \text{ J/g}^{\circ}\text{C} * (70-25) \text{ }^{\circ}\text{C}) * 2.77 * 10^{-7} \text{ kWh/J} \Rightarrow Q2 = 0.28 \text{ kWh (for normalization 2)}$$

$$*Q1 \text{ for methanol} = (79200 \text{ g} * 2.48 \text{ J/g}^{\circ}\text{C} * (70-25) \text{ }^{\circ}\text{C}) * 2.77 * 10^{-7} \text{ kWh/J}$$

$$\Rightarrow Q1 = 2.45 \text{ kWh (for normalization 1)}$$

$$Q2 \text{ for methanol} = (473106 \text{ g} * 2.48 \text{ J/g}^{\circ}\text{C} * (70-25) \text{ }^{\circ}\text{C}) * 2.77 * 10^{-7} \text{ kWh/J}$$

$$\Rightarrow Q2 = 14.63 \text{ kWh (for normalization 2)}$$

$$*Q1 \text{ for water} = (150000 \text{ g} * 4.18 \text{ J/g}^{\circ}\text{C} * (70-25) \text{ }^{\circ}\text{C}) * 2.77 * 10^{-7} \text{ kWh/J}$$

$$\Rightarrow Q1 = 7.82 \text{ kWh (for normalization 1)}$$

$$Q2 \text{ for water} = (896033 \text{ g} * 4.18 \text{ J/g}^{\circ}\text{C} * (70-25) \text{ }^{\circ}\text{C}) * 2.77 * 10^{-7} \text{ kWh/J}$$

$$\Rightarrow Q2 = 46.69 \text{ kWh (for normalization 2)}$$

$$*Q1 \text{ for sodium hydroxide} = (1500 \text{ g} * 4.18 \text{ J/g}^{\circ}\text{C} * (70-25) \text{ }^{\circ}\text{C}) * 2.77 * 10^{-7} \text{ kWh/J}$$

$$\Rightarrow Q1 = 0.03 \text{ kWh (for normalization 1)}$$

$$Q2 \text{ for sodium hydroxide} = (8960 \text{ g} * 4.18 \text{ J/g}^{\circ}\text{C} * (70-25) \text{ }^{\circ}\text{C}) * 2.77 * 10^{-7} \text{ kWh/J}$$

$$\Rightarrow Q2 = 0.17 \text{ kWh (for normalization 2)}$$

$$\text{Total Heat Energy for Normalization 1} = (0.01+0.05+2.45+7.82+0.03) \text{ kWh}$$

$$\Rightarrow Q1 = 10.35 \text{ kWh}$$

Total Heat Energy for Normalization 2 = (0.06+0.28+14.63+46.69+0.17) kWh

$$\Rightarrow Q2 = 61.81 \text{ kWh}$$

### Heat Energy for Drying

To calculate the volume of the PAN fiber after distilled water washing, it has been assumed that the initial density of fiber which is  $1.18 \text{ g/cm}^3$  is constant. Then, by using the mass and density information, fiber volume has been estimated as 1258.94 mL and 7520.32 mL for normalization 1 and 2, respectively. Also, the porosity of fiber has been assumed again to be the same as the initial condition value (0.76) presented in Table 3.8. Then, the volume of distilled water which is held inside the fiber has been calculated as 956.79 mL and 5715.44 mL for normalization 1 and 2 by using the fiber volume and porosity information and mass of distilled water that should be heated and evaporated in the gram unit is equal to these volume results. Finally, the required heat to increase water temperature from  $20 \text{ }^\circ\text{C}$  to  $60 \text{ }^\circ\text{C}$  can be estimated below.

$$Q1 = (956.79 \text{ g} * 2.48 \text{ J/g} * \text{K} * (60-25) \text{ }^\circ\text{C}) * 2.77 * 10^{-7} \text{ kWh/J}$$

$$\Rightarrow Q1 = 0.04 \text{ kWh (for normalization 1)}$$

$$Q2 = (5715.44 \text{ g} * 2.48 \text{ J/g} * \text{K} * (60-25) \text{ }^\circ\text{C}) * 2.77 * 10^{-7} \text{ kWh/J}$$

$$\Rightarrow Q2 = 0.23 \text{ kWh (for normalization 2)}$$

Then, the required energy for the evaporation of water is estimated below.

$$Q1 \text{ for Evaporation} = (2358 \text{ kJ/kg} * 0.957 \text{ kg} * 1000 \text{ J/kJ}) * 2.77 * 10^{-7} \text{ kWh/J}$$

$$\Rightarrow Q1 = 0.62 \text{ kWh}$$

$$Q2 \text{ for Evaporation} = (2358 \text{ kJ/kg} * 5.715 \text{ kg} * 1000 \text{ J/kJ}) * 2.77 * 10^{-7} \text{ kWh/J}$$

$$\Rightarrow Q2 = 3.73 \text{ kWh}$$

Total Heat Energy for Normalization 1 = (0.04+0.62) kWh  $\Rightarrow$  Q1 = 0.66 kWh

Total Heat Energy for Normalization 2 = (0.23+3.73) kWh  $\Rightarrow$  Q2 = 3.96 kWh

Related energy data and normalized versions of them to produce PAN-AO adsorbent are listed in Table 3.10

Table 3.10: Energy Requirement and Operational Temperature Values for PAN-AO Adsorbent Production Processes

Process Name	Temperature	Energy Values for 1 kg PAN-AO	Energy Values for 1 kg U Production
Amidoximation	70 °C	10.35 kWh	61.81 kWh
Drying	60 °C	0.66 kWh	3.96 kWh
Total Energy		<b>11.01 kWh</b>	<b>65.8 kWh</b>

#### 3.2.2.1.2.4 Adsorbed Uranium Calculations for PAN-AO Adsorbent

The results provided by Pan et al.'s (2020) article revealed that after 56 days, 6.02 g U was obtained by using a 1 kg PAN-AO adsorbent. However, this result was obtained after using this adsorbent only once. After the desorption process, the adsorbent can be reused. Also, no more than 50 uses of the same amidoximated adsorbent for uranium recovery purposes are economically feasible as specified in the literature (Flicker Byers & Schneider, 2016). Therefore, the breakthrough curve has been drawn by considering a 3% loss after every use to reach the optimum cycle number for PAN-AO adsorbent, and the optimum cycle or reuse number has been accepted as 50 cycles. The related curve is presented in Figure 3.4.

The results declare that 156.9 g uranium can be obtained by using 1 kg adsorbent after the 50th usage based on the results presented in Figure 3.4. Also, the inclusion of the biofouling effect is valid for this adsorbent.

#### 3.2.2.2 Elution Process Selection and Estimation

##### 3.2.2.2.1 Elution Process Selection

Until this point, only the adsorption step has been considered. However, the desorption process must be applied to obtain uranium as yellowcake. In literature, various

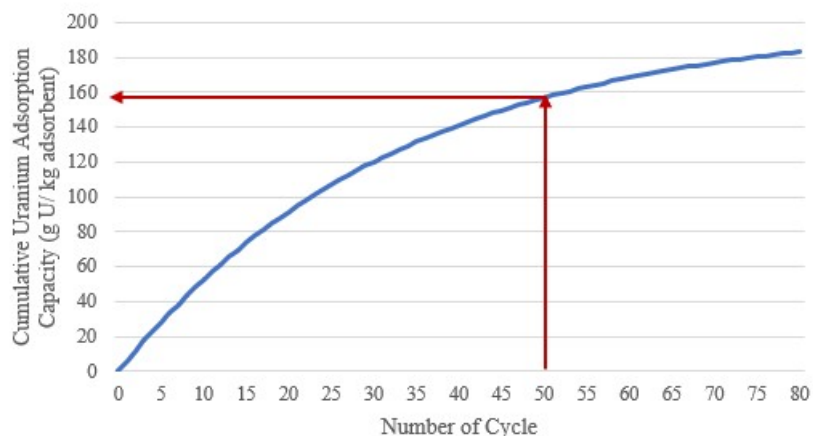


Figure 3.4: Breakthrough Curve for Optimum Cycle for PAN-AO Adsorbent

techniques are used for this purpose. Detailed information about them is listed in Table 3.11 by comparing all these methods. If HCl elution has been chosen as a uranium desorption method, amidoximated adsorbent material can be used no more than 5-6 cycles because of the acid damage on it, and physical damage can be seen after even 3 cycles (Seko et al., 2004). Also, conditioning is required in every cycle after applying HCl elution (C. M. Wai, 2017). Therefore, this method has not been preferred for our study since the desired recycling ratios for both adsorbent scenarios cannot be achieved. Since the third method is the most environmentally friendly and also is a cost-effective method to desorb the uranium from the amidoximated fiber,  $\text{KHCO}_3 + \text{NaOH}$  soaking was chosen as an elution method or chemical based on the information presented in Table 3.11. Furthermore, NaOH is used for the removal of natural organic matters (NOM) in this method, but in our case, since we deal with the brine produced from desalination plants, most natural organic matters had been dissociated already (Wongsawaeng et al., 2021).

### 3.2.2.2.2 Required Eluant Amount Estimation

In the article presented by Pan et al. (2017), the molarity of potassium bicarbonate required for uranium elution is given as 3 M, but there is no information about the volume of this chemical. In the study by Flicker Byers et al., (2018), a similar system to our work was tested in the natural environment. The same adsorbent (AF1 adsorbent)

Table 3.11: Pros and Cons of Uranium Elution Methods and Their Experimental Conditions

Elution Method	Pros and Cons	Chemical Consumption and Condition	Reference
Acid Leaching with HCl	<ul style="list-style-type: none"> <li>*Causing shrinkage of polymeric adsorbents</li> <li>*Before reuse, the necessity for alkaline conditioning</li> <li>*Physical damage to polymer fibers</li> </ul>	<ul style="list-style-type: none"> <li>*10 mL 0.02M HCl for 0.1 g of dried fiber at 30 °C for 2 hours (Mg and Ca elution)</li> <li>*10 mL 0.05M HCl for 0.1 g of dried fiber at 30 °C for 2 hours (Ni, Mn, and Zn elution)</li> <li>*5 mL 0.05M HCl + 5% w/v L-ascorbic acid (0.25g) for 0.05 g of dried fiber at 30 °C for 2 hours (Fe elution ) *</li> <li>0.05 M HCl + 1 % thiourea (x / 100) for dried fiber at 30 °C for 2 hours (Cu elution)</li> <li>* 0.5 M HCl for dried fiber at 30 °C for 2 hours (U elution)</li> </ul>	<ul style="list-style-type: none"> <li>(J. Kim et al., 2013) (Kuo et al., 2017) (Suzuki et al., 2000)</li> </ul>
The mixture of Na <sub>2</sub> CO <sub>3</sub> and H <sub>2</sub> O <sub>2</sub>	<ul style="list-style-type: none"> <li>*Milder than acid elution</li> <li>*Decreasing uranium capacity because of H<sub>2</sub>O<sub>2</sub> existence</li> <li>*After the elution adsorbent was digested in aqua regia (3HCl:HNO<sub>3</sub>) at 85 °C</li> <li>*Other ions can be eluted in this way, but it has less number compared to the third option.</li> <li>*The pH of Na<sub>2</sub>CO<sub>3</sub> is different from the seawater pH</li> </ul>	<ul style="list-style-type: none"> <li>*10 mL 1 M Na<sub>2</sub>CO<sub>3</sub> for 20 mg fiber at room temperature</li> <li>*10 mL 0.1 M H<sub>2</sub>O<sub>2</sub> for 20 mg fiber at room temperature</li> <li>*0.5 M Tiron should be used for iron removal</li> <li>* 1:1 glutarimidedioxime and vanadium ions for vanadium removal from solution</li> </ul>	<ul style="list-style-type: none"> <li>(Kuo et al., 2017)(C. M. Wai, 2017) (Pan et al., 2014)</li> </ul>
KHCO <sub>3</sub> + NaOH soaking	<ul style="list-style-type: none"> <li>*Extremely mild to the adsorbent because of the pH closeness with seawater</li> <li>*Cost-effective</li> <li>*Environmentally friendly</li> <li>*No need for hot alkaline treatment for reuse</li> <li>*Most of the ions can be eluted in this way</li> <li>*The pH of KHCO<sub>3</sub> is closer to the seawater pH (pH is important to occur good or stable form of uranium carbonate ions.)</li> </ul>	<ul style="list-style-type: none"> <li>*10 mL 3 M KHCO<sub>3</sub> for 20 mg fiber at 20 °C for 24 hours</li> <li>* 0.5 M NaOH for fiber at room temperature for DOM removal</li> </ul>	<ul style="list-style-type: none"> <li>(Kuo et al., 2017) (C. M. Wai, 2017) (Pan et al., 2017) (Pan et al., 2015)</li> </ul>

and same elution method were chosen in this article. Therefore, the parameters listed in this article have been used for the required potassium bicarbonate calculation and the ratio of used chemicals for the 1 tonne of adsorbent was specified as 0.03. That is, 30 kg  $\text{KHCO}_3$  solution is required for 1000 kg of adsorbent (Byers et al., 2018). Then, by using this relation and calculated fiber mass information which is 6.09 kg and 9.02 kg for AF1 first and second normalization, the required potassium bicarbonate amounts have been calculated as 0.047 g and 0.07 g. Also, the mass ratio between water and  $\text{KHCO}_3$  has been found via the trial-and-error method by using 3 M information. Then, the required water masses for AF1 normalization scenarios have been calculated as 0.14 g and 0.2 g. However, these chemicals are used for only 1 cycle, but as explained in the "Adsorbed Uranium Calculations for AF1 Adsorbent" part, AF1 adsorbent material will be used 40 times in this study. Therefore, the required chemical amount should be multiplied by 40, and the final potassium bicarbonate amount can be written as 1.89 kg and 2.8 kg for AF1 normalization cases. Also, overall water requirements have been estimated as 5.42 kg and 8.03 kg for 40 cycles for them. Finally, by using density information of water and potassium bicarbonate, the overall volume of elution solution has been calculated as 6.29 L and 9.32 L.

Then, the same steps have been followed for the PAN-AO adsorbent, and the required  $\text{KHCO}_3$  amount has been estimated as 0.39 kg and 2.47 kg for the first and second normalization cases. Then, the amount of water has been estimated as 1.11 kg and 7.09 kg.

The total amount of potassium bicarbonate solution used in the elution of uranium from AF1 and PAN-AO adsorbent is summarized in Table 3.14 for both normalization scenarios.

### **3.2.2.2.3 Purification by Vanadium Elution from Concentrated Solution**

After elution, the obtained solution purity is not high because of the competing ion which is vanadium (Yuan et al., 2021). That is, vanadium is another ion that is adsorbed via amidoximated adsorbent. While adsorbed vanadium amount is equal to 15.33 g per 1 kg AF1 adsorbent (Oyola & Dai, 2016), this amount is 6.38 g for PAN adsorbent (Pan et al., 2020). Moreover, 33% of adsorbed vanadium can be eluted

with potassium bicarbonate solution (C. M. Wai, 2017). That is, 0.7 kg and 1.1 kg vanadium can be eluted via AF1 adsorbent for normalization 1 and 2, respectively under these circumstances. On the other hand, in PAN adsorbent normalization 1 and 2 cases 0.06 kg and 0.35 kg vanadium can be obtained. Vanadium must be removed from the solution to increase the uranium content of the solution to make a fair comparison with conventional methods. In the literature precipitation, solvent extraction, and ion exchange are the most common methods to extract vanadium from distinct leach liquors (Cheira, 2020). Their advantages and disadvantages are listed in Table 3.12.

Table 3.12: Vanadium Elution Methods Comparison

Name of Method	Precipitation	Solvent Extraction	Ion Exchange	References
Efficiency	Low	High	Low	(Z. Zhu et al., 2013)
Selectivity	Low	High	Low	(Shi et al., 2017) (Z. Zhu et al., 2013)
Cost	Cheap	Medium	Costly	(Sole et al., 2011) (Udayar et al., 2013) (Zhang et al., 2014) (Z. Zhu et al., 2013)
Operation	Simple	Medium and Fast Kinetics	Hard and Slow Kinetics	(Sole et al., 2011) (Zhang et al., 2014) (Z. Zhu et al., 2013)

By considering the information presented in Table 3.12, solvent extraction has been chosen as an elution technique from the pregnant solution because efficiency and selectivity are more important criteria for this study. Moreover, different chemicals are used to extract vanadium depending on the characteristics of the solution. To illustrate, vanadium can be extracted from acidic solution using phosphorous based extractants such as di(2-ethylhexyl) phosphoric acid (D2EHPA), tri-n-octyl-phosphine oxide (TOPO or Cyanex 923) and tri-butyl-phosphate (TBP) (J. Kumar et al., 2010). Among these materials, D2EHPA is the most common extractant type to remove vanadium (Alibrahim et al., 2008). However, since in the adsorbent elution step of this study potassium bicarbonate that contributes to the solution alkalinity increase is used, suitable extractants should be used to remove vanadium from the alkaline solution. In the vanadium removal from alkaline media quaternary amines like Alamine 336 or Aliquat 336 can be used at room temperature (El-Nadi et al., 2009) (J. Kumar et al., 2010). Third phase formation is one of the biggest problems in this technique because it causes the efficiency reduction (Crouse, 1956). However, by using con-

venient modifiers like isodecanol, this effect can be minimized (Z. Zhu et al., 2013). For this study, the steps or chemicals presented in the article presented by Zhu et al. (2013) have been analyzed. Organic media including Aliquat and isodecanol in Shell-sol D70 was developed and ammonium sulfate and sodium bicarbonate were used to scrub uranium and vanadium from the solution, respectively based on the information presented in this article.

### Chemical Requirements for Uranium and Vanadium Separation

The required mass calculation has been completed by considering the given aqueous/organic or A:O ratio and other values listed in Table 3.13 in the article discussed by Zhu et al. (2013).

Table 3.13: Chemical Used in Uranium and Vanadium Separation from Alkaline Media (Z. Zhu et al., 2013)

<b>Name of Chemicals</b>	<b>Value</b>
A:O ratio for 3% Aliquat 336 & 3% Isodecanol in Shellsol D70	10:01
Density of Sodium Carbonate (g/L)	50
The density of Ammonium Sulfate (g/L)	150

By using the A:O ratio and volume of  $\text{KHCO}_3$  solution used for uranium elution from amidoximated fiber and calculated in the "Required Eluant Amount Estimation" part, the overall volume of the organic solution has been calculated as 0.63 L and 0.93 L for AF1 both normalization cases. Then, the required masses of these chemicals have been estimated as 0.019 kg and 0.028 kg by using the 3% relationship for them. Also, by using density information of Aliquat 336 which is  $\rho_{\text{Aliquat336}} = 0.88 \text{ g/cm}^3$  (Mikkola et al., 2006) and isodecanol which is  $\rho_{\text{isodecanol}} = 0.84 \text{ g/cm}^3$  (Mirci, 2009), volumes of these chemicals have been found and these value have been used for volume of Shellsol D70 solution. The amount of required Shellsol D70 solution have been found as 0.47 kg and 0.69 kg by using density of Shellsol D70 which is  $\rho_{\text{ShellsolD70}} = 0.796 \text{ g/cm}^3$  for AF1 normalization scenarios (Soldenhoff et al., 2005). Then, the required sodium carbonate and ammonium sulfate amounts have been estimated by using the density information given in Table 3.13 and the total organic

phase volume. Finally, while the required sodium carbonate amount can be listed as 0.031 kg and 0.047 kg, ammonium sulfate requirements have been estimated as 0.094 kg and 0.140 kg for both normalization cases.

The same procedure has been followed for PAN adsorbent, and the results of required chemicals for vanadium and uranium separation from alkaline media are also summarized in Table 3.14.

Table 3.14: Summary of Chemical Amounts Required for Carbonate Elution and Vanadium and Uranium Separation for AF1 and PAN Adsorbents and both Normalization Cases

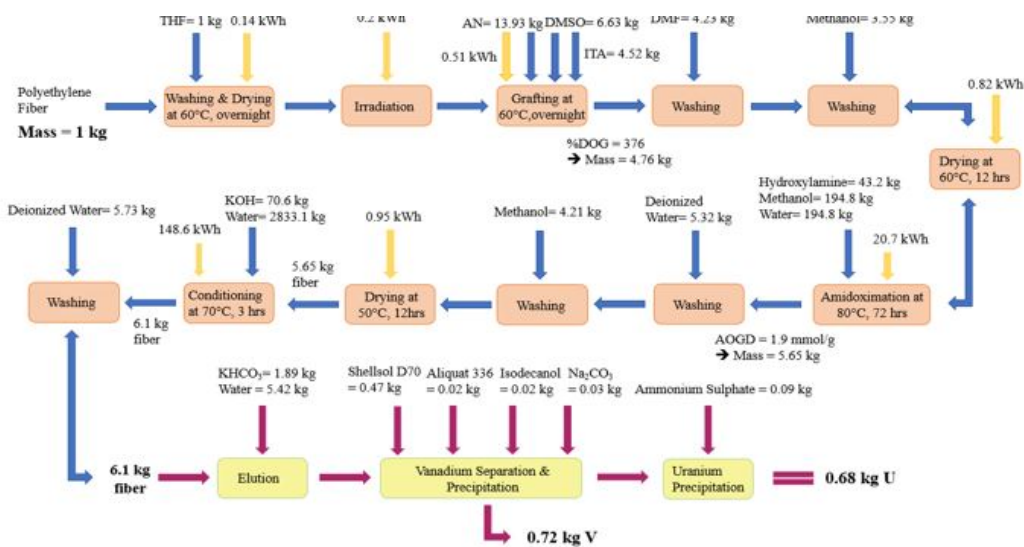
Name of Chemicals	AF1 Adsorbent		PAN Adsorbent	
	Normalization 1	Normalization 2	Normalization 1	Normalization 2
Potassium Bicarbonate	1.89 kg	2.80 kg	0.41 kg	2.47 kg
Water	5.42 kg	8.03 kg	1.19 kg	7.09 kg
Aliquat 336	0.02 kg	0.03 kg	0.004 kg	0.025 kg
Isodecanol	0.02 kg	0.03 kg	0.004 kg	0.03 kg
Shellsol D70	0.47 kg	0.62 kg	0.1 kg	0.61 kg
Ammonium Sulfate	0.09 kg	0.14 kg	0.02 kg	0.12 kg
Sodium Carbonate	0.03 kg	0.05 kg	0.006 kg	0.04 kg

The required amount of chemicals, energy, and process steps to produce uranium from brine via AF1 adsorbent are shown in the case of both normalization scenarios in Figure 3.5.

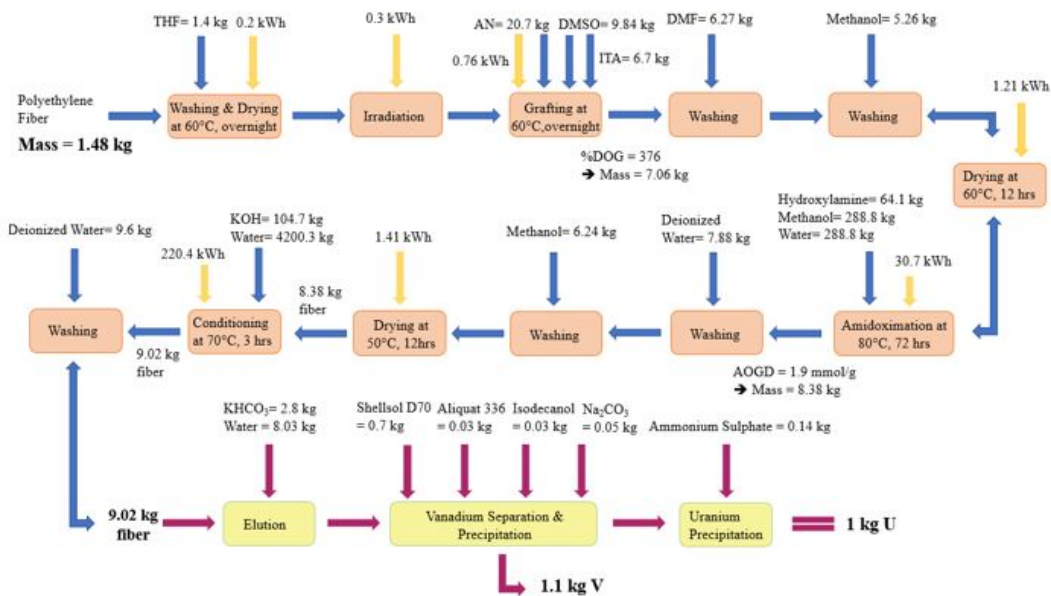
All the relevant items required for uranium production from brine via PAN-AO adsorbent in the case of normalization 1 and 2 are summarized in Figure 3.6.

### 3.2.2.3 Disposal Calculations

Waste characteristics that are created during the uranium recovery from brine processes and their treatment methods are listed in Table 3.15. It is claimed that incineration can be a common disposal solution for all these chemicals based on the information presented in this table.



(a)



(b)

Figure 3.5: Process Steps and Chemicals and Energy Requirements of AF1 Adsorbent Production for Normalization 1 (a) & Normalization 2 (b)

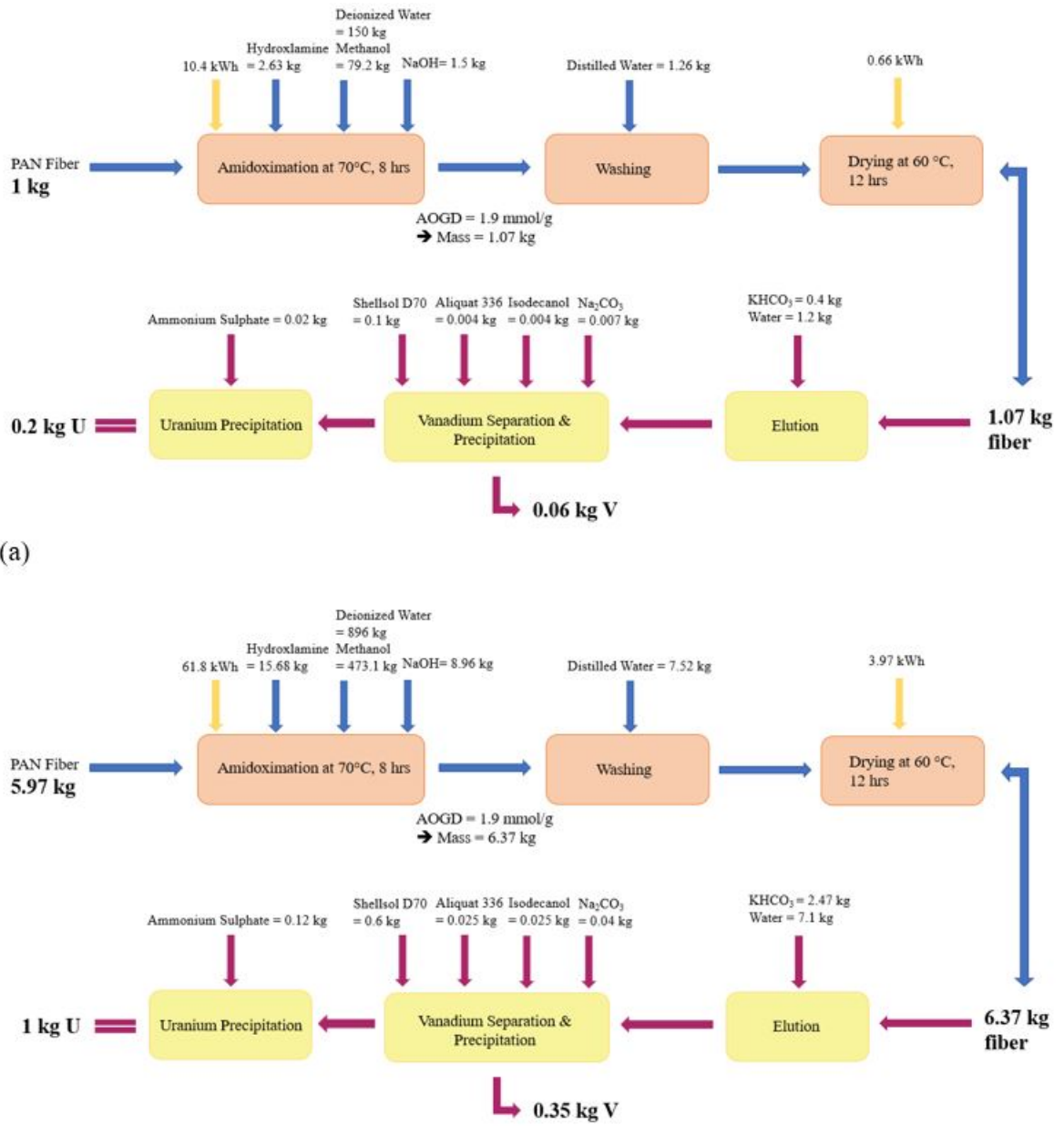


Figure 3.6: Process Steps and Chemicals and Energy Requirements of PAN-AO Adsorbent Production for Normalization 1 (a) and Normalization 2 (b)

Table 3.15: Disposal Methods of Waste Produced from Uranium Recovery from Brine Processes

Name of Chemical	Characteristics	Treatment Method	Reference
Dimethyl Formamide	Organic Solvent Waste	Incineration	(Long et al., 2001)
Methanol	Hazardous Waste	Incineration	(U. E. P. Agency, 2006)
Acrylonitrile	Hazardous Waste	Incineration	(Bonner et al., 1981) (U. E. P. Agency, 2006)
Dimethyl Sulfoxide	Organic Solvent Waste	Incineration	(Amelio et al., 2014)
Itaconic Acid	Organic Waste	Incineration	(Steiger et al., 2013)
Hydroxylamine	Inorganic Chemical Reagent Waste	Incineration	(Hydrochloride & Supplier, n.d.)
Potassium Hydroxide	Hazardous Waste	Incineration	(U. E. P. Agency, 2006)
Used Fiber	Hazardous Waste	Incineration	Suggested Method in this article
Potassium Bicarbonate	Organic Salt Waste	Incineration	(EPA, 2009)
Sodium Hydroxide	Hazardous Waste	Incineration	(Hong et al., 2017)

### 3.2.2.3.1 AF1 Adsorbent Disposal Amount

Acrylonitrile, itaconic acid, hydroxylamine, and potassium hydroxide react with polyethylene fiber and contribute to the fiber formation or structure. Also, potassium bicarbonate, sodium carbonate, and ammonium sulfate react with uranium and vanadium ions and contribute to product formation, so these chemicals form a waste as a consumed fiber form after 40 cycles. The chemicals named tetrahydrofuran, methanol, water, dimethylformamide, and dimethyl sulfoxide can be reused and recycled with a ratio of 90% as specified in the section on the adaptation of experimental values to realistic values. Moreover, it is specified that recycling methods like distillation and condensation are available for the organic chemicals used in solvent extraction in the literature (Cheremisinoff, 1995). In a study conducted by Wu et al. (2011), up to a 99% recycling rate was obtained for an organic composite solvent. Therefore, the amount of waste formed by these chemicals for 1 kg of uranium production from brine via adsorbent technologies is comparatively lower than the main waste flow produced by consumed fiber. The methodology used in the disposal of waste produced from the URFB system with AF1 adsorbent is summarized in Table 3.16.

Table 3.16: Disposal Methodology for AF1 Adsorbent Case

<b>Name of Chemical</b>	<b>Disposal Method</b>
Acrylonitrile	
Itaconic Acid	
Hydroxylamine	
Potassium Hydroxide	Contribution of fiber structure and form a waste
Potassium Bicarbonate	
Sodium Carbonate	
Ammonium Sulfate	
Tetrahydrofuran	
Methanol - Water	
Dimethyl Formamide	Reuse and recycle methods are available, neglect
Dimethyl Sulfoxide	
Chemicals Organic	
Consumed Fiber	Main waste source

The main waste source of this system is classified as hazardous waste and is the unrecyclable or un-reusable adsorbent itself. Therefore, it is declared that 9.02 kg of hazardous waste is formed by the AF1 adsorbent scenario by considering the assumptions that have been made in this study. Moreover, based on the Ecoinvent v3.6 database, the electrical and thermal energy recoveries from the incineration the process were included as 4.75 kWh and 0.35 kWh per 1 kg of hazardous waste with efficiencies of 10% and 74.4%, respectively.

### **3.2.2.3.2 PAN-AO Adsorbent Disposal Amount**

The similar methodology and assumptions applied for the AF1 adsorbent scenario are valid for waste disposal of the URFB system with PAN-AO adsorbent case since the processes and consumed chemicals during these processes are similar to each other. The name of chemicals and applied assumptions for their disposal are listed in Table 3.17. It is claimed that 6.37 kg of hazardous waste is produced by the PAN-AO adsorbent scenario by taking into account the assumptions that have been made in this study.

Table 3.17: Disposal Methodology for PAN Adsorbent Case

Name of Chemical	Disposal Method
Hydroxylamine	
Sodium Hydroxide	
Potassium Bicarbonate	Contribution of fiber structure and form a waste
Sodium Carbonate	
Ammonium Sulfate	
Methanol - Water	
Chemicals Organic	Reuse and recycle methods are available, neglect
Consumed Fiber	Main waste source

### 3.2.2.4 Recycling of Adsorbents

The amount of required chemicals and energy and produced waste for 1 kg U production from brine by using two distinct adsorbents are presented in Table 3.18. These values have been used in the modeling part of these systems in SimaPro. Moreover, to understand the cycling effect on the chemical and energy amount required for the URFB system with amidoximated adsorbent, adsorbent capacities have been changed. While AF1 uranium capacity has been changed from 110.81 g to 71.78 g, PAN adsorbent uranium capacity has been modified from 156.9 g to 106.96 g by halving the cycle numbers (from 40 cycles to 20 cycles for AF1 adsorbent, from 50 cycles to 25 cycles for PAN-AO adsorbent). Then, all calculations made in the previous sections for input and output have been repeated for both normalization cases of AF1 and PAN-AO adsorbents. No experimental conditions like temperature have been changed during this procedure. The inventory data for URFB systems via AF1 and PAN-AO adsorbents to produce 1 kg of uranium in different recycling ratios have been listed in Table 3.18. Moreover, the details of datasets are presented in Appendix A.1. While using Ecoinvent v3.6 dataset, it has been considered that data covers as many countries as possible to reach more comprehensive results.

Table 3.18: Input and Output Data for Uranium Recovery from Brine via AF1 and PAN-AO Adsorbents for Different Cycles (Ecoinvent)

<b>Inputs for AF1 Adsorbent</b>	<b>Amount (40 Cycles)</b>	<b>Amount (20 Cycles)</b>	<b>Inputs for PAN-AO Adsorbent</b>	<b>Amount (50 Cycles)</b>	<b>Amount (25 Cycles)</b>
Water, salt, ocean (m3)	303030.3	303030.3	Water, salt, ocean (m3)	303030.3	303030.3
HDPE Resin (kg)	1.48	2.3	PAN Fibers (kg)	5.97	8.8
Acrylonitrile (kg)	4.21	6.5	Hydroxylamine (kg)	1.69	2.5
Succinic Acid (kg)	1.37	2.1	Potassium Carbonate (kg)	2.47	1.8
Hydroxylamine (kg)	1.32	2.0	Sodium Hydroxide (kg)	0.97	1.42
Potassium Carbonate (kg)	2.8	2.2	Sodium Carbonate (kg)	0.04	0.03
Potassium Hydroxide (kg)	0.78	1.2	Ammonium Sulfate (kg)	0.12	0.09
Sodium Carbonate (kg)	0.05	0.04	Electricity (kWh)	65.8	96.5
Ammonium Sulfate (kg)	0.14	0.11			
Electricity (kWh)	254.9	393.5			
<b>Outputs for AF1 Adsorbent</b>	<b>Amount (40 Cycles)</b>	<b>Amount (20 Cycles)</b>	<b>Outputs for PAN-AO Adsorbent</b>	<b>Amount (50 Cycles)</b>	<b>Amount (25 Cycles)</b>
Hazardous Waste (kg)	9.02	13.9	Hazardous Waste (kg)	6.37	9.35

### **3.2.3 Life Cycle Impact Assessment**

In the Life Cycle Impact Assessment (LCIA), the environmental impact of the system or process is evaluated quantitatively (Hauschild, 2018). The LCIA method using International Reference Life Cycle Data System (ILCD) 2011 Midpoint+ is implemented to evaluate 16 impact categories including IRE and IRHH as a midpoint category for its compatibility with prior LCA studies on uranium and other metal recovery (Farjana et al., 2018) (Farjana et al., 2019) (Z. Li et al., 2019). In addition, EF 3.0 method currently recommended by the European Commission (Saouter et al., 2018) has also been used to conduct LCA analysis to provide extra data and the results have been shown in Figures B.1, B.2, B.3 and B.4.

## **3.3 RESULTS AND DISCUSSION**

The interpretation step that is the last step in LCA is covered under this heading by describing the important issues and evaluating the data sensitivity, completeness and consistency in this section. The major findings and limitations of this study along with the recommendations are also argued.

### **3.3.1 Characterization Results**

#### **3.3.1.1 AF1 Adsorbent**

The analysis for AF1 adsorbent showed that HW disposal (47.7%), electricity (24.3%), potassium bicarbonate (7.0%), and hydroxylamine (16.1%) consumption are the main reason for high HTC results (Figure 3.7). Moreover, the same parameters were responsible for the HTNC results with a different ratios which were 17.7%, 15.1%, 14.0%, and 42.2% respectively. The same pattern is valid also for FET, but again different contributions were observed as 12.4%, 26.2%, 15.8%, and 36.6% respectively. Lastly, MFRRD is caused by the ratio of 1.6% HW waste disposal, 4.2% electricity, 2.9% potassium bicarbonate, and 91.7% hydroxylamine consumption. Hence, the AF1 adsorbent preparation step is in charge of the highest portion of environmental impact.

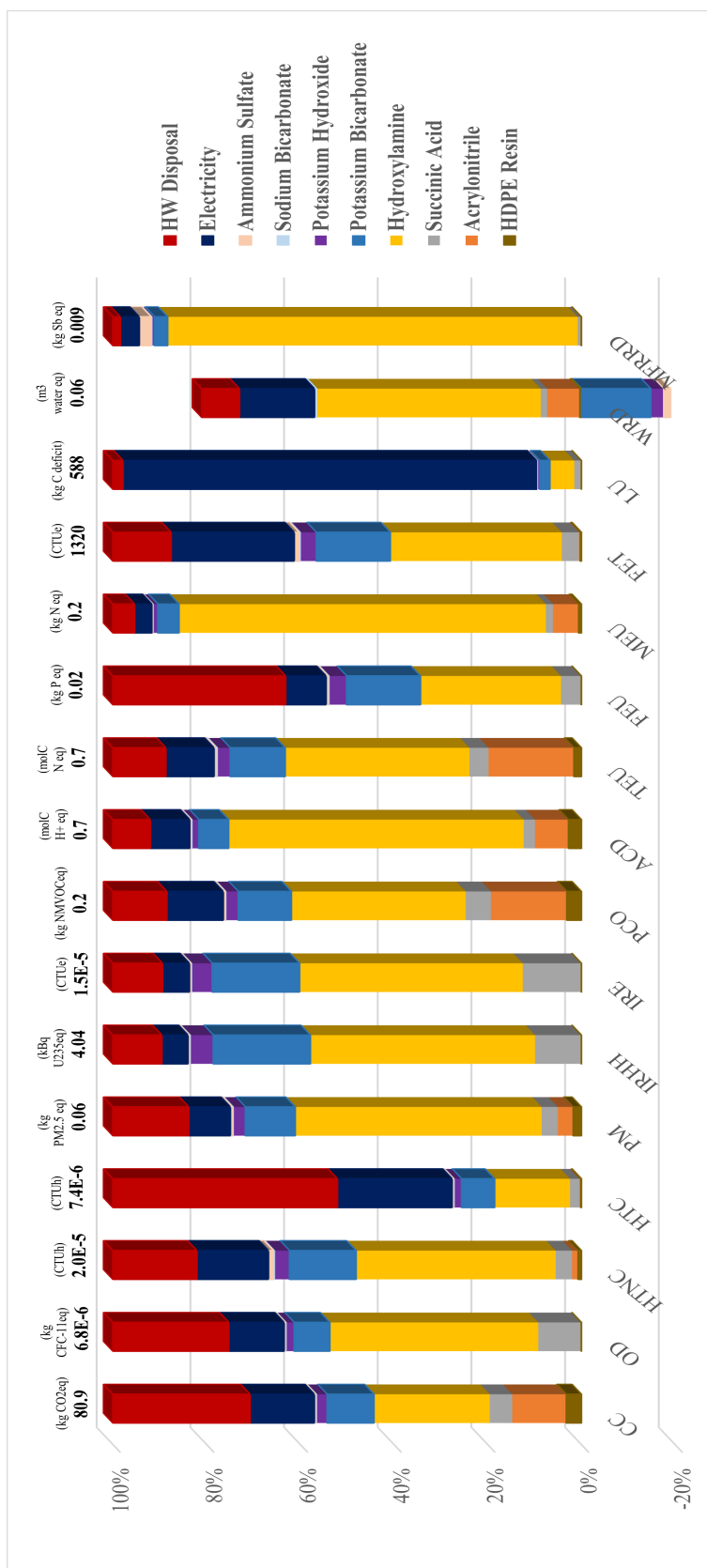


Figure 3.7: Characterization Results of Uranium Recovery from brine via AF1 Adsorbent Method

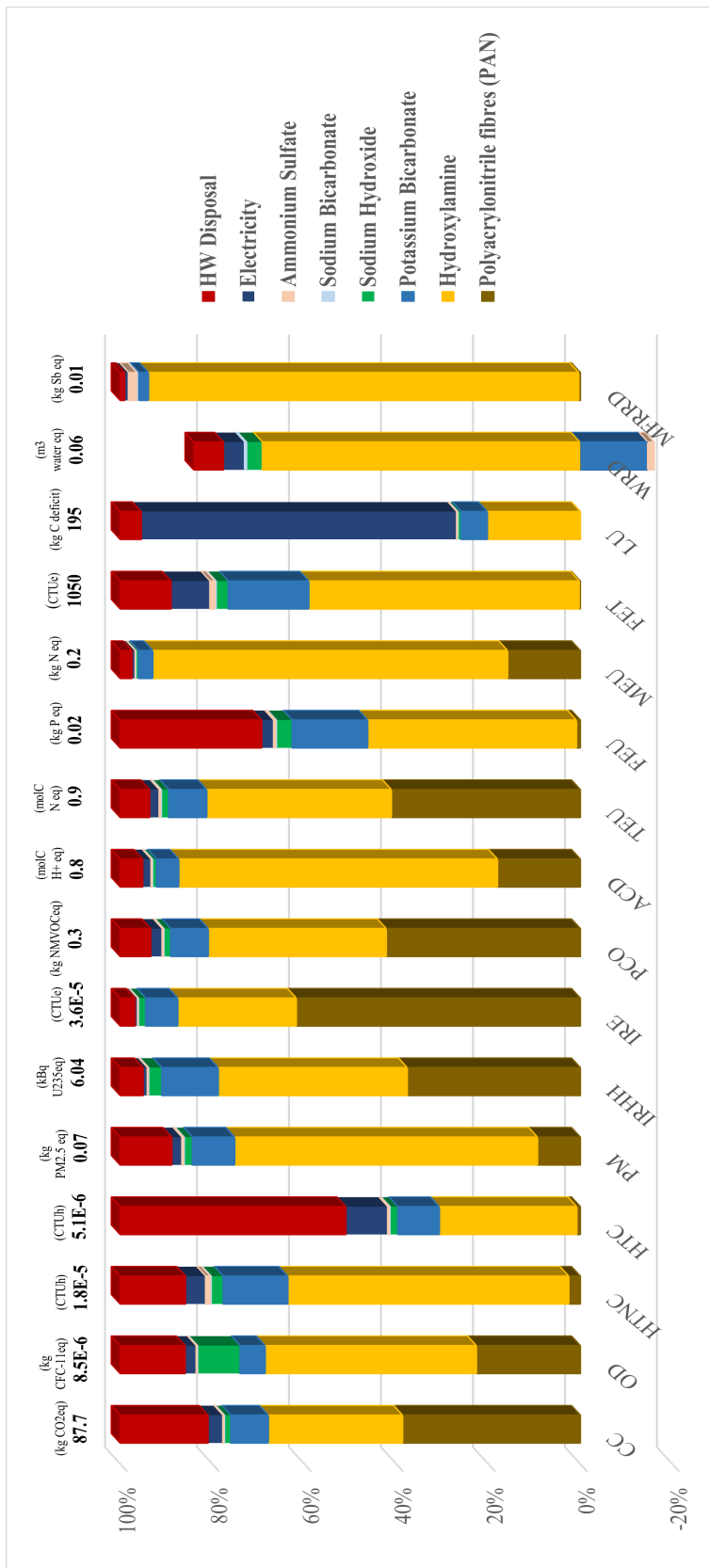


Figure 3.8: Characterization Results of Uranium Recovery from brine via PAN-AO Adsorbent Method

### 3.3.1.2 PAN-AO Adsorbent

Characterization results of PAN-AO adsorbent showed that HTC ( $5.1 \times 10^{-6}$  CTUh), HTNC ( $1.8 \times 10^{-5}$  CTUh), FET (1050 CTUe), and MFRRD (0.01 kg Sb eq) have the highest environmental impact categories in normalization (Figure 3.8). For these impact categories HW disposal, potassium bicarbonate, and hydroxylamine consumption are responsible for these loads. While the related ratios were estimated as 48.9%, 8.9%, and 29.8% for the first impact category, 13.9%, 13.7%, and 59.9% are the results for the second one, respectively. For FET, the ratio of HW disposal and potassium bicarbonate consumptions were 11.0% and 17.5%, respectively, and the rest of 58.9% springs from hydroxylamine utilization. MFRRD was caused by the ratio of 1.0% HW disposal, 2.3% potassium bicarbonate, and 93.5% hydroxylamine consumption. Therefore, in this adsorbent, the role of electricity has less importance than in the former, and the importance of PAN-AO adsorbent preparation and adsorption step is similar in both cases. Also, negative values in WRD data are seen in Figure 3.7 and Figure 3.8 because the credits are larger than the environmental burdens. Moreover, hydroxylamine is the hot spot chemical for both adsorbent scenarios since it is a toxic and mutagenic chemical depending on the consumption of energy and raw materials named ammonium nitrite and sulfur dioxide to produce this chemical and waste disposal (Fernando et al., 2002). AF1 scenarios overall resulted in lower environmental impacts than PAN-AO in 9 out of 16 impact categories indicating that the environmental impact of AF1 is lower than the other adsorbents under study.

### 3.3.1.3 Different Energy Scenarios

To understand the effect of the electricity source on the overall results of adsorbent scenarios, the main energy source of these methods has been changed from solar to coal, diesel, nuclear, and wind, respectively. Firstly, these results have been compared with solar cases and then conventional scenarios. During the comparison process, the results of adsorbent methods are divided by the results of in-situ leaching, open-pit, and underground techniques, separately. If this result is higher than 1, it shows that the environmental load of this case is higher than conventional mining methods, so it is an undesirable case. These situations are shown in red color in the Tables 3.19 and 3.20 below. On the contrary, if this result is lower than 1, it is a desirable situation

and represented by green color. Lastly, the case where the results are equal to  $1 \pm 0.05$  is shown in yellow color in the same tables. Overall, when the energy source is converted from solar to nuclear, the biggest drawback is a considerable increase in the environmental load on the IRE impact category in all cases depending on carbon-14 emissions to the air from the nuclear power plants during electricity production, nuclear fuel production, and low-level radioactive waste treatment. However, in all cases, a decrease in the LU impact category has been observed. Also, the results presented in the IRHH impact category of all adsorbent methods still is substantially lower than the outcomes of all conventional mining methods depending on the radon-222 emissions to air from tailing treatment.

Table 3.19: All Energy Sources Results Comparison of AF1 Case with Conventional Mining Results

	In-Situ Leaching					Open-Pit					Underground				
	Coal	Diesel	Nuclear	Solar	Wind	Coal	Diesel	Nuclear	Solar	Wind	Coal	Diesel	Nuclear	Solar	Wind
CC	2.28	1.05	0.51	0.57	0.55	5.04	2.31	1.13	1.26	1.22	3.74	1.72	0.84	0.93	0.91
OD	0.37	1.03	1.77	0.35	0.35	1.27	3.49	5.98	1.19	1.19	0.75	2.07	3.54	0.71	0.70
HTNC	0.06	0.01	0.01	0.01	0.02	0.07	0.01	0.01	0.01	0.02	0.07	0.01	0.01	0.01	0.02
HTC	0.17	0.06	0.06	0.07	0.09	0.18	0.06	0.07	0.08	0.09	0.18	0.06	0.07	0.08	0.09
PM	0.23	0.15	0.07	0.07	0.08	0.25	0.16	0.08	0.08	0.09	0.24	0.16	0.07	0.07	0.08
IRHH	0.0001	0.0002	0.01	0.0001	0.0001	0.0001	0.0002	0.01	0.0001	0.0001	0.0001	0.0002	0.01	0.0001	0.0001
IRE	0.33	0.94	23.57	0.30	0.34	0.98	2.77	69.47	0.88	0.99	0.63	1.79	44.88	0.57	0.64
PCO	0.57	0.78	0.10	0.10	0.11	1.53	2.10	0.26	0.27	0.30	0.99	1.37	0.17	0.18	0.19
ACD	1.47	0.78	0.29	0.31	0.33	3.00	1.60	0.60	0.63	0.68	2.32	1.24	0.46	0.49	0.53
TEU	0.58	0.83	0.09	0.10	0.11	1.61	2.31	0.26	0.27	0.30	1.01	1.45	0.16	0.17	0.19
FEU	0.90	0.13	0.13	0.13	0.19	3.09	0.45	0.47	0.46	0.66	3.07	0.45	0.46	0.46	0.66
MEU	0.08	0.11	0.03	0.03	0.03	1.74	2.23	0.63	0.60	0.63	1.05	1.35	0.38	0.36	0.38
FET	0.14	0.06	0.06	0.07	0.42	0.16	0.06	0.06	0.08	0.47	0.16	0.06	0.06	0.08	0.47
LU	0.66	0.71	0.20	1.62	0.32	1.41	1.50	0.43	3.44	0.67	1.07	1.15	0.33	2.62	0.51
WRD	0.12	0.01	0.12	0.01	0.02	1.41	0.17	1.36	0.16	0.22	2.15	0.26	2.09	0.24	0.34
MFRRD	0.03	0.03	0.04	0.03	0.04	0.04	0.04	0.05	0.04	0.05	0.04	0.04	0.05	0.04	0.05

According to the AF1 case results shown in Table 3.19, every scenario of AF1 has lower environmental impact than in-situ leaching method results in all impact categories except for CC, ACD, OD and IRE. As compared to the second conventional mining method which is open-pit, higher environmental impact has been observed in CC and OD impact categories in all AF1 scenarios and the AF1 case supported by coal energy is not a favorable method as compared to the open-pit mining method. When all underground mining results are compared with all AF1 scenario outcomes, the cases derived from fossil fuels are the most undesirable cases because of the higher environmental load in various impact categories. AF1 case powered by wind energy

gives the lowest environmental impacts as compared to in-situ leaching and underground mining techniques in all impact categories.

Table 3.20: All Energy Sources Results Comparison of PAN Case with Conventional Mining Results

	In-Situ Leaching					Open-Pit					Underground				
	Coal	Diesel	Nuclear	Solar	Wind	Coal	Diesel	Nuclear	Solar	Wind	Coal	Diesel	Nuclear	Solar	Wind
CC	1.06	0.74	0.60	0.62	0.61	2.34	1.64	1.33	1.36	1.35	1.74	1.21	0.99	1.01	1.01
OD	0.44	0.61	0.80	0.44	0.44	1.50	2.08	2.72	1.48	1.48	0.89	1.23	1.61	0.88	0.88
HTNC	0.02	0.01	0.01	0.01	0.01	0.03	0.01	0.01	0.01	0.01	0.03	0.01	0.01	0.01	0.01
HTC	0.08	0.05	0.05	0.05	0.05	0.08	0.05	0.05	0.05	0.06	0.08	0.05	0.05	0.05	0.06
PM	0.11	0.09	0.07	0.07	0.07	0.12	0.10	0.08	0.08	0.08	0.12	0.10	0.08	0.08	0.08
IRHH	0.0002	0.0002	0.002	0.0002	0.0002	0.0002	0.0002	0.002	0.0001	0.0002	0.0001	0.0002	0.002	0.0001	0.0001
IRE	0.72	0.87	6.71	0.71	0.72	2.11	2.57	19.79	2.09	2.12	1.36	1.66	12.79	1.35	1.37
PCO	0.24	0.30	0.12	0.12	0.13	0.66	0.81	0.33	0.33	0.34	0.43	0.53	0.21	0.22	0.22
ACD	0.66	0.48	0.36	0.36	0.37	1.35	0.99	0.73	0.74	0.75	1.04	0.76	0.56	0.57	0.58
TEU	0.25	0.31	0.12	0.12	0.12	0.69	0.87	0.34	0.34	0.35	0.43	0.54	0.21	0.21	0.22
FEU	0.31	0.11	0.11	0.11	0.13	1.07	0.39	0.39	0.39	0.44	1.07	0.39	0.39	0.39	0.44
MEU	0.05	0.06	0.04	0.04	0.04	1.08	1.20	0.79	0.78	0.79	0.65	0.73	0.48	0.47	0.48
FET	0.07	0.05	0.05	0.05	0.15	0.08	0.06	0.06	0.06	0.16	0.08	0.06	0.06	0.06	0.16
LU	0.29	0.30	0.17	0.54	0.20	0.62	0.64	0.37	1.14	0.43	0.47	0.49	0.28	0.87	0.33
WRD	0.04	0.01	0.04	0.01	0.01	0.48	0.16	0.46	0.15	0.17	0.73	0.24	0.71	0.23	0.26
MFRRD	0.04	0.04	0.04	0.04	0.04	0.05	0.05	0.05	0.05	0.05	0.05	0.05	0.05	0.05	0.05

According to the PAN-AO scenario results presented in Table 3.20, even if the energy source is changed from solar to another one, still PAN-AO scenarios have the lowest environmental impact in nearly all impact categories except for CC with a very low ratio and IRE as compared to the in-situ leaching technique. Also, all impact results presented in diesel and wind scenarios are lower than the results of this technique. When the PAN-AO scenario results are compared with the open-pit mining results, all outcomes are higher than the open-pit results in CC, OD, and IRE categories. Although the PAN-AO coal scenario seems the worst case among all PAN-AO adsorbent alternatives, still it gives better results in 10 out of 16 impact categories as compared to open-pit mining. Compared to the underground mining results presented in Table 3.22, all energy scenarios of PAN-AO yield higher results in the IRE impact category, but still, they can be classified as an alternative method to the underground mining technique.

In the case of comparison between entire AF1 and PAN-AO energy scenarios in all impact categories, although AF1 cases give the worst results in nearly all impact categories except for MFRRD, the best results have also been obtained in AF1 nuclear and AF1 solar cases in most of the impact categories (10 out of 16). The results presented

in Figures 3.9 and 3.10 reveal that deciding on the best energy source for any system or process is not straightforward because every energy source may have handicaps in different impact categories based on their geography and climate. Therefore, our systems have been modeled also by applying the 50% ratios in different energy sectors to the 50% solar energy, and the results of this analysis are presented in Figures B.5 and B.6. In all cases, increases in specific impact categories have been observed when switching from just solar energy to combination of solar and other energy sources, such as 50% solar and 50% coal. When the outcome in any impact category was at least nearly twofold that of the solar scenario alone, the impact categories listed in Table 3.21 have been classified as the most affected. For example, when wind energy is included as another energy source of URFB systems, FET impact category is affected by this change most with nearly 3.6 times higher result than only solar energy case. Based on those scenarios changing the additional energy source is inadequate to obtain the best results among all conventional mining methods in all impact categories, so other improvements should be applied to decrease these loads.

Table 3.21: Name of the Most Affected Impact Categories based on the Energy Scenarios

<b>Name of Second Energy Source</b>	<b>Most Affected Impact Categories</b>
Coal	CC, HTNC, PM, PCO, ACD, TEU, FEU, MEU & WRD
Diesel	OD, IRE, PCO, TEU & MEU
Nuclear	OD, IRHH, IRE & WRD
Wind	FET

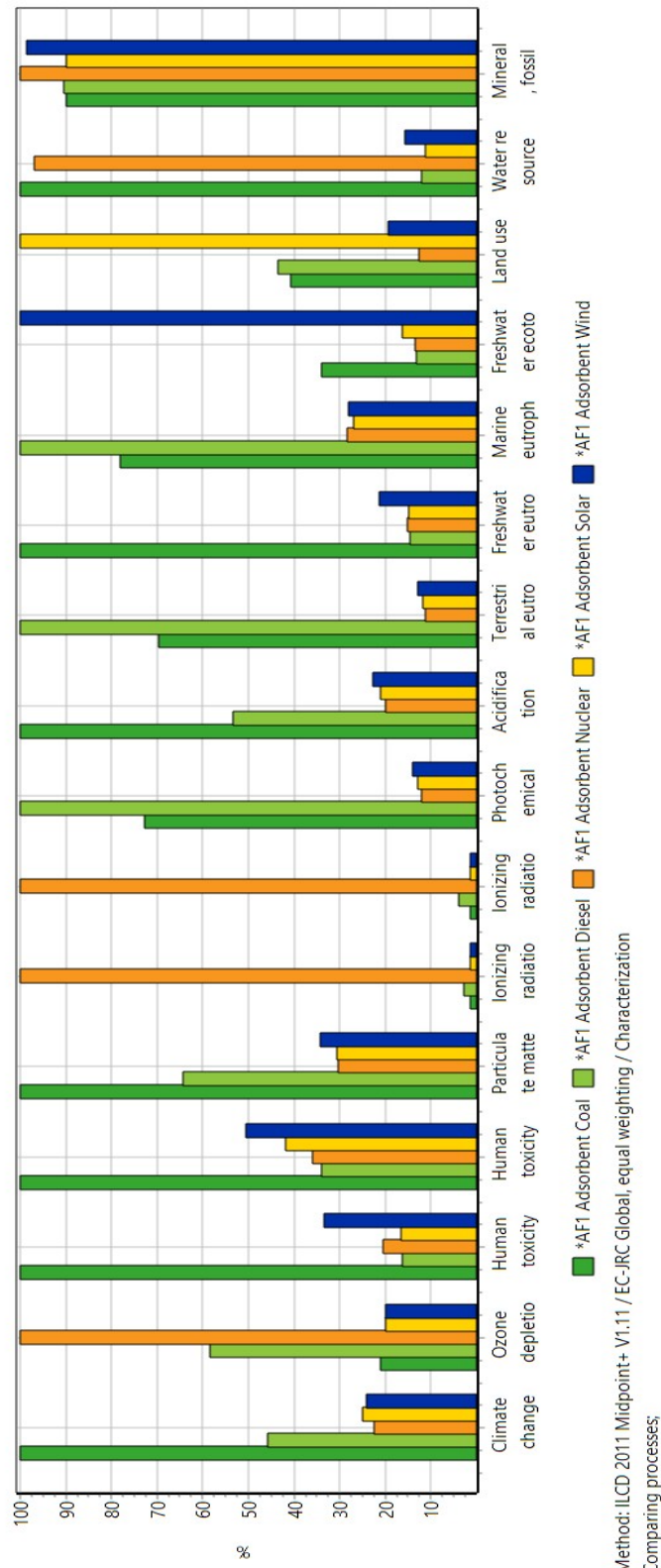


Figure 3.9: Characterization Results of Uranium Recovery from brine via AF1 Adsorbent for Different Energy Sources

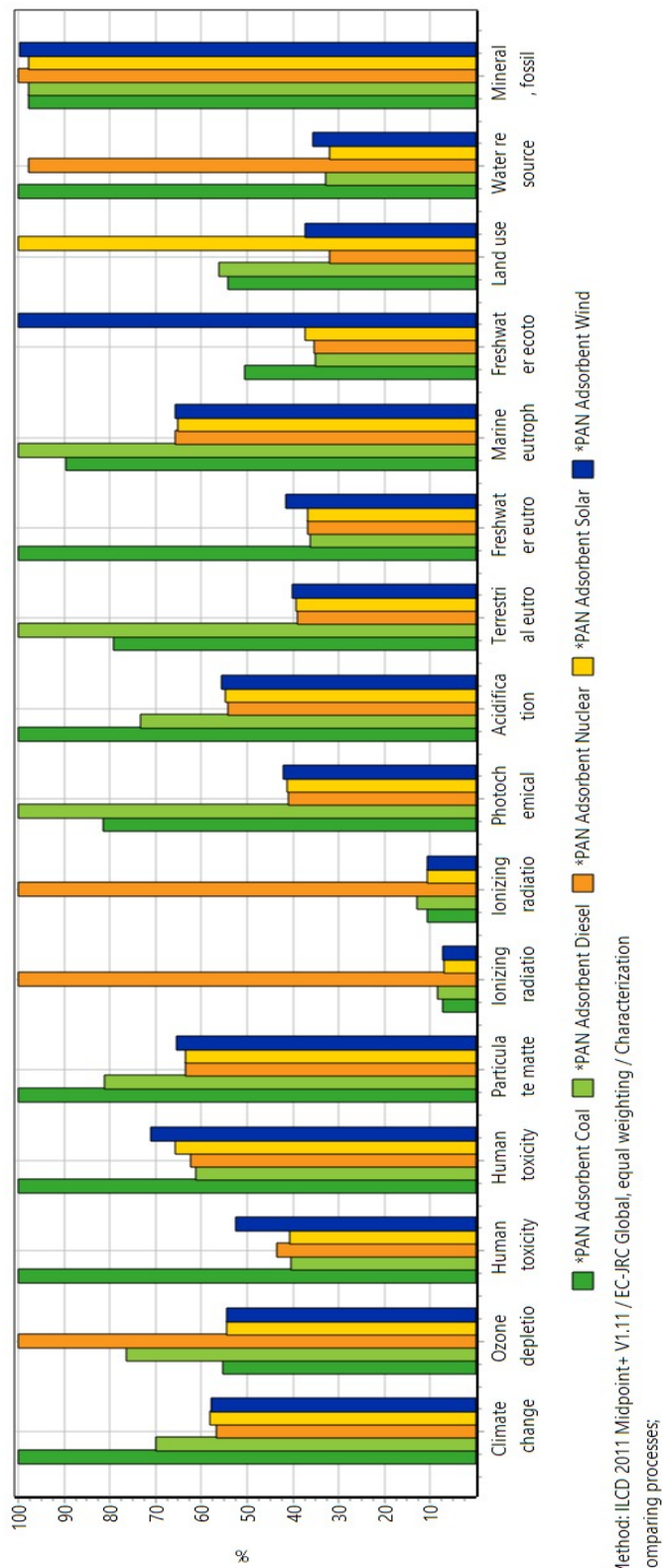


Figure 3.10: Characterization Results of Uranium Recovery from brine via PAN-AO Adsorbent for Different Energy Sources

### **3.3.2 Comparative Results of Adsorbent and Conventional Uranium Recovery Methods**

The overall results of this study presented in Table 3.22 reveal that uranium extraction by using AF1 and PAN-AO adsorbents have a lower impact than conventional methods for all impact categories except for CC, OD, and LU. After these results have been obtained, a detailed analysis has been conducted to detect the main pollutants and the processes of the relevant uranium extraction methods in all impact categories, and the result of this analysis are presented in Table 3.23. The requirement of hydroxylamine is the main contributor to hazardous waste production during the URFB process. The carbon-dioxide emissions to the air from mainly hazardous waste disposal and liquid ammonia used in hydroxylamine production are responsible for the impact in the CC impact category. Also, the main contributors to environmental load in the OD category for URFB processes are the air pollutant of methane, tetrachloro- (CFC-10) and methane, bromotrifluoro- (Halon 1301), which are released from the sodium hydroxide used in the hydroxylamine production required for adsorbent preparation and used in the hazardous waste treatment. Although open-pit gives the best results in these categories, the difference between adsorbent technologies and open-pit method results is low. The highest difference is in the LU category with nearly 3.5 times. Conventional uranium extraction techniques show the highest environmental load in HTNC, IRHH, and FET categories as compared to the adsorbent methods. The variations between them and adsorbent technologies are changing from nearly 20 to 104 times. The biggest change is obtained in the IRHH category. Ionizing radiation exposure to humans leads to DNA alteration that results in some serious health problems like cancer and damage to the immune system (Lumniczky et al., 2021). Furthermore, the worst scenario springs from in-situ leaching applications because of the diesel burned in the diesel-electric generating set, the heat requirement, and the tailing from uranium milling which are also the reasons of environmental load in other conventional uranium mining alternatives. Among all methods, uranium recovery via AF1 adsorbent is the method that has the lowest environmental load in nearly all categories except for LU. The reason is explained by the supply of energy requirements for uranium recovery via this adsorbent with solar energy that requires a high land area. Therefore, in the industrial application of uranium extraction via

adsorbent technologies, supplying all energy with solar energy may not be logical, so hybrid energy sources should be evaluated by considering the features of the region. As compared to all conventional uranium mining methods, the environmental impact of the PAN-AO scenario is the lowest in all impact categories except for CC, OD, and IRE. The main sources of the environmental load in the IRE impact category are carbon-14 emissions to air and cesium-137 emissions to water generated during the production of PAN fiber which is the raw material of PAN-AO adsorbent.

Moreover, the results obtained by EF 3.0 method and presented in Figures B.1, B.2, B.3 and B.4 declare that the characterization results of all uranium recovery methods are not different from the results calculated by ILCD 2011+ method except for the HTNC, HTC and FET impact categories with two orders of magnitude difference because EF 3.0 method has been developed for improving toxicological analysis and provide results in a more sensitive level for toxicological values (Fazio et al., 2018).

HTC, HTNC, FET, and IRHH are the most critical impact categories among all conventional uranium mining alternatives according to the normalization and single score results declared in Figures 3.11 and 3.12. In all these categories, conventional uranium mining methods show the highest impact with the highest ratio of up to 8500 times as compared to uranium recovery with adsorbent methods. In all conventional mining methods, uranium tailing treatment is the main reason for the high environmental load in HTC, HTNC, FET, and IRHH impact categories mainly caused by chromium VI, arsenic, vanadium copper emission to water, and radon-222 emission to air, respectively. In the uranium recovery methods with adsorbent, zinc, arsenic, and copper emissions to water and radon-222 and carbon-14 emissions to air depending on the hydroxylamine production are the main pollutants in HTNC, FET, and IRHH impact categories. Additionally, chromium VI is the contaminant produced during HW treatment and has the highest impact in the HTC category for both adsorbents. The in-situ leaching method gives the worst results among all techniques except for IRHH and LU impact categories. Although in the other mining and adsorbent methods comparison, the results are quite similar in CC and OD impact categories, adsorbent scenarios lead to less environmental impact in other categories except for LU in the AF1 adsorbent case depending on the land requirement for solar energy. Moreover, the single score results of uranium recovery with adsorbent methods are

displayed in Figure 3.13 by narrowing the data range in Figure 3.12 to make the data more observable. The results claim that the most important impact categories for uranium recovery with adsorbent methods are HTNC, HTC, FET and MFRRD depending on the hydroxylamine production and HW disposal.

Although adsorbent technologies have a less environmental impact than the conventional mining methods in most impact categories, they still have some negative impacts on the environment and society because of the high energy requirements in AF1 adsorbent preparation, and required chemicals like hydroxylamine, and HW disposal.

As mentioned in European Green Deal, environmental challenges including loss of biodiversity, climate change, and deforestation can be dealt with by providing resource efficiency and a competitive economy while mobilizing industry for a clean and circular economy (Commission et al., 2019). This study contributes not only to sustainable development goals but also to the circular economy due to the recovery of material from brine concerned as waste generated from desalination plants which is one of the greatest strengths of this system. Another promising feature of adsorbent methods is that they offer an alternative to cleaner nuclear energy sources produced in terrestrial deposits that have limits and will eventually deplete in the next 135 years (N. E. Agency & Agency, 2021).

Although URFB can be implemented in all desalination plant types such as plants by reverse osmosis, solar desalination plants are advantageous over other systems because solar panels which are required for adsorbent preparation and brine have already been found to supply the energy demand. Therefore, the implementation of URFB on solar desalination plants would be much easier than in the other types of plants. Similarly, the impact of the transportation step, which is not included in this study, could be mitigated with the construction of adsorbent systems that are located close to the desalination systems. Furthermore, a synergistic approach should be considered for desalination and nuclear plants, which also have to be located close to each other. While the energy required for desalination plant operation can be provided by nuclear power plants (Zheng et al., 2014), the required raw material for nuclear power plants can be supplied by uranium recovery systems with amidoximated adsorbents.

Table 3.22: Characterization Results of Uranium Recovery from Brine via Amidoximated Adsorbents and Conventional Uranium Extraction and Mining Methods (Ecoinvent)

Name of Impact Category	Unit	Total Impact				
		AF1	PAN-AO	In-situ Leaching	Open pit	Underground
<b>Climate change (CC)</b>	kg CO <sub>2</sub> eq	80,9	87,7	142,2	64,4	86,8
<b>Ozone depletion (OD)</b>	kg CFC-11eq	6,80E-06	8,50E-06	1,90E-05	5,70E-06	9,60E-06
<b>Human toxicity, non-cancer effects (HTNC)</b>	CTUh	2,00E-05	1,80E-05	2,00E-03	1,70E-03	1,70E-03
<b>Human toxicity, cancer effects (HTC)</b>	CTUh	7,40E-06	5,10E-06	1,00E-04	9,60E-05	9,60E-05
<b>Particulate matter (PM)</b>	kg PM2.5 eq	0,06	0,06	0,91	0,83	0,85
<b>Ionizing radiation HH (IRHH)</b>	kBq U235 eq	4,04	6,04	40125	40282	41303
<b>Ionizing radiation E (interim) (IRE)</b>	CTUe	1,50E-05	3,60E-05	5,10E-05	1,70E-05	2,70E-05
<b>Photochemical ozone formation (PCO)</b>	kg NMVOC eq	0,21	0,26	2,07	0,77	1,18
<b>Acidification (ACD)</b>	molc H+ eq	0,71	0,83	2,29	1,12	1,45
<b>Terrestrial eutrophication (TEU)</b>	molc N eq	0,73	0,92	7,53	2,70	4,30
<b>Freshwater eutrophication (FEU)</b>	kg P eq	0,02	0,02	0,17	0,05	0,05
<b>Marine eutrophication (MEU)</b>	kg N eq	0,19	0,24	6,36	0,31	0,51
<b>Freshwater ecotoxicity (FET)</b>	CTUe	1318	1051	19360	17388	17208
<b>Land use (LU)</b>	kg C deficit	588	195	362	171	224
<b>Water resource depletion (WRD)</b>	m3 water eq	0,07	0,06	4,85	0,42	0,27
<b>Mineral, fossil &amp; resource depletion (MFRRD)</b>	kg Sb eq	0,01	0,01	0,29	0,22	0,22

Table 3.23: Main Pollutants and Processes Released in All Uranium Extraction Methods in All Impact Categories

Impact Categories	Main Pollutants and Relevant Processes in AFI Recovery Method (a)	Main Pollutants and Relevant Processes in PAN-AO Recovery Method (b)	Main Pollutants and Relevant Processes in Open-Pit Mining (c)	Main Pollutants and Relevant Processes in Underground Mining (d)	Main Pollutants and Relevant Processes in In-situ Leaching (e)
CC	CO <sub>2</sub> (air) from HW disposal	CO <sub>2</sub> (air) from PAN fiber production	CO <sub>2</sub> (air) from heat production	CO <sub>2</sub> (air) from diesel burned diesel-electric generating set for (c), (d) and (e)	CO <sub>2</sub> (air) from diesel burned diesel-electric generating set for both (d) and (e)
OD	Methane, tetrachloro- (CFC-10) (air) and methane, bromotrifluoro- (Halon 1301) (air) from hydroxylamine production for both (a) and (b)	CO <sub>2</sub> (air) from PAN fiber production			
HTNC	Zinc and Arsenic (water) from hydroxylamine production for both (a) and (b)				
HTC	Chromium VI (water) from HW disposal for both (a) and (b)				
PM	Sulfur dioxide (air) from hydroxylamine production for both (a) and (b)				
IRHH	Radon-222 from hydroxylamine production	Carbon-14 (air) from PAN fiber production			
IRE	Carbon-14 (air) from hydroxylamine production	Carbon-14 (air) from PAN fiber production			
PCO	Nitrogen oxides (air) from hydroxylamine production	Nitrogen dioxides (air) from PAN fiber production			
ACD	Sulfur dioxide (air) from hydroxylamine production for both (a) and (b)		Sulfur dioxide (air) from sulfuric acid consumption in uranium milling	Sulfur dioxide (air) from sulfuric acid consumption in uranium milling and Nitrogen oxides (air) from diesel burned in the diesel-electric generating set	Nitrogen oxides (air) from diesel burned in diesel-electric generating set
TEU	Nitrogen oxides (air) from hydroxylamine production	Nitrogen dioxides (air) from PAN fiber production			
FEU	Phosphate (water) from HW disposal	Phosphate (water) from hydroxylamine production			
MEU	Ammonium, ion (water) from hydroxylamine production for both (a) and (b)		Nitrogen oxides (air) from blasting activities	Nitrogen oxides (air) from diesel burned in diesel-electric generating set for (c), (d) and (e)	Phosphate (water) from acid leaching step
FET	Copper (water) from hydroxylamine production for both (a) and (b)		Vanadium and Copper (water) from uranium tailing treatment for both (c) and (d)		Vanadium (water) from acid leaching step
LU	Transformation to area (raw material) from solar panel for both (a) and (b)		Transformation to area (raw material) from uranium tailing treatment for both (c) and (d)		Transformation to area (raw material) from diesel burned in diesel-electric generating set
WRD	Water (raw material) from hydroxylamine production for both (a) and (b)		Water (raw material) from heat production for both (c) and (d)		Water (raw material) from acid leaching step
MFRRD	Gold (raw material) from hydroxylamine production for both (a) and (b)		Uranium (raw material) from mining activities for (c), (d) and (e)		

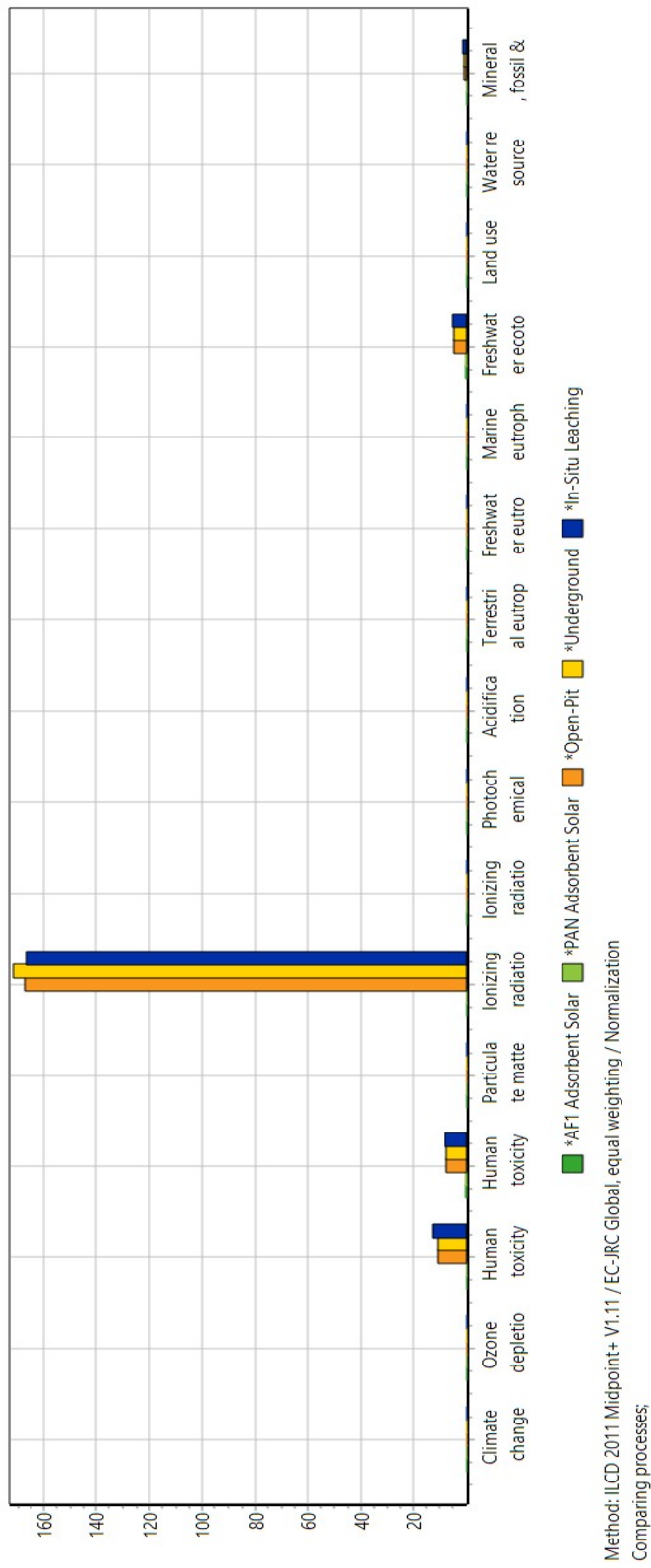


Figure 3.11: Normalization Results from Comparison for Uranium Recovery via Amidoximated Adsorbents and Conventional Uranium Extraction and Mining Methods



Figure 3.12: Comparative Single Score Results for All Uranium Mining Methods



Figure 3.13: Comparative Single Score Results for Only Uranium Recovery with Adsorbent Methods

### 3.3.3 Sensitivity Analysis

Variations in methods, data, and assumptions lead to alteration of results and these alterations are determined with sensitivity analysis by comparing the base case with modified cases (Finkbeiner et al., 2006). In our sensitivity analysis, 4 main impact categories, which are CC, HTC, FET, and MFRRD, have been considered as they are directly related to the goal and scope of this study and responsible for the high portion of total environmental load. All input values have been changed one by one with perturbation ratios of  $\pm 10\%$ ,  $\pm 25\%$ , and  $\pm 50\%$  to clearly comprehend their actual effects on the system. The results have been obtained from these perturbed parameters by using ILCD 2011 Midpoint+. Positive and negative perturbation ratio results for uranium extraction via AF1 adsorbent are shown in Tables 3.24 and 3.25. Furthermore, all results are given on a percentage basis. The colored cells represent the highest importance degree among all parameters and variations. On the one hand, sensitivity analysis results for uranium extraction via PAN-AO adsorbent are given in Tables 3.26 and 3.27. The outcomes of all perturbation ratios and impact categories for uranium extraction with AF1 and PAN-AO adsorbents are combined and presented in Figure 3.14.

Table 3.24: Sensitivity Results (%) of Uranium Recovery via AF1 adsorbent (Only Positive Perturbation Ratio)

	Climate Change			Human Toxicity, Cancer Effects			Freshwater Ecotoxicity			Mineral, Fossil & Ren, Resource Depletion		
	10%	25%	50%	10%	25%	50%	10%	25%	50%	10%	25%	50%
<b>HDPE (kg)</b>	0,28	0,76	1,56	0,02	0,001	0,03	0,02	0,05	0,1	0,001	0,003	0,01
<b>Acrylonitrile (kg)</b>	1,10	2,83	5,70	0,003	0,05	0,13	0,03	0,08	0,15	0,01	0,01	0,03
<b>Succinic acid (kg)</b>	0,41	1,14	2,34	0,16	0,47	0,97	0,35	0,91	1,82	0,07	0,18	0,36
<b>Hydroxylamine (kg)</b>	2,39	6,13	12,32	1,56	4,00	8,03	3,61	9,16	18,32	8,62	21,89	43,78
<b>Potassium carbonate (kg)</b>	0,95	2,45	4,94	0,67	1,73	3,48	1,58	3,94	7,89	0,28	0,69	1,39
<b>Potassium hydroxide (kg)</b>	0,16	0,52	1,13	0,12	0,38	0,8	0,31	0,85	1,75	0,06	0,15	0,31
<b>Sodium Bicarbonate (kg)</b>	0,05	0,03	0,02	0,03	0,02	0,002	0,005	0,04	0,09	0,003	0,02	0,05
<b>Ammonium Sulphate (kg)</b>	0,02	0,02	0,11	0,01	0,04	0,12	0,07	0,21	0,5	0,18	0,54	1,27
<b>Electricity (kWh)</b>	1,32	3,38	6,81	2,42	6,09	12,21	2,63	6,57	13,14	0,40	1,01	2,02
<b>Hazardous Waste Disposal (kg)</b>	2,90	7,35	14,49	4,81	12,08	23,77	1,25	3,14	6,16	0,16	0,40	0,78

Table 3.25: Sensitivity Results (%) of Uranium Recovery via AF1 adsorbent (Only Negative Perturbation Ratio)

	Climate Change			Human Toxicity, Cancer Effects			Freshwater Ecotoxicity			Mineral, Fossil & Ren, Resource Depletion		
	10%	25%	50%	10%	25%	50%	10%	25%	50%	10%	25%	50%
HDPE (kg)	-0,37	-0,85	-1,65	-0,04	-0,05	-0,08	-0,02	-0,05	-0,1	0,001	0,003	-0,01
Acrylonitrile (kg)	-1,2	-2,92	-5,83	-0,06	-0,1	-0,18	-0,03	-0,08	-0,15	-0,01	-0,01	-0,03
Succinic acid (kg)	-0,54	-1,27	-2,47	-0,23	-0,54	-1,04	-0,37	-0,94	-1,85	-0,07	-0,18	-0,36
Hydroxylamine (kg)	-2,48	-6,23	-12,41	-1,62	-4,06	-8,09	-3,61	-9,16	-18,32	-8,62	-21,89	-43,78
Potassium carbonate (kg)	-1,04	-2,54	-5,03	-0,73	-1,78	-3,54	-1,58	-3,94	-7,89	-0,28	-0,69	-1,39
Potassium hydroxide (kg)	-0,29	-0,65	-1,22	-0,2	-0,45	-0,86	-0,36	-0,9	-1,75	-0,06	-0,16	-0,31
Sodium Bicarbonate (kg)	-0,06	-0,08	-0,1	-0,04	-0,06	-0,07	-0,05	-0,09	-0,14	-0,03	-0,05	-0,08
Ammonium Sulphate (kg)	-0,07	-0,14	-0,2	-0,05	-0,11	-0,18	-0,07	-0,28	-0,5	-0,18	-0,72	-1,27
Electricity (kWh)	-1,42	-3,47	-6,9	-2,48	-6,14	-12,26	-2,63	-6,57	-13,13	-0,4	-1,01	-2,01
Hazardous Waste Disposal (kg)	-3,03	-7,25	-14,71	-4,91	-11,82	-24,03	-1,27	-3,05	-6,22	-0,16	-0,39	-0,79

Table 3.26: Sensitivity Results (%) of Uranium Recovery via PAN-AO adsorbent (Only Positive Perturbation Ratio)

	Climate Change			Human Toxicity, Cancer Effects			Freshwater Ecotoxicity			Mineral, Fossil & Ren, Resource Depletion		
	10%	25%	50%	10%	25%	50%	10%	25%	50%	10%	25%	50%
PAN (kg)	4,08	9,90	19,62	0,08	0,19	0,39	0,02	0,05	0,10	0,04	0,09	0,18
Hydroxylamine (kg)	2,94	7,43	14,68	3,01	7,61	15,04	5,92	14,97	29,60	9,41	23,80	47,04
Potassium Carbonate (kg)	0,82	2,07	4,04	0,91	2,29	4,47	1,77	4,45	8,70	0,21	0,52	1,02
Sodium Hydroxide (kg)	0,13	0,35	0,71	0,16	0,43	0,87	0,25	0,66	1,33	0,04	0,09	0,19
Sodium Bicarbonate (kg)	0,01	0,01	0,03	0,01	0,02	0,04	0,03	0,06	0,12	0,01	0,02	0,04
Ammonium Sulphate (kg)	0,04	0,06	0,14	0,06	0,09	0,22	0,18	0,27	0,63	0,30	0,45	1,06
Electricity (kWh)	0,33	0,81	1,36	0,92	2,28	4,58	0,85	2,12	4,26	0,09	0,22	0,43
Hazardous Waste Disposal (kg)	1,88	4,88	9,66	4,85	12,54	24,85	1,09	2,81	5,58	0,09	0,24	0,47

Table 3.27: Sensitivity Results (%) of Uranium Recovery via PAN-AO adsorbent (Only Negative Perturbation Ratio)

	Climate Change			Human Toxicity, Cancer Effects			Freshwater Ecotoxicity			Mineral, Fossil & Ren, Resource Depletion		
	10%	25%	50%	10%	25%	50%	10%	25%	50%	10%	25%	50%
PAN (kg)	-3,69	-9,52	-19,23	-0,07	-0,19	-0,38	-0,02	-0,05	-0,09	-0,03	-0,09	-0,18
Hydroxylamine (kg)	-2,94	-7,25	-14,51	-3,01	-7,43	-14,86	-5,92	-14,62	-29,25	-9,41	-23,25	-46,49
Potassium Carbonate (kg)	-0,82	-2,04	-4,04	-0,91	-2,25	-4,47	-1,77	-4,38	-8,7	-0,21	-0,51	-1,02
Sodium Hydroxide (kg)	-0,15	-0,35	-0,72	-0,18	-0,43	-0,89	-0,28	-0,66	-1,36	-0,04	-0,09	-0,19
Sodium Bicarbonate (kg)	0,004	-0,01	-0,03	-0,01	-0,02	-0,04	-0,02	-0,06	-0,12	-0,01	-0,02	-0,04
Ammonium Sulphate (kg)	-0,02	-0,06	-0,12	-0,03	-0,09	-0,19	-0,09	-0,27	-0,54	-0,15	-0,45	-0,91
Electricity (kWh)	-0,33	-0,82	-1,63	-0,92	-2,29	-4,58	-0,85	-2,13	-4,26	-0,09	-0,22	-0,43
Hazardous Waste Disposal (kg)	-2	-4,7	-9,48	-5,15	-12,08	-24,39	-1,16	-2,71	-5,47	-0,1	-0,23	-0,46

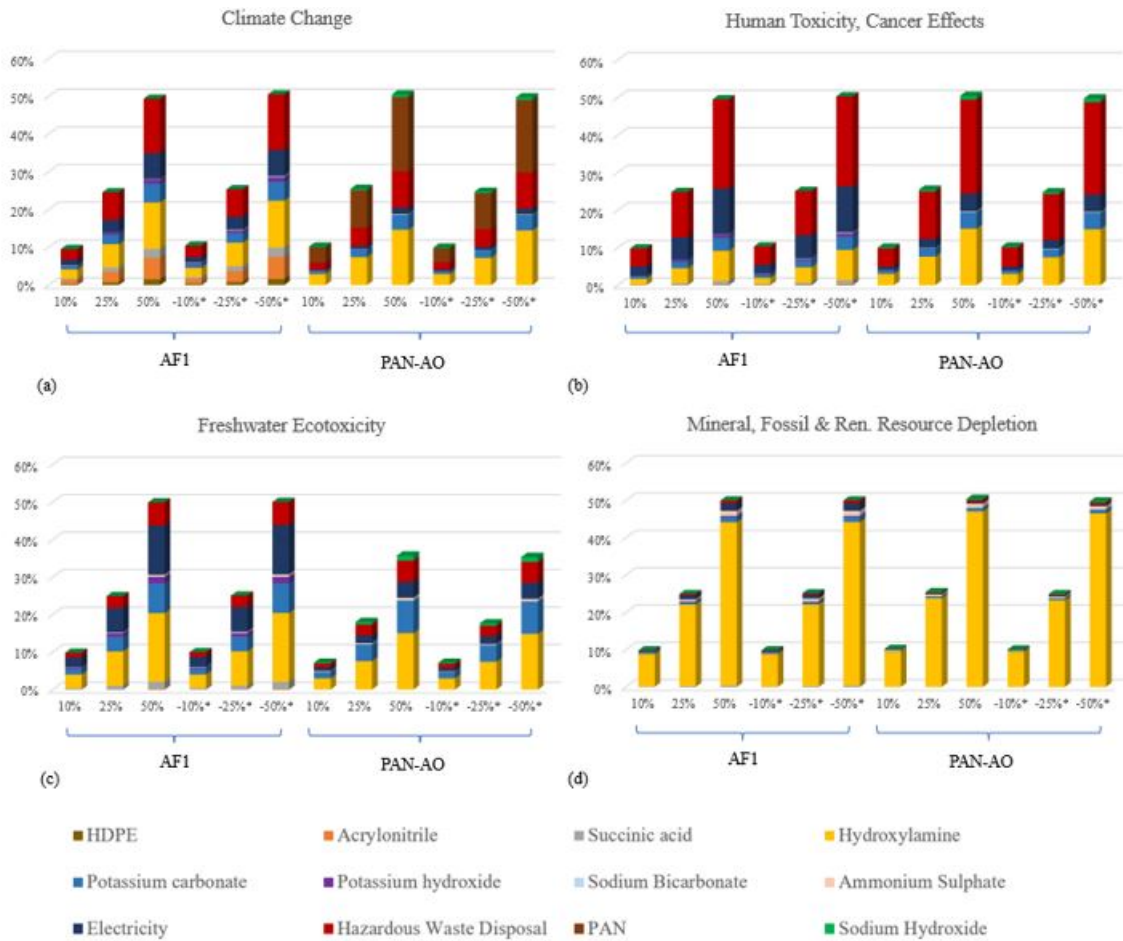


Figure 3.14: Sensitivity Analysis Results of Uranium Extraction in (a) CC, (b) HTC, (c) FET, and (d) MFRRD Impact Categories for AF1 and PAN-AO Adsorbent Methods (\* means negative perturbation ratio, and all results are given in absolute value.)

Uranium stripping with AF1 adsorbent sensitivity results revealed that HW disposal is the most sensitive parameter in CC and HTC impact categories compared to the base case (Figures 3.14a and 3.14b). This was an expected result because of the use of toxic materials during adsorbent production. Ammonium sulphate and sodium bicarbonate are the least sensitive parameters for the CC impact category, while HDPE or the raw material of AF1 adsorbent is one of the least susceptible parameters for the HTC impact category. For FET and MFRRD impact categories, hydroxylamine is the most sensitive parameter (Figures 3.14c and 3.14d). While the FET category has the highest system response of around 19% for hydroxylamine, in the MFRRD category a system response variation of nearly 44% is observed for hydroxylamine among all

parameters. This response level is the highest in all impact categories because of the use of high raw metals such as gold and silver during hydroxylamine production. The least sensitive parameters are HDPE for the MFRRD category, and sodium bicarbonate and HDPE for CC, HTC, and FET categories due to their non-toxic nature.

For the second adsorbent scenario even though PAN fiber was the most sensitive parameter in the CC impact category because of the CO<sub>2</sub> emission during the production of this material, this parameter was only introduced for PAN adsorbent production scenarios (Figure 3.14a). Therefore, we should mention that HW disposal and hydroxylamine were also sensitive parameters in this category. Similarly, HW disposal is the most susceptible parameter in the HTC impact category due to the toxic nature of the used adsorbent material (Figure 3.14b). For FET and MFRRD impact categories, hydroxylamine is the most sensitive parameter (Figures 3.14c and 3.14d). While the highest system response results in 15% for hydroxylamine in the FET impact category because of its toxic nature, and MFRRD category has the highest response of 47% for hydroxylamine because of high raw material consumption during its production. Also, the least sensitive parameters are evaluated as sodium bicarbonate in CC, HTC, and MFRRD categories, and PAN for the FET category due to its non-toxic nature.

Combining all the sensitivity results it was concluded that PAN adsorbent production is more vulnerable than AF1 adsorbent production. Overall, the most sensitive parameters for both adsorbent systems were established as HW disposal and hydroxylamine especially because of their impact on the ecosystem, humans, environment, and resources. Sensitivity results in absolute values presented in Figure 3.14 demonstrate that electricity and hydroxylamine used in the adsorbent preparation step and HW disposal are the most critical parameters for the first scenario. In the second case, PAN fiber and hydroxylamine consumed in the generation of adsorbent and HW disposal are listed as the most sensitive parameters. Yet, it should be noted that this study is based on data available in pilot-scale laboratory experiments and due to the limited information in the literature, some assumptions have been made. At this point, sensitivity analysis provides information on which steps, chemicals, or assumptions are the most crucial for such an assessment. Once uranium recovery is performed on large or industrial scales, energy requirements for processes such as drying can

be decreased by energy recovery systems such as a heat exchanger, and necessary chemical amounts such as PAN fiber and hydroxylamine can be minimized by considering reuse and recycle options instead of using incineration methods (Piccinno et al., 2016). Furthermore, to reduce the environmental impacts caused by currently required chemicals like hydroxylamine, more eco-friendly chemicals can replace them before these systems are industrialized.

Additionally, adjusting the input and output values with specified ratios in sensitivity analysis may be impossible in practice, depending on the reaction's minimum or maximum chemical requirements. Thus, a data range for hydroxylamine, one of the most sensitive compounds for both adsorbent cases, has been identified, and further analysis has been undertaken to determine the worst and best case scenarios based on hydroxylamine consumption. The amount of this chemical is highly dependent on the degree of grafting or conversion ratio. For AF1 adsorbent, the applicable grafting degree range is denoted by 97%-385% (Oyola & Dai, 2016)(Das, Tsouris, et al., 2016)(Das, Oyola, et al., 2016) (Flicker Byers & Schneider, 2016) (Hu et al., 2016), while the relevant conversion ratio range is stated by 1.2% and 46.3% (Horzum et al., 2012) (H. Zhao et al., 2015) for PAN-AO adsorbent. Table A.2 contains the exact values of these conversion factors. By applying the listed degree of grafting or conversion factors, it is calculated that AF1 adsorbent production requires between 1.19 kg and 5.45 kg hydroxylamine, whereas the required amount of hydroxylamine is between 0.18 kg and 7.26 kg for PAN-AO adsorbent.

The findings in Figure 3.15 demonstrate that when AF1's and PAN-AO's worst-case scenario based on hydroxylamine consumption is compared to open-pit and underground mining methods, they still achieve the greatest outcomes in all impact categories except CC, OD, IRE, ACD, MEU, and LU, which have a fourfold difference. Additionally, AF1 worst-case scenario outperforms the in-situ leaching method in almost all impact categories except for LU. Furthermore, it achieves the best results as compared to the in-situ leaching technique in nearly all impact categories apart from CC, OD, IRE, and LU. In brief, adsorbent methods give better results in at least 10 out of 16 impact categories than conventional uranium mining methods outcomes even under the worst conditions depending on the hydroxylamine consumption. Moreover, when AF1's best-case scenario based on the hydroxylamine usage is compared to the

underground and in-situ leaching methods, the best results are obtained from AF1 case in nearly entire impact categories except for LU. However, it performs poorly in only CC and OD along with the LU impact categories with the highest 3.4 times greater result as compared to the open-pit mining technique. Furthermore, in comparison to open-pit mining, the PAN-AO's best-case scenario achieves the best performance in practically all impact categories except IRE. Additionally, it outperforms in-situ leaching and underground mining techniques in all impact categories. Finally, when the worst-case scenarios of adsorbent methods are examined, it is concluded that AF1 gives the best results in nearly all impact categories apart from HTC and LU impact categories. However, this pattern alters in the comparison between AF1's and PAN-AO's best-case scenarios. That is, PAN-AO yields better results in almost all impact categories except for IRE with the highest 1.9 times greater outcome.



### **3.3.4 Recycling of Adsorbent Scenarios**

Since the demand for raw materials and the required energy strongly depends on the reuse number of the adsorbent in this study, the role of reuse or regeneration of adsorbent with a series number of adsorption-desorption processes may be crucial. To observe the real effect of recycling on environmental impacts, all inputs and outputs listed in Table 3.18 have been recalculated by halving the recycle numbers to 20 and 25 or changing the total uranium capacities for AF1 and PAN-AO. While the amount of chemicals for adsorbent elution is reduced, the required energy and chemicals for an adsorbent production increase with the number of cycles of reuse. Overall, environmental impacts in all impact categories represented in Figure 3.16 increase with the cycle number reduction. However, they are still competitive alternatives even in this case in most impact categories such as PCO, HTC, and IRHH as compared to the conventional uranium mining methods. The results strongly indicate that once the recycling of the adsorbent is improved the environmental impact of the uranium recovery will decrease.

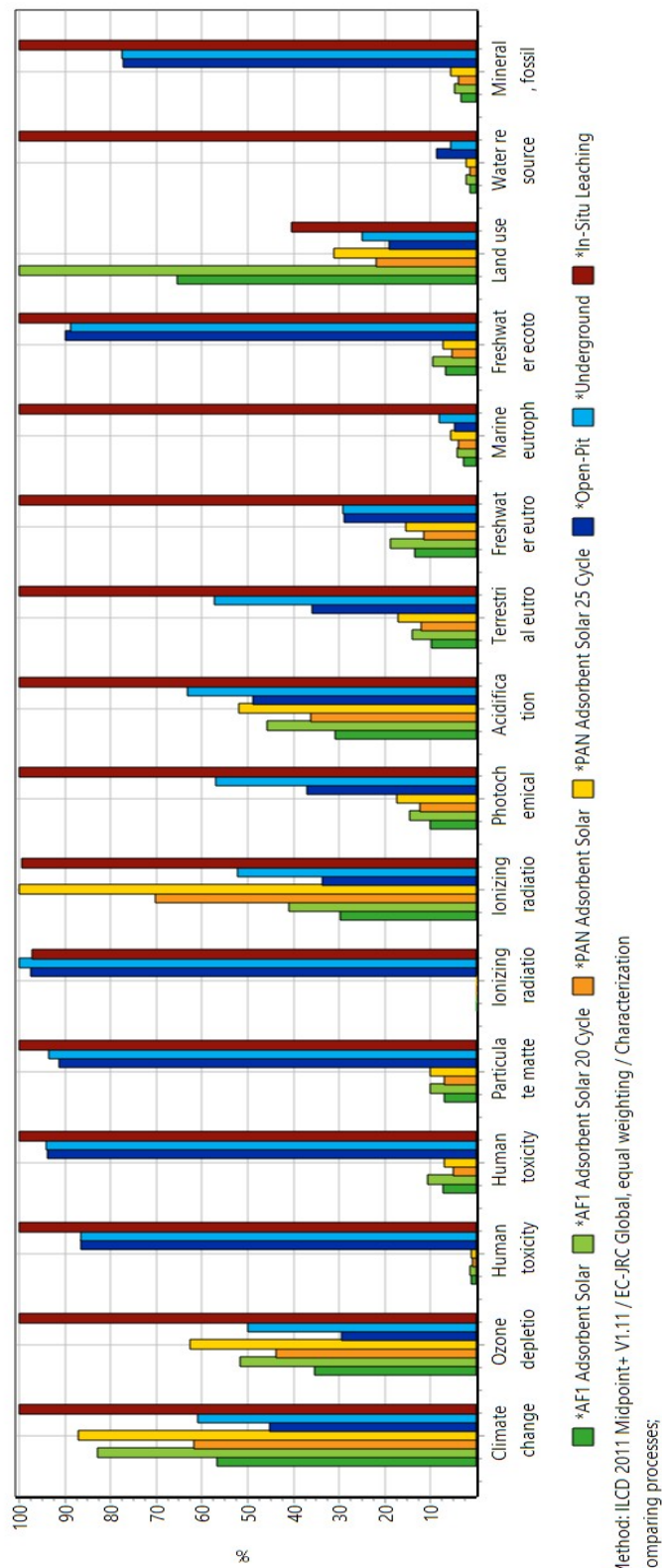


Figure 3.16: Comparative Characterization Results of AF1 and PAN-AO Adsorbents for Different Cycles or Reuse Numbers and Conventional Uranium Mining Methods

### 3.3.5 Comparison of Results with Literature

To understand the potential of adsorbents in uranium mining, the results given above have been compared with the conventional uranium mining findings given in the literature. The study conducted by (Haque & Norgate, 2014) which covers environmental impacts of uranium mining with in-situ leaching focused on just GHG emissions as an impact category and used the Australian Impact Method. Total GHG emissions were estimated as 38.0 kg CO<sub>2</sub>-eq for 1 kg yellowcake production and our overall impact is 142 kg CO<sub>2</sub>-eq by using IPCC 2013 GWP 100a method for in-situ leaching. The main difference between our result and the result provided by (Haque & Norgate, 2014) is due to the heat and electricity requirement differences. Moreover, distinctive databases, assumptions such as ore grade and recovery rate, and methods were also used in both studies. Another article published by (D. J. Parker et al., 2016) focused on the GHG emission intensities of Canadian uranium mining and milling with a cradle-to-gate approach. In the article, mainly 3 large uranium sites that have different uranium mining techniques were discussed using IPCC 2013 GWP 100a method. While underground mining was applied in the first area, open-pit was used for the third option. However, the second uranium site cannot be compared with the scenarios covered in this particular study. Therefore, only the first and third options have been selected to be compared with our results. (D. J. Parker et al., 2016) calculated that for the underground and open-pit mining, using the data provided in the study we have calculated the GHG emission impacts values as 86.5 kg CO<sub>2</sub>-eq and 64.2 kg CO<sub>2</sub>-eq. Although results for underground mining are close and the results for open-pit mining seem unrelatable, making such a comparison is unrealistic because different assumptions such as the inclusion of infrastructure and construction, and inventories were applied for these separate studies. Furthermore, since electricity and heat requirements calculated for our study are higher than the study conducted by (D. J. Parker et al., 2016), more emissions have been obtained in our study. Also, while in these articles researchers modeled their system on a site-specific based, our system has been modeled as representative of the rest of the world scenario. For AF1 and PAN-AO adsorbents, GHG emissions values have been calculated as 82.3 kg CO<sub>2</sub>-eq and 88.9 kg CO<sub>2</sub>-eq respectively by using IPCC 2013 GWP 100a method. However, these results are not enough to compare the results with the given example

studies because different assumptions and system boundaries are valid for different studies. (Farjana et al., 2018) conducted a comparative life cycle assessment of conventional uranium methods with different methodologies by considering Australian circumstances, and different assumptions about system boundaries were made and different databases were used by the authors. The variations between our study and (Farjana et al., 2018) that are presented in Figure 3.17 are mainly caused by specifying different system boundaries. The results show that in-situ leaching is still the most harmful uranium recovery method among nearly all impact categories under these circumstances. Also, although open-pit and underground techniques appear to be a more environmentally friendly way to produce uranium as compared to the other adsorbent cases, in 6 out of 16 impact categories, CC, OD IRE, ACD, FEU, and LU, system responses of adsorbent technologies are not so much different from them with a maximum of 3.5 times higher results. However, in the other 10 categories of adsorbent methods, environmental loads are considerably lower than the results of conventional mining methods with a maximum of 2800 times in the IRHH impact category.

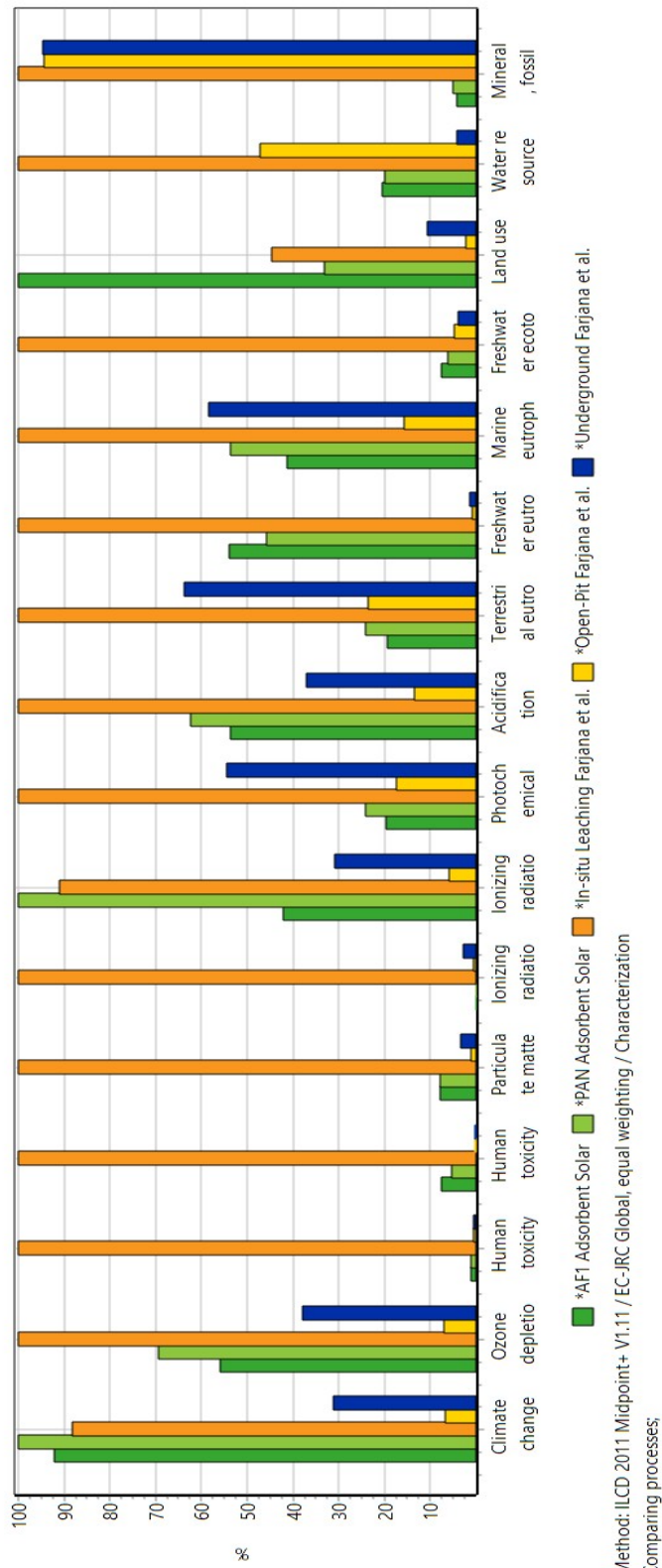


Figure 3.17: Comparative Characterization Results of Adsorbent Calculated in Our Study and Compiled Conventional Mining Methods given in (Farjana et al., 2018)

### **3.3.6 Environmental Sustainability Concept of This Study**

Environmental sustainability is a part of the United Nations SDGs to solve the main problems, including environmental challenges, faced by people all over the world (Leal Filho et al., 2019). In this context, this study reflects the environmental sustainability of the system which helps to achieve some of the SDGs by evaluating the industrialization of a uranium recovery system that shows parallelism with affordable and clean energy (SDG 7) and responsible consumption and production (SDG 12), decent work and economic growth (SDG 8) and industry, innovation, and infrastructure (SDG 9) goals, due to the innovative sustainable uranium extraction process that could provide new job opportunities while converting waste to an energy source. Within the scope of SDG 13 called “climate action”, this study can be considered a mitigation activity because of reducing the dependency on fossil fuel energy sources and GHG emissions. Since this study compares the eutrophication impact of uranium extraction methods with sustainable options and using adsorbents to minimize acidification, it helps to reach the life below water goal known as SDG 14. Furthermore, this study reveals that there is a sustainable way to extract uranium when compared to conventional methods which may cause deforestation and land degradation. That is why, it is directly linked to SDG 15 which includes the protection, restoration, and promotion of sustainable use of terrestrial ecosystems to deal with desertification, land degradation, and loss of biodiversity.

### 3.4 CONCLUSION

Laboratory values for adsorbents used to extract uranium from brine were scaled up to estimate the potential industrial application of this process and also to be compared with conventional uranium mining. The energy source effect on the environmental analysis results has also been considered in this study. Sensitivity analysis has been performed for all system inputs by changing perturbation ratios of  $\pm 10\%$ ,  $\pm 25\%$ , and  $\pm 50\%$  and the recycling of the adsorbent concept has also been introduced to detect its impact on our results. Finally, all results have been compared with the outcomes presented in the literature and the environmental sustainability concept of this study has been discussed.

According to the results, the main outcomes of this study are listed below:

- Extraction of uranium from brine is an applicable process as long as proper adsorbents are produced industrially.
- Adsorbent technologies have less environmental load than conventional uranium mining methods in HTNC, IRHH, and FET impact categories.
- AF1 adsorbent has less negative environmental impact than PAN-AO adsorbent in most impact categories.
- Hydroxylamine and HW disposal are the most sensitive parameters for adsorbent scenarios.
- The environmental impacts of solar scenarios in both adsorbent cases are less than the other energy alternatives.

## CHAPTER 4

### LIFE CYCLE ASSESSMENT OF DESALINATION PLANT COMBINED WITH URFB SYSTEM

#### 4.1 INTRODUCTION

The shortage of fresh water sources is one of the biggest problems in today's world depending on the growth in the human population together with the consumption of water sources for different purposes such as domestic and irrigation. Although 1.4 billion km<sup>3</sup> of water is found in the world, only 0.5% of this amount is accessible clean water (Humplik et al., 2011). The remaining part is salty water and salts can be separated from the water by desalination technologies to provide further fresh water sources (Youssef et al., 2014).

Various kinds of desalination methods and plants are applied in the world. Although the RO system dominates the desalination market in especially Europe because of the lower energy consumption and higher efficiency (Abdullah et al., 2021) (Curto et al., 2021), thermal desalination technologies have advantages in terms of simplicity of operation, higher permeate quality, and ability to deal with water with higher salt content (Fritzmman et al., 2007b). Therefore, there has been a rising trend toward global thermal desalination installed capacity in time (Curto et al., 2021). In the comparison of MSF and MED, MED did not compete with the MSF technology because of the scaling problem and higher capital and operational expenditures in the past. However, a new design solution with operation at a lower top brine temperature (the maximum temperature at which steam can heat seawater) and a cost-effective material usage overcame these problems (Mezher et al., 2011). Moreover, MED electricity requirement and carbon footprint are lower than MSF, so it started to gain ground and became competitive with MSF (Bhojwani et al., 2019). However, high

thermal energy consumption in the MED system which has been also discussed in chapter 2 is the main issue of this technology, so research has been emphasized the integration of MED systems and renewable energy sources that can meet the energy requirement of MED systems and improvement of the system performance by modeling (Mata-Torres et al., 2019). As a renewable energy source, solar energy has an important role and dominates the market as compared to other alternatives (Jijakli et al., 2012). Solar technologies can be separated into two categories: photovoltaic (PV) and solar thermal like concentrating solar power (CSP) or non-concentrating solar power (Qin et al., 2017). The main difference between these two categories is related to what solar energy is directly converted into. While sunlight is converted directly to electricity in the former alternative, it is switched to heat in the latter one. CSP technologies are more suitable for the thermal-based desalination technologies depending on the heat requirement for system operation (Compain, 2012). Moreover, CSP technologies cover mainly line focusing systems named linear Fresnel and parabolic trough and point focusing systems called the solar tower and parabolic dish (Saghafifar & Gabra, 2020). Parabolic trough collectors (PTC) are primarily used in solar heat for industrial processes (SHIP) and electricity production among the CSP plants. Also, PTC dominates the CSP market because of its maturity (Raturi, 2019). The comparative analysis of all CSP technologies is given in Table A.4. Moreover, flat plate collectors and evacuated tube collectors are the most well-known collector types for non-concentrating solar power fields. The former is more common and has simple design that is capable of generating heat up to 100°C above the surrounding temperature. The efficiency of the latter collector type is higher, but it is also costly as compared to the flat plate collectors (Sokhansefat et al., 2018).

Although desalination plants contribute to quality freshwater production, they can have adverse effects on the environment. To fulfill the sustainable development of all types of desalination methods, a detailed investigation about controlling these impacts should be completed with the LCA approach (Esmailion, 2020). Prior environmental impact of the commercial RO, MSF, and MED desalination facilities with and without renewable energy systems was conducted using real plant data with CML 2 baseline 2000, Eco-Points 97, and Eco-Indicator 99 methods (Raluy et al., 2005). The results of prior work declared that operation is the most harmful stage based on

energy consumption. However, compared to fossil fuel-driven desalination plants, this impact can be reduced up to 70% by integrating renewable energy sources into these plants. Another systematic LCA of membrane and thermal desalination plants was conducted comparatively by (Vince et al., 2008). In this paper, IMPACT 2002+ was used to evaluate the environmental impacts quantitatively. Operation phase and chemical consumption were decided as the main reasons for environmental load in this system based on the outcomes of the study. Other examples of LCA studies about desalination plants conducted in the last 10 years are presented depending on distinct features such as LCIA methods and software in Table 4.1. Moreover, further analyses named economic (Aleisa & Al-Shayji, 2018) (Do Thi et al., 2021), social (Abdul Ghani et al., 2020) (Uche et al., 2014), political (Do Thi et al., 2021), quantitative microbial risk assessment (QMRA) (Kobayashi et al., 2015) and mathematical modeling of the system (Aleisa & Heijungs, 2020) (Alhaj & Al-Ghamdi, 2019)(Alhaj et al., 2022)(Mannan et al., 2019) along with the LCA have been followed to achieve more comprehensive and sustainable analysis in the field of desalination.

The LCA studies presented in Table 4.1 were conducted for different desalination technologies and locations by using various techniques. In the literature, there is a tendency to work on the LCA studies of membrane-based desalination systems like RO, and limited studies have been conducted for analyzing the environmental impact of thermal desalination systems for different countries by considering the geographical features of these regions. Various kinds of impact assessment methods named CML 2001, ReCiPe, IPCC 2013, and IMPACT 2002+ have commonly been used to calculate environmental load in distinct impact categories such as global warming potential (GWP), ozone depletion potential (ODP), acidifying potential (AP) and marine eutrophication (MEU). Also, the study conducted by (Do Thi et al., 2021) was unique due to the inclusion of brine impact into the system boundary of the thermal desalination system.

Although the results of all these studies presented in Table 4.2 differ from each other depending on the different geographical conditions, system boundaries, and assumptions that have been made, the role of energy source selection on results has been discussed in all of them by investigating different energy sources like mainly solar (Aleisa & Al-Shayji, 2018) (Alhaj & Al-Ghamdi, 2019)(Alhaj et al., 2022) (Do Thi

Table 4.1: Desalination LCA Studies Performed in the last 10 years

No	Authors	Location	Inflow	Name of Technology	Goal of the Study	Functional Unit	System Boundary	Method&Software	Data Quality
1	(Jfakli et al., 2012)	Abu Dhabi	BW	RO	Evaluating the environmental impacts of solar energy driven desalination plants	1250 L freshwater daily	Operation and construction	Eco-indicator 99, SimaPro	Ecoinvent Database, publicly available sources, and design
2	(Salcedo et al., 2012)	Spain	SW	RO	Deciding the best performance of desalination plant integrated with solar rankine system both environmentally and economically	1 m <sup>3</sup> freshwater	Operation* (construction is excluded)	CML 2001, MINPL in GAMS	Ecoinvent Database and design
3	(Tarnacki et al., 2012)	Spain, Germany, France, the Netherlands, and Portugal	SW	RO, MD	Detecting the environmental impact of desalination technologies in the case of various facility locations, feed water types, and energy sources	1 m <sup>3</sup> desalinated water	Processing or operation, construction, and dismantling processes are not included	CML 2001, NR	MD: pilot or laboratory plants RO: Literature Data Ecoinvent V2.2 Database
4	(Al-Sarkal & Arafa, 2013)	United Arab Emirates	SW	RO	Analyzing the environmental burden of two different pretreatment methods named sedimentation and ultrafiltration applied in SWRO desalination plant	1 m <sup>3</sup> treated water	Operation for only pre-treatment steps, construction and processing*	Eco-Indicator 99(H), SimaPro	Sedimentation-based: Real plants data Ultrafiltration-based: Design data
5	(Anroes et al., 2013)	Spain	SW	RO	Analyzing the environmental load of urban water cycle	1 m <sup>3</sup> potable water	Construction, operation, distribution, consumption and disposal (treatment plant construction is excluded.)	CML 2001, Manual	Ecoinvent Database and publicly available sources
6	(Antipova et al., 2013)	Spain	SW	RO	Detecting the best environmental and economic performance of desalination plant integrated with solar rankine system with a thermal storage	1 m <sup>3</sup> potable water	Construction and operation*	CML 2001, MINPL in GAMS	Ecoinvent Database, publicly available sources and design
7	(Del Bogghi et al., 2013)	Italy	SW	RO, MSF, MED, MVC	Evaluating the progress of the LCA study of the potable water supply in Sicily	1 m <sup>3</sup> treated water	Collection, processing, and distribution of water*	Manual Calculation in GWP, ODP, AP, POCP, and EP impact categories	Real plants data
8	(Godskesen et al., 2013)	Denmark	SW	RO	Carrying out the environmental analysis of various urban water supply alternatives	1 m <sup>3</sup> potable water	Operation, distribution, and disposal (in disposal, only energy is included)	EDIP 1997, GaBi	PE Database, data from municipalities, and publicly available sources
9	(Shahabi et al., 2014)	Australia	SW	RO	Detecting the environmental impacts of renewable energy driven desalination plant	1 m <sup>3</sup> treated water	Construction, operation and transportation (decommissioning is excluded)	IPCC 2007, SimaPro	Ecoinvent and Australian Databases and publicly available sources
10	(Uebe et al., 2014)	Spain	SW	RO	Evaluating the environmental impacts of water supply processes and water use	1 m <sup>3</sup> served water	Assembly and processing*	ReCiPe 2008, SimaPro	Real plants data
11	(Kobayashi et al., 2015)	Australia	SW	RO	Analyzing the environmental impact of the water supply systems on human health by using two different approaches named LCA and QRA to assist water management	18 GL per year of water flow	Operation phase only, construction, transportation, and demolition steps are excluded	ReCiPe Endpoint and Manual Calculations, GaBi 6	Publicly available documents about real plants and Ecoinvent Database
12	(Shahabi, McHugh, & Ho, 2015)	Australia and USA	SW	RO	Detecting and comparing the environmental burden of two scenarios of desalination plants named open intake and bench well	1 m <sup>3</sup> desalinated water	Construction and operation	CML 2001, SimaPro	Economic input-output model and conceptual design
13	(Shahabi, McHugh, Anda, et al., 2015)	Australia	SW	RO	Comparing the different desalination systems based on geography with environmental and cost analysis	1 m <sup>3</sup> desalinated water	Construction, operation and distribution	CML 2001, SimaPro	Ecoinvent and Australian Databases, publicly available sources, economic input-output model and conceptual design

\*: Brine is excluded or unspecified, NR: Not Reported, SW: Seawater, BW: Brackish Water, RO: Reverse Osmosis, MSF: Multi-stage Flash Distillation, MED: Multiple-effect Distillation, SPMD: Solar-powered Membrane Distillation, MVC: Mechanical Vapor Compression, GWP: global warming potential, AP: acidifying potential, POCP: ozone creating potential, EP: oxygen consumption potential, QRA: Quantitative Risk Assessment, MINLP: Mixed Integer Nonlinear Programming, ELCD: European Reference Life Cycle Database, USLCI: the United States Life Cycle Inventory, SIOD: the Swiss Input and Output Database, MAW: Mine-affected Water, SUW: Surface Water, GW: Ground Water, RWV: Recycled Wastewater

Table 4.1: Desalination LCA Studies Performed in the last 10 years continue..

No	Authors	Location	Inflow	Name of Technology	Goal of the Study	Functional Unit	System Boundary	Method&Software	Data Quality
14	(Cherif et al., 2016)	Tunisia	BW	RO	Analyzing the environmental impacts of hybrid renewable energy driven desalination plants	1 m <sup>3</sup> permeate water	Construction and operation*	Embodied Energy, Manual	Publicly available sources and design
15	(Garfi et al., 2016)	Spain	SW	RO	Evaluating the environmental burden and economy of different drinking water supply systems	1 m <sup>3</sup> potable water	Only operation, facilities construction, maintenance and decommissioning and transportation are excluded	CML 2 baseline, SimaPro	Ecoinvent Database, real plants data and publicly available sources
16	(Y. Li et al., 2016)	China	SW	RO, MED	Detecting the environmental impacts of three water supply methods	1 m <sup>3</sup> water that is withdrawn from water media	Construction and operation & maintenance, dismantling is excluded*	CML2011 and USEtox, GaBi	GaBi Database, real plants data and publicly available sources
17	(Aleisa & Al-Shayji, 2018)	Kuwait	SW	RO, MSF, MED	Evaluating the environmental impact and financial aspects of thermal and membrane desalination systems integrated with different energy sources	1 m <sup>3</sup> desalinated water	Only operation, infrastructure is excluded*	CML 2001, SimaPro	ELCD Database and publicly available sources
18	(Al-Shayji & Aleisa, 2018)	Kuwait	SW	RO, MSF	Analyzing the environmental burden of different existing desalination plants	1 ton of desalination water	Only operation, construction, infrastructure, transportation are excluded*	CML 2001, SimaPro	Ecoinvent Database and publicly available sources
19	(A. H. Al-Kaabi & Mackey, 2019)	Arabian Gulf	SW	RO	Evaluating the environmental impact of two desalination facilities applying different pre-treatment methods named open intake and subsurface intake	1 m <sup>3</sup> desalinated water	Only operation, construction, and distribution are excluded*	CML 2001, GaBi	ThinkStep GaBi Database, publicly available sources, and real plants data
20	(Alhaji & Al-Ghandi, 2019)	Qatar	SW	MED	Evaluating the environmental impacts of solar energy driven desalination plant	1 m <sup>3</sup> Freshwater	Construction and operation*	ReCiPe 2016, GaBi	Publicly available sources and ESS model
21	(Goga et al., 2019)	South Africa	SW, MAW	RO	Quantifying the environmental burden of different membrane-based desalination scenarios	1 m <sup>3</sup> potable water	Construction and operation, decommissioning is excluded	ReCiPe: Midpoint, SimaPro	Ecoinvent Database and feasibility study of real plant
22	(Mannan et al., 2019)	Qatar	SW	MSF	Analyzing the environmental burden of desalination plant under different gain output ratios	1 m <sup>3</sup> high-quality desalinated water	Only operation, infrastructure, construction are excluded*	ReCiPe, GaBi	Data generation with VDS software, GaBi Database and publicly available sources
23	(Tarpani et al., 2019)	Northern Chile	BW	MED	Detecting the environmental impacts of small scale desalination plant utilizing different energy sources	1 m <sup>3</sup> desalinated water for agricultural usage	Infrastructure, operation, decommissioning and transportation*	ReCiPe, GaBi	Ecoinvent Database and real plants data
24	(Abdul Ghani et al., 2020)	Malaysia	SW	RO	Deciding the social actors in organizing the environmental complications throughout the small-scale desalination process from environmental and social perspectives	1 m <sup>3</sup> desalinated water	Installation, operation, and post-installation	Eco-indicator 99, SimaPro	Ecoinvent Database and blue book
25	(Aleisa & Hejijungs, 2020)	Kuwait	SW	MSF	Evaluating the environmental impacts of desalination plant utilizing different fossil fuel types	1 m <sup>3</sup> desalinated water	Only operation*	CML-IA, SimaPro	Ecoinvent and ELCD Databases and publicly available sources
26	(Meron et al., 2020)	Israel	SW, BW, SUW, GW	RO	Detecting the environmental burden of centralized water system	1 m <sup>3</sup> potable water	Infrastructure, construction, decommissioning, transportation, operation and distribution	ReCiPe & AWARE, SimaPro	Ecoinvent Database, publicly available reports and personal communications

\*: Brine is excluded or unspecified, NR: Not Reported, SW: Seawater, BW: Brackish Water, RO: Reverse Osmosis, MSF: Multi-stage Flash Distillation, MED: Membrane Distillation, SPMD: Solar-powered Membrane Distillation, MVC: Mechanical Vapor Compression, GWP: global warming potential, ODP: ozone depleting potential, AP: acidifying potential, POCP: ozone creating potential, EP: oxygen consumption potential, QRA: Quantitative Risk Assessment, MINLP: Mixed Integer Nonlinear Programming, ELCD: European Reference Life Cycle Database, USLCI: the United States Life Cycle Inventory, SIOI: the Swiss Input and Output Database, MAW: Mine-affected Water, SUW: Surface Water, GW: Ground Water, RWW: Recycled Wastewater

Table 4.1: Desalination LCA Studies Performed in the last 10 years continue..

No	Authors	Location	Inflow	Name of Technology	Goal of the Study	Functional Unit	System Boundary	Method&Software	Data Quality
27	(Abdul Ghani et al., 2021)	Malaysia	SW	RO	Analyzing the environmental impact of desalination plant	1 m <sup>3</sup> desalinated water	Installation and operation	ReCipe 2016, SimaPro	Ecoinvent Database and publicly available sources
28	(A. Al-Kaabi et al., 2021)	Qatar	SW	RO	Detecting the operational life cycle impacts of desalination plants utilizing the same treatment technology to identify the water quality impact on the results	1 m <sup>3</sup> desalinated water	Only operation, construction is excluded*	CML 2001, GaBi	ThinkStep GaBi Database, real plants data, publicly available sources, and AqMB software
29	(Do Thi et al., 2021)	Saudi Arabia	SW	MSF, MED, RO	Analyzing the environmental impact of power sources	1 m <sup>3</sup> product water	Operation, storage, and distribution (construction and material transportation are excluded)*	ReCipe 2016, IPCC 2013, IMPACT 2002+, SimaPro	Publicly available reports, the real plants data and studies
30	(Ghani et al., 2021)	Malaysia	SW	RO	Analyzing the environmental impact of desalination plant with carbon footprint assessment	1 m <sup>3</sup> treated water	Construction and operation, dismantling stage is excluded*	IPCC 2013, SimaPro	Ecoinvent Database, real plants data and manual calculations
31	(Najjar et al., 2021)	Lebanon	SW	RO	Evaluating the environmental load of desalination plant integrated driven hybrid energy	1 m <sup>3</sup> desalinated water	Construction, transportation, operation, and decommissioning	Impact 2002+, SimaPro	Ecoinvent Database, publicly available sources, HOMER Pro, real plant data and personal communication
32	(Pazouki et al., 2021)	Australia	SW, RWW	RO	Evaluating and comparing the environmental impacts of conventional desalination plants with two desalination plant configurations depending on different inflows and processes	1 m <sup>3</sup> desalinated water	Construction, operation, transportation, and disposal	CML-IA, SimaPro	Ecoinvent Database, publicly available sources, and manual calculations
33	(Tarpani et al., 2021)	Brazil	SW	RO	Deciding the urban water supply method that has the lowest environmental impacts comparatively	1000 m <sup>3</sup> potable water	Operation, infrastructure and transportation*	ReCipe, openLCA	Ecoinvent Database, publicly available sources and data adaptation
34	(Alhaj et al., 2022)	Qatar	SW	MED	Detecting the environmental impacts of solar energy driven desalination plant	1 m <sup>3</sup> freshwater	Construction and operation*	ReCipe 2016, GaBi	Publicly available sources, real plant data and ESS model
35	(Siefan et al., 2022)	Jordan	SW	SPMD, MD	Evaluating the environmental impacts of thermal desalination technology under different energy sources	1 m <sup>3</sup> distillate water	Operation, construction of only electricity distribution network and transportation, system construction and end-of-life are excluded*	ReCipe 2016 Endpoint, SimaPro	Ecoinvent 3, USLCl, SIOD, Industry Data 2.0 and real plant data

\*: Brine is excluded or unspecified, NR: Not Reported, SW: Seawater, BW: Brackish Water, RO: Reverse Osmosis, MSF: Multi-stage Flash Distillation, MED: Multiple-effect Distillation, MD: Membrane Distillation, SPMD: Solar-powered Membrane Distillation, MVC: Mechanical Vapor Compression, GWP: global warming potential, ODP: ozone depleting potential, AP: acidifying potential, POCP: ozone creating potential, EP: oxygen consumption potential, QRA: Quantitative Risk Assessment, MINLP: Mixed Integer Nonlinear Programming, ELCD: European Reference Life Cycle Database, USLCl: the United States Life Cycle Inventory, SIOD: the Swiss Input and Output Database, MAW: Mine-affected Water, SUW: Surface Water, GW: Ground Water, RWW: Recycled Wastewater

Table 4.2: The Main Contributors Affecting the LCA Results in Desalination Technologies based on the Previously Presented LCA Studies

No	Authors	Energy Consumption	Chemical Consumption	Design configuration	Location	Inlet Characteristic	Gain Ratio	Construction	Waste Disposal	Plant Capacity	Time
1	(Jijakli et al., 2012)	✓	✓		✓						
2	(Salcedo et al., 2012)	✓		✓							✓
3	(Tarnacki et al., 2012)	✓				✓					
4	(Al-Sarkal & Arafat, 2013)	✓		✓							
5	(Amores et al., 2013)	✓			✓				✓		
6	(Antipova et al., 2013)	✓		✓	✓						✓
7	(Del Borghi et al., 2013)	✓									
8	(Godskesen et al., 2013)	✓			✓	✓					
9	(Shahabi et al., 2014)	✓		✓	✓				✓		
10	(Uche et al., 2014)	✓									
11	(Kobayashi et al., 2015)	✓									
12	(Shahabi, McHugh, & Ho, 2015)	✓		✓				✓			
13	(Shahabi, McHugh, Anda, et al., 2015)	✓			✓			✓			
14	(Cherif et al., 2016)	✓		✓	✓						
15	(Garfi et al., 2016)	✓									
16	(Y. Li et al., 2016)	✓		✓				✓			
17	(Aleisa & Al-Shayji, 2018)	✓		✓							
18	(Al-Shayji & Aleisa, 2018)	✓									
19	(A. H. Al-Kaabi & Mackey, 2019)	✓		✓	✓						
20	(Alhaj & Al-Ghamdi, 2019)	✓		✓				✓			
21	(Goga et al., 2019)	✓		✓					✓		
22	(Mannan et al., 2019)	✓					✓				
23	(Tarpani et al., 2019)	✓			✓						
24	(Abdul Ghani et al., 2020)	✓		✓					✓		
25	(Aleisa & Hejjungs, 2020)	✓						✓			
26	(Merou et al., 2020)	✓									✓
27	(Abdul Ghani et al., 2021)	✓		✓					✓		
28	(A. Al-Kaabi et al., 2021)	✓		✓	✓	✓					
29	(Do Thi et al., 2021)	✓									
30	(Ghani et al., 2021)	✓		✓	✓					✓	
31	(Najjar et al., 2021)	✓		✓				✓			
32	(Pazouki et al., 2021)	✓		✓							
33	(Tarpani et al., 2021)	✓		✓				✓			
34	(Alhaj et al., 2022)	✓		✓				✓			
35	(Siefan et al., 2022)	✓		✓	✓						

et al., 2021) (Mannan et al., 2019) (Tarpani et al., 2019), biomass (Tarpani et al., 2019) and wind (Alhaj et al., 2022) as an alternative for fossil fuel energy sources to reduce the environmental load. Also, a detailed analysis of the energy source effect on desalination plant LCA results has been completed in all studies except for the studies numbered 10, 13, 15, 17, 18, 24, 25, 27, 30. All results show that the environmental impact caused by thermal desalination technologies can be reduced by the integration of renewable energy with these technologies. To illustrate, it was concluded that nearly a 99% reduction in environmental impacts can be achieved by changing the electricity mix involving %100 renewable energy (Y. Li et al., 2016). Also, distinctive solar energy technologies named PV, PTC, and linear Fresnel collector have been analyzed in detail (Aleisa & Al-Shayji, 2018)(Alhaj et al., 2022) and it was concluded that linear Fresnel collector gives better results as compared to the PTC (Alhaj et al., 2022). Moreover, the most vulnerable impact categories have been listed as AP (Y. Li et al., 2016), GWP (Aleisa & Al-Shayji, 2018) (Al-Shayji & Aleisa, 2018) (Y. Li et al., 2016), MEU (Aleisa & Al-Shayji, 2018)(Al-Shayji & Aleisa, 2018), human toxicity (Alhaj & Al-Ghamdi, 2019)(Alhaj et al., 2022)(Mannan et al., 2019), marine sediment ecotoxicity (Aleisa & Heijungs, 2020) and ozone depletion (Alhaj et al., 2022)(Mannan et al., 2019) in the literature. In these impact categories, the main factors are chemical utilization and design configuration along with the energy consumption. To illustrate, it is claimed that chemical usage has strongly effect on the impact categories named ozone depletion potential (A. H. Al-Kaabi & Mackey, 2019), acidification potential (A. H. Al-Kaabi & Mackey, 2019) and marine aquatic ecotoxicity potential (Aleisa & Heijungs, 2020) (A. Al-Kaabi et al., 2021) and water depletion (Tarpani et al., 2021). Moreover, the construction process shows a considerable contribution to terrestrial ecotoxicity and mineral resource scarcity impact categories (Meron et al., 2020).

Furthermore, nearly 57% of the studies (20 out of 35) did not include the brine disposal step into their system boundaries specifying that it causes a lower environmental impact than the operational phase depending on the energy utilization. However, brine still causes serious impacts on marine life because of the toxic nature (Zhou et al., 2013) (Panagopoulos et al., 2019). The remaining 43% of the LCA studies (15 out of 35) cover the brine disposal phase, but none of them included its potential in

the metal recovery field in their system boundaries.

Moreover, desalination plants is a necessity for some regions with no or difficult access to clean water like an island, but the environmental impact of this technology has to be analyzed first to prevent the possible adverse effects on the environment and human health. This study focus on the LCA study of the middle-scale MED plant integrated with URFB systems and solar facility considering the Mediterranean's conditions that are suitable for installation of solar technologies due to solar irradiance.

## **4.2 METHODOLOGY**

Life cycle assessment (LCA) is executed by compiling and evaluating the system inputs and outputs to detect the possible environmental load of any product or process system during its life cycle (Guinee et al., 2011). The assessment includes the ISO 14040 that covers goal and scope definition, life cycle inventory (LCI), life cycle impact assessment (LCIA), and results interpretation (Buyle et al., 2013). Environmental impacts of the system are considered for sustainable system design besides its economic and social impacts (Heijungs et al., 2010).

### **4.2.1 Goal and Scope Definition**

Before combining the desalination plant and URFB system to detect its environmental impact, LCA of only middle-scale solar-driven MED system conditions has been conducted from a cradle-to-gate perspective first and this system is presented as a second system in the Figure 4.1. The parameters named global warming (GW), stratospheric ozone depletion (SOD), ionizing radiation (IR), ozone formation human health (OFHH), fine particulate matter formation (FPMF), ozone formation terrestrial ecosystems (OFTE), terrestrial acidification (TA), freshwater eutrophication (FEU), marine eutrophication (MEU), terrestrial ecotoxicity (TE), freshwater ecotoxicity (FE), marine ecotoxicity (ME), human carcinogenic toxicity (HTC), human non-carcinogenic toxicity (HTNC), land use (LU), mineral resource scarcity (MRS), fossil resource scarcity (FRS) and water consumption (WC) were decided as the parameters to be analyzed with this analysis. Moreover, the system has been modeled by a consequential approach and allocation is avoided. The functional unit of the second system has been specified as “1 m<sup>3</sup> of distillate production” to be able to make a

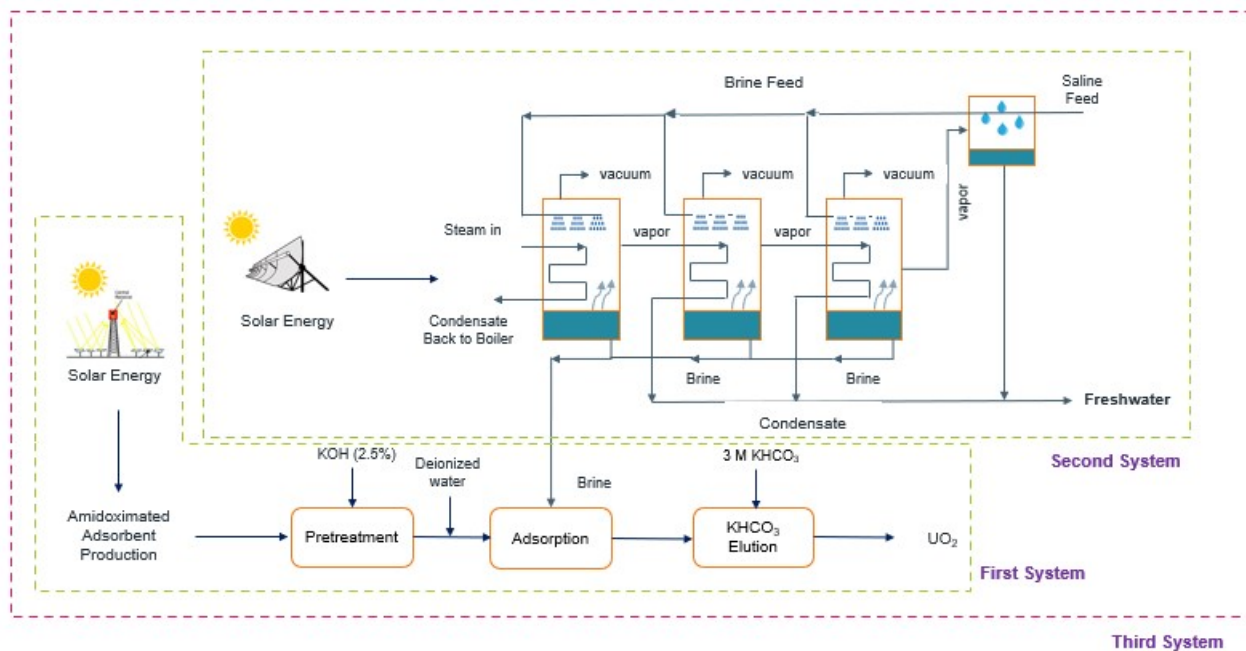


Figure 4.1: Overview of Systems Investigated in This Study

consistent comparison with the presented studies in the literature. Then, the modeled system has been combined with URFB systems, but the functional unit of the study has been changed to “1 kg of uranium production as yellowcake with a purity of 90%” and this system is called the third system in Figure 4.1. SimaPro 9.2.0.1. (PhD version) has been used as an LCA software to quantify the environmental impact of this study. The system boundary of the second system includes solar field construction and decommissioning, MED infrastructure, MED decommissioning, and operation of the plant, and a detailed representation of the MED system boundary are demonstrated in Figure 4.2. Additionally, while the brine is released into the ocean in the second system, it is used as a raw material for uranium production in the third system. Also, the transportation step is not included in the boundaries of these systems.

#### 4.2.2 Inventory Analysis

The material and energy data have been collected according to the system boundary and the main LCA design parameters are presented in Table 4.3. The data about solar field construction, operation, and decommissioning have been obtained from ecoinvent v3.6 Database by applying linear scale down procedure (Alhaj et al., 2022)

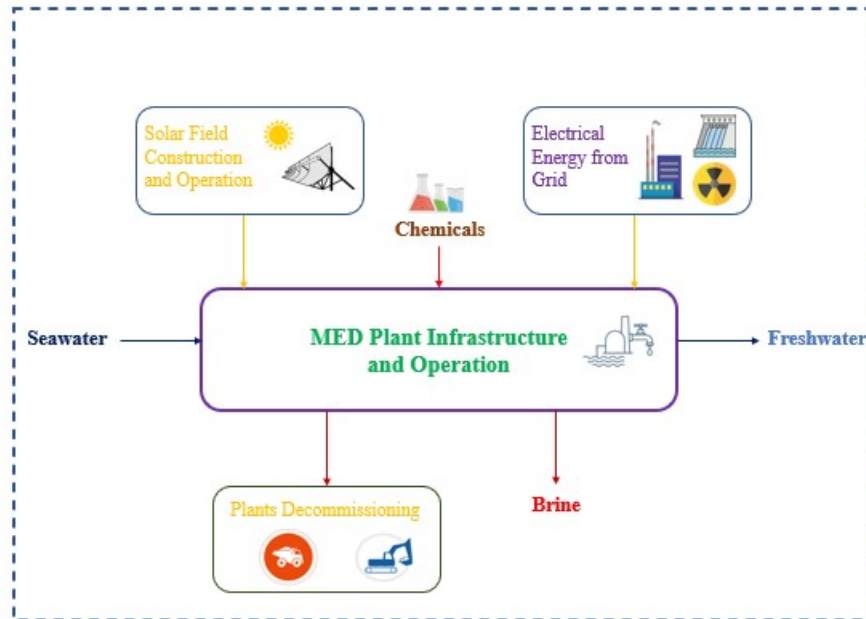


Figure 4.2: The System Boundary of Solar-Driven MED Plant Investigated in This Study

to 50 MW capacity plant to 3.5 MW capacity plant that has been evaluated by ESS model results (Taylan, 2019). The data for MED infrastructure and decommissioning has been taken by the study conducted by (Tarpani et al., 2019), the required area for MED plant that is proportional to distillate amount has been provided by Plataforma Solar de Almeria (PSA-CIEMAT) during the field trip to Spain. A detailed design of the MED plant is shown in Figure A.1 and the system schema of PTC+MED plant is represented in Figure 4.3. Also, the results of custom code developed by Plataforma Solar de Almeria (PSA-CIEMAT) about the amount of raw seawater, brine, and energy consumption during the MED operational stage have been processed in LCI. Thermal and electrical energy requirements for MED operation have been calculated as 88.57 and 0.78 kWh per 1 m<sup>3</sup> fresh water production. The real plant values presented in the article (Do Thi et al., 2021) have been used for the chemicals consumed throughout MED operation. All inputs and outputs values used in the solar-driven MED plant are presented in detail in Table A.3. Although the data quality is assured by the ecoinvent v3.6 database, model results, and literature values, the following assumptions were made to fill the gaps:

- The plant lifetime is 25 years.
- All electricity is supplied from the electricity grid which is %100 fuel oil-based.

Table 4.3: Important Design Parameters of Solar-Driven MED LCA to Produce 1 m<sup>3</sup> Distillate

Name of Parameters	Description	References
Lifetime	25 years	Assumption
Electrical Energy Utilization	0.78 kWh	PSA-CIEMAT
Thermal Energy Utilization	88.57 kWh	PSA-CIEMAT
MED Infrastructure and Decommissioning Inventory	Data from existing plants	(Tarpani et al., 2019)
MED Operation Inventory	Data from existing studies for operational chemicals and input material from nature with design	(Do Thi et al., 2021) and PSA-CIEMAT
Construction, Operation and Decommissioning of Solar Field Inventory	Application of linear scale down procedure	Ecoinvent Database

After all data was collected for 1 m<sup>3</sup> freshwater production, they have been arranged for the third system or desalination plant combined with the URFB system with the functional unit of 1 kg U production. Since uranium concentration in a typical brine sample is equal to 0.0066 mg/L (Wiechert et al., 2018), 151515.15 m<sup>3</sup> brine is required to produce 1 kg of U. When 41.7 m<sup>3</sup> of distillate is generated, 69.3 m<sup>3</sup> of brine from 190.6 m<sup>3</sup> of seawater is also produced from our MED plant system (Figure A.1). The freshwater and seawater amounts processed in the MED desalination plant when producing 1 kg of U are calculated below:

$$\text{The Amount of Distillate} = 151515.15 \text{ m}^3 \text{ brine} * 41.7 \text{ m}^3 \text{ distillate} / 69.3 \text{ m}^3 \text{ brine}$$

$$*\text{Total Amount of Distillate} = 91171.5 \text{ m}^3 = 91171.5 \text{ tons}$$

$$\text{Total Amount of Seawater} = 151515.15 \text{ m}^3 \text{ brine} * 111.09 \text{ m}^3 \text{ seawater} / 69.3 \text{ m}^3 \text{ brine}$$



Midpoint have been used to estimate the environmental impact of the solar-driven MED plant integrated with the URFB system.

### **4.3 RESULTS and DISCUSSION**

This section covers the interpretation stage, which is the final step in the LCA process, by discussing the critical issues and analyzing the data's sensitivity, completeness, and consistency. The study's main results and limitations, as well as its suggestions, are also debated.

#### **4.3.1 Characterization and Normalization Results of Solar-Driven MED Plant**

The characterization results declare that the electricity production mix based on 100% fuel oil and MED operation are responsible for the main environmental impact of the system in all impact categories except for MEU (Figure 4.4). The solar field construction stage has nearly the same environmental impact as the MED operation phase in MEU depending on the nitrate release to water due to the heat transfer fluid itself named diphenyl ether compound. While electricity mix is the main reason for environmental load in 8 out of 18 impact categories with the highest percentage of nearly 83 depending on the airborne emissions from heavy fuel combustion and petroleum consumption, this ratio is valid for the MED operation stage also with the highest percentage of approximately 73 due to mainly waterborne emissions from phosphoric acid, sodium bisulfite, and chlorine production and brine release to ocean along with the raw material consumption. Moreover, the contribution of electricity mix and MED operation are nearly equal to each other in the IR impact category (0.016 kBq Co-60 eq) because of the radon-222 and carbon-14 emission to air from the end of life treatment of electricity mix and the production of the required chemicals named sodium bisulfite, phosphoric acid, and chlorine for MED operation.

The results of the normalization analysis declare that there are five critical toxicity-related impact categories named TE, FE, ME, HTC, and HTNC (Figure 4.5). Based on the characterization results presented in Figure 4.4, the contribution of the electricity mix is greater than the effect of the MED operation stage in only 1 of these 5 impact categories with the ratio of nearly 72% depending on the vanadium, copper, and nickel emissions to air from the heavy fuel combustion process. In FE,

HTC, and HTNC impact categories, phosphoric acid production is responsible for these loads depending on the copper, chromium IV, and zinc released to water from disposal activities and sulfuric acid utilization required to produce phosphoric acid. Also, sodium bisulfite production has also an important role in load in the HTNC impact category due to the electricity consumption to produce sodium hydroxide used in sodium bisulfite manufacture. Moreover, brine discharge from the MED operation process contributes the highest impact in the ME impact category.

Also, the solar collector type has been changed from PTC to flat-plate collector to analyze the impact of collector type on environmental analysis results by using the inventory found in Ecoinvent 3.6 database. The results presented in Figure B.7 claim that the MED plant driven by PTC collector gives the best results in all impact categories as compared to flat plate collector, but the difference between them is lower than the 1.6 orders of magnitude and the biggest differences are observed in mainly eutrophication and toxicity related impact categories depending on the electricity consumption of flat-plate system from different sources like hard coal.

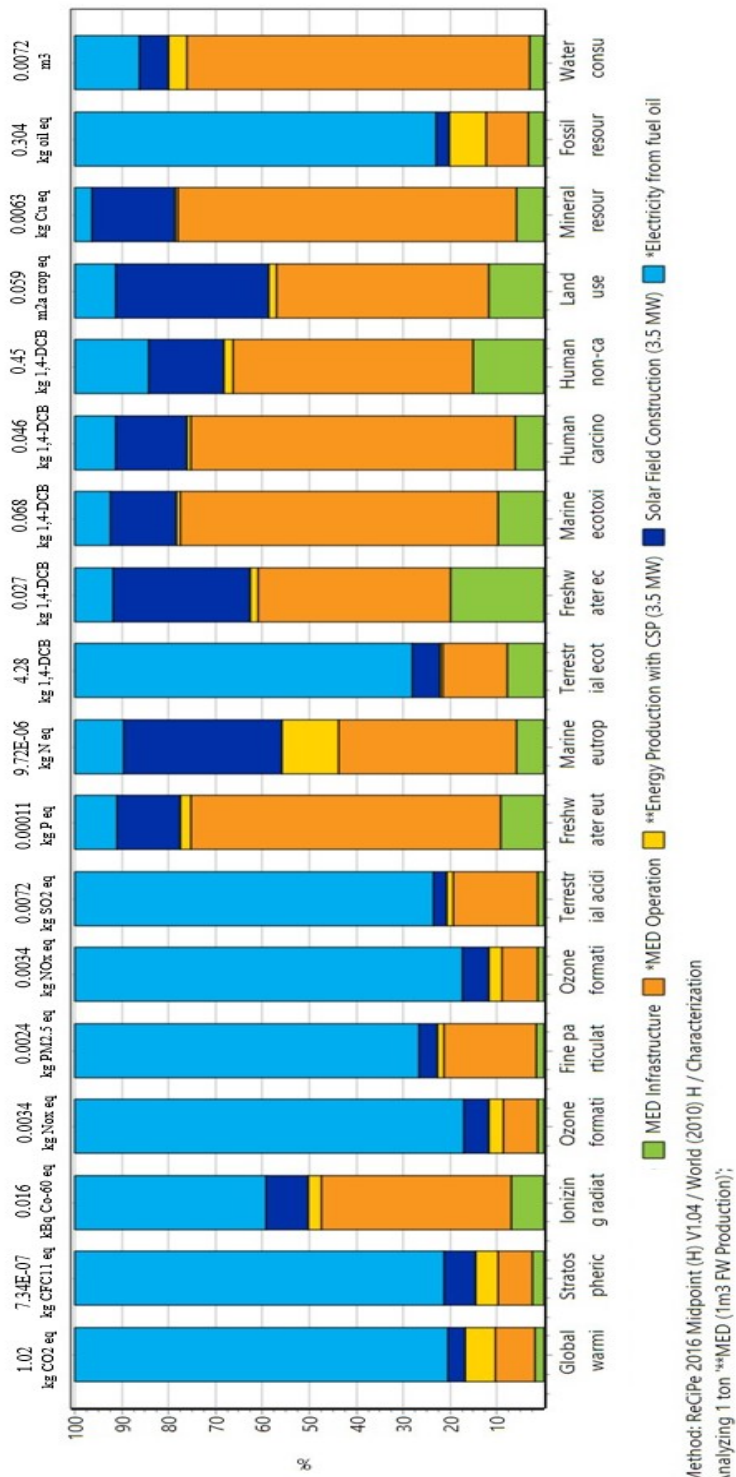


Figure 4.4: Characterization Result of Solar Driven MED Plant

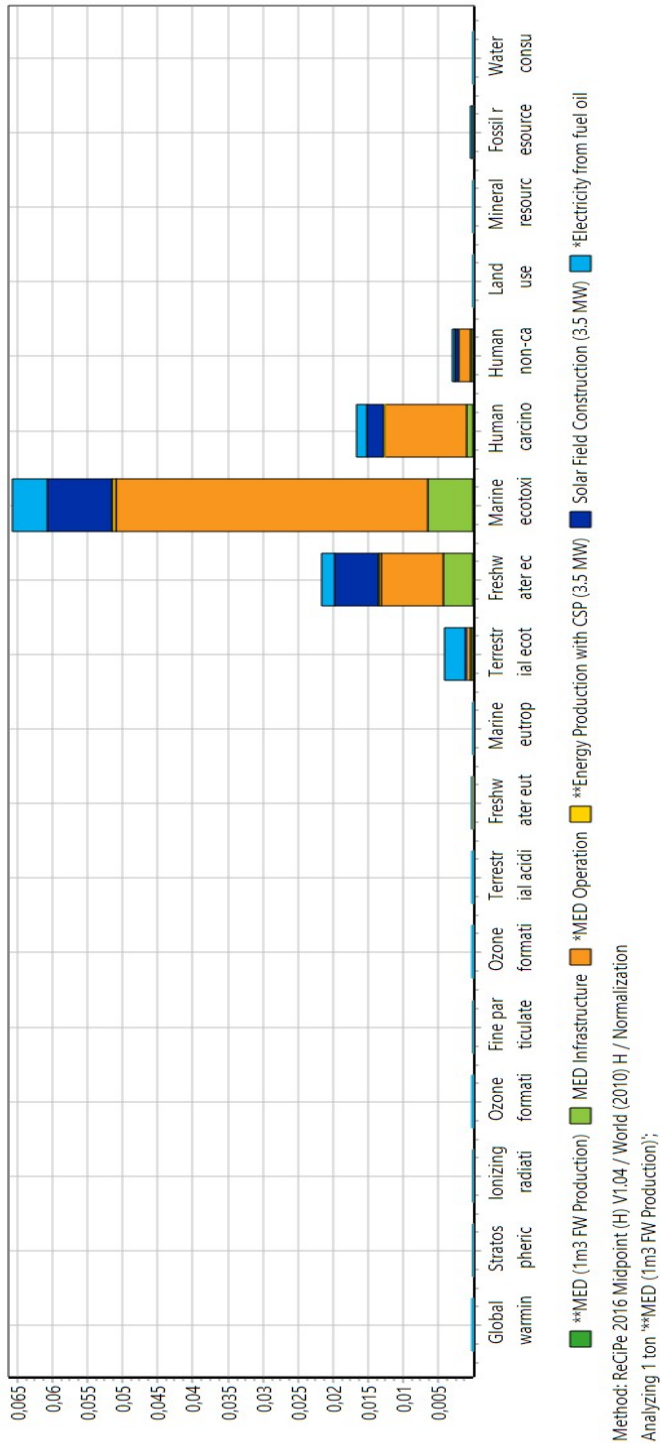


Figure 4.5: Normalization Result of Solar Driven MED Plant

The characterization and normalization results of this study show a similarity with the literature results in terms of the main system stage that leads to considerable impacts on the system. It is stated that the consumption of 100% fuel oil to generate electricity is one of the main reasons for the environmental impact resulting from the MED plant investigated in this study, but the dependency on fossil fuels can be reduced by the installation of renewable energy sources in this study area. Moreover, the chemicals that cause a considerable environmental load can be replaced with more environmentally friendly ones. For example, sulfuric acid can be substituted for phosphoric acid utilized as an antiscalant agent (Alhaj et al., 2022). Also, the environmental impact of the MED plant integrated with the solar field can be decreased by technological developments that help to increase the efficiency of the system. In the study presented by (Aly et al., 2022), the energy consumption reduction with the highest percentage of 70 was achieved with a novel integration of absorption compressor to MED. Moreover, it should be an alternative management method for brine disposal due to the high impact in the ME impact category. Uranium recovery from brine can be an alternative way discussed in Chapter 3 of this study (Altay et al., 2022). Also, surrogate heat transfer fluids may be used instead of using a diphenyl-ether compound that is the main parameter being harmful to the environment in the MEU category. The environmental impact of the ternary mixture of molten salt composed of  $\text{NaNO}_2$ ,  $\text{NaNO}_3$  and  $\text{KNO}$  compounds was evaluated lower than the fluid used in this study based on the results of the LCA study carried out by (Batuecas et al., 2017), so it can be used as an alternative heat transfer fluid to reduce the load in our study. Moreover, the transportation stage has not been included in this study, but it may also contribute a considerable impact depending on the geographical features of the study area.

#### **4.3.2 Sensitivity Analysis**

When the model, data, and assumptions used in the LCA study are changed, the results of the study are affected by these alterations. In sensitivity analysis, these variations are analyzed by comparing base case scenario results with the modified ones (Wei et al., 2015). GW, FE, ME, and HTC have been decided as 4 main impact categories analyzed within the scope of sensitivity analysis of this study since these categories have a critical position in the environmental load of the system and have a direct relationship with the goal and scope of this study.

Two sensitivity analyses have been carried out to investigate the most sensitive system stage and how variations in electricity grid source would reflect on the environmental load. In the first analysis, all input values found in every stage have been altered with perturbation ratios of  $\pm 10\%$ ,  $\pm 25\%$ , and  $\pm 50\%$  and the electricity grid mixes of various countries named the United Kingdom, France, Brazil, Spain, and Turkey as an alternative for electricity grid of 100% fuel oil-based have been defined in the second sensitivity analysis. During the selection of these countries, attention was paid to the fact that the dominant energy source was different from each other and the pioneering in the field of solar technologies and geographical features. For example, while natural gas is the main source of electricity production in the United Kingdom (UK) (G. Zhao & Baker, 2022), nuclear and hydropower dominate France (FR) (Dong et al., 2018) and Brazil (BR) (Paim et al., 2019) electricity mixes, respectively. In Spain (SP), the share of renewable energy in electricity production is higher than most European countries based on the ecoinvent v3.6 Database, and Spain has been considered as one of the pioneer countries in the area of CSP technology development (Baharoon et al., 2015). Finally, Turkey (TR) was chosen as one of the countries to be analyzed since it is located in the Mediterranean region and it has high solar potential (Sözen et al., 2005). Moreover, the majority of the electrical energy produced in Turkey comes from fossil fuels (Atilgan & Azapagic, 2016b). The electricity sources of these countries are presented in detail in Table 4.4. Finally, the scenario where all the energy is supplied from the sun, or the system can meet its own energy has also been considered. After all scenarios are defined clearly, the results have been evaluated with the same impact assessment method named ReCiPe 2016 Midpoint.

Table 4.4: Electricity Sources of the Selected Countries in 2016 (Ecoinvent 3.6)

<b>Share in the Grids of Countries (%)</b>					
<b>Energy Sources</b>	<b>TR</b>	<b>SP</b>	<b>BR</b>	<b>FR</b>	<b>UK</b>
Coal (Hard coal, lignite, etc.)	33,09%	16,54%	2,97%	1,49%	10,83%
Oil	0,42%	4,32%	3,37%	0,32%	0,20%
Natural Gas	29,42%	11,70%	13,57%	4,32%	44,62%
Wind	6,33%	21,64%	3,69%	3,97%	11,20%
Geothermal	1,81%	0,00%	0,00%	0,00%	0,00%
Solar	0,00%	2,22%	0,00%	0,00%	0,00%
Hydropower	27,15%	17,29%	62,81%	12,61%	2,52%
Heat and Power Cogeneration (Biogas, woodchips, etc.)	1,77%	1,23%	4,44%	1,77%	5,81%
Nuclear	0,00%	24,64%	2,61%	75,17%	24,83%
Others	0,00%	0,43%	5,23%	0,35%	0,00%

The absolute results of the first sensitivity analysis presented in Figure 4.6 reveal that energy production with fuel oil is the most sensitive system stage in the GW impact category with the highest system response of nearly 40% due to the heavy metal, particle, and toxic chemical emissions to air during combustion of fuel (Figure 4.6a). For the FE impact category, the most susceptible system phases have been detected as MED operation and solar field construction with the highest percentages of nearly 21 and 15, respectively due to the toxic nature of chemicals consumed during the operation of the MED plant and waste disposal of power block being a part of the solar field (Figure 4.6b). The highest system response culminates in nearly 35% for the MED operation stage in both impact categories named ME and HTC because of the potential toxicity of brine to marine life and the treatment of waste generated in phosphoric acid manufacture (Figure 4.6c and 4.6d). The first sensitivity analysis results show similarity with the outcomes of the study conducted by (Y. Li et al., 2016). The biggest system response was also observed in the operation stage when the energy source is switched to 100 % renewable energy among other system parameters named transportation of materials and concrete consumption in their study. While the

variation in the GW impact category was estimated as nearly 50% with total renewable energy utilization, approximately 79% reduction has been detected in our study depending on mainly electricity mix and energy amount differences.

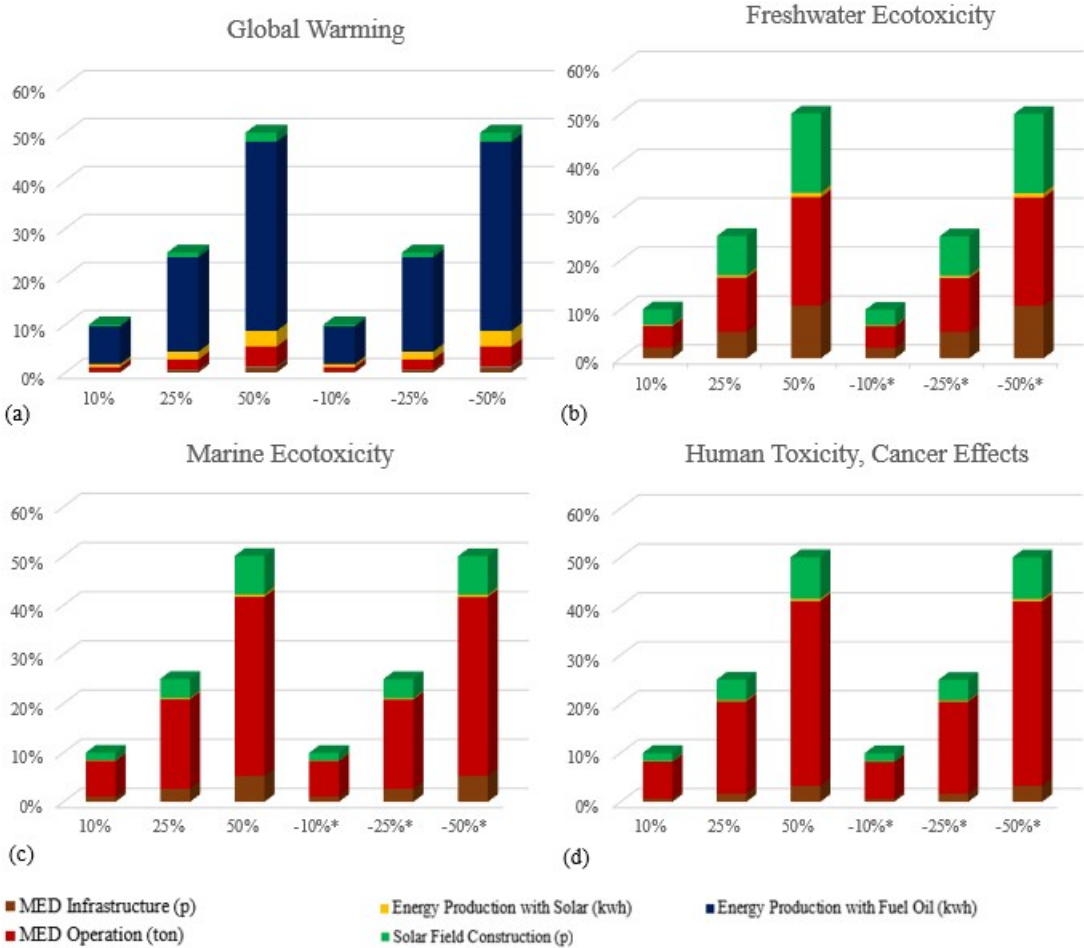


Figure 4.6: Sensitivity Analysis Results in (a) GW, (b) FE, (c) ME, and (d) HTC Impact Categories for Solar-Driven MED Plant (\* refer to negative perturbation ratio and all results are presented in absolute value.)

The second analysis of the electricity mix variation impact on results declares that the negative variance is observed in only the GW impact category in all alternative grid cases (Figure 4.7). While the best case scenario has been seen in the totally solar grid case with the reduction in all impact categories with the highest percentages of approximately 79 in the GW category, Turkey's grid has resulted in the worst case due to the dependency of lignite in its grid. Also, environmental load in all impact

categories except for the GW shows a substantial increase with the ratio up to 45% in HTC in the Turkey grid due to the emission of zinc, arsenic, and nickel to water. In the Spain scenario, while the decline with the percentage of 56 has been detected only in the GW category like Turkey case, the environmental loads have risen in HTC and FE categories with a ratio of almost 12% due to the arsenic, nickel, and zinc release to water due to hard coal consumption. Alterations of the grid from 100% fuel oil-based to France have resulted in the environmental impact reduction in all impact categories as in the totally solar case and the variance ratios in these categories except for GW are close to each other. In the Brazil grid, only an increase has been seen in the FE impact category, but this ratio is close to 0. Finally, the environmental loads in GW and ME impact categories have reduced with the grid source change to the United Kingdom, but the reduction percentage in the latter impact category is nearly 0. The average increase ratio is equal to 4% in the other impact categories because of the hard coal consumption. The comparative sensitivity results of this study declare that France’s grid based on nuclear energy is the most environmentally benign alternative as compared to the other countries’ grids to produce electricity for the MED plant (Figure 4.7).

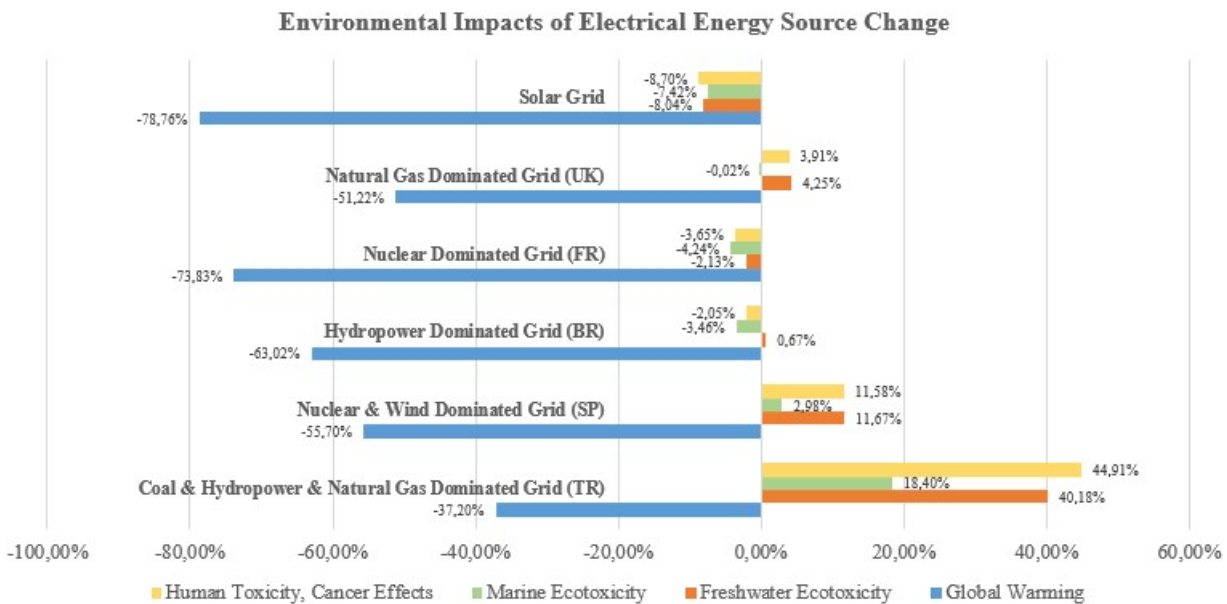


Figure 4.7: Electricity Mix Impact on Results in GW, FE, ME, and HTC Impact Categories for Solar-Driven MED Plant

The second sensitivity analysis results show parallelism with the study results presented by (Do Thi et al., 2021). When the energy source is changed from oil to natural gas, renewable or nuclear dominant sources, it was deduced that the impact on human health can be reduced significantly. In the study conducted by (Tarpani et al., 2019), biomass and solar energy were also considered as energy sources for small-scale MED plants for isolated communities to produce distillate being used for agricultural purposes. The results of this study declare that the best results are obtained in solar-powered scenarios. Although consumption of biomass as a thermal energy source has increased the toxicity impact potential, the reduction in climate change potential, air impacts, and terrestrial acidification potential have been observed as compared to the current diesel-based operating scenario. Moreover, the transportation of the pellets has contributed a considerable environmental impact in several impact categories based on the results of this study. Biomass has not been considered as an alternative energy source directly in our study since it can show an alteration depending on composition, availability, and characteristics from time to time and from one place to another. Furthermore, the results of the study presented by (Mannan et al., 2019) about solar energy integration with MSF desalination plant claim that introduction of solar energy to MSF system by 20% ratio causes a 15% reduction in CO<sub>2</sub> emission. Although all thermal energy was supplied with the solar energy in their system, their emission results for different system configurations are still higher than the result of this study (0.21 kg CO<sub>2</sub> eq) depending on mainly different amounts of energy requirements (Figure 4.7).

#### **4.3.3 Comparative Characterization and Normalization Results of Solar-Driven MED Plant Combined with URFB System**

Once a solar-driven MED plant is integrated with URFB systems, the overall impact listed in Table 4.5 and Table B.1 increases considerably as compared to the results of the first, given in Table 3.22, and second, presented in Figure 4.4, systems depending on mainly the high volume of freshwater production with MED plant. The main pollutant sources and the most sensitive impact categories of the combined system are identical to those of the second system. However, it is not favorable to compare the results of URFB systems and solar-driven MED plants integrated with URFB directly because of the difference in the final products and functional units of these

systems. For example, while only 1 kg uranium is produced in the first system of this study, 91171.5 m<sup>3</sup> of fresh water along with the 1 kg of uranium is generated in the third or combined system. In the case of the second system, the results may be compared when the functional unit of the second study is changed from 1 m<sup>3</sup> of freshwater production to 91171.5 m<sup>3</sup> of freshwater production. Therefore, the solar-driven MED plant presented in the second study and the combination of this system with URFB systems including their worst and base case scenarios based on hydroxylamine consumption can be analyzed together and the effect of URFB systems on the environmental performance of MED plants can be studied in depth. The results of this analysis shown in Figure 4.8 declare that although integration of URFB systems to MED plants leads to an increase in environmental pollution slightly in the MEU impact category for base-case scenarios due to the hydroxylamine consumption in the adsorbent production stage, it reduces the environmental load with the ratio of approximately 46% in ME impact category because of preventing the release of brine to the ocean as compared to the all adsorbent scenarios. However, the disparity between the outcomes of the worst case adsorbent and only MED plant scenarios in the MEU impact category is more visible with a nearly 1.2 times difference. Moreover, the impacts in other impact categories remain unchanged with this modification for all scenarios due to mainly the same amount of electricity generation from fuel oil during desalination processes.

Additionally, there are six comparable impact categories named CC, OD, PM, FEU, MEU and WRD between ILCD 2011 Midpoint+ and ReCiPe 2016 Midpoint impact assessment methods depending on the units of measurement (Colucci et al., 2021). The characterization results obtained by ILCD 2011 Midpoint+ method and presented in Appendix B.1 claim that there is no significant difference between the findings estimated by ReCiPe 2016 Midpoint method in the relevant impact categories except for the MEU impact category with two orders of magnitude depending on the different characterization factors and emission compartment consideration (Acero et al., 2016).

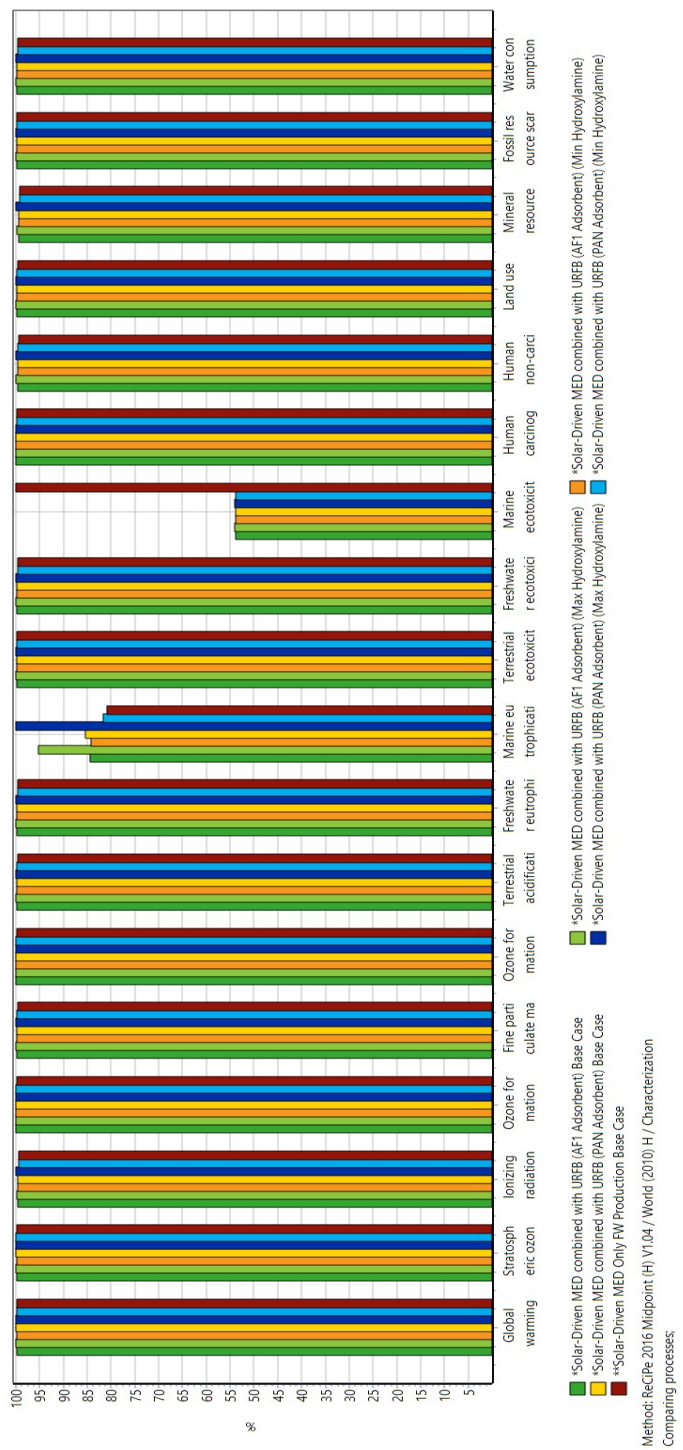


Figure 4.8: Comparative Characterization Results of Solar-Driven MED Plant and Solar-Driven MED Plant Integrated with URFB Systems via AFI and PAN-AO Adsorbents (ReCiPe 2016 Midpoint)

Table 4.5: The Characterization Results of Solar-Driven MED System Integrated with URFB via AF1 and PAN-AO Adsorbent (ReCiPe 2016 Midpoint)

<b>Impact Category</b>	<b>MED combined with URFB System (AF1) Base Case</b>	<b>MED combined with URFB System (PAN-AO) Base Case</b>
Global warming (kg CO2 eq)	93238	93244
Stratospheric ozone depletion (kg CFC11 eq)	0.067	0.067
Ionizing radiation (kBq Co-60 eq)	1484	1485
Ozone formation, Human health (kg NOx eq)	308.4	308.5
Fine particulate matter formation (kg PM2.5 eq)	214.7	214.7
Ozone formation, Terrestrial ecosystems (kg NOx eq)	312.1	312.2
Terrestrial acidification (kg SO2 eq)	655.8	655.8
Freshwater eutrophication (kg P eq)	9.96	9.95
Marine eutrophication (kg N eq)	0.928	0.939
Terrestrial ecotoxicity (kg 1,4-DCB)	393422	393411
Freshwater ecotoxicity (kg 1,4-DCB)	2425	2424
Marine ecotoxicity (kg 1,4-DCB)	3340	3339
Human carcinogenic toxicity (kg 1,4-DCB)	4227	4226
Human non-carcinogenic toxicity (kg 1,4-DCB)	40827	40820
Land use (m2a crop eq)	5366	5363
Mineral resource scarcity (kg Cu eq)	578.3	578.3
Fossil resource scarcity (kg oil eq)	27791	27797
Water consumption (m3)	659.5	659.5

#### **4.3.3.1 Comparison of Results with Conventional Reverse Osmosis Integrated with URFB Systems**

To understand the potential of URFB systems in other desalination methods, the LCA results of MED plant combined with URFB system have been compared with the outcomes of RO plant integrated with URFB systems after functional units of both studies are equalized to 1 kg of U production. According to the RO plant inventory given in ecoinvent v3.6 Database, the drinking water production is achieved with seawater reverse osmosis with conventional pretreatment using two stages configuration and enhanced membrane modules. Moreover, the recovery rate of this plant is specified as 55%, but this ratio is equal to 37.5% for the MED plant depending on the working principle and system configuration differences (Figure A.1). While this dissimilarity brings about the production of different amounts of freshwater (185185.2 m<sup>3</sup> distillate from RO facility and 91171.5 m<sup>3</sup> distillate from MED plant), the amount of uranium that can be produced from both systems is equal to each other. Furthermore, the main disposal method of RO membrane is specified as landfill and it is assumed that the composition of brine obtained from both plants are similar to each other to make a comparison between them (Fard et al., 2015) (Ahmad et al., 2019) (Wiechert et al., 2018).

The characterization results of the base case MED using 100% fuel oil to generate electricity and conventional RO plants integrated with URFB systems claim that the environmental impact of MED plant combined with URFB system is lower than the impact of RO plant in all impact categories with the lowest ratio of nearly 2.7 times (Figure 4.9). However, it should be noted that the overall amount of freshwater produced in the RO plant is approximately 2 times higher than the distillate amount generated in the MED facility based on the recovery ratios of the systems investigated in this study. Moreover, the environmental load of the URFB system is very low when compared to both desalination systems. Electricity production from mainly hard coal, chemical consumption like sulfuric acid during operation, production and disposal of polyvinylidenechloride used as filtration material in RO desalination are the main causes of the high load in RO plants combined with URFB systems. The released pollutants and the processes that cause these pollutants to spread during 1 kg of uranium generation from RO plant combined with URFB system are summarized

in different impact categories in Table B.2.

Similar to the MED plant results, normalization results of the RO system combined with URFB systems declare that TE, FE, ME, HTC, and HTNC are the most critical impact categories due to mainly electricity production from hard coal (Figure 4.10) (Table B.2). The system results of the RO plant integrated with URFB systems are considerably higher than the outcomes of the MED plant combined with URFB systems in the listed critical impact categories based on the normalization results of this study.

Moreover, to reduce the impact caused by the electricity generation of the combined RO plant, the electricity source has been altered from mainly hard coal to solar one as in the combined MED plant and totally solar cases for both plants have been compared. The results of this analysis shown in Figure 4.11 assert that the solar-driven RO plant with URFB system still gives the worst results as compared to the solar-driven MED plant with URFB in all impact categories. In this case, the impact gap between two desalination technologies widened in some impact categories such as LU due to the elimination of land area used for coal mining activities, while it closed in other impact categories like IR.

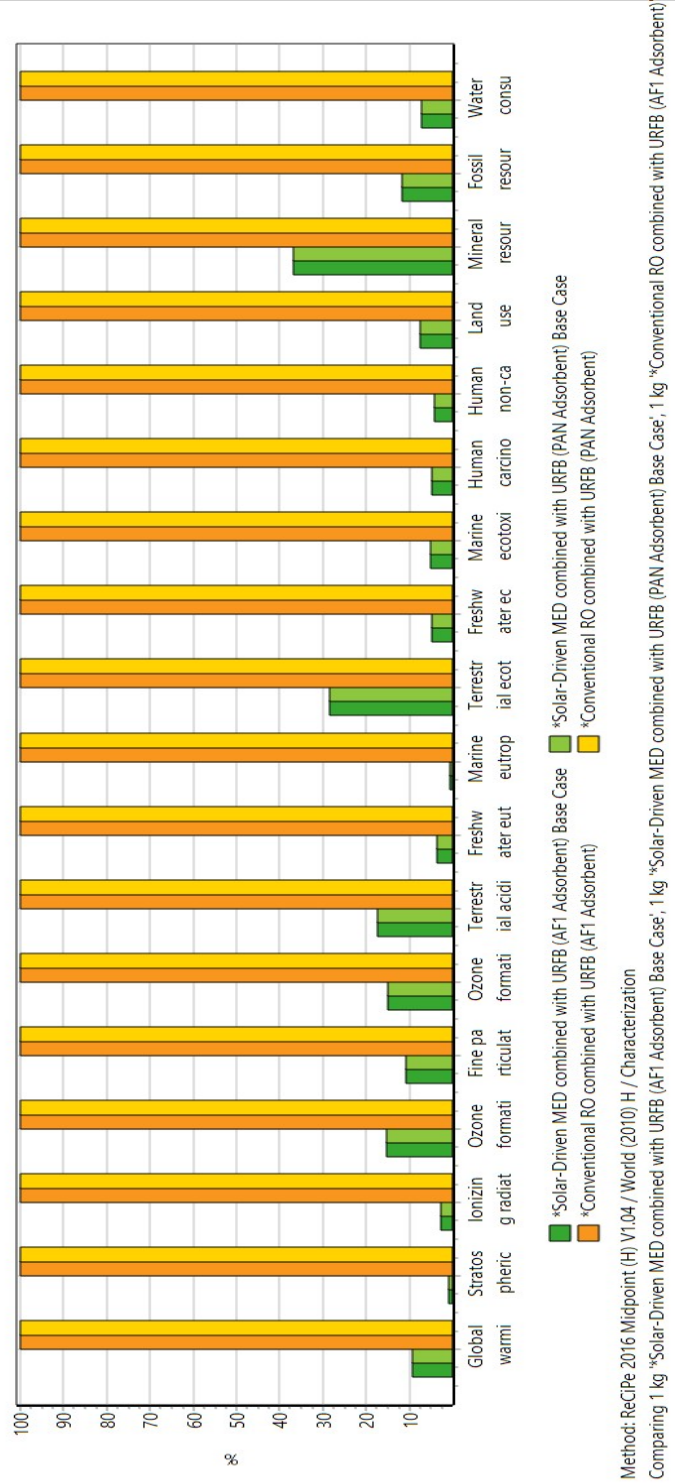


Figure 4-9: Comparative Characterization Results of Base Case Solar-Driven MED Plant and Conventional RO Plant Combined with URFB Systems (ReCiPe 2016)

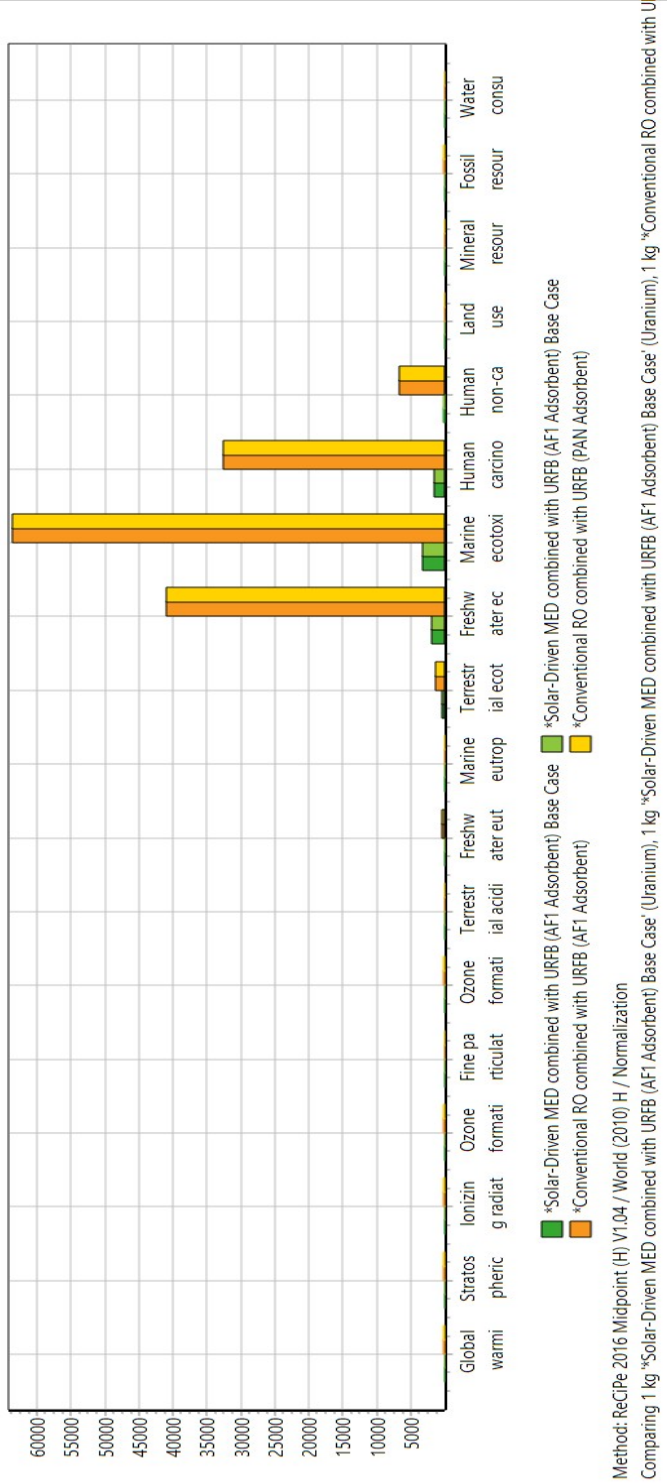


Figure 4.10: Comparative Normalization Results of Base Case Solar-Driven MED and RO Plants Combined with URFB Systems (ReCiPe 2016)

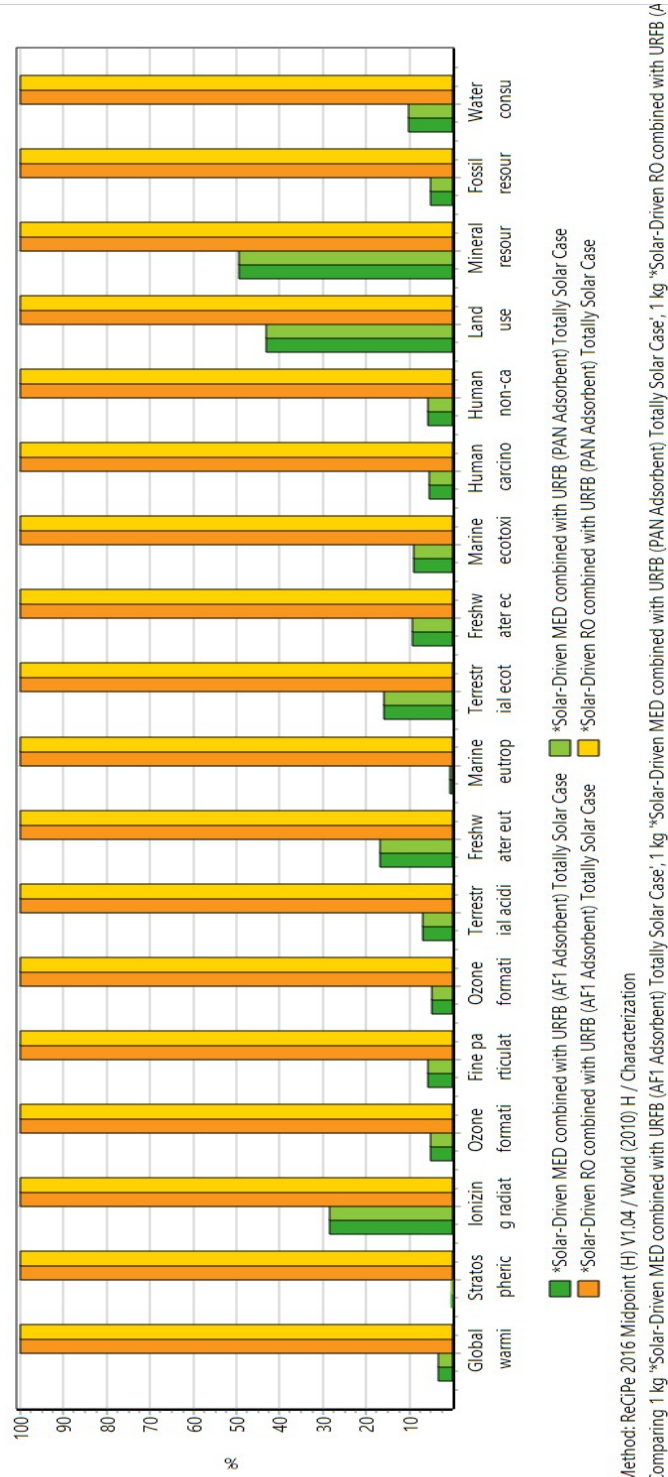
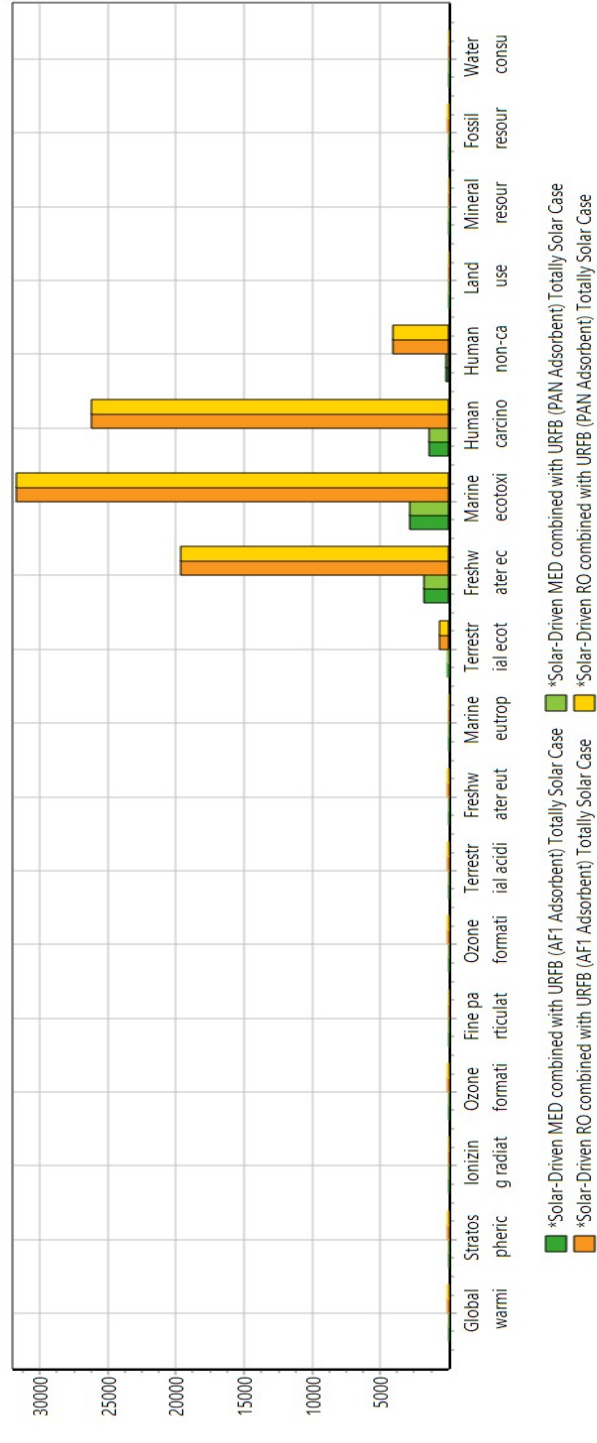


Figure 4.11: Characterization Results Comparison of Totally Solar Case Solar-Driven MED Plant Combined with URFB Systems and Conventional Reverse Osmosis Method Combined with URFB Systems (ReCiPe 2016)

Although the overall impact has been reduced with the energy source alteration in RO plant integrated with URFB systems (Figure B.8), the most critical impact categories have not changed depending on mainly plastic waste disposal and polyvinylidenechloride production based on the results presented in Figure 4.12. The study conducted by (Lawler et al., 2015) claims that the most study about water treatment systems emphasize the operation stage of processes covering energy and chemical consumption and there is no study conducted before about the impact of RO membranes production and their disposal methods adequately, so they assessed these impacts with an LCA approach including different end-of-life disposal alternatives such as reuse, incineration, and landfill by using ReCiPe 2016 Midpoint. The results of this study show that direct reuse of membrane in a secondary plant, where harsh water conditions are available and regular membrane replacement is required, has the lowest environmental impact among all disposal alternatives. Also, it is asserted that energy recovery in an electric arc furnace in the process of steel production by using consumed membrane for a substitute carbon source is an environmentally favorable alternative in end-of-life disposal of RO membranes by particularly reducing the volume of waste. On the other hand, landfill gives the worst results among all disposal methods. Based on the results of this study, it can be said that the impact of our RO desalination system integrated with URFB can also be reduced by changing the end-of-life option of RO membranes.



Method: ReCiPe 2016 Midpoint (H) V1.04 / World (2010) H / Normalization  
 Comparing 1 kg \*Solar-Driven MED combined with URFB (AF1 Adsorbent) Totally Solar Case, 1 kg \*Solar-Driven RO combined with URFB (PAN Adsorbent) Totally Solar Case

Figure 4.12: Normalization Results Comparison of Totally Solar Case Solar-Driven MED Plant Combined with URFB Systems and Conventional Reverse Osmosis Method Combined with URFB Systems (ReCiPe 2016)

#### 4.4 CONCLUSION

The LCA analysis has been conducted from cradle to gate perspective to first evaluate the environmental impact resulting in the middle-scale solar-driven MED plant designed for the Mediterranean region. The ReCiPe 2016 Midpoint has been used as an impact assessment method to evaluate the impact of this system and sensitivity analyses have been performed to detect the most harmful step and the influence of electricity source on results. Then, the solar driven-MED system has been combined with the URFB systems and the results have been compared with the only solar-driven MED plant findings to analyze the impact of the URFB system on the results of conventional desalination plants. Finally, the environmental impacts of MED and RO plants combined with URFB systems that can produce 1 kg of uranium by using distinct energy sources have been compared to detect the potential of URFB systems in other desalination technologies.

According to the results of this study, the main outcomes of this study are discussed below:

- Electricity production mix with 100% fuel oil and chemical consumption mainly phosphoric acid and brine release to the ocean during solar-driven MED operation are the main reasons for high environmental load in nearly all impact categories for freshwater production via solar-driven MED plant.
- The most sensitive system stages are MED operation and electricity production with fuel oil.
- Totally solar case scenario gives the most environmentally favorable results when compared to other grid mix alternatives in GW, FE, ME, and HTC impact categories.
- Although URFB systems integrated into MED and RO desalination plants have negligible impacts nearly in all impact categories, it contributes to impact reduction by nearly half in the ME impact category.
- RO combined with URFB systems has higher environmental loads than MED plant integrated with URFB systems in all impact categories.

## CHAPTER 5

### CONCLUSION AND RECOMMENDATION

This study covers mainly two LCA analyses. The first analysis aims to evaluate the environmental impact of the uranium extraction system from brine with amidoximated adsorbents by scaling up the laboratory system values to estimate the potential industrial application of this process and compare them with conventional uranium mining methods by using ILCD 2011 Midpoint+ as an impact assessment method. Up to date, the literature has focused on improving different uranium adsorbent types without considering an environmental load of uranium mining from seawater. However, the industrialization of this process requires an assessment before application. This study provided the first LCA analysis of uranium recovery from brine. Moreover, different energy and adsorbent recycling scenarios have been investigated to observe the system response to the modification of energy sources and adsorbent recycling numbers. Furthermore, sensitivity analysis has been completed by applying  $\pm 10\%$ ,  $\pm 25\%$ , and  $\pm 50\%$  perturbation ratios to define the most sensitive system parameters in the URFB system in four impact categories named CC, HTC, FET, and MFRRD.

The main outcomes of the first LCA analysis are summarized below:

- If adsorbents are produced industrially for uranium extraction from an aqueous media, it would be an applicable technology.
- The environmental impact of adsorbent technologies is lower than the load of conventional uranium mining methods in HTNC, IRHH, and FET impact categories.
- AF1 adsorbent scenario has a lower environmental load than the PAN-AO adsorbent method in most impact categories.

- The most sensitive system parameters of adsorbent scenarios are hydroxylamine and HW disposal.
- Solar scenarios have a lower environmental impact than the other energy alternatives.

One of the main limitations of this study is the exclusion of parameters that vary for every application like infrastructure and transportation which can lead to higher results in real life. Moreover, a process-based LCA has been conducted in this study, but the results can be affected by the geographical properties of the study area. Similarly, there can be some deviations originating from the usage of lab-based data in this study. Therefore, pilot-scale implementation of recovery of uranium from brine will provide a better approximation that may be more reliable than the assumptions that have been made in this study. Even though solar applications have been demonstrated to be the most environmentally friendly application of the system, using only solar energy adsorbent may not be practical in industrial applications because of the high land requirement. Therefore, there is a need for future studies focusing on reducing the amount of used chemicals, finding alternative chemicals used in adsorbent production, and improving the energy-saving systems and disposal methods via environmentally-sound alternatives. Furthermore, while the predicted uranium recovery cost using adsorbent methods is about 5.4 times higher than the market price of uranium extraction using conventional uranium mining technologies (75 \$/kgU by 2020), the estimated recovery cost will be reduced by the development of a more efficient adsorbent (Wongsawaeng et al., 2021).

The objective of the second analysis is to detect the environmental impact of solar-driven MED desalination plants integrated with URFB systems to understand the applicability of URFB technology in the desalination field. Firstly, the environmental impact of the solar-driven MED plant that produces brine and releases it to the ocean has been analyzed with a cradle-to-gate perspective by using the ReCiPe impact assessment method. Moreover, the first sensitivity analysis was conducted to detect the most sensitive system stage in only solar-driven MED plants by modifying the perturbation ratios as  $\pm 10\%$ ,  $\pm 25\%$ , and  $\pm 50\%$ . In the second analysis, the electricity mix was changed from complete fuel oil to totally solar, United Kingdom, France, Brazil,

Spain, and Turkey mixes to understand the effect of electricity sources on environmental impact results in the MED plant. Then, solar-driven MED and URFB integrated version of this system has been compared to understand the URFB processes' effects on MED desalination plant impact results. Finally, the comparative LCA analysis of the environmental load of MED and RO desalination plants integrated with URFB systems using different energy sources has been conducted to understand the potential of this technology in other desalination alternatives.

The results of the second LCA study declare that:

- The main reasons for environmental impact in solar-driven MED plants are electricity consumption with complete fuel oil and chemical usage mainly phosphoric acid and brine discharge to the ocean during MED operation.
- MED operation and electricity production are the most sensitive system stages.
- The most environmentally favorable energy scenario is the totally solar case as compared to the other grid mix scenarios in GW, FE, ME, and HTC impact categories.
- Integration of URFB systems to MED and RO desalination plants results in negligible impacts on the results nearly in all impact categories except for the ME impact category, where a reduction of nearly 50% ratio has been achieved.
- RO plant combined with URFB system gives the worst results when compared to the MED plant with URFB in all impact categories.

One of the limitations of the second environmental analysis is the detection of the electricity impact on results in only 4 impact categories and the results may be different in other impact categories. To illustrate, all impacts can be reduced in the relevant impact categories by applying the France grid where nuclear energy dominates the market, but the opposite situation can be seen in the IR impact category (Farjana et al., 2018). Moreover, the transportation stage has not been included in the system boundary of this study, but results may vary depending on mainly geographical features and the fuel source. Also, although the environmental loads of the RO plant integrated with the URFB system are higher than the MED plant combined with URFB to produce 1 kg of uranium in all impact categories, the freshwater amount produced

in the RO plant is roughly two times higher than the amount of distillate obtained from MED plant with URFB due to the different recovery ratios, but recovery ratio can be different for even in the same technology (Meneses et al., 2010) (Ezzeghni & El-Bourawi, 2016). Furthermore, even though the integration of the URFB system into desalination plants does not have significant environmental impacts on results in nearly all impact categories, a detailed economical analysis has to be completed to decide whether this option is economically viable or not. However, it can be said that the economy of this system strongly depends on the reusability of adsorbent material, electricity and capital costs covering total construction of plants (Atilgan & Azapagic, 2016a). Also, large-scale desalination plants can be more applicable for the integration of URFB systems since a high amount of brine is required and the other metals extraction along with uranium may be considered in further studies. Also, re-using the heated water for desalination purposes and then using the brine for uranium recovery will provide a sustainable circulation of the water and minerals. Furthermore, although it seems that desalination plants integrated with URFB systems contribute to the provision of employment by creating new jobs and provide energy security by generating raw materials for nuclear power plant, a detailed social analysis has to be conducted by considering health and safety standards.

To conclude, the industrial application of uranium recovery from brine offers an alternative method to conventional uranium mining methods in a more environmentally-friendly way. Also, this system can be integrated with already installed or planned to be built desalination plants so that it can contribute to uranium production by reducing the impact in marine ecotoxicity and offering an alternative solution to brine disposal. Moreover, the hot water arising from the nuclear plants can be used to heat seawater or brackish water used in thermal desalination plants and uranium can be produced from brine as a waste from desalination plants for nuclear power plants. Therefore, further studies about combining desalination and nuclear technologies should be investigated since there is a huge potential to establish a mutualistic relationship between these technologies.

## REFERENCES

- Abdul Ghani, L., Ali, N., Nazaran, I. S., Hanafiah, M. M., et al. (2021). Environmental performance of small-scale seawater reverse osmosis plant for rural area water supply. *Membranes*, *11*(1), 40.
- Abdul Ghani, L., Nazaran, I. S., Ali, N., Hanafiah, M. M., et al. (2020). Improving prediction accuracy of socio-human relationships in a small-scale desalination plant. *Sustainability*, *12*(17), 6949.
- Abdullah, N., Yusof, N., Ismail, A., & Lau, W. (2021). Insights into metal-organic frameworks-integrated membranes for desalination process: A review. *Desalination*, *500*, 114867.
- Acero, A. P., Rodriguez, C., & Citroth, A. (2016). Lcia methods. *Impact Assessment Methods in Life Cycle Assessment and Their Impact Categories*. [Google Scholar].
- Agency, N. E., & Agency, I. A. E. (2021). *Uranium 2020*. <https://doi.org/https://doi.org/https://doi.org/10.1787/d82388ab-en>
- Agency, U. E. P. (2006). Consolidated list of chemicals subject to the emergency planning and community right-to-know act (epcra) and section 112 (r) of the clean air act.
- Ahmad, M., Garudachari, B., Al-Wazzan, Y., Kumar, R., & Thomas, J. P. (2019). Mineral extraction from seawater reverse osmosis brine of gulf seawater. *Desalin Water Treat*, *144*, 45–56.
- Ahmed, F. E., Khalil, A., & Hilal, N. (2021). Emerging desalination technologies: Current status, challenges and future trends. *Desalination*, *517*, 115183.
- Albaiti, A., Liliyasi, L., & Sumarna, O. (2016). The study of mental model on n-hexane-methanol binary system (the validation of physical chemistry practicum procedure). *Jurnal Pendidikan IPA Indonesia*, *5*(1), 6–13.

- Aleisa, E., & Al-Shayji, K. (2018). Ecological–economic modeling to optimize a desalination policy: Case study of an arid rentier state. *Desalination*, *430*, 64–73.
- Aleisa, E., & Heijungs, R. (2020). Leveraging life cycle assessment and simplex lattice design in optimizing fossil fuel blends for sustainable desalination. *The International Journal of Life Cycle Assessment*, *25*(4), 744–759.
- Alhaj, M., & Al-Ghamdi, S. G. (2019). Technical and environmental perspectives on solar-driven seawater desalination: A case study of multi-effect distillation. *World Environmental and Water Resources Congress 2019: Groundwater, Sustainability, Hydro-Climate/Climate Change, and Environmental Engineering*, 440–448.
- Alhaj, M., Tahir, F., & Al-Ghamdi, S. G. (2022). Life-cycle environmental assessment of solar-driven multi-effect desalination (med) plant. *Desalination*, *524*, 115451.
- Alibrahim, M., Shlewit, H., & Alike, S. (2008). Solvent extraction of vanadium (iv) with di (2-ethylhexyl) phosphoric acid and tributyl phosphate. *Periodica Polytechnica Chemical Engineering*, *52*(1), 29–33.
- Al-Kaabi, A., Al-Sulaiti, H., Al-Ansari, T., & Mackey, H. R. (2021). Assessment of water quality variations on pretreatment and environmental impacts of swro desalination. *Desalination*, *500*, 114831.
- Al-Kaabi, A. H., & Mackey, H. R. (2019). Environmental assessment of intake alternatives for seawater reverse osmosis in the arabian gulf. *Journal of environmental management*, *242*, 22–30.
- Al-Qaraghuli, A., & Kazmerski, L. L. (2012). *Comparisons of technical and economic performance of the main desalination processes with and without renewable energy coupling* (tech. rep.). National Renewable Energy Lab.(NREL), Golden, CO (United States).
- Al-Sarkal, T., & Arafat, H. A. (2013). Ultrafiltration versus sedimentation-based pretreatment in fujairah-1 ro plant: Environmental impact study. *Desalination*, *317*, 55–66.
- Al-Shayji, K., & Aleisa, E. (2018). Characterizing the fossil fuel impacts in water desalination plants in kuwait: A life cycle assessment approach. *Energy*, *158*, 681–692.

- Altay, M. B., Kalıncıoğlu, C., & Kurt, Z. (2022). Comparative life cycle assessment of uranium recovery from brine. *Resources, Conservation and Recycling*, *181*, 106237.
- Aly, S., Jawad, J., Manzoor, H., Simson, S., Lawler, J., & Mabrouk, A. N. (2022). Pilot testing of a novel integrated multi effect distillation-absorber compressor (med-ab) technology for high performance seawater desalination. *Desalination*, *521*, 115388.
- Amelio, A., Genduso, G., Vreysen, S., Luis, P., & Van der Bruggen, B. (2014). Guidelines based on life cycle assessment for solvent selection during the process design and evaluation of treatment alternatives. *Green Chemistry*, *16*(6), 3045–3063.
- Amores, M. J., Meneses, M., Pasqualino, J., Antón, A., & Castells, F. (2013). Environmental assessment of urban water cycle on mediterranean conditions by lca approach. *Journal of cleaner production*, *43*, 84–92.
- Anand, K., Sharma, R., & Mehta, P. S. (2011). Experimental investigations on combustion, performance and emissions characteristics of neat karanja biodiesel and its methanol blend in a diesel engine. *Biomass and bioenergy*, *35*(1), 533–541.
- Antipova, E., Boer, D., Cabeza, L. F., Guillén-Gosálbez, G., & Jiménez, L. (2013). Multi-objective design of reverse osmosis plants integrated with solar rankine cycles and thermal energy storage. *Applied energy*, *102*, 1137–1147.
- Athanasopoulos, N., Sikoutris, D., Panidis, T., & Kostopoulos, V. (2012). Numerical investigation and experimental verification of the joule heating effect of polyacrylonitrile-based carbon fiber tows under high vacuum conditions. *Journal of composite materials*, *46*(18), 2153–2165.
- Atilgan, B., & Azapagic, A. (2016a). An integrated life cycle sustainability assessment of electricity generation in turkey. *Energy Policy*, *93*, 168–186.
- Atilgan, B., & Azapagic, A. (2016b). Renewable electricity in turkey: Life cycle environmental impacts. *Renewable Energy*, *89*, 649–657.
- Ayou, D. S., Currás, M. R., Salavera, D., Garcia, J., Bruno, J. C., & Coronas, A. (2014). Performance analysis of absorption heat transformer cycles using ionic liquids based on imidazolium cation as absorbents with 2, 2, 2-trifluoroethanol as refrigerant. *Energy Conversion and Management*, *84*, 512–523.

- Bahar, R., Hawlader, M., & Woei, L. S. (2004). Performance evaluation of a mechanical vapor compression desalination system. *Desalination*, *166*, 123–127.
- Baharoon, D. A., Rahman, H. A., Omar, W. Z. W., & Fadhl, S. O. (2015). Historical development of concentrating solar power technologies to generate clean electricity efficiently—a review. *Renewable and Sustainable Energy Reviews*, *41*, 996–1027.
- Bardi, U. (2010). Extracting minerals from seawater: An energy analysis. *Sustainability*, *2*(4), 980–992.
- Barlev, D., Vidu, R., & Stroeve, P. (2011). Innovation in concentrated solar power. *Solar energy materials and solar cells*, *95*(10), 2703–2725.
- Batuecas, E., Mayo, C., Diaz, R., & Pérez, F. (2017). Life cycle assessment of heat transfer fluids in parabolic trough concentrating solar power technology. *Solar Energy Materials and Solar Cells*, *171*, 91–97.
- Best, F., Driscoll, M. et al. (1980). Proceedings of a topical meeting on the recovery of uranium from seawater. *Massachusetts Inst. of Tech.*
- Bhojwani, S., Topolski, K., Mukherjee, R., Sengupta, D., & El-Halwagi, M. M. (2019). Technology review and data analysis for cost assessment of water treatment systems. *Science of the Total Environment*, *651*, 2749–2761.
- Bonner, T., Cornett, C., Desai, B., Fullenkamp, J., & Hughes, T. (1981). *Engineering handbook for hazardous waste incineration. final report march-september 1981* (tech. rep.). Monsanto Research Corp., Dayton, OH (USA).
- Brander, M., Tipper, R., Hutchison, C., & Davis, G. (2008). Technical paper: Consequential and attributional approaches to lca: A guide to policy makers with specific reference to greenhouse gas lca of biofuels.
- Brook, B. W., Alonso, A., Meneley, D. A., Misak, J., Blee, T., & van Erp, J. B. (2014). Why nuclear energy is sustainable and has to be part of the energy mix. *Sustainable Materials and Technologies*, *1*, 8–16.
- Buyle, M., Braet, J., & Audenaert, A. (2013). Life cycle assessment in the construction sector: A review. *Renewable and sustainable energy reviews*, *26*, 379–388.
- Byers, M. F., Haji, M. N., Slocum, A. H., & Schneider, E. (2018). Cost optimization of a symbiotic system to harvest uranium from seawater via an offshore wind turbine. *Ocean Engineering*, *169*, 227–241.

- Campbell, M., Frame, J., Dudgey, N., Kiel, G., Mesec, V., Woodfield, F., Binney, S., Jante, M., Anderson, R., & Clark, G. (1979). *Extraction of uranium from seawater: Chemical process and plant design feasibility study* (tech. rep.). Bendix Field Engineering Corp., Grand Junction, CO (USA); Exxon Nuclear Co . . .
- Castro, M., Alcanzare, M., Esparcia, E., & Ocon, J. (2020). A comparative techno-economic analysis of different desalination technologies in off-grid islands. *Energies*, *13*(9), 2261.
- Cau, G., & Cocco, D. (2014). Comparison of medium-size concentrating solar power plants based on parabolic trough and linear fresnel collectors. *Energy procedia*, *45*, 101–110.
- Chase, M. W. (1996). Nist-janaf thermochemical tables for oxygen fluorides. *Journal of physical and chemical reference data*, *25*(2), 551–603.
- Cheira, M. F. (2020). Solvent extraction of uranium and vanadium from carbonate leach solutions of ferruginous siltstone using cetylpyridinium carbonate in kerosene. *Chemical Papers*, *74*(7), 2247–2266.
- Cheremisinoff, P. N. (1995). *Waste minimization and cost reduction for the process industries*. Elsevier.
- Cherif, H., Champenois, G., & Belhadj, J. (2016). Environmental life cycle analysis of a water pumping and desalination process powered by intermittent renewable energy sources. *Renewable and Sustainable Energy Reviews*, *59*, 1504–1513.
- Chouyyok, W., Pittman, J. W., Warner, M. G., Nell, K. M., Clubb, D. C., Gill, G. A., & Addleman, R. S. (2016). Surface functionalized nanostructured ceramic sorbents for the effective collection and recovery of uranium from seawater. *Dalton Transactions*, *45*(28), 11312–11325.
- Colucci, V., Manfreda, G., Mendecka, B., Talluri, L., & Zuffi, C. (2021). Lca and exergo-environmental evaluation of a combined heat and power double-flash geothermal power plant. *Sustainability*, *13*(4), 1935.
- Commission, E. et al. (2019). The european green deal. *Eur. Comm*, *53*, 24.
- Compain, P. (2012). Solar energy for water desalination. *Procedia Engineering*, *46*, 220–227.
- Council, N. R. et al. (2012). Uranium mining in virginia: Scientific, technical, environmental, human health and safety, and regulatory aspects of uranium mining and processing in virginia.

- Crouse, D. J. (1956). *Progress report on uranium extraction with organonitrogen compounds*. Oak Ridge National Laboratory.
- Curto, D., Franzitta, V., & Guercio, A. (2021). A review of the water desalination technologies. *Applied Sciences*, *11*(2), 670.
- Das, S., Oyola, Y., Mayes, R. T., Janke, C. J., Kuo, L.-J., Gill, G., Wood, J. R., & Dai, S. (2016). Extracting uranium from seawater: Promising series adsorbents. *Industrial & Engineering Chemistry Research*, *55*(15), 4110–4117.
- Das, S., Tsouris, C., Zhang, C., Kim, J., Brown, S., Oyola, Y., Janke, C., Mayes, R., Kuo, L.-J., Wood, J. R., et al. (2016). Enhancing uranium uptake by amidoxime adsorbent in seawater: An investigation for optimum alkaline conditioning parameters. *Industrial & Engineering Chemistry Research*, *55*(15), 4294–4302.
- Del Borghi, A., Strazza, C., Gallo, M., Messineo, S., & Naso, M. (2013). Water supply and sustainability: Life cycle assessment of water collection, treatment and distribution service. *The International Journal of Life Cycle Assessment*, *18*(5), 1158–1168.
- Deng, R., Xie, L., Lin, H., Liu, J., & Han, W. (2010). Integration of thermal energy and seawater desalination. *Energy*, *35*(11), 4368–4374.
- Do Thi, H. T., Pasztor, T., Fozer, D., Manenti, F., & Toth, A. J. (2021). Comparison of desalination technologies using renewable energy sources with life cycle, pestle, and multi-criteria decision analyses. *Water*, *13*(21), 3023.
- Dong, J., Tang, Y., Nzihou, A., Chi, Y., Weiss-Hortala, E., Ni, M., & Zhou, Z. (2018). Comparison of waste-to-energy technologies of gasification and incineration using life cycle assessment: Case studies in finland, france and china. *Journal of Cleaner Production*, *203*, 287–300.
- Drioli, E., Ali, A., & Macedonio, F. (2015). Membrane distillation: Recent developments and perspectives. *Desalination*, *356*, 56–84.
- Dulama, M., Iordache, M., & Deneanu, N. (2013). Treatment of uranium contaminated wastewater—a review.
- Ekvall, T. (2019). Attributional and consequential life cycle assessment. *Sustainability assessment at the 21st century*. IntechOpen.

- El-Nadi, Y., Awwad, N., & Nayl, A. (2009). A comparative study of vanadium extraction by aliquat-336 from acidic and alkaline media with application to spent catalyst. *International Journal of Mineral Processing*, 92(3-4), 115–120.
- Elsaid, K., Kamil, M., Sayed, E. T., Abdelkareem, M. A., Wilberforce, T., & Olabi, A. (2020). Environmental impact of desalination technologies: A review. *Science of The Total Environment*, 748, 141528.
- EPA. (2009). Us epa, pesticide product label, armicarb 100, 05/30/2012. [https://www3.epa.gov/pesticides/chem\\_search/ppls/005905-00541-20120530.pdf](https://www3.epa.gov/pesticides/chem_search/ppls/005905-00541-20120530.pdf)
- Esmailion, F. (2020). Hybrid renewable energy systems for desalination. *Applied Water Science*, 10(3), 1–47.
- Espinoza, D., Goycoolea, M., Moreno, E., & Newman, A. (2013). Minelib: A library of open pit mining problems. *Annals of Operations Research*, 206(1), 93–114.
- Ezzeghni, U., & El-Bourawi, M. (2016). Exergy analysis of a 10,000 m<sup>3</sup>/day tajoura swro desalination plant. *The 1st International Conference on Chemical, Petroleum, and Gas Engineering (ICCPGE 2016) 20th–22th December*.
- Fard, A. K., Manawi, Y. M., Rhadfi, T., Mahmoud, K. A., Khraisheh, M., & Benyahia, F. (2015). Synoptic analysis of direct contact membrane distillation performance in qatar: A case study. *Desalination*, 360, 97–107.
- Farjana, S. H., Huda, N., Mahmud, M. P., & Lang, C. (2018). Comparative life-cycle assessment of uranium extraction processes. *Journal of cleaner production*, 202, 666–683.
- Farjana, S. H., Huda, N., Mahmud, M. P., & Lang, C. (2019). Life-cycle assessment of solar integrated mining processes: A sustainable future. *Journal of Cleaner Production*, 236, 117610.
- Favre-Reguillon, A., Lebuzit, G., Foos, J., Guy, A., Draye, M., & Lemaire, M. (2003). Selective concentration of uranium from seawater by nanofiltration. *Industrial & engineering chemistry research*, 42(23), 5900–5904.
- Favre-Réguillon, A., Lebuzit, G., Foos, J., Guy, A., Sorin, A., Lemaire, M., & Draye, M. (2005). Selective rejection of dissolved uranium carbonate from seawater using cross-flow filtration technology. *Separation science and technology*, 40(1-3), 623–631.
- Fazio, S., Castellani, V., Sala, S., Schau, E., Secchi, M., Zampori, L., & Diaconu, E. (2018). Supporting information to the characterisation factors of recom-

- mended of life cycle impact assessment methods. *New models and differences with ILCD. EUR*, 28888.
- Fernando, P. N., Egwu, I. N., & Hussain, M. S. (2002). Ion chromatographic determination of trace hydroxylamine in waste streams generated by a pharmaceutical reaction process. *Journal of Chromatography A*, 956(1-2), 261–270.
- Filatov, V., & Afanas' ev, V. (1992). Differential heat-flux calorimeter. *Izv. Vysshikh. Uchebn. Zaved., Khim. Khim. Tekhnol*, 35(8), 97–100.
- Finkbeiner, M., Inaba, A., Tan, R., Christiansen, K., & Klüppel, H.-J. (2006). The new international standards for life cycle assessment: Iso 14040 and iso 14044. *The international journal of life cycle assessment*, 11(2), 80–85.
- Flicker Byers, M., & Schneider, E. (2016). Optimization of the passive recovery of uranium from seawater. *Industrial & Engineering Chemistry Research*, 55(15), 4351–4361.
- Fritzmann, C., Löwenberg, J., Wintgens, T., & Melin, T. (2007a). State-of-the-art of reverse osmosis desalination. *Desalination*, 216(1), 1–76. <https://doi.org/https://doi.org/10.1016/j.desal.2006.12.009>
- Fritzmann, C., Löwenberg, J., Wintgens, T., & Melin, T. (2007b). State-of-the-art of reverse osmosis desalination. *Desalination*, 216(1-3), 1–76.
- Garfi, M., Cadena, E., Sanchez-Ramos, D., & Ferrer, I. (2016). Life cycle assessment of drinking water: Comparing conventional water treatment, reverse osmosis and mineral water in glass and plastic bottles. *Journal of cleaner production*, 137, 997–1003.
- Gertsch, R. E., & Bullock, R. L. (1998). *Techniques in underground mining: Selections from underground mining methods handbook*. SME.
- Ghani, L. A., Ali, N., Nazaran, I. S., Hanafiah, M. M., Yatim, N. I., et al. (2021). Carbon footprint-energy detection for desalination small plant adaptation response. *Energies*, 14(21), 7135.
- Giwa, A., Dufour, V., Al Marzooqi, F., Al Kaabi, M., & Hasan, S. (2017). Brine management methods: Recent innovations and current status. *Desalination*, 407, 1–23.
- Godskesen, B., Hauschild, M., Rygaard, M., Zambrano, K., & Albrechtsen, H.-J. (2013). Life-cycle and freshwater withdrawal impact assessment of water supply technologies. *Water research*, 47(7), 2363–2374.

- Goga, T., Friedrich, E., & Buckley, C. (2019). Environmental life cycle assessment for potable water production—a case study of seawater desalination and mine-water reclamation in south africa. *Water SA*, 45(4), 700–709.
- Grasselli, M., Carbajal, M. L., Yoshii, F., & Sugo, T. (2003). Radiation-induced gma/d-maa graft copolymerization onto porous pe hollow-fiber membrane. *Journal of applied polymer science*, 87(10), 1646–1653.
- Grolier, J.-P., Roux-Desgranges, G., Berkane, M., Jimenez, E., & Wilhelm, E. (1993). Heat capacities and densities of mixtures of very polar substances 2. mixtures containing n, n-dimethylformamide. *The Journal of Chemical Thermodynamics*, 25(1), 41–50.
- Guard, U. C. (1999). Chemical hazard response information system (chris)-hazardous chemical data. *Commandant Instruction*, 16465.
- Guerrero-Pérez, M. O., & Banares, M. A. (2015). Metrics of acrylonitrile: From biomass vs. petrochemical route. *Catalysis Today*, 239, 25–30.
- Guinee, J. B., Heijungs, R., Huppes, G., Zamagni, A., Masoni, P., Buonamici, R., Ekvall, T., & Rydberg, T. (2011). Life cycle assessment: Past, present, and future.
- Hamrin, H. (1980). *Guide to underground mining: Methods and applications*. Atlas Copco.
- Haque, N., & Norgate, T. (2014). The greenhouse gas footprint of in-situ leaching of uranium, gold and copper in australia. *Journal of Cleaner Production*, 84, 382–390.
- Hauschild, M. Z. (2018). Introduction to lca methodology. *Life cycle assessment* (pp. 59–66). Springer.
- Hauschild, M. Z., Rosenbaum, R. K., & Olsen, S. I. (2018). *Life cycle assessment* (Vol. 2018). Springer.
- Heijungs, R., Huppes, G., & Guinée, J. B. (2010). Life cycle assessment and sustainability analysis of products, materials and technologies. toward a scientific framework for sustainability life cycle analysis. *Polymer degradation and stability*, 95(3), 422–428.
- Hogle, B. P., Shekhawat, D., Nagarajan, K., Jackson, J. E., & Miller, D. J. (2002). Formation and recovery of itaconic acid from aqueous solutions of citraconic

- acid and succinic acid. *Industrial & engineering chemistry research*, 41(9), 2069–2073.
- Hong, J., Han, X., Chen, Y., Wang, M., Ye, L., Qi, C., & Li, X. (2017). Life cycle environmental assessment of industrial hazardous waste incineration and land-filling in china. *The International Journal of Life Cycle Assessment*, 22(7), 1054–1064.
- Hore-Lacy, I. (2016). Uranium for nuclear power: Resources, mining and transformation to fuel.
- Horzum, N., Shahwan, T., Parlak, O., & Demir, M. M. (2012). Synthesis of amidoximated polyacrylonitrile fibers and its application for sorption of aqueous uranyl ions under continuous flow. *Chemical Engineering Journal*, 213, 41–49.
- Hu, J., Ma, H., Xing, Z., Liu, X., Xu, L., Li, R., Lin, C., Wang, M., Li, J., & Wu, G. (2016). Preparation of amidoximated ultrahigh molecular weight polyethylene fiber by radiation grafting and uranium adsorption test. *Industrial & Engineering Chemistry Research*, 55(15), 4118–4124.
- Huang, G., Li, W., Liu, Q., Liu, J., Zhang, H., Li, R., Li, Z., Jing, X., & Wang, J. (2018). Efficient removal of uranium (vi) from simulated seawater with hyperbranched polyethylenimine (hpei)-functionalized polyacrylonitrile fibers. *New Journal of Chemistry*, 42(1), 168–176.
- Humplik, T., Lee, J., O’hern, S., Fellman, B., Baig, M., Hassan, S., Atieh, M., Rahman, F., Laoui, T., Karnik, R., et al. (2011). Nanostructured materials for water desalination. *Nanotechnology*, 22(29), 292001.
- Hydrochloride, H., & Supplier, 3. (n.d.). SECTION 2: Hazard(s) identification [Accessed: 2022-2-8].
- Irena, I. (2012). Renewable energy technologies: Cost analysis series. *Concentrating solar power*, 4(5).
- Jijakli, K., Arafat, H., Kennedy, S., Mande, P., & Theeyattuparampil, V. V. (2012). How green solar desalination really is? environmental assessment using life-cycle analysis (lca) approach. *Desalination*, 287, 123–131.
- Joshi, S. S., Aminabhavi, T. M., Balundgi, R. H., & Shukla, S. S. (1990). Densities and viscosities of binary liquid mixtures of nitrobenzene with cyclohex-

- ane and n, n-dimethylformamide. *Journal of Chemical and Engineering Data*, 35(2), 185–187.
- Kanno, M. (1984). Present status of study on extraction of uranium from sea water. *Journal of Nuclear Science and Technology*, 21(1), 1–9.
- Karakosta, C., Pappas, C., Marinakis, V., & Psarras, J. (2013). Renewable energy and nuclear power towards sustainable development: Characteristics and prospects. *Renewable and Sustainable Energy Reviews*, 22, 187–197.
- Kim, J., Tsouris, C., Mayes, R. T., Oyola, Y., Saito, T., Janke, C. J., Dai, S., Schneider, E., & Sachde, D. (2013). Recovery of uranium from seawater: A review of current status and future research needs. *Separation Science and Technology*, 48(3), 367–387.
- Kim, J., Tsouris, C., Oyola, Y., Janke, C. J., Mayes, R. T., Dai, S., Gill, G., Kuo, L.-J., Wood, J., Choe, K.-Y., et al. (2014). Uptake of uranium from seawater by amidoxime-based polymeric adsorbent: Field experiments, modeling, and updated economic assessment. *Industrial & Engineering Chemistry Research*, 53(14), 6076–6083.
- Kim, L. K. (2018). *Uranium mining and milling* (tech. rep.). Lawrence Livermore National Lab.(LLNL), Livermore, CA (United States).
- Kluitenberg, G. (2002). 5.2 heat capacity and specific heat. *Methods of Soil Analysis: Part 4 Physical Methods*, 5, 1201–1208.
- Ko, T.-H., Ting, H.-Y., & Lin, C.-H. (1988). Thermal stabilization of polyacrylonitrile fibers. *Journal of applied polymer science*, 35(3), 631–640.
- Kobayashi, Y., Peters, G. M., Ashbolt, N. J., Heimersson, S., Svanström, M., & Khan, S. J. (2015). Global and local health burden trade-off through the hybridisation of quantitative microbial risk assessment and life cycle assessment to aid water management. *Water research*, 79, 26–38.
- Krishna, I. M., Manickam, V., Shah, A., & Davergave, N. (2017). *Environmental management: Science and engineering for industry*. Butterworth-Heinemann.
- Kubaschewski, O., Alcock, C. B., & Spencer, P. (1993). *Materials thermochemistry*. revised. Pergamon Press Ltd, Headington Hill Hall, Oxford OX 3 0 BW, UK, 1993. 363.
- Kucera, J. (2015). *Reverse osmosis: Industrial processes and applications*. John Wiley & Sons.

- Kumar, H., Mathad, R., Ganesh, S., Sarma, K., & Haramaghatti, C. (2011). Electron-beam-induced modifications in high-density polyethylene. *Brazilian Journal of Physics*, *41*(1), 7–14.
- Kumar, J., Kim, J.-S., Lee, J.-Y., & Yoon, H.-S. (2010). Solvent extraction of uranium (vi) and separation of vanadium (v) from sulfate solutions using alamine 336. *Journal of radioanalytical and nuclear chemistry*, *285*(2), 301–308.
- Kumar, J. R., Kim, J.-S., Lee, J.-Y., & Yoon, H.-S. (2011). A brief review on solvent extraction of uranium from acidic solutions. *Separation & Purification Reviews*, *40*(2), 77–125.
- Kuo, L.-J., Janke, C. J., Wood, J. R., Strivens, J. E., Das, S., Oyola, Y., Mayes, R. T., & Gill, G. A. (2016). Characterization and testing of amidoxime-based adsorbent materials to extract uranium from natural seawater. *Industrial & Engineering Chemistry Research*, *55*(15), 4285–4293.
- Kuo, L.-J., Pan, H.-B., Wai, C. M., Byers, M. F., Schneider, E., Strivens, J. E., Janke, C. J., Das, S., Mayes, R. T., Wood, J. R., et al. (2017). Investigations into the reusability of amidoxime-based polymeric adsorbents for seawater uranium extraction. *Industrial & Engineering Chemistry Research*, *56*(40), 11603–11611.
- Ladshaw, A. P., Wiechert, A. I., Das, S., Yiacoumi, S., & Tsouris, C. (2017). Amidoxime polymers for uranium adsorption: Influence of comonomers and temperature. *Materials*, *10*(11), 1268.
- Lawler, W., Alvarez-Gaitan, J., Leslie, G., & Le-Clech, P. (2015). Comparative life cycle assessment of end-of-life options for reverse osmosis membranes. *Desalination*, *357*, 45–54.
- Leal Filho, W., Tripathi, S. K., Andrade Guerra, J., Giné-Garriga, R., Orlovic Lovren, V., & Willats, J. (2019). Using the sustainable development goals towards a better understanding of sustainability challenges. *International Journal of Sustainable Development & World Ecology*, *26*(2), 179–190.
- Lebedev, B., Rabinovich, I., Milov, V., & Lityagov, V. Y. (1978). Thermodynamic properties of tetrahydrofuran from 8 to 322 k. *The Journal of Chemical Thermodynamics*, *10*(4), 321–329.

- Lee, Y. E., & Koh, K.-K. (2002). Decision-making of nuclear energy policy: Application of environmental management tool to nuclear fuel cycle. *Energy Policy*, 30(13), 1151–1161.
- Leridon, H. (2020). World population outlook: Explosion or implosion? *Population Societies*, (1), 1–4.
- Li, Y., Xiong, W., Zhang, W., Wang, C., & Wang, P. (2016). Life cycle assessment of water supply alternatives in water-receiving areas of the south-to-north water diversion project in china. *Water Research*, 89, 9–19.
- Li, Z., Diaz, L. A., Yang, Z., Jin, H., Lister, T. E., Vahidi, E., & Zhao, F. (2019). Comparative life cycle analysis for value recovery of precious metals and rare earth elements from electronic waste. *Resources, Conservation and Recycling*, 149, 20–30.
- Lienhard, I., & John, H. (2005). *A heat transfer textbook*. phlogiston press.
- Liu, L., & Cheng, Q. (2020). Mass transfer characteristic research on electro dialysis for desalination and regeneration of solution: A comprehensive review. *Renewable and Sustainable Energy Reviews*, 134, 110115.
- Long, G., Meek, M., Lewis, M., et al. (2001). *N, n-dimethylformamide*. World health organization.
- Lu, Z., & Xu, L. (2010). Freezing desalination process. *Thermal desalination processes*, 2.
- Lubis, M. R., & Holtzaple, M. T. (2012). Performance evaluation of an innovative-vapor-compression-desalination system. *Aceh International Journal of Science and Technology*, 1(1), 1–13.
- Lumniczky, K., Impens, N., Armengol, G., Candéias, S., Georgakilas, A. G., Hornhardt, S., Martin, O. A., Rödel, F., & Schae, D. (2021). Low dose ionizing radiation effects on the immune system. *Environment international*, 149, 106212.
- Macfarlane, A. M., & Miller, M. (2007). Nuclear energy and uranium resources. *Elements*, 3(3), 185–192.
- Mannan, M., Alhaj, M., Mabrouk, A. N., & Al-Ghamdi, S. G. (2019). Examining the life-cycle environmental impacts of desalination: A case study in the state of qatar. *Desalination*, 452, 238–246.

- Manos, M. J., & Kanatzidis, M. G. (2012). Layered metal sulfides capture uranium from seawater. *Journal of the American Chemical Society*, *134*(39), 16441–16446.
- Mata-Torres, C., Zurita, A., Cardemil, J. M., & Escobar, R. A. (2019). Exergy cost and thermoeconomic analysis of a rankine cycle+ multi-effect distillation plant considering time-varying conditions. *Energy Conversion and Management*, *192*, 114–132.
- McCombie, C., & Jefferson, M. (2016). Renewable and nuclear electricity: Comparison of environmental impacts. *Energy Policy*, *96*, 758–769.
- Mehta, J. S. (n.d.). A comparative study of sea water desalination technologies driven by solar power.
- Meneses, M., Pasqualino, J. C., Céspedes-Sánchez, R., & Castells, F. (2010). Alternatives for reducing the environmental impact of the main residue from a desalination plant. *Journal of Industrial Ecology*, *14*(3), 512–527.
- Menyah, K., & Wolde-Rufael, Y. (2010). Co2 emissions, nuclear energy, renewable energy and economic growth in the us. *Energy policy*, *38*(6), 2911–2915.
- Meron, N., Blass, V., & Thoma, G. (2020). A national-level lca of a water supply system in a mediterranean semi-arid climate—Israel as a case study. *The International Journal of Life Cycle Assessment*, *25*(6), 1133–1144.
- Mezher, T., Fath, H., Abbas, Z., & Khaled, A. (2011). Techno-economic assessment and environmental impacts of desalination technologies. *Desalination*, *266*(1-3), 263–273.
- Micale, G., Rizzuti, L., & Cipollina, A. (2009). *Seawater desalination: Conventional and renewable energy processes* (Vol. 1). Springer.
- Michopoulos, Y., & Rode, B. M. (1991). Monte carlo simulation of liquid hydroxylamine: Structure and physical properties. *Physica Scripta*, *1991*(T38), 84.
- Mikkola, J.-P., Virtanen, P., & Sjöholm, R. (2006). Aliquat 336®—a versatile and affordable cation source for an entirely new family of hydrophobic ionic liquids. *Green Chemistry*, *8*(3), 250–255.
- Miller, S., Shemer, H., & Semiat, R. (2015). Energy and environmental issues in desalination. *Desalination*, *366*, 2–8.
- Mirci, L. E. (2009). New synthetic esters with a complex structure considered as tribological fluids. *Lubrication Science*, *21*(4), 160–168.

- Moradi, G., Zinadini, S., Dabirian, F., & Rajabi, L. (2019). Polycitrate-para-aminobenzoate alumoxane nanoparticles as a novel nanofiller for enhancement performance of electrospun pan membranes. *Separation and Purification Technology*, *213*, 224–234.
- Morillo, J., Usero, J., Rosado, D., El Bakouri, H., Riaza, A., & Bernaola, F.-J. (2014). Comparative study of brine management technologies for desalination plants. *Desalination*, *336*, 32–49.
- Mu, D., Xin, C., & Zhou, W. (2020). Life cycle assessment and techno-economic analysis of algal biofuel production. *Microalgae Cultivation for Biofuels Production*, 281–292.
- Muhammad-Sukki, F., Ramirez-Iniguez, R., McMeekin, S. G., Stewart, B. G., & Clive, B. (2010). Solar concentrators. *Int. J. Appl. Sci*, *1*(1), 1–15.
- Müller-Steinhagen, H., & Trieb, F. (2004). Concentrating solar power. *A review of the technology. Ingenia Inform QR Acad Eng*, *18*, 43–50.
- Muralikrishna, I. V., & Manickam, V. (2017). Chapter five - life cycle assessment. In I. V. Muralikrishna & V. Manickam (Eds.), *Environmental management* (pp. 57–75). Butterworth-Heinemann. <https://doi.org/https://doi.org/10.1016/B978-0-12-811989-1.00005-1>
- Muthu, S. S. (2014). 6—estimating the overall environmental impact of textile processing: Life cycle assessment (lca) of textile products.
- Na, C.-K., Park, H.-J., & Kim, B.-G. (2012). Optimal amidoximation conditions of acrylonitrile grafted onto polypropylene by photoirradiation-induced graft polymerization. *Journal of applied polymer science*, *125*(1), 776–785.
- Najjar, E., Al-Hindi, M., Massoud, M., & Saad, W. (2021). Life cycle assessment of a seawater reverse osmosis plant powered by a hybrid energy system (fossil fuel and waste to energy). *Energy Reports*, *7*, 448–465.
- Negewo, B. D. (2012). *Renewable energy desalination: An emerging solution to close the water gap in the middle east and north africa*. World Bank Publications.
- Nixon, J., Dey, P., & Davies, P. (2010). Which is the best solar thermal collection technology for electricity generation in north-west india? evaluation of options using the analytical hierarchy process. *Energy*, *35*(12), 5230–5240.

- Norgate, T., Haque, N., & Koltun, P. (2014). The impact of uranium ore grade on the greenhouse gas footprint of nuclear power. *Journal of cleaner production*, *84*, 360–367.
- Oshita, K., Seo, K., Sabarudin, A., Oshima, M., Takayanagi, T., & Motomizu, S. (2008). Synthesis of chitosan resin possessing a phenylarsonic acid moiety for collection/concentration of uranium and its determination by icp-aes. *Analytical and bioanalytical chemistry*, *390*(7), 1927–1932.
- Oyola, Y., & Dai, S. (2016). High surface-area amidoxime-based polymer fibers co-grafted with various acid monomers yielding increased adsorption capacity for the extraction of uranium from seawater. *Dalton Transactions*, *45*(21), 8824–8834.
- Paim, M.-A., Dalmarco, A. R., Yang, C.-H., Salas, P., Lindner, S., Mercure, J.-F., de Andrade, J. B. S. O., Derani, C., da Silva, T. B., Viñuales, J. E., et al. (2019). Evaluating regulatory strategies for mitigating hydrological risk in Brazil through diversification of its electricity mix. *Energy Policy*, *128*, 393–401.
- Pan, H.-B., Kuo, L.-J., Wai, C. M., Miyamoto, N., Joshi, R., Wood, J. R., Strivens, J. E., Janke, C. J., Oyola, Y., Das, S., et al. (2016). Elution of uranium and transition metals from amidoxime-based polymer adsorbents for sequestering uranium from seawater. *Industrial & Engineering Chemistry Research*, *55*(15), 4313–4320.
- Pan, H.-B., Kuo, L.-J., Wood, J., Strivens, J., Gill, G. A., Janke, C. J., & Wai, C. M. (2015). Towards understanding KOH conditioning of amidoxime-based polymer adsorbents for sequestering uranium from seawater. *RSC Advances*, *5*(122), 100715–100721.
- Pan, H.-B., Liao, W., Wai, C. M., Oyola, Y., Janke, C. J., Tian, G., & Rao, L. (2014). Carbonate-H<sub>2</sub>O<sub>2</sub> leaching for sequestering uranium from seawater. *Dalton transactions*, *43*(28), 10713–10718.
- Pan, H.-B., Wai, C. M., Kuo, L.-J., Gill, G., Tian, G., Rao, L., Das, S., Mayes, R. T., & Janke, C. J. (2017). Bicarbonate elution of uranium from amidoxime-based polymer adsorbents for sequestering uranium from seawater. *ChemistrySelect*, *2*(13), 3769–3774.

- Pan, H.-B., Wai, C. M., Kuo, L.-J., Gill, G. A., Wang, J. S., Joshi, R., & Janke, C. J. (2020). A highly efficient uranium grabber derived from acrylic fiber for extracting uranium from seawater. *Dalton Transactions*, 49(9), 2803–2810.
- Panagopoulos, A., Haralambous, K.-J., & Loizidou, M. (2019). Desalination brine disposal methods and treatment technologies-a review. *Science of the Total Environment*, 693, 133545.
- Parker, B., Zhang, Z., Rao, L., & Arnold, J. (2018). An overview and recent progress in the chemistry of uranium extraction from seawater. *Dalton Transactions*, 47(3), 639–644.
- Parker, D. J., McNaughton, C. S., & Sparks, G. A. (2016). Life cycle greenhouse gas emissions from uranium mining and milling in Canada. *Environmental Science & Technology*, 50(17), 9746–9753.
- Patel, S. K., Biesheuvel, P. M., & Elimelech, M. (2021). Energy consumption of brackish water desalination: Identifying the sweet spots for electrodialysis and reverse osmosis. *ACS ES&T Engineering*, 1(5), 851–864.
- Paulillo, A., Dodds, J. M., Palethorpe, S. J., & Lettieri, P. (2021). Reprocessing vs direct disposal of used nuclear fuels: The environmental impacts of future scenarios for the UK. *Sustainable Materials and Technologies*, 28, e00278.
- Pazouki, P., Lu, H. R., El Hanandeh, A., Biswas, W., Bertone, E., Helfer, F., & Stewart, R. A. (2021). Comparative environmental life cycle assessment of alternative osmotic and mixing dilution desalination system configurations. *Desalination*, 504, 114963.
- Piccinno, F., Hischer, R., Seeger, S., & Som, C. (2016). From laboratory to industrial scale: A scale-up framework for chemical processes in life cycle assessment studies. *Journal of Cleaner Production*, 135, 1085–1097.
- Piro, M. H., & Lipkina, K. (2020). 8 - mining and milling. In M. H. Piro (Ed.), *Advances in nuclear fuel chemistry* (pp. 315–329). Woodhead Publishing. <https://doi.org/10.1016/B978-0-08-102571-0.00009-4>
- Qin, J., Hu, E., Nathan, G. J., & Chen, L. (2017). Concentrating or non-concentrating solar collectors for solar aided power generation? *Energy Conversion and Management*, 152, 281–290.
- Raluy, R. G., Serra, L., & Uche, J. (2005). Life cycle assessment of water production technologies-part 1: Life cycle assessment of different commercial desalina-

- tion technologies (msf, med, ro)(9 pp). *The International Journal of Life Cycle Assessment*, 10(4), 285–293.
- Raturi, A. K. (2019). Renewables 2019 global status report.
- Rebitzer, G., Ekvall, T., Frischknecht, R., Hunkeler, D., Norris, G., Rydberg, T., Schmidt, W.-P., Suh, S., Weidema, B. P., & Pennington, D. W. (2004). Life cycle assessment: Part 1: Framework, goal and scope definition, inventory analysis, and applications. *Environment international*, 30(5), 701–720.
- Romanchuk, A. Y., Slesarev, A. S., Kalmykov, S. N., Kosynkin, D. V., & Tour, J. M. (2013). Graphene oxide for effective radionuclide removal. *Physical Chemistry Chemical Physics*, 15(7), 2321–2327.
- Ruan, S., Yang, E.-H., & Unluer, C. (2021). Production of reactive magnesia from desalination reject brine and its use as a binder. *Journal of CO2 Utilization*, 44, 101383.
- Sachs, J. D., Schmidt-Traub, G., & Williams, J. (2016). Pathways to zero emissions. *Nature Geoscience*, 9(11), 799–801.
- Saghafifar, M., & Gabra, S. (2020). A critical overview of solar assisted carbon capture systems: Is solar always the solution? *International Journal of Greenhouse Gas Control*, 92, 102852.
- (SAIC), S. A. I. C., & Curran, M. A. (2006). Life-cycle assessment: Principles and practice.
- Salcedo, R., Antipova, E., Boer, D., Jiménez, L., & Guillén-Gosálbez, G. (2012). Multi-objective optimization of solar rankine cycles coupled with reverse osmosis desalination considering economic and life cycle environmental concerns. *desalination*, 286, 358–371.
- Saouter, E., Biganzoli, F., Ceriani, L., Versteeg, D., Crenna, E., Zampori, L., Sala, S., & Pant, R. (2018). Environmental footprint: Update of life cycle impact assessment methods—ecotoxicity freshwater, human toxicity cancer, and non-cancer. *European Union, Luxembourg*.
- Savenko, A. (1997). Coprecipitation of uranium with iron (iii) hydroxide formed in sea water by the oxidation of iron (ii). *Oceanographic Literature Review*, 1(44), 26.
- Seko, N., Katakai, A., Tamada, M., Sugo, T., & Yoshii, F. (2004). Fine fibrous amidoxime adsorbent synthesized by grafting and uranium adsorption–elution

- cyclic test with seawater. *Separation science and technology*, 39(16), 3753–3767.
- Shahabi, M. P., McHugh, A., Anda, M., & Ho, G. (2014). Environmental life cycle assessment of seawater reverse osmosis desalination plant powered by renewable energy. *Renewable Energy*, 67, 53–58.
- Shahabi, M. P., McHugh, A., Anda, M., & Ho, G. (2015). Comparative economic and environmental assessments of centralised and decentralised seawater desalination options. *Desalination*, 376, 25–34.
- Shahabi, M. P., McHugh, A., & Ho, G. (2015). Environmental and economic assessment of beach well intake versus open intake for seawater reverse osmosis desalination. *Desalination*, 357, 259–266.
- Shatat, M., & Riffat, S. B. (2014). Water desalination technologies utilizing conventional and renewable energy sources. *International Journal of Low-Carbon Technologies*, 9(1), 1–19.
- Sherazi, T. A. (2016). Graft polymerization. In E. Drioli & L. Giorno (Eds.), *Encyclopedia of membranes* (pp. 886–887). Springer Berlin Heidelberg. [https://doi.org/10.1007/978-3-662-44324-8\\_274](https://doi.org/10.1007/978-3-662-44324-8_274)
- Shi, Q., Zhang, Y., Huang, J., Liu, T., Liu, H., & Wang, L. (2017). Synergistic solvent extraction of vanadium from leaching solution of stone coal using d2ehpa and pc88a. *Separation and Purification Technology*, 181, 1–7.
- Siefan, A., Rachid, E., Elashwah, N., AlMarzooqi, F., Banat, F., & van der Merwe, R. (2022). Desalination via solar membrane distillation and conventional membrane distillation: Life cycle assessment case study in Jordan. *Desalination*, 522, 115383.
- Silva, D. A. L., Nunes, A. O., Piekarski, C. M., da Silva Moris, V. A., de Souza, L. S. M., & Rodrigues, T. O. (2019). Why using different life cycle assessment software tools can generate different results for the same product system? a cause–effect analysis of the problem. *Sustainable Production and Consumption*, 20, 304–315.
- Simbolotti, G. (2013). Concentrating solar power, IEA-ETSAP and Irena.
- Simons, A., & Bauer, C. (2012). Life cycle assessment of the European pressurized reactor and the influence of different fuel cycle strategies. *Proceedings of the*

- Institution of Mechanical Engineers, Part A: Journal of Power and Energy*, 226(3), 427–444.
- Singh, H., & Gupta, C. (2000). Solvent extraction in production and processing of uranium and thorium. *Mineral Processing and Extractive Metallurgy Review*, 21(1-5), 307–349.
- Sodaye, H., Nisan, S., Poletiko, C., Prabhakar, S., & Tewari, P. (2009). Extraction of uranium from the concentrated brine rejected by integrated nuclear desalination plants. *Desalination*, 235(1-3), 9–32.
- Sokhansefat, T., Kasaeian, A., Rahmani, K., Heidari, A. H., Aghakhani, F., & Mahian, O. (2018). Thermoeconomic and environmental analysis of solar flat plate and evacuated tube collectors in cold climatic conditions. *Renewable Energy*, 115, 501–508.
- Soldenhoff, K., Shamieh, M., & Manis, A. (2005). Liquid–liquid extraction of cobalt with hollow fiber contactor. *Journal of Membrane Science*, 252(1-2), 183–194.
- Sole, K. C., Cole, P. M., Feather, A. M., & Kotze, M. H. (2011). Solvent extraction and ion exchange applications in africa’s resurging uranium industry: A review. *Solvent extraction and ion exchange*, 29(5-6), 868–899.
- Sözen, A., Arcaklioğlu, E., Özalp, M., & Kanit, E. G. (2005). Solar-energy potential in turkey. *Applied Energy*, 80(4), 367–381.
- Steiger, M. G., Blumhoff, M. L., Mattanovich, D., & Sauer, M. (2013). Biochemistry of microbial itaconic acid production. *Frontiers in Microbiology*, 4, 23.
- Stephenson, R. M. (2012). *Handbook of the thermodynamics of organic compounds*. Springer Science & Business Media.
- Suzuki, T., Saito, K., Sugo, T., Ogura, H., & Oguma, K. (2000). Fractional elution and determination of uranium and vanadium adsorbed on amidoxime fiber from seawater. *Analytical sciences*, 16(4), 429–432.
- Tamada, M. (2010). Current status of technology for collection of uranium from seawater. *International Seminar On Nuclear War And Planetary Emergencies—42nd Session*, 243–252.
- Tanaka, H., Nosoko, T., & Nagata, T. (2000). Parametric investigation of a basin-type-multiple-effect coupled solar still. *Desalination*, 130(3), 295–304.

- Tang, N., Liang, J., Niu, C., Wang, H., Luo, Y., Xing, W., Ye, S., Liang, C., Guo, H., Guo, J., et al. (2020). Amidoxime-based materials for uranium recovery and removal. *Journal of Materials Chemistry A*, 8(16), 7588–7625.
- Tarnacki, K., Meneses, M., Melin, T., Van Medevoort, J., & Jansen, A. (2012). Environmental assessment of desalination processes: Reverse osmosis and memstill®. *Desalination*, 296, 69–80.
- Tarpani, R. R. Z., Lapolli, F. R., Recio, M. Á. L., & Gallego-Schmid, A. (2021). Comparative life cycle assessment of three alternative techniques for increasing potable water supply in cities in the global south. *Journal of Cleaner Production*, 290, 125871.
- Tarpani, R. R. Z., Miralles-Cuevas, S., Gallego-Schmid, A., Cabrera-Reina, A., & Cornejo-Ponce, L. (2019). Environmental assessment of sustainable energy options for multi-effect distillation of brackish water in isolated communities. *Journal of Cleaner Production*, 213, 1371–1379.
- Taylan, G. (2019). *Techno-economic analysis of middle-size PTC power plant for a university campus*.
- Tsouris, C. (2017). Uranium extraction: Fuel from seawater. *Nature Energy*, 2(4), 1–3.
- Tsouris, C., Mayes, R. T., Janke, C. J., Dai, S., Das, S., Liao, W.-P., Kuo, L.-J., Wood, J., Gill, G., Byers, M. F., et al. (2015). *Adsorbent alkali conditioning for uranium adsorption from seawater: adsorbent performance and technology cost evaluation* (tech. rep.). Oak Ridge National Lab.(ORNL), Oak Ridge, TN (United States).
- Uche, J., Martínez-Gracia, A., & Carmona, U. (2014). Life cycle assessment of the supply and use of water in the segura basin. *The International Journal of Life Cycle Assessment*, 19(3), 688–704.
- Udayar, T., Yahorava, V., & Kotze, M. (2013). Impact of impurities on performance of strong-base resin for recovery of uranium from sulphuric acid leach liquors. *Uranium extraction technology*. (1993). INTERNATIONAL ATOMIC ENERGY AGENCY. <https://www.iaea.org/publications/1463/uranium-extraction-technology>
- Vanderzee, C. E., & Westrum Jr, E. F. (1970). Succinic acid. heat capacities and thermodynamic properties from 5 to 328 k. an efficient drying procedure. *The Journal of Chemical Thermodynamics*, 2(5), 681–687.

- Vince, F., Aoustin, E., Bréant, P., & Marechal, F. (2008). Lca tool for the environmental evaluation of potable water production. *Desalination*, 220(1-3), 37–56.
- Wai, C., Tian, G., & Janke, C. (2014). *Innovative elution processes for recovering uranium from seawater* (tech. rep.). Univ. of Idaho.
- Wai, C. M. (2017). *Innovative elution processes for recovering uranium and transition metals from amidoxime-based adsorbents* (tech. rep.). Univ. of Idaho, Moscow, ID (United States).
- Wang, J., & Zhuang, S. (2019). Extraction and adsorption of u (vi) from aqueous solution using affinity ligand-based technologies: An overview. *Reviews in Environmental Science and Bio/Technology*, 18(3), 437–452.
- Water, U. (2018). 2018 un world water development report, nature-based solutions for water.
- Wei, W., Larrey-Lassalle, P., Faure, T., Dumoulin, N., Roux, P., & Mathias, J.-D. (2015). How to conduct a proper sensitivity analysis in life cycle assessment: Taking into account correlations within lci data and interactions within the lca calculation model. *Environmental science & technology*, 49(1), 377–385.
- Wiechert, A. I., Ladshaw, A. P., Gill, G. A., Wood, J. R., Yiacoumi, S., & Tsouris, C. (2018). Uranium resource recovery from desalination plant feed and reject water using amidoxime functionalized adsorbent. *Industrial & Engineering Chemistry Research*, 57(50), 17237–17244.
- Wongsawaeng, D., Wongjaikham, W., Hosemann, P., Swantomo, D., & Basuki, K. T. (2021). Direct uranium recovery from brine concentrate using amidoxime adsorbents for possible future energy source. *International Journal of Energy Research*, 45(2), 1748–1760.
- Wunderlich, B., & Jones, L. (1969). Heat capacities of solid polymers. *Journal of Macromolecular Science, Part B*, 3(1), 67–79.
- Youssef, P., Al-Dadah, R., & Mahmoud, S. (2014). Comparative analysis of desalination technologies. *Energy Procedia*, 61, 2604–2607.
- Yuan, Y., Yu, Q., Cao, M., Feng, L., Feng, S., Liu, T., Feng, T., Yan, B., Guo, Z., & Wang, N. (2021). Selective extraction of uranium from seawater with biofouling-resistant polymeric peptide. *Nature Sustainability*, 4(8), 708–714.

- Yun, C. (1982). *Development of a process for continuous extraction of uranium from seawater* (tech. rep.). International Atomic Energy Agency.
- Zhang, J.-h., Zhang, W., Zhang, L., & Gu, S.-q. (2014). A critical review of technology for selective recovery of vanadium from leaching solution in v2o5 production. *Solvent extraction and ion exchange*, 32(3), 221–248.
- Zhao, G., & Baker, J. (2022). Effects on environmental impacts of introducing electric vehicle batteries as storage-a case study of the united kingdom. *Energy Strategy Reviews*, 40, 100819.
- Zhao, H., Liu, X., Yu, M., Wang, Z., Zhang, B., Ma, H., Wang, M., & Li, J. (2015). A study on the degree of amidoximation of polyacrylonitrile fibers and its effect on their capacity to adsorb uranyl ions. *Industrial & Engineering Chemistry Research*, 54(12), 3101–3106.
- Zhao, X., Feng, M., Jiao, Y., Zhang, Y., Wang, Y., & Sha, Z. (2020). Lithium extraction from brine in an ionic selective desalination battery. *Desalination*, 481, 114360.
- Zheng, X., Chen, D., Wang, Q., & Zhang, Z. (2014). Seawater desalination in china: Retrospect and prospect. *Chemical engineering journal*, 242, 404–413.
- Zhongming, Z., Linong, L., Wangqiang, Z., Wei, L., et al. (2019). International energy outlook 2019 projects nearly 50% increase in world energy usage by 2050, led by growth in asia.
- Zhou, J., Chang, V. W.-C., & Fane, A. G. (2011). Environmental life cycle assessment of reverse osmosis desalination: The influence of different life cycle impact assessment methods on the characterization results. *Desalination*, 283, 227–236.
- Zhou, J., Chang, V. W.-C., & Fane, A. G. (2013). An improved life cycle impact assessment (lcia) approach for assessing aquatic eco-toxic impact of brine disposal from seawater desalination plants. *Desalination*, 308, 233–241.
- Zhu, G., Wendelin, T., Wagner, M. J., & Kutscher, C. (2014). History, current state, and future of linear fresnel concentrating solar collectors. *Solar Energy*, 103, 639–652.
- Zhu, Z., Pranolo, Y., & Cheng, C. Y. (2013). Uranium solvent extraction and separation from vanadium in alkaline solutions. *Separation Science and Technology*, 48(9), 1402–1408.

Zimek, Z. (2018). *Pre-feasibility study of setting up an electron beam r&d facility*.

Instytut Chemii i Techniki Jądrowej= Institute of Nuclear Chemistry and ...

Zuckermandl, E., & Pauling, L. (1965). Evolutionary divergence and convergence in proteins. *Evolving genes and proteins* (pp. 97–166). Elsevier.

## **Appendix A**

### **APPENDIX**

#### **A.1 DETAILS OF INVENTORIES**

Table A.1: Details of Inventory for Uranium Recovery via AF1 and PAN-AO Adsorbent Methods

AF1 Inventory	PAN Inventory	Energy Inventory
Water, salt, ocean	Water, salt, ocean	Electricity, high voltage {RoW}  electricity production, hard coal   Conseq, U
High density polyethylene resin, at plant/RNA	Polyacrylonitrile fibres (PAN), from acrylonitrile and methacrylate, prod. mix, PAN w/o additives EU-27 S	Diesel, burned in diesel-electric generating set {GLO}  market for   Conseq, U
Acrylonitrile, at plant/RNA	Hydroxylamine {RoW}  market for hydroxylamine   Conseq, U	Electricity, high voltage {RoW}  electricity production, nuclear, boiling water reactor   Conseq, U
Succinic acid{GLO}  market for succinic acid   Conseq, U	Potassium carbonate {GLO}  market for   Conseq, U	Electricity, high voltage {RoW}  electricity production, solar tower power plant, 20 MW   Conseq, U
Hydroxylamine {RoW}  market for hydroxylamine   Conseq, U	Sodium hydroxide, without water, in 50% solution state {GLO}  market for   Conseq, U	Electricity, high voltage {RoW}  electricity production, wind, >3MW turbine, onshore   Conseq, U

Table A.1: Details of Inventory for Uranium Recovery via AF1 and PAN-AO Adsorbent Methods

AF1 Inventory	PAN Inventory	Energy Inventory
Potassium carbonate {GLO}  market for   Conseq, U	Sodium bicarbonate {GLO}  market for sodium bicarbonate   Conseq, U	Heat, central or small-scale, other than natural gas {RoW}  operation, solar collector system, Cu flat plate collector, one-family house, for combined system   Conseq, U
Potassium hydroxide {GLO}  market for   Conseq, U	Ammonium sulfate, as N {GLO}  market for   Conseq, U	
	Hazardous waste, for incineration {RoW}  treatment of hazardous waste, hazardous waste incineration   Conseq, U	
Sodium bicarbonate {GLO}  market for sodium bicarbonate   Conseq, U		
Ammonium sulfate, as N {GLO}  market for   Conseq, U		

Table A.2: Conversion Factors (%) for Amidoximated Adsorbent Production

Name of Adsorbent	Degree of Grafting (%) or Conversion Factor (%)	References
AF1	97%, 187%, 286%, 316%, 356%, %376 & 385%	(Oyola & Dai, 2016)
	~300%	(Das, Tsouris, et al., 2016)
	154%-354%	(Das, Oyola, et al., 2016)
	250%	(Flicker Byers & Schneider, 2016)
	360%	(Hu et al., 2016)
PAN-AO	1.2%, 2.8%, 4.7%, 10.8%, 25.4% & 46.3%	(H. Zhao et al., 2015)
	30%	(Horzum et al., 2012)

Table A.3: The Inventory of Solar Driven MED Plant

Infrastructure of MED Plant		
Name of Input	Amount for 1m <sup>3</sup> FW Production	References
<i>Sand Filter</i>		
Silica Sand (filter media) (kg)	0,001359942	
Polyvinyl chloride (pipes and valves) (kg)	0,000130055	
Chromium Steel (pipe clamping frame) (kg)	0,000200043	
<i>Anti-fouling Dispenser (to prevent scale formation)</i>		
High Density polyethylene (tank) (kg)	6,9988E-05	
Polypropylene (sensor, dosage pump and pump body) (kg)	3,99543E-05	
Polyvinyl Chloride (valves) (kg)	1,00565E-05	
Polyvinyl fluoride (valves and dosage pump) (kg)	1,00565E-05	
Tetrafluoroethylene (diaphragm) (kg)	1,35899E-06	
<i>Brackish Water Tank</i>		
Polypropylene (tank) (kg)	0,000949935	
Polyphenylene sulfide (level sensor) (kg)	1,00565E-05	
Polyvinyl Chloride (valves) (kg)	8,99652E-05	
Chromium steel (vacuum pump) (kg)	0,000139976	
<i>Multi-effect Distillation (8 effects)</i>		
Chromium steel (effects, condensator and valve actuator) (kg)	0,00835997	(Tarpani et al., 2019)
Polyphenylene sulfide (level sensor) (kg)	1,00565E-05	
Polypropylene (valves, valves actuators and water meter) (kg)	5,00109E-05	
Polypropylene (control block) (kg)	2,03849E-06	
<i>Distillate water tank</i>		
Polypropylene (lung) (kg)	0,000949935	
High density polyethylene (distilled water tank) (kg)	0,000589938	
Polyphenylene sulfide (level sensor) (kg)	1,00565E-05	
Polypropylene (level sensor) (kg)	5,00109E-05	
Polypropylene (valves, valves actuators and water meter) (kg)	0,000200043	
Polypropylene (control block) (kg)	2,03849E-06	
Chromium steel (vacuum pump) (kg)	0,000139976	
<i>Other Equipment</i>		
Polypropylene (tanks) (kg)	0,002039982	
Chromium steel (heat exchanger and heat pump) (kg)	0,000479996	
Chromium steel (centrifugal pumps) (kg)	0,000290009	
Copper (pipes) (kg)	8,00446E-05	
Polyvinyl chloride (valves) (kg)	3,00337E-05	
<i>Area (m<sup>2</sup>)</i>		
Occupation, industrial area (m <sup>2</sup> a)	1,85502E-06	PSA-CIEMAT
Transformation, from grassland, natural (non-use) (m <sup>2</sup> )	3,71005E-05	
Transformation, to industrial area (m <sup>2</sup> )	3,71005E-05	
Operation of MED Plant		
Name of Input	Amount for 1m <sup>3</sup> FW Production	References
Chlorine (disinfectant) (kg/m <sup>3</sup> )	0,0185	
Phosphoric Acid (Antiscalant) (kg/m <sup>3</sup> )	0,027	

Sodium Bisulfite (Chlorine removal) (kg/m <sup>3</sup> )	0,018	(Doi et al., 2021)
Propylene Glycol (kg/m <sup>3</sup> )	0,0009	
Calcium Hydroxide (kg/m <sup>3</sup> )	0,0005	
Thermal Energy from PTC (kwh/m <sup>3</sup> )	32,77	
Electrical Energy from GRID	0,78	PSA-CIEMAT
Raw Seawater (m <sup>3</sup> )	2,664028777	
<b>Decommissioning of MED Plant</b>		
<b>Name of Input</b>	<b>Amount for 1m<sup>3</sup> FW Production</b>	<b>References</b>
Inert Landfill (kg)	0,01629539	(Tarpani et al., 2019)
<b>Construction of Solar Plant</b>		
<b>Name of Input</b>	<b>Amount for 1m<sup>3</sup> FW Production</b>	<b>Reference</b>
*Concentrated solar power plant, solar thermal parabolic trough, 50 MW {RoW}  concentrated solar power plant construction, solar thermal parabolic trough, 50 MW   Conseq, U		
<u>Area (m<sup>2</sup>)</u>		
Occupation, industrial area (m <sup>2</sup> a)	0,010723932	
Transformation, from grassland, natural (non-use) (m <sup>2</sup> )	0,000357464	
Transformation, to industrial area (m <sup>2</sup> )	0,000357464	
Building, hall, wood construction (m <sup>2</sup> )	2,63604E-07	
Excavation, hydraulic digger (m <sup>3</sup> )	6,41147E-06	
Road (my)	1,20741E-05	
Steel, unalloyed (kg)	1,78652E-06	ECOINVENT
Water supply network (km)	1,11815E-09	
Wire drawing, steel (kg)	1,78652E-06	
Collector field area, solar thermal parabolic trough, 50 mw (p)	2,79537E-10	
Heat transport fluid system, solar thermal parabolic trough, 50 mw (p)	2,79537E-10	
Power block, solar thermal parabolic trough, 50 mw (p)	2,79537E-10	
*Concentrated solar power plant, solar thermal parabolic trough, 50 MW {ZA}  concentrated solar power plant construction, solar thermal parabolic trough, 50 MW   Conseq, U		
<u>Area (m<sup>2</sup>)</u>		
Occupation, industrial area (m <sup>2</sup> a)	0,00151792	
Transformation, from grassland, natural (non-use) (m <sup>2</sup> )	5,05973E-05	
Transformation, to industrial area (m <sup>2</sup> )	5,05973E-05	
Building, hall, wood construction (m <sup>2</sup> )	3,73118E-08	
Excavation, hydraulic digger (m <sup>3</sup> )	9,07512E-07	
Road (my)	1,70902E-06	
Steel, unalloyed (kg)	2,52874E-07	ECOINVENT
Water supply network (km)	1,58269E-10	
Wire drawing, steel (kg)	2,52874E-07	
Collector field area, solar thermal parabolic trough, 50 mw (p)	3,95672E-11	
Heat transport fluid system, solar thermal parabolic trough, 50 mw (p)	3,95672E-11	
Power block, solar thermal parabolic trough, 50 mw (p)	3,95672E-11	
<b>Operation of Solar Plant</b>		
<b>Name of Input</b>	<b>Amount for 1m<sup>3</sup> FW Production</b>	<b>Reference</b>
Benzene (for heat transfer fluid lost) (kg)	0,00011903	

Diphenylether-compound (for heat transfer fluid lost) (kg)	0,000330141	ECOINVENT
Water, deionised (for cleaning) (kg)	0,22939	
Heat, district or industrial, natural gas (MJ) (for back up firing)	0,88479	

### Decommissioning of Solar Plant

Name of Input	Amount for 1m <sup>3</sup> FW Production	Reference
*Concentrated solar power plant, solar thermal parabolic trough, 50 MW {RoW}  concentrated solar power plant construction, solar thermal parabolic trough, 50 MW   Conseq, U		
Decommissioned road (my)	1,20741E-05	ECOINVENT
Waste reinforcement steel (kg)	1,23962E-09	
Waste reinforcement steel (kg)	1,78528E-06	
*Concentrated solar power plant, solar thermal parabolic trough, 50 MW {ZA}  concentrated solar power plant construction, solar thermal parabolic trough, 50 MW   Conseq, U		
Decommissioned road (my)	1,70902E-06	ECOINVENT
Waste reinforcement steel collection (kg)	1,64368E-07	
Waste reinforcement steel recycling (kg)	8,85058E-08	

### OUTPUTS

Name of Output	Amount for 1m <sup>3</sup> FW Production	References
Chlorine (kg)	0,0007	(Do Thi et al., 2021)
Phosphoric acid (kg)	0,01	
Copper (from corrosion of structural materials) (kg)	0,00002	
Propylene glycol (kg)	0,00009	
Sodium chloride (kg)	45	
Waste heat (MJ)	114,24	

Table A.4: CSP Technologies Comparison

TECHNOLOGY	PARABOLIC TROUGH	FRESNEL MIRROR REFLECTOR	SOLAR TOWER	DISH STIRLING	REFERENCES
Maturity of technology	Very Mature	Mature	Most Recent	Recent	(Barlev et al., 2011)
Capacity in unit MW	10-300	10-200	10-150	0.01-0.4	(Müller-Steinhagen & Trieb, 2004) (Irena, 2012)
Concentration (radiant power density at the collector/ radiant power density of the sun without any concentration)	70-80	25-100	300-1000	1000-3000	(Müller-Steinhagen & Trieb, 2004)
Peak Solar Efficiency	21%	20%	20%	29%	(Müller-Steinhagen & Trieb, 2004)
Annual Solar Efficiency (net power generation/ incident beam radiation)	10-15%	9-11%	8-10%	16-18%	(Müller-Steinhagen & Trieb, 2004)
Thermal Cycle Efficiency	30-40% (steam turbine)	30-40% (steam turbine)	30-40% (steam turbine) 45-55% (combined cycle)	30-40% Stirl. 20-30% (gas turbine)	(Müller-Steinhagen & Trieb, 2004)
Land use m <sup>2</sup> /MWh*year	2	2.5	2-2.5	1-1.15	(Müller-Steinhagen & Trieb, 2004)
Heat Transfer Fluid	synthetic oil, water/stream	water/stream	air, molten salt, water/stream	Air	(Negewo, 2012)
Thermal Storage Media	molten salt, concrete, PCM	molten salt, concrete, PCM	molten salt, ceramics, PCM	-	(Negewo, 2012)
Land use Factor	0.25-0.35	0.6-0.8	0.2-0.25	-	(Negewo, 2012)

Table A.4: CSP Technologies Comparison

TECHNOLOGY	PARABOLIC TROUGH	FRESNEL MIRROR REFLECTOR	SOLAR TOWER	DISH STIRLING	REFERENCES
Land use (ha/MW)	2	2-5	2-2.5	1-1.15	(Simbolotti, 2013)
Construction Time, yr	1-3	1-2	1-3	1	(Simbolotti, 2013)
Operating T range (C)	350-550	390	250-565	550-750	(Irena, 2012)
Steam Conditions (C/bar)	380 to 540/100	260/50	540/100 to 160	n.a.	(Irena, 2012)
Maximum slope of solar field (%)	<1-2	<4	<2-4	10% or more	(Irena, 2012)
Thermodynamic Power Cycle	Rankine	Rankine	Brayton, Rankine	Stirling, Brayton	(Irena, 2012)
Water requirement (m <sup>3</sup> /MWh)	3 (wet cooling) 0.3 (dry cooling)	3 (wet cooling) 0.2 (dry cooling)	2-3 (wet cooling) 0.25 (dry cooling)	0.05-0.1 (mirror washing)	(Irena, 2012)
Storage with molten salt	commercially available	possible, but not proven	commercially available 5700-6400	possible, but not proven	(Irena, 2012)
Cost of Solar Field (2010 USD/KW)	3900-4100 (no storage) 6300-8300(6hrs storage)	Cheaper than the Parabolic Trough	(6 to 7.5 hrs storage) 8100-9000 (12 to 15 hrs storage)	Higher than the all technology	(Irena, 2012) (Simbolotti, 2013)
Power Unit	steam turbine	steam turbine	gas turbine, steam turbine	stirling engine	(Müller-Steinhagen & Trieb, 2004) (Negewo, 2012)
Lifetime, yr	30	20-30	30	<15	(Simbolotti, 2013) (G. Zhu et al., 2014)

Table A.4: CSP Technologies Comparison

TECHNOLOGY	PARABOLIC TROUGH	FRESNEL MIRROR REFLECTOR	SOLAR TOWER	DISH STIRLING	REFERENCES
Advantages	*Long term proven reliability and durability	*Simple structure and easy field construction	*High temperature allows high efficiency of power cycle	* Small amount of water requirement for mirror cleaning	(Irena, 2012)
	*Better solution for large area because of higher optical efficiency	*Tolerance for slight slopes	*Tolerates non-flat sites		(Negewo, 2012)
Disadvantages	*High concentration	*Direct steam generation proven	* Available storage technologies, but still they did not prove in long term		(Cau & Cocco, 2014)
	*Limited temperature of heat transfer fluid hampering efficiency and effectiveness	*Better solution for the small area because of larger energy production per m <sup>2</sup> .		*High solar efficiency	(Müller-Steinhagen & Trieb, 2004)
Disadvantages	*Complex structure, high precision required during field construction	*Thinner than a conventional lens			(Irena, 2012)
	*Requires flat land area	*Requirement of less material than a conventional lens			
Disadvantages	*Good tracking system requirement	*Capability of separating the direct and diffuse light			
Disadvantages		*Storage for direct steam generation (phase change material) in very early stage			
		*Imperfection on the edges of the facets, causing the rays improperly focused at the receiver	*High maintenance and equipment cost	*Very high cost compares to the other solar concentrator types	(Negewo, 2012)
Disadvantages					(Muhammad-Sukki et al., 2010)
					(Nixon et al., 2010)

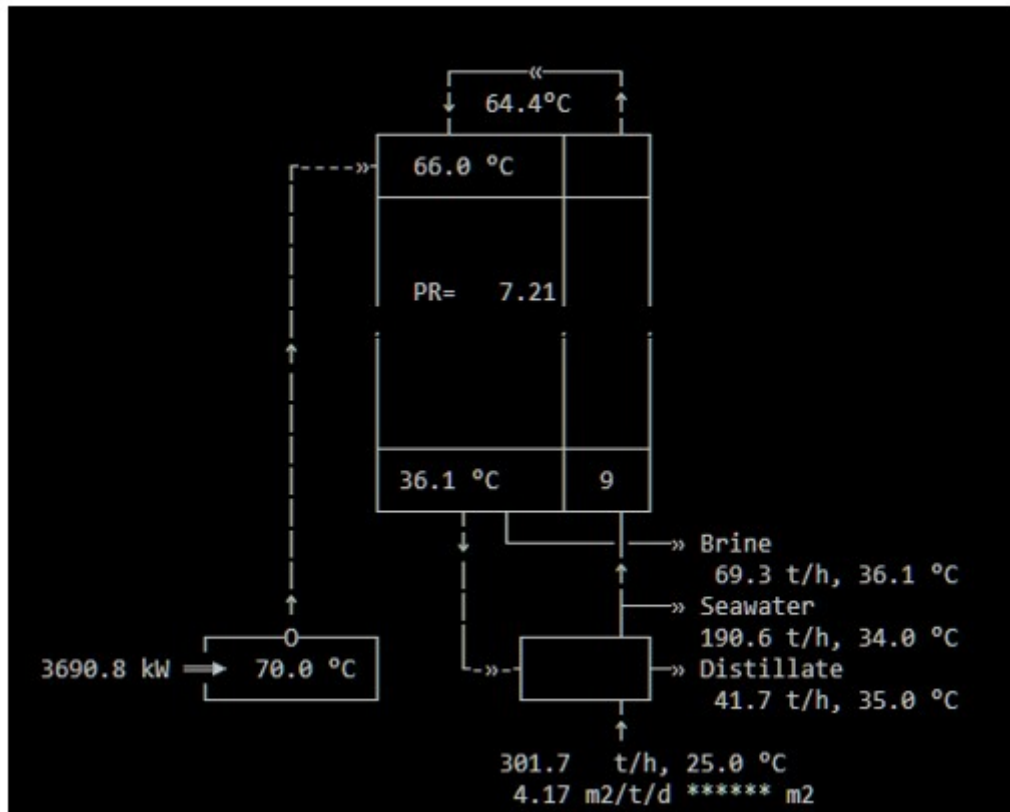


Figure A.1: MED Plant Chart Designed by PSA-CIEMAT



## **Appendix B**

### **APPENDIX**

#### **B.1 COMPARATIVE CHARACTERIZATION AND NORMALIZATION RESULTS WITH DIFFERENT IMPACT CATEGORIES**



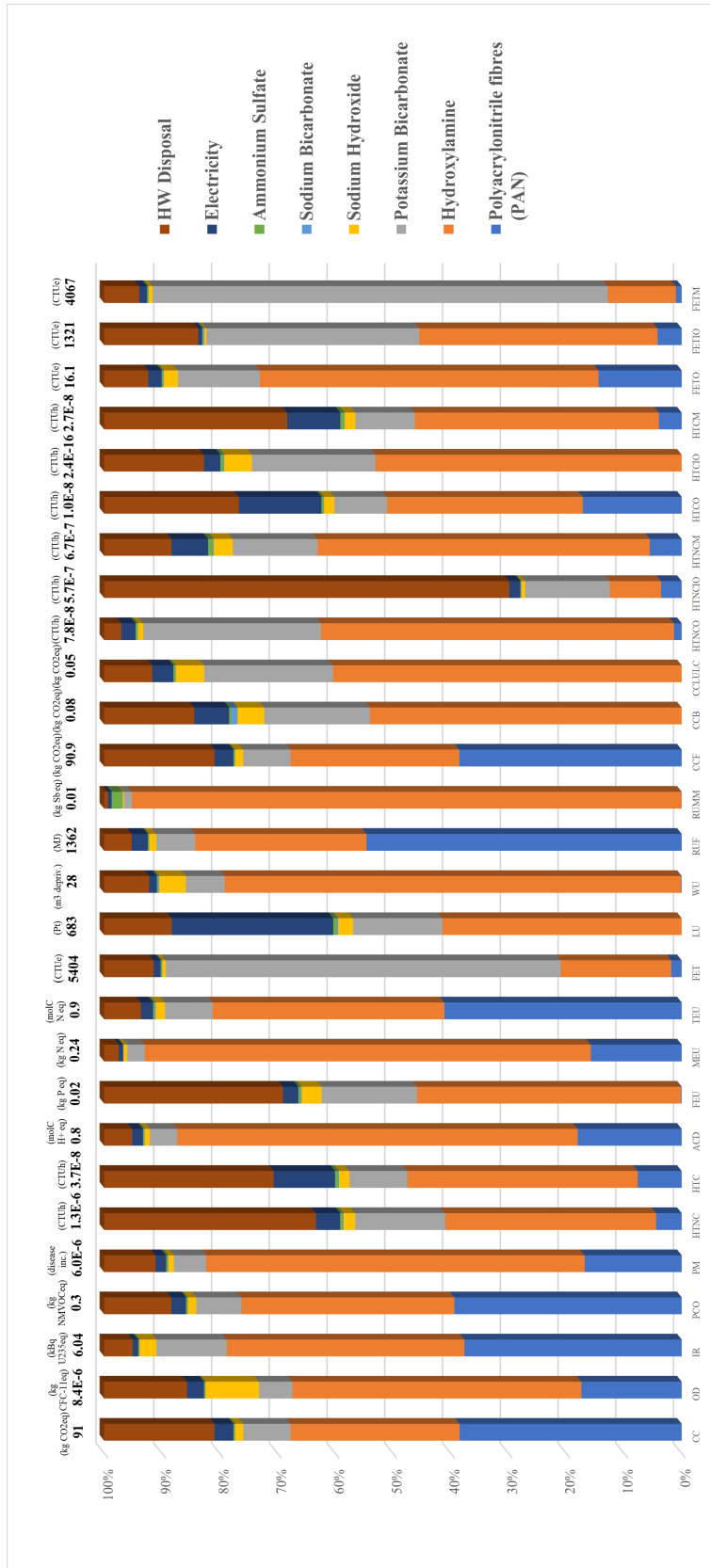


Figure B.2: Characterization Results of Uranium Recovery from brine via PAN-AO Adsorbent with EF 3.0 Method



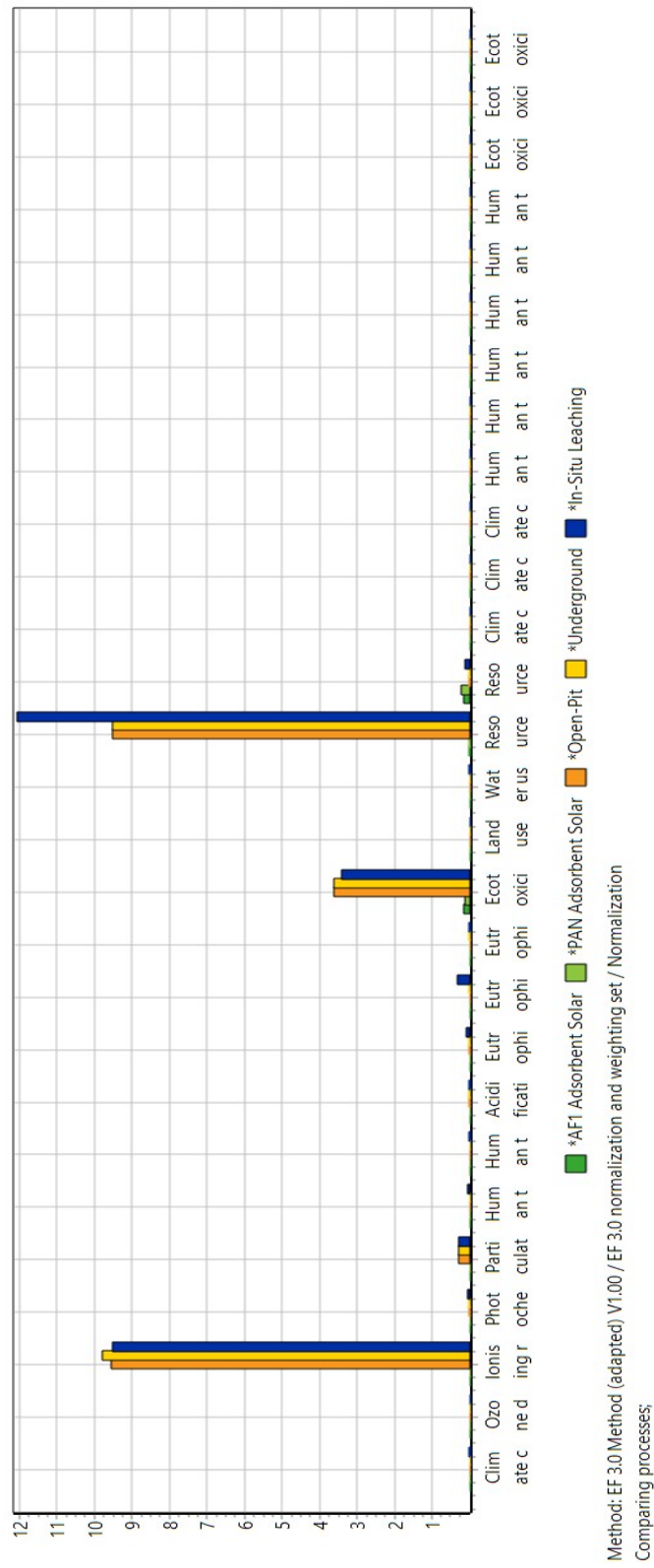


Figure B.4: Comparative Normalization Results of Uranium Recovery from Brine via Amidoximated Adsorbents and Conventional Uranium Extraction and Mining Methods with EF 3.0 Method

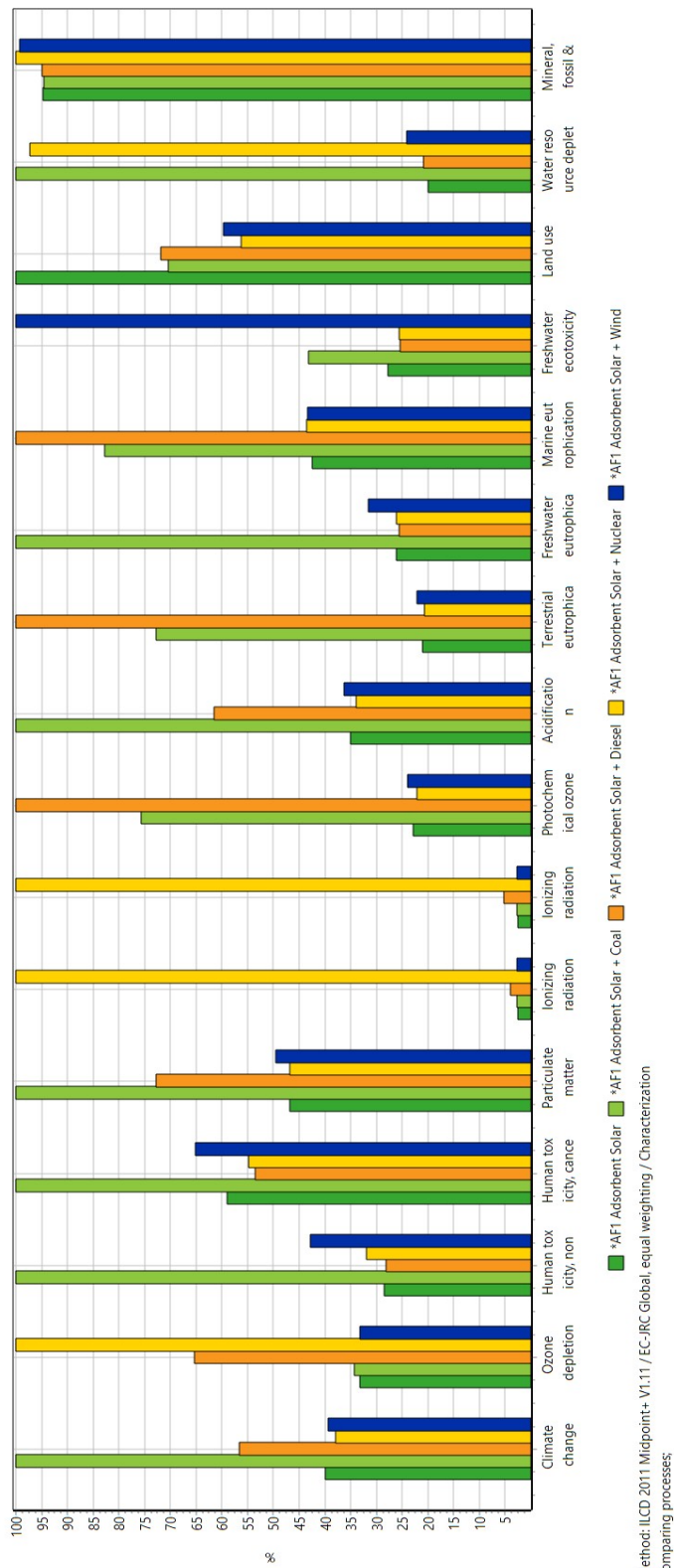


Figure B.5: Comparative Characterization Results of URFB Systems with Distinct Combined Energy Sources with ILCD 2011 Midpoint+ Method (AF1 Adsorbent)

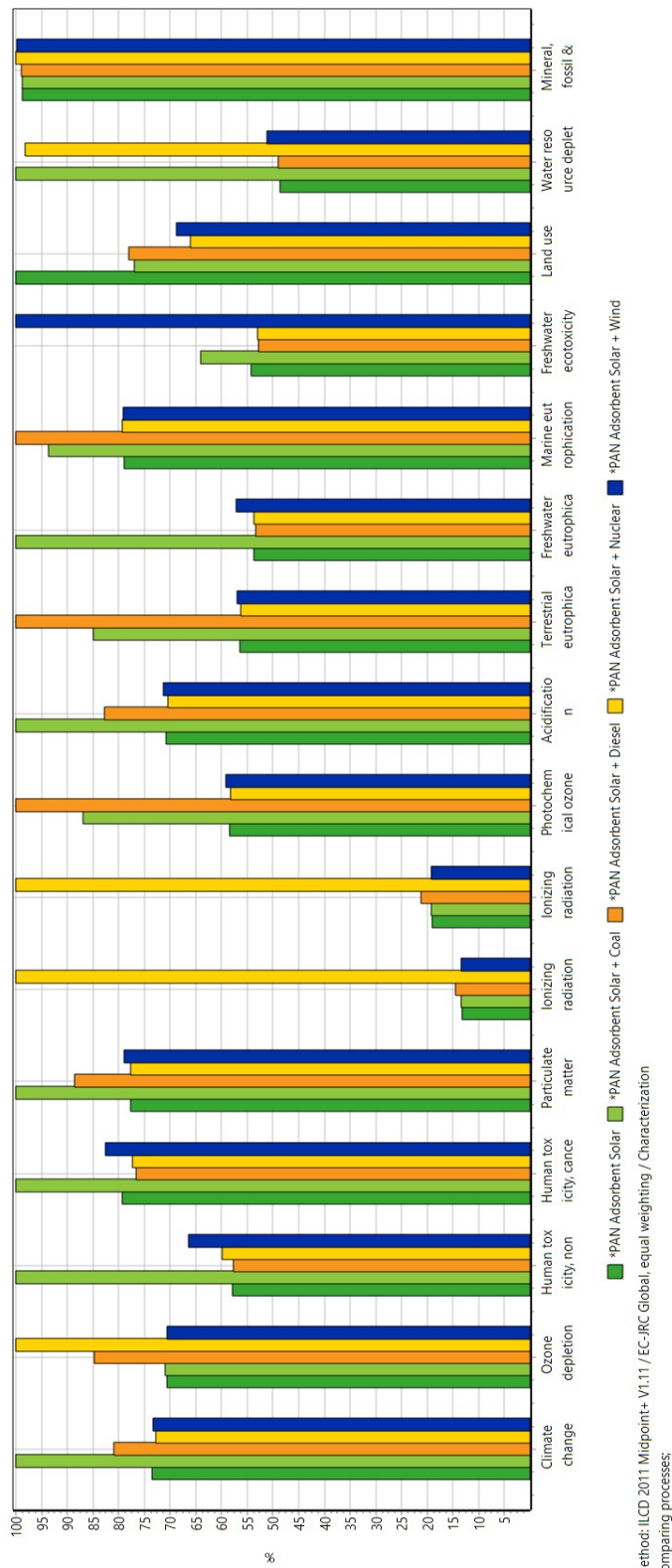
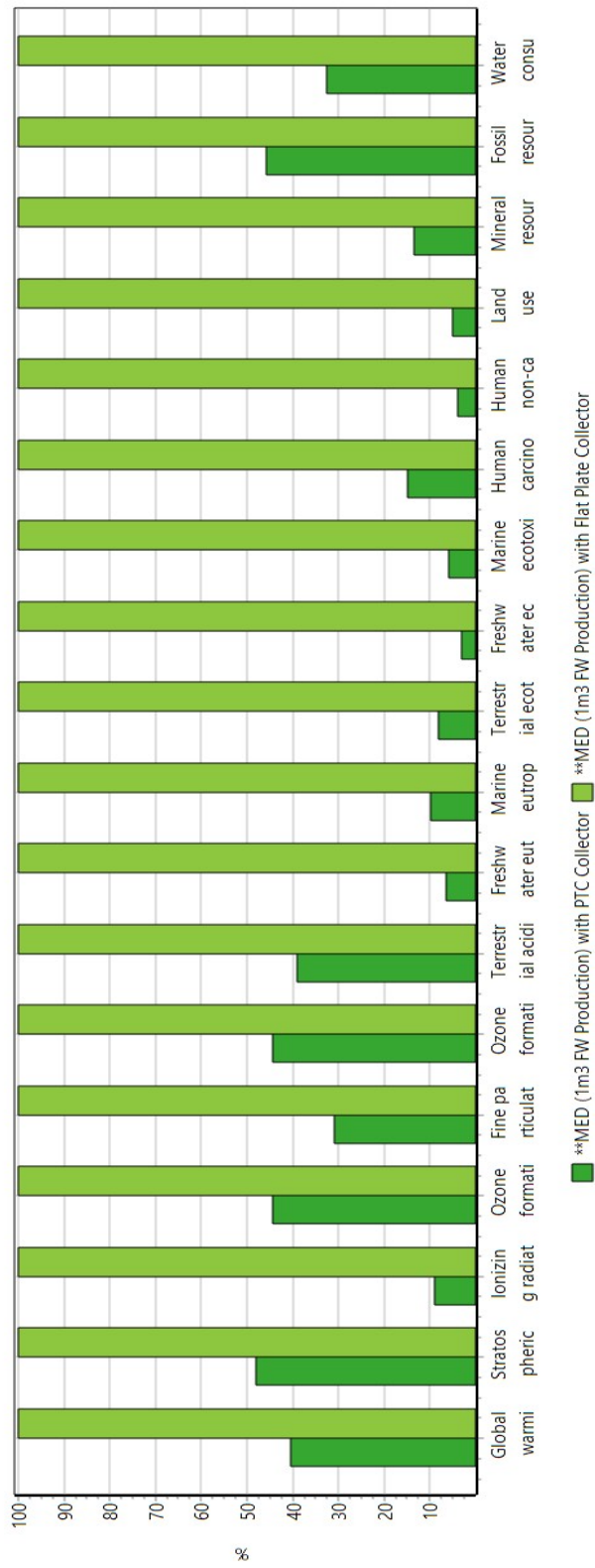


Figure B.6: Comparative Characterization Results of URFB Systems with Distinct Combined Energy Sources with ILCD 2011 Midpoint+ Method (PAN-AO Adsorbent)



Method: ReCiPe 2016 Midpoint (H) V1.04 / World (2010) H / Characterization  
 Comparing 1 ton \*\*MED (1m3 FW Production) with PTC Collector' with 1 ton \*\*MED (1m3 FW Production) with Flat Plate Collector';

Figure B.7: Comparative Characterization Results of MED Plant Driven by PTC and Flat Plate Collectors with ReCiPe 2016 Midpoint Method

Table B.1: The Characterization Results of Solar-Driven MED System Integrated with URFB via AF1 and PAN-AO Adsorbent with ILCD 2011 Midpoint+ Method

<b>Impact Category</b>	<b>Solar-Driven MED</b>	<b>Solar-Driven MED</b>
	<b>combined with URFB (AF1 Adsorbent) Base Case</b>	<b>combined with URFB (PAN Adsorbent) Base Case</b>
Climate change (kg CO2 eq)	92226	92233
Ozone depletion (kg CFC-11 eq)	0,015	0,015
Human toxicity, non-cancer effects (CTUh)	0,012	0,012
Human toxicity, cancer effects (CTUh)	0,006	0,006
Particulate matter (kg PM2.5 eq)	73,4	73,4
Ionizing radiation HH (kBq U235 eq)	5340	5342
Ionizing radiation E (interim) (CTUe)	0,033	0,033
Photochemical ozone formation (kg NMVOC eq)	380,7	380,7
Acidification (molc H+ eq)	940,7	940,8
Terrestrial eutrophication (molc N eq)	1306	1307
Freshwater eutrophication (kg P eq)	12,7	12,7
Marine eutrophication (kg N eq)	120,7	120,7
Freshwater ecotoxicity (CTUe)	885218	884950
Land use (kg C deficit)	514596	514203
Water resource depletion (m3 water eq)	158,4	158,4
Mineral, fossil & ren resource depletion (kg Sb eq)	3,25	3,25

Table B.2: Main Pollutants and Relevant Processes Causing to Spread These Pollutants During 1 kg of U Production from RO Plant Combined With URFB System

<b>Impact Categories</b>	<b>Main Pollutants and Released Media</b>	<b>Relevant Processes</b>
GW	CO <sub>2</sub> , fossil (air)	Electricity and polyvinylidenechloride production
SOD	Hydrocarbons, chlorinated (air)	Polyvinylidenechloride and seawater RO module production
IR	Radon 222 (air)	Electricity production
OFHH	Nitrogen oxides (air)	Electricity and polyvinylidenechloride production
FPMF	Sulfur dioxide and particulates, <2.5 um (air)	Electricity and polyvinylidenechloride production
OFTE	Nitrogen oxides (air)	Electricity and polyvinylidenechloride production
TA	Sulfur dioxide (air)	Electricity and polyvinylidenechloride production
FEU	Phosphate (water)	Mining activities during electricity production
MEU	Nitrogen, organic (water)	Plastic Waste Disposal
TE	Copper (air)	Electricity production
FE	Copper and Zinc (water)	Electricity production
ME	Copper and Zinc (water)	Electricity production
HTC	Chromium VI (water)	Polyvinylidenechloride production
HTNC	Zinc and Arsenic (water)	Mining activities during electricity production and plastic waste disposal
LU	Occupation, urban green areas (raw material)	Mining activities during electricity production
MRS	Gold (raw material)	Sulfuric acid, electricity, and sodium hydrogen sulfite production
FRS	Gas, natural (raw material)	Electricity production
WC	Water (raw material)	Electricity and polyvinylidenechloride production

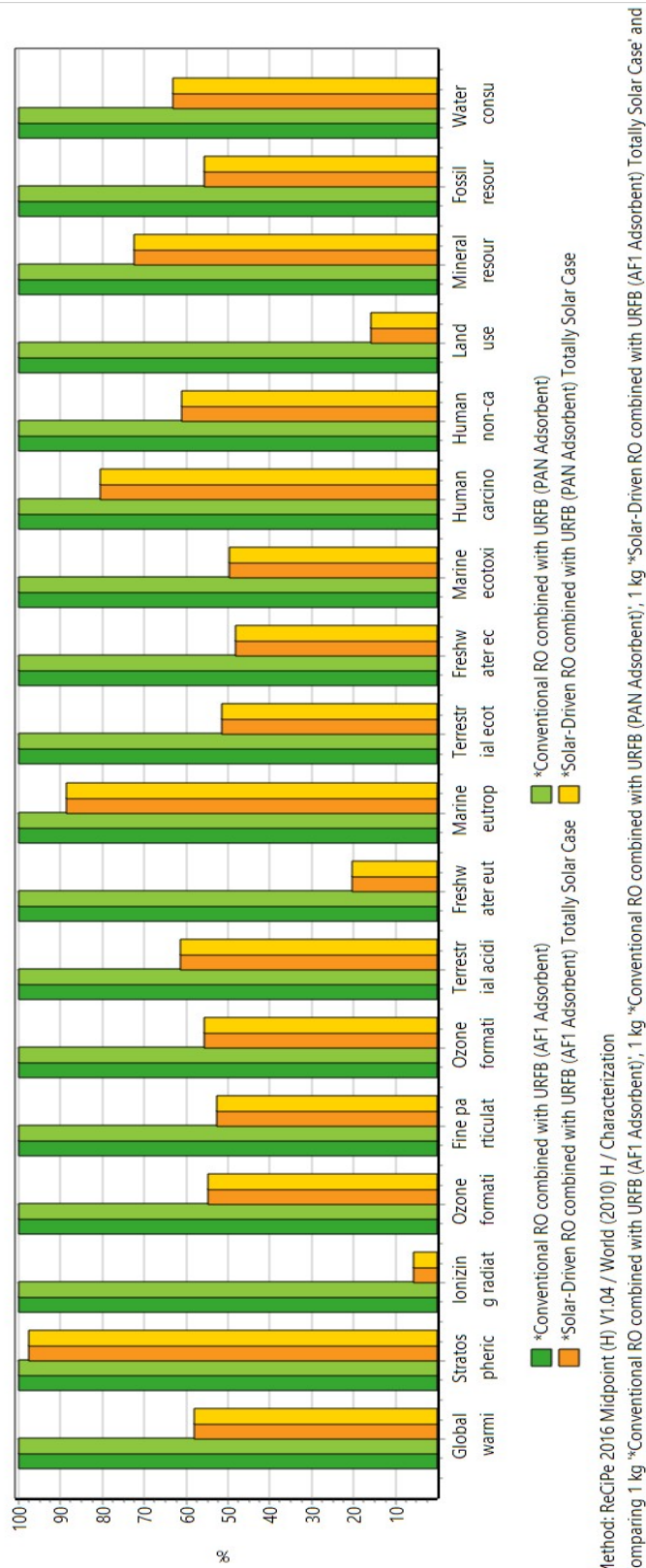


Figure B.8: Comparative Characterization Results of Totally Solar Case and Conventional RO Plants Case Combined With URFB Systems with ReCiPe 2016 Midpoint+